

**Development of crop factor (K_c) using lysimeters and examination of
the effect of irrigation outset timing on physiological and anatomical
aspects in wine vineyards**

Thesis for degree of
"Doctor of Philosophy"

By Sarel Munitz

Submitted to the Senate of the Hebrew University of Jerusalem

December 2019

**Development of crop factor (K_c) using lysimeters and examination of
the effect of irrigation outset timing on physiological and anatomical
aspects in wine vineyards**

Thesis for degree of
"Doctor of Philosophy"

By Sarel Munitz

Submitted to the Senate of the Hebrew University of Jerusalem

December 2019

This work was carried out under the supervision of:

Prof. Amnon Schwartz

The Robert H. Smith Institute of Plant Sciences and Genetics in Agriculture, Faculty of
Agriculture, Food and Environment, The Hebrew University of Jerusalem, Rehovot, Israel.

Declaration

This thesis summarizes my own research.

Dr. Noa Ohana-Levi, has contributed to the data analysis presented in chapters 3.4 & 3.5.

Dr. Ilana Shtein, a post-doc in our lab, has contributed to the anatomy work presented in chapter 3.7.

Sarel Munitz

Rehovot, December 2019

Acknowledgment

I would like to express my appreciation and gratitude to my advisors. The first, Dr. Yishai Netzer for leading me through all the stages of the research, in the field and at the lab. I cannot overestimate his tremendous contribution to this work, and I am grateful for that. And the second Prof. Amnon Schwartz who supported me through all the research period. I also wish to thank my advisory committee Dr. Giora Ben-Ari and Dr. Or Sperling for their helpful comments.

I would like to thank Dr. Noa Ohana-Levi, for her help with lysimeters data analysis, and to Dr. Ilana shtein for her assistance with the plant anatomy.

I wish to thank to the Ministry of Science and Technology, Israel; the Ministry of Agriculture and Rural Development, Israel and the Israeli Wine Grape Council for founding these researches.

Special thanks to the dedicated growers : Yoav David, Itamar Weis, Yedidia Spitz and Shlomi Choen.

I would also like to thank the team of Teperberg Winery, Udi Gliksman, Shiki Rauchberger and Olivier Fratty for their collaboration.

I would like to particularly thank Yechezkel Harroch, Bentzi Green, Yossi Shteren, Alon Katz, Ben hazut, David Kimchi, Gilad gersman, Alon chores, Yedidia sweid, Daniel Mintz and Yair hayat for assisting in the field measurements.

To Yotam Zait my lab member for many enjoyable moments, suggestions, support and lunch breaks.

And most important to my family: words cannot express how grateful I am for their support.

Abstract

Wine grapevine cultivation is rapidly expanding all over the world and particularly in Israel. In order to produce high quality wine (color and aroma), drought stress must be induced during some stages of the growing season (mainly in red varieties). A skilled irrigation method must be imposed in order to enable quality grape wine production without causing damage to vines.

Such Skilled irrigation needs to be based upon reliable data from crop water use. In perennial crop like vines, the constant changes in canopy size and atmospheric conditions must be an integral part in water use evaluation. In the current study, vine water use (ET_c) was measured using 6 drainage lysimeters. The relationship between crop evapotranspiration (ET_c) and reference evapotranspiration (ET_o) is termed the crop coefficient (K_c) (Allen et al. 1998). ET_c and K_c changes during the growing season due to phenological development and agro technical practices. These factors include: canopy management treatments, trellis type, row and inter row spacing and more factors. The objective of the present study is to determine seasonal crop water use of *Vitis vinifera* 'Cabernet Sauvignon' (used for red wine production) grown under unlimited water supply in the central mountain region of Israel. A derivative of the objective is to correlate K_c to leaf area index (LAI).

The irrigation model which is being developed in this study, can help farmers to control vine growing via skilled irrigation model. Meteorological data can be obtained from nearby meteorological station (free data of more than 145 cross – country widespread meteorological stations is available in internet). Canopy size can be obtained from estimation from pictures or by Sunscan device (delta T). In the future we plan to build internet site in which farmers can fill in all the data of their vineyard, choose from pictures the vine which resembles the most in their leaf area to the vines in their vineyard, and get water amounts for irrigation. In this way the Israeli farmers will get skilled irrigation method which will enable them to grow higher quality grapes with less water.

One of the most critical aspects in a skilled irrigation method is the irrigation initiation timing during growing season, which depends on winter rains, soil texture, scion and variety cultivated. The aim of current research is to develop physiological tools for scheduling irrigation initiation in wine grapevines.

The current irrigation trial was constructed during the winter of 2014 in a commercial vineyard of 'Cabernet Sauvignon'. Irrigation initiation was determined by measurement of midday stem water potential, which is a very reliable and integrative water stress indicator. The water potential threshold were: Budbreak, -0.6 MPa, -0.8 MPa, -1.0 MPa and -1.2 MPa. After irrigation initiation all treatments were similarly irrigated according to RDI strategy.

The following physiological measurements were taken weekly: midday stem water potential, gas exchange parameters and canopy size. In addition, four trunk dendrometers per treatment were installed. At the end of growing season 12 petioles and shoots per treatment (in triplicates) were sampled, cross sectioned, stained and photographed for computer analysis. Vessel diameter and specific hydraulic conductivity were calculated. At harvest yield parameters of all vines were measured separately. Wine was made (micro vinification) from each replication separately.

From 2014 - 2016 obtained results, it seems that early irrigation onset is directly correlated to increasingly more vigorous vegetative growth, bigger berry mass, higher yield and inferior wine quality. The long term effect of irrigation delay on vine performance should be carefully examined in the future.

Contents

1. Introduction.....	7
1.1 Deficit irrigation in vineyards for wine production– backroad.....	7
1.2.1 Crop & reference evapotranspiration, crop coefficients and leaf area.....	8
1.2.2 Wine grapevine water consumption measurements.....	9
1.3 Deficit irrigation implementation strategies.....	10
1.4 Functional anatomy effect on water status.....	11
2. Results.....	12
2.1: Chapter 1:.....	12
Water consumption, crop coefficient and leaf area relations of a <i>Vitis vinifera</i> cv. “Cabernet Sauvignon” vineyard.....	
2.2: Chapter 2:.....	22
Evaluation of Seasonal Water Use and Crop Coefficients for Cabernet Sauvignon Grapevines As the Base for Skilled regulated irrigation.....	
2.3: Chapter 3:.....	30
The effect of irrigation initiation timing on vegetative growth, physiological parameters and yield components in 'Cabernet Sauvignon' grapevines.....	
2.4: Chapter 4:.....	55
Multiseasonal grapevine water consumption - drivers and forecasting.....	
2.5: Chapter 5:.....	68
Evaluation of within-season grapevine evapotranspiration patterns and drivers using generalized additive models.....	
2.6: Chapter 6:.....	82
Structural memory in grapevines: Early season water availability affects late season drought stress severity.....	
2.7: Chapter 7:.....	91
From structural constraints to hydraulic function in three <i>Vitis</i> rootstocks.....	
3. Discussion and conclusions.....	103
3.1.1 water consumption and crop coefficient.....	103
3.1.2 Evaporation : transpiration ratio.....	103
3.1.3 Leaf area index and crop coefficient relationship.....	104
3.2.1 Water availability effect on physiological parameters.....	104
3.2.2 Drought stress effect on vegetative growth	106
3.2.3 Water availability effect on anatomical structure.....	107
3.2.4 4 Irrigation regime effect on yield components.....	108
4. Reference.....	109
5. Hebrew summary (תקציר בעברית).....	115

1. Introduction

1.1 Deficit irrigation in vineyards for wine production– backroad

Most cultivated vineyards worldwide (7.4 million ha) are located at semi-arid and arid regions, in which water resources are scarce (Chaves et al. 2007). In those areas water shortage is likely the most dominant environmental constraint (Chaves et al., 2010; Cifre et al., 2005; Patakas et al., 2005; Schultz, 2016), so vineyard irrigation management is essential there in order to enable sustainable production of grapevines (Feres and Evans, 2006; Romero et al., 2010b). In cultivation of wine grape, water has additional importance, since skilled vineyard irrigation management is considered the main tool for effective control of vegetative growth and wine quality (Bravdo et al., 1985; Chaves et al., 2010; Feres and Evans, 2006; Keller et al., 2008; Munitz et al., 2016; Romero et al., 2010b). Imposing an appropriate drought stress level at a suitable phenological stage can improve wine quality with causing minimal yield reduction (Girona et al., 2009; Intrigliolo and Castel, 2010; Munitz et al., 2016; Romero et al., 2013; Williams and Araujo, 2002). Conversely, imposing severe drought stress at inappropriate phenological stages can result in significant yield loss and even a decrease in quality in extreme cases (Bravdo et al., 1985; Chaves et al., 2010; Esteban et al., 2001; Grimes and Williams, 1990; Medrano et al., 2003; Munitz et al., 2016). Continuous severe drought stress conditions will lead to dramatic vegetative growth reduction and shorten the lifespan of the vineyard. A non-stress irrigation approach is also problematic, since excessive irrigation is costly and may cause vigorous vegetative growth that leads to shading of clusters and reduced quality (Bureau et al., 2000; Chorti et al., 2010; Gao and Cahoon, 1994; Morrison and Noble, 1990). In addition, over-irrigating may increase the need for more canopy management practices and also can lead to percolation of water below the root zone, leaching nitrates and other chemicals into groundwater reservoirs (Di and Cameron, 2002; Keller, 2005; Watts et al., 1991). Moreover, excessive irrigation can contribute to fungal infection and cluster rotting.

In semi-arid regions such as Israel, the degree of deficit irrigation that should be imposed in the vineyard depends considerably on the wine category planned to be produced from the grapes (Munitz et al., 2016). In practice, severer deficit irrigation regime is imposed at certain phenological stages for production of high-quality red wines, in order to increase berries quality. Drought stress is considered to increase grape quality by two main mechanisms. One is increased skin-to-pulp ratio (that results from decreased berry size), raising the concentration of phenolic

substances and anthocyanins that can be extracted from berries skin to the must (Bravdo et al., 1985; Keller et al., 2008; Kennedy et al., 2002). The other is an enhancing effect of drought stress on the biosynthesis of precursors in the metabolic pathway of color and aroma compounds, resulting in increased concentration of them in the berry skin (Castellarin et al., 2007; Chaves et al., 2010; Ollé et al., 2011; Zarrouk et al., 2012).

1.2.1 Crop & reference evapotranspiration, crop coefficients and leaf area.

The term evapotranspiration (ET) refers to the total amount of water that is evaporated (E) from the soil surface and transpired (T) through the plant canopy (Allen et al., 2006). During the past century, studies have been conducted to determine the role of meteorological variables in generating evapotranspiration from agricultural fields (Allen et al., 1998; Briggs and Shantz, 1916; Fuchs et al., 1987; Pierce, 1958; Tao et al., 2009; Widstoe, 1909). In 1948 Howard Penman published the equation that describes the standard climatological factors affecting evaporation from an open water source (Penman, 1948). Later on, the Penman-Monteith equation was developed to approximate plant evapotranspiration (ET_o) based on temperature, relative humidity, radiation, and wind speed (Monteith, 1965). The United Nations Food and Agriculture Organization (FAO) adopted the Penman–Monteith equation as the standard methods for evapotranspiration modeling. The main factors affecting ET are the canopy area and architecture, evaporative power of the atmosphere (ET_o), stomatal conductance and soil type (Allen et al., 2006). Crop evapotranspiration (ET_c) is the evapotranspiration of certain crop, measured at field condition under optimal water availability, full fertilization and disease-free (no biotic & abiotic stress). The reference evapotranspiration (ET_o) of a well-watered 12-cm-high grassy surface that fully covers the ground is calculated using meteorological data from the FAO Penman-Monteith equation (Allen et al., 2006; Doorenbos and Pruitt, 1977). Measuring crop evapotranspiration (ET_c) and relating it to reference evapotranspiration (ET_o) is the standard procedure for determination of crop coefficient (K_c) used for skilled irrigation management (Allen et al., 2006; Netzer et al., 2009; Williams et al., 2003). K_c is defined as the ratio between the actual crop evapotranspiration (ET_c) and reference evapotranspiration (ET_o), i.e. $K_c = ET_c/ET_o$. K_c varies along the growing season as a function of canopy area (LAI) dynamics, the solar radiation intercepted by the canopy and the phenological stage of the crop (Allen et al., 2006; Doorenbos and Pruitt, 1977; Evans et al., 1993; Jagtap and Jones, 1989; Netzer et al., 2009; Peacock et al., 1987; Williams et al., 2003). Leaf area has a substantial effect on vine water consumption (ET_c), due to stomatal response to meteorological conditions. A larger leaf area signifies a larger transpiring surface. Conversely, a larger leaf area generates a wider shaded ground area and a

reduction in the relative portion of evaporation from the ground. Leaf area is typically described by using leaf area index (LAI) which is defined as one-sided green leaf area per unit ground surface area ($\text{m}^2 \text{m}^{-2}$) allocated to a single plant. This ratio standardizes the canopy area to the ground surface allocated to the plant, which enables to compare leaf area among different crops and between various plots that differ in their planting density or other characteristics. Studies on water consumption in vineyards have established LAI as a driver of vine water consumption (ET_c), mostly due to its effect on K_c . The K_c values of grapevines may vary with agricultural practices and trellising architecture (Williams and Ayars, 2005; Williams and Fidelibus, 2016). As a consequence of all mentioned above, a comprehensive irrigation model enabling imposing precise water availability conditions, should be based on changes in water consumption as a function of climate conditions (ET_o) and canopy area (LAI) (Allen et al., 2006; Netzer et al., 2009).

1.2.2 Wine grapevine water consumption measurements.

Grapevine ET_c has been measured and estimated with different techniques such as microclimatological methods (Carrasco-Benavides et al., 2012; Oliver and Sene, 1992; Yunusa et al., 2004), soil moisture (Prior and Grieve, 1987; Van Zyl and Van Huyssteen, 1980), sap flow sensors (Chatelet et al., 2008) and remote sensing (Carrasco-Benavides et al., 2012; Consoli et al., 2006; Lopes et al., 2010; Rozenstein et al., 2018; Vanino et al., 2015). Another technique is lysimetry, which is considered the standard technique for measuring ET_c (Hatfield 1990, Howell et al., 1995, Prueger 1997). Lysimeters have been used to measure the water consumption of many woody agricultural species such as apple (Girona et al., 2011; Mpelasoka et al., 2001; Ro, 2001), almond (García-Tejero et al., 2015; Heilmeyer et al., 2002; Lorite et al., 2012) and olive (Ben-Gal et al., 2010; Deidda et al., 1990). In field-grown grapevines, lysimeters have been used to measure ET_c of a range of cultivars under different climate and soil conditions with drainage (Evans et al., 1993; Netzer et al., 2009; Prior and Grieve, 1987) and weighting methods (López-Urrea et al., 2012; Picón et al., 2012; Williams et al., 2003). Measurement of water consumption under field conditions, using vines that are similar in their dimensions and physiological performance to those grown in a commercial vineyard, is beneficial for assessing the actual ET_c dynamics of the vineyard.

Defining the factors that affect dynamics throughout the season and evaluating expected physiological and vegetative performance may assist in understanding ET_c patterns and provide projection models for vineyards with no direct ET_c measurements (Ohana-Levi et al., 2019). At a

given location, grapevine ET_c variability is usually similar over different seasons, aside from specific variations due to particular, distinct meteorological events (e.g. Montoro et al. 2008). Along each season, there is high variability in vine water consumption as the crop growth cycle progresses (Evans et al. 1993, Zhang et al. 2010, López-Urrea et al. 2012, Munitz et al. 2019). Commonly, studies classify within-seasonal sub-periods, such as phenological growth stages or months, for specific definition of intra-seasonal variation in crop-related dynamics (Azevedo et al. 2008, Zhang et al. 2010, López-Urrea et al. 2012). While some studies have dealt with the impact of meteorological and vegetative factors on vine water consumption (López-Urrea et al. 2012, Montoro et al. 2017, Wang et al. 2019), there is still a lack of information on relative importance of each predictor on water consumption.

1.3 Deficit irrigation implementation strategies.

Application of water at a rate lower than the full ET_c requirement is termed ‘deficit irrigation’, in which water reduction is relative to maximum crop consumption (% of ET_c), and is gained by multiplying ET_c by ‘water stress coefficient’ (K_s). There are two main strategies for application of deficit irrigation: Sustained deficit irrigation (SDI) and regulated deficit irrigation (RDI). In the SDI method, an equal proportion of ET_c is applied throughout vine phenological development, resulting in constantly increasing drought stress along the growing season (Ferreeres and Soriano 2007, Chalmers et al. 2010, Williams 2012, Shellie 2014). In contrast, the RDI method introduces alternation of water stress coefficients (K_s) along the course of the irrigation period, imposing differential drought stress levels at diverse periods along the growing season (Fernandes-Silva et al., 2019; Girona et al., 2009; Intrigliolo and Castel, 2010; Romero et al., 2010a; Santesteban et al., 2011). The theory behind the RDI method is that vines respond differently to drought stress conditions at various phenological stages (Girona et al., 2009; Hardie and Considine, 1976; Keller et al., 2008; Munitz et al., 2016; Netzer et al., 2019; Romero et al., 2013). Inducing the precise drought stress level at the adequate phenological stage, enables to achieve balanced vegetative growth, reduced berry size, and results in only a moderate yield loss (Chaves et al., 2010; Fernandes-Silva et al., 2019; Keller et al., 2008; Netzer et al., 2019; Romero et al., 2013). Our previous studies showed that applying high water amounts during stage I of berry development (fruit set to bunch closure) and reducing irrigation level during stages II & III (bunch closure to harvest) resulted in increased vegetative growth (represented by LAI and pruning weight), improved morphological and anatomical parameters (such as trunk diameter, annual ring area and calculated hydraulic conductivity) and high yields combined with improved wine quality (Munitz et al., 2018, 2016; Netzer et al., 2019). There is a lack of available information in the literature on

the effect of water availability during springtime (budbreak to bunch closure) on canopy development and yield parameters. This knowledge is a key factor for developing and implanting a skilled irrigation model for vineyards, based on canopy area and meteorological parameters (Munitz et al., 2019, 2016). A strong indicator of plant water status must be monitored routinely while imposing any skilled deficit irrigation method, in order to validate that the desirable level of drought stress is achieved. Midday stem water potential (Ψ_s) measured by pressure chamber (Scholander et al., 1965) is considered the most reliable and sensitive indicator of vine water status (Acevedo-Opazo et al., 2010; Choné et al., 2001; Munitz et al., 2016; Patakas et al., 2005; Santesteban et al., 2019; Williams and Araujo, 2002). Reference values of Ψ_s are available in the literature, enabling easy interpretation of measured Ψ_s values to the real water status of vines. Picón-Toro (2012) calculated that in grapevines, evapotranspiration is maximal down to Ψ_s of -0.5 to -0.6 MPa, while Ψ_s value of -1.4 MPa is considered as an indicator of severe drought stress (Leeuwen et al., 2009; Munitz et al., 2016; Romero et al., 2010b).

1.4 Functional anatomy effect on water status.

Soil water availability is the main factor affecting vine water status, thus determining the vegetative growth of the vines (Medrano et al., 2003; Munitz et al., 2018, 2016; Padgett-Johnson et al., 2003; Pellegrino et al., 2005; Santesteban et al., 2011), but there are more factors involved. One of the additional factors affecting vine water status is the hydraulic architecture of the xylem tissue – which is responsible for conducting the available water found in the soil- through the trunk, to the canopy of the vines. The xylem tissue conducting elements are dead cells termed tracheids and vessels. Wide diameter vessels are considered to be more hydraulically efficient, but tend to be more vulnerable getting nonfunctional (embolism) during drought stress events (Sperry and Tyree, 1988; Lo Gullo and Salleo, 1991; Hargrave et al., 1994; Cai and Tyree, 2010; Christman et al., 2012; Scoffoni et al., 2016). On the other hand, low diameter vessels are more acclimated to drought stress conditions, but their ability to conduct water to the canopy is limited. The accepted "air-seeding" theory suggests that the increased vulnerability to drought stress of wide vessels is linked to their enlarged total area of intervessel pits. A wide pit area raises the average size of the "rare" largest pore, consequently increasing the risk of air seeding, which in turn will cause the vessel to be nonfunctional (Choat et al., 2003; Wheeler et al., 2005; Jansen et al., 2009; Cai and Tyree, 2010). Different levels of water availability may alter the xylem structure and hydraulic conductivity, those will affect the adaptivity of the vines to later drought stress conditions. Furthermore, the interaction between scion and rootstock of the vine can also effect its anatomical structure (Shtein et al., 2016).

2. Results:

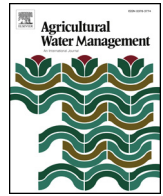
2.1: Chapter 1:

Water consumption, crop coefficient and leaf area relations of a *Vitis vinifera* cv.

“Cabernet Sauvignon” vineyard

Sarel Munitz, Amnon Schwartz and Yishai Netzer

Published in agricultural water management April 2019



Water consumption, crop coefficient and leaf area relations of a *Vitis vinifera* cv. 'Cabernet Sauvignon' vineyard

Sarel Munitz^{b,c}, Amnon Schwartz^c, Yishai Netzer^{a,b,*}

^a Department of Chemical Engineering, Biotechnology and Materials, Ariel University, Ariel 40700, Israel

^b The Eastern Regional Research and Development Center, Ariel 40700, Israel

^c R.H. Smith Institute of Plant Science and Genetics in Agriculture, Faculty of Agriculture, Food and Environment, The Hebrew University of Jerusalem, Rehovot 76100, Israel

ARTICLE INFO

Keywords:

Crop coefficient
Drainage lysimeters
Evapotranspiration
Leaf area index
Vitis vinifera
Water consumption

ABSTRACT

Most cultivated vineyards worldwide are located in semi-arid and arid regions with a limited water supply. Skilled vineyard water management is considered the main tool for controlling vegetative growth and grape quality and for ensuring vineyard sustainability. Imposing an appropriate drought stress at a suitable phenological stage can improve wine quality with almost no yield reduction. A comprehensive irrigation model enabling precise vineyard irrigation should be based on changes in vine water consumption as a function of climate conditions and canopy area.

In 2011, six drainage lysimeters were constructed within a commercial 'Cabernet Sauvignon' vineyard located in the central mountains of Israel. Data were collected during six successive years from 2012 – 2017. The daily vine water consumption, ET_c ($L day^{-1}$), was calculated by subtracting the amount of collected drainage (over a 24 h period) from the amount of applied irrigation during the same time period.

Seasonal water consumption (ET_c) was $715 mm season^{-1}$ on average, while seasonal calculated reference evapotranspiration (ET_o) was $1237 mm season^{-1}$ on average. Maximal crop coefficient (K_c) was $0.8 - 0.9$, meaning that actual water consumption was lower than the calculated reference evapotranspiration. Maximal leaf area index (LAI) was 0.9 to $1.7 m^2 m^{-2}$. The multi-seasonal linear correlation between LAI and K_c was strongly positive and significant.

The robust multiyear relationship between LAI & K_c proves that measuring canopy area of wine grapevines is a reliable approach for estimating their K_c . The LAI to K_c relationship that we have established can be used as a basis for developing a comprehensive irrigation model for wine grapevines that integrates both climatic conditions and canopy area.

1. Introduction

Most cultivated vineyards worldwide are located in semi-arid and arid regions, in which water resources are scarce (Chaves et al. 2007). Precise vineyard water management is essential in those areas to enable sustainable production of grapevines (Ferreles and Evans, 2006; Romero et al., 2010). In wine grape cultivation, water has additional importance, since skilled vineyard water management is considered the main tool for controlling vegetative growth and grape quality and for ensuring vineyard sustainability (Bravdo et al., 1985; Chaves et al., 2010; Fereres and Evans, 2006; Keller et al., 2008; Munitz et al., 2016; Romero et al., 2010). Imposing an appropriate drought stress at a suitable phenological stage can improve wine quality with almost no yield reduction (Girona et al., 2009; Intrigliolo and Castel, 2010; Munitz

et al., 2016; Romero et al., 2013; Williams and Araujo, 2002). Conversely, imposing severe drought stress at inappropriate phenological stages can cause significant yield loss and even a decrease in quality in extreme cases (Bravdo et al., 1985; Chaves et al., 2010; Esteban et al., 2001; Grimes and Williams, 1990; Medrano et al., 2003; Munitz et al., 2016). Continuous severe drought stress will dramatically reduce vegetative growth and shorten the lifespan of the vineyard. A non-stress irrigation strategy is also problematic, since excessive irrigation is costly and may cause vigorous vegetative growth that leads to shading of clusters and reduced quality (Bureau et al., 2000; Chorti et al., 2010; Gao and Cahoon, 1994; Morrison and Noble, 1990). In addition, over-irrigating may increase the need for canopy management practices and also lead to percolation of water below the root zone, leaching nitrates and other chemicals into groundwater reservoirs (Di and Cameron,

* Corresponding author.

E-mail address: ynetzer@gmail.com (Y. Netzer).

<https://doi.org/10.1016/j.agwat.2019.03.051>

Received 8 January 2019; Received in revised form 29 March 2019; Accepted 29 March 2019

Available online 16 April 2019

0378-3774/ © 2019 Elsevier B.V. All rights reserved.

2002; Keller, 2005; Watts et al., 1991). Moreover, excessive irrigation may lead to fungal infection and cluster rotting. A comprehensive irrigation model enabling precise vineyard irrigation should be based on changes in vine water consumption as a function of climate conditions and canopy area (Allen et al., 2006; Netzer et al., 2009).

The term evapotranspiration (ET) refers to the total amount of water that is transpired through the plant canopy and evaporated from the soil surface (Allen et al., 2006). The main factors affecting ET are the canopy area and architecture, evaporative power of the atmosphere (ET_o), stomatal conductance and soil type (Allen et al., 2006). The reference evapotranspiration (ET_o) of a well-watered 12-cm-high grassy surface that fully covers the ground is calculated using meteorological data from the FAO Penman-Monteith equation (Allen et al., 2006; Doorenbos and Pruitt, 1977). Measuring crop evapotranspiration (ET_c) and relating it to reference evapotranspiration (ET_o) is the standard procedure for determination of crop coefficient (K_c) used for skilled irrigation management (Allen et al., 2006; Netzer et al., 2009; Williams et al., 2003). K_c is defined as the ratio between the actual crop evapotranspiration (ET_c) and reference evapotranspiration (ET_o), i.e. $K_c = ET_c/ET_o$. Since biotic and abiotic stress on the crop may affect its water consumption (Allen et al., 1998; Netzer et al., 2014), standard K_c needs to be determined on plants that are disease-free, well-fertilized and achieving full production, grown in a large field under optimum soil water conditions (Allen et al., 2006). K_c varies along the growing season as a function of leaf area index (LAI) dynamics, the solar radiation intercepted by the canopy and the phenological stage of the crop (Allen et al., 2006; Doorenbos and Pruitt, 1977; Evans et al., 1993; Jagtap and Jones, 1989; Netzer et al., 2009; Peacock et al., 1987; Williams et al., 2003). The K_c values of grapevines may vary with agricultural practices and trellising architecture (Williams and Ayars, 2005; Williams and Fidelibus, 2016). K_c has two components – K_{ce} , soil evaporation, and K_{cb} , plant transpiration, i.e. $K_c = K_{ce} + K_{cb}$ (Allen et al., 2006).

Grapevine ET_c has been measured and estimated with different techniques such as microclimatological methods (Carrasco-Benavides et al., 2012; Oliver and Sene, 1992; Yunusa et al., 2004), soil moisture (Van Zyl and Van Huyssteen, 1980; Prior and Grieve, 1987), sap flow sensors (Dragoni et al., 2006; Intrigliolo et al., 2009; Trambouze and Voltz, 2001; Yunusa et al., 1997) and remote sensing (Carrasco-Benavides et al., 2012; Consoli et al., 2006; Lopes et al., 2010; Rozenstein et al., 2018; Vanino et al., 2015). Another technique is lysimetry, which is considered the standard technique for measuring ET_c (Hatfield 1990, Howell et al., 1995, Prueger 1997). Lysimeters have been used to measure the water consumption of many woody agricultural species such as apple (Girona et al., 2011; Mpelasoka et al., 2001; Ro, 2001), almond (García-Tejero et al., 2015; Heilmeyer et al., 2002; Lorite et al., 2012) and olive (Ben-Gal et al., 2010; Deidda et al., 1990). In field-grown grapevines, lysimeters have been used to measure ET_c of a range of cultivars under different climate and soil conditions with drainage (Evans et al., 1993; Netzer et al., 2009; Prior and Grieve, 1987) and weighting methods (López-Urrea et al., 2012; Picón et al., 2012; Williams et al., 2003).

The objectives of the present research are:

- 1) To determine the seasonal curves of ET_c and K_c of mature *Vitis vinifera* cv. Cabernet Sauvignon vines trained to a vertical shoot positioning (VSP) training system grown in a semi-arid region.
- 2) To establish the relationship between LAI and K_c . This relationship forms the basis for developing a comprehensive irrigation model considering climate conditions, canopy area and grapevine specific features.

2. Materials and methods

2.1. Experiment design and vineyard structure

The study was carried out during six successive years from 2012 to

2017 at 'Kida' vineyard, located in the central mountain region of Israel (lat 32.2 °N, long. 35.1 °E), 759 m above sea level. The climate at the experimental site is characterized as semi-arid with predominant winter rainfall of 415 mm, warm days (maximum > 30 °C) and relatively cool nights (minimum < 20 °C) during the growing season. The soil is deep, stone-free terra rossa comprising 36.4% sand, 30.6% silt and 33% clay, with bulk density of 1.25 g cm⁻³. The commercial vineyard was planted during 2007 with *Vitis vinifera* cv. 'Cabernet Sauvignon' vines grafted onto 110 Richter rootstock. During 2011, similar four-year-old vines were replanted, one in each of the six lysimeter tanks. Vine spacing was 3 m between rows and 1.5 m between vines, i.e. 2222 vines per hectare. Lysimeters were constructed while conserving commercial vineyard spacing. Row orientation was east/west and the vines were trained to a VSP training system with two foliage wires. The vines were designed as a bi-lateral cordon and pruned during the winter to 16 spurs (8 per cordon), each comprising two buds. Except for irrigation, lysimeter vines were treated by following the local commercial vineyard growing practices (pest and weed control, canopy management, pruning).

2.2. Lysimeters – structure and maintenance

Each of the six lysimeter tanks was 1.2 m in diameter and 1.3 m in height, for a total volume of 1.47 m³. The lysimeters were filled with local soil (terra rossa) packed to the original bulk density while conserving soil layers. In order to avoid edge row effects, the lysimeters tanks were located in the second row of the vineyard (S1, 2). To ensure drainage of water from the lysimeter tank into the receiver tank, the bottom of each lysimeter tank was packed with 30 cm of rock wool. The lysimeters were buried in the ground with their top surfaces aligned with the soil surface. Two 10-m-long drainage pipe lines (50.8 mm in diameter) connected to the base of each lysimeter tank led to a 2.5-m-deep underground tunnel located 7 m outside the vineyard. For more technical details about lysimeter construction see the supplementary information (S1-3).

Each lysimeter was irrigated separately with a tailor-made, computer-controlled system (Crystal vision, Kibbutz Samar, Israel). To ensure 'optimum soil water conditions' (Allen et al., 2006) the daily irrigation amount exceeded the vines' estimated daily water consumption (ET_o) by 5–10 %. During 2011–2012, daily irrigation began at 6:00 am and lasted for 4–8 hours depending on the amount of water that was applied. During 2013–2017, irrigation was set on an hourly basis, i.e. 24 irrigations pulses per day. The drip line of each lysimeter was connected to a separate, high-precision flowmeter (RS Pro Turbine Flow Meter, RS Components Ltd., Birchington Road, Corby, Northants, NN17 9RS, UK) and equipped with four CNL (compensated non-leakage) 1 L h⁻¹ drip emitters spaced 30 cm apart (Netafim, Israel). The drainage water from each lysimeter was collected separately in a receiver tank (tailor-made 30-L round container) placed on a scale (load cell Model 1042, Vishay, Measurements Group, Rayleigh, NC, USA) and its weight was recorded every 15 min (S3). The drainage tank was automatically emptied each day between 11:46 and 11:59 pm. The data were recorded on the system data logger and downloaded on a daily basis via cellular communication. The drainage scales and the high-precision flowmeters were calibrated manually twice a week.

2.3. Crop and reference evapotranspiration and crop coefficient calculations

The daily vine water consumption - ET_c (L day⁻¹), was calculated by subtracting the amount of water collected as drainage in the receiver tank (over a 24 h period) from the amount of irrigation applied to the lysimeter tank during the same time period. Daily crop evapotranspiration - ET_c (mm day⁻¹) was calculated by multiplying the daily vine water consumption by 0.222 (2222 vines ha⁻¹ divided by 10,000 m²). Daily reference evapotranspiration (ET_o) was calculated

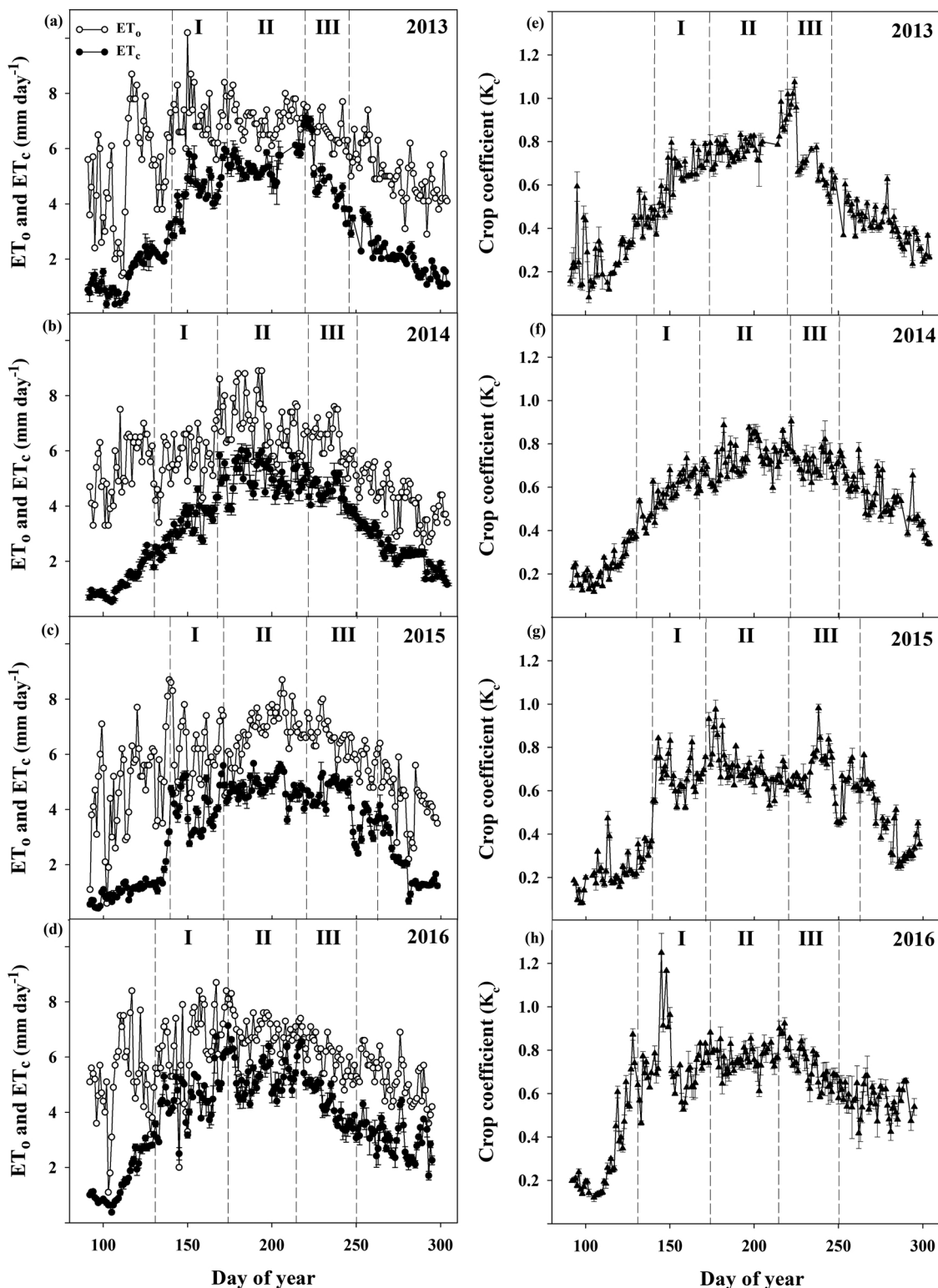


Fig. 1. (a – d) Seasonal curves of measured evapotranspiration (ET_c) and calculated evapotranspiration (ET_0). (e – h) Seasonal curves of crop coefficient (K_c). Phenological stages (I, II, III) are marked by dashed lines. Each point is the mean of six lysimeters. Vertical bar denotes one standard error. Measured from 2013 to 2016 in a 'Cabernet Sauvignon' vineyard, Kida Israel.

according to the Penman-Monteith equation. The daily crop coefficient (K_c) was calculated by dividing the daily crop evapotranspiration ET_c ($mm\ day^{-1}$) by the daily reference evapotranspiration ET_0 ($mm\ day^{-1}$) according to FAO paper no. 56 (Allen et al., 2006, 1998). Growing degree days (GDD) were calculated using the base temperature of $10\ ^\circ C$ as used previously for grapevines by several authors (Evans et al., 1993;

Netzer et al., 2009; Williams et al., 2003). The meteorological data used for calculating ET_0 and GDD were obtained from a meteorological station located 50 m east of the lysimeter installation. The meteorological station was equipped with a data logger (CR1000, Campbell science, Logan, UT, USA), combined temperature and humidity sensor at 2 m height (HMP155, Vaisala, Helsinki, Finland), wind speed and

Table 1
Seasonal ET_c, ET_o and irrigation amounts. 'Cabernet sauvignon', 'Kida' vineyard. 2012–2017.

Irrigation field (mm season ⁻¹)	Irrigation lysimeters(mm season ⁻¹)	ET _o (mm season ⁻¹)	ET _c (mm season ⁻¹)	Year
		1205	780	2012
64	1571	1321	746	2013
53	1326	1203	698	2014
39	1206	1197	671	2015
25	1403	1322	668	2016
33	1270	1173	724	2017
43	1355	1237	715	Average

direction sensor at 10 m height (05103LM, Young, Traverse City, MI, USA), solar radiation sensor at 2 m height (CM11, Kipp & zonen, Delft, The Netherlands) and automatic rainfall gauge (00.15189.002 000, Lambrecht, Gottingen, Germany).

2.4. Leaf Area Index measurements

Leaf Area Index (LAI) of the six lysimeter-grown vines and of the six adjacent field-grown vines was measured weekly during each growing season using a canopy analysis system (SunScan model SS1-R3-BF3; Delta-T Devices, Cambridge, UK). This system, which uses a line quantum sensor array of 64 sensors, sensitive to photosynthetic active radiation (PAR), was operated using the standard protocol recommended by the manufacturer, and all measurements were conducted while the zenith angle was below 30°. Each sample comprised 16 equally-spaced observations (10 cm apart), starting from the center of the row to half the distance between adjacent rows, with the sensor array positioned parallel to the rows. The LAI values obtained by this method were compared with measurements obtained after destructive defoliation of leaves from 39 vines (3 cultivars from 6 sites), using an area meter (model 3100; Li-Cor, Lincoln, Nebraska). The two measurement methods were found to be highly correlated with a linear relationship (S4, R² = 0.922; P < 0.001). For more information about LAI measurements see Netzer et al., (2009).

2.5. Stem water potential measurements

Midday stem water potential (Ψ_s) of the six lysimeter-grown vines and the six adjacent field-grown vines was measured weekly at solar noon (from 12:00 to 14:30). The measurements were conducted using a pressure chamber (model Arimad 3000, MRC, Hulon, Israel) according to the procedures of Boyer (1995). One sunlit, mature, fully-expanded leaf from each vine was double bagged 2 h prior to measurement with plastic bags covered with aluminum foil. The time elapsing between leaf excision and chamber pressurization was less than 15 s. In the field-grown vines, measurements were conducted at the same time, one day before irrigation (irrigation was applied once a week).

2.6. Phenological stages

The growing season was divided into three phenological stages as defined by Kennedy (2002): Stage I - from full bloom to bunch closure, stage II - from bunch closure to veraison (color change to red) and stage III - from veraison to harvest.

2.7. Soil evaporation measurements

On two different occasions during each growing season, the soil surface of three lysimeter tanks was covered with white plastic sheets, while the soil surface of the other three lysimeter tanks remained uncovered. Soil evaporation in all lysimeters was measured for four days.

Subsequently, the covers were transferred to the uncovered lysimeter tanks and the next day another four days of soil evaporation were measured. Soil evaporation was measured by subtracting the average water consumption of the three covered lysimeters from the average water consumption of the three uncovered lysimeters.

2.8. Yield, must composition and pruning mass

Each of the six lysimeter-grown vines and the six adjacent field-grown vines were harvested separately. Total yield was weighed and the number of bunches per vine was recorded. One hundred berries from lysimeter-grown vines and from field-grown vines were randomly sampled, and berry mass was determined. After weighing the berries, they were crushed, and the pH and sugar content (TSS) of the must was measured (after filtration). During the winter period, the pruning mass of each of the lysimeter-grown and field-grown vines was recorded separately.

3. Results

3.1. Crop and reference evapotranspiration and crop coefficient

The seasonal course of crop and reference evapotranspiration was similar across the growing seasons (Fig. 1a-d). Measured crop evapotranspiration, ET_c, was at its minimum at the beginning of the growing season (DOY 90–110, budbreak) with values of 1.0–1.5 mm day⁻¹. From budbreak onwards, a constant increase in ET_c was recorded until the middle of stage II (DOY 190–210), reaching values of 4–6 mm day⁻¹. Subsequently, a constant decline in ET_c was recorded, reaching values of 3–4 mm day⁻¹ at harvest and 1.5–2 mm day⁻¹ in early fall (DOY 280–300, Fig. 1a-d). The seasonal sum of ET_c was similar across the trial years (668–780 mm season⁻¹), averaging 715 mm season⁻¹ (Table 1). The seasonal trend of the calculated reference evapotranspiration (ET_o) was similar to that of ET_c, but of smaller magnitude (higher values during budbreak and fall). ET_o values at budbreak were 3–4 mm day⁻¹, rising to a peak of 6–8 mm day⁻¹ during the middle of stage II (DOY 190–210) and then decreasing to 3.5–4.5 mm day⁻¹ during early fall (DOY 280–300, Fig. 1a-d). The seasonal sum of ET_o was steady over the trial years (1173–1321 mm season⁻¹), averaging 1237 mm season⁻¹ (Table 1). Except for a few occasions (mainly at 2013 DOY 215, Fig. 1a), the calculated ET_o values were higher than the measured ET_c values. The seasonal irrigation amounts applied to lysimeter vines exceeded the sum of ET_o by 9.5%, on average, according to the irrigation plan. Field vines were irrigated with 43 mm season⁻¹ (Table 1) from DOY 180 to DOY 200, an RDI irrigation strategy similar to that being applied to the local commercial vineyards.

The seasonal pattern of K_c was similar across the growing seasons (Fig. 1e-h). K_c was minimal at the beginning of the growing season (DOY 90–110), in the range 0.15–0.25, then increased gradually, reaching maximum values of 0.6–0.8 at the middle of stage II (DOY 190–210). Subsequently, a constant decline in K_c was recorded, with values of 0.35–0.55 in early fall (DOY 280–300, Fig. 1e-h). The effect of hedging and catch wire lifting are reflected in the sharp decline in K_c (Fig. 1e DOY 215, Fig. 1g DOY 240, Fig. 1h DOY 145). A strong second-degree polynomial relationship was found between K_c and DOY (R² = 0.92, Fig. 2a) between crop coefficient and GDD (R² = 0.9, Fig. 2b).

3.2. Grapevine phenology, vegetative growth and water status

The phenological stages occurred at similar dates across the growing seasons (Fig. 3a-h). Full bloom was recorded at DOY 125–135, bunch closure at DOY 160–175, veraison at DOY 210–215 and harvest at DOY 245–260. No pronounced differences were recorded between the phenological development of lysimeter vines and that of adjacent field vines.

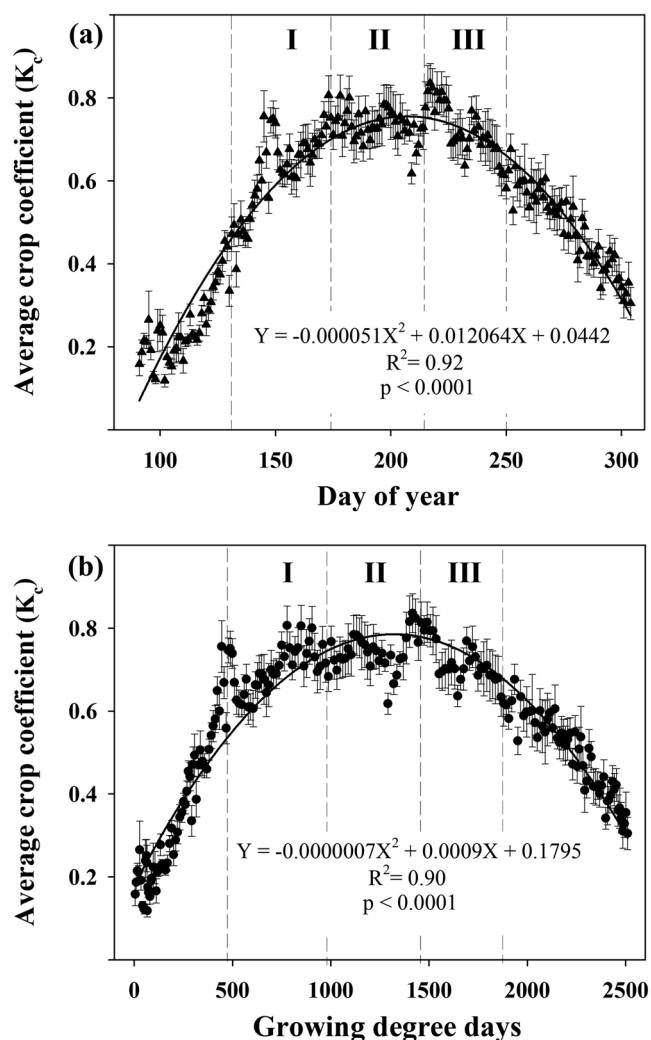


Fig. 2. (a) Development of crop coefficient (K_c) as a function of day of year. (b) Development of crop coefficient (K_c) as a function of growing degree days. Phenological stages (I, II, III) are marked by dashed lines. Each point is the mean of six lysimeters. Vertical bar denotes one standard error. Measured from 2012 to 2017 in a 'Cabernet Sauvignon' vineyard, Kida Israel.

The seasonal course of LAI of lysimeter and field vines was similar along the growing seasons (Fig. 3a-d). A steep increase in LAI was recorded from budbreak until the middle of stage I (DOY 150–165), at which LAI reached a maximum of $0.9 - 1.2 \text{ m}^2 \text{ m}^{-2}$ (exceptionally high values of $1.7 \text{ m}^2 \text{ m}^{-2}$ were measured during 2016). Subsequently, LAI stabilized in both lysimeter and field vines (Fig. 3a-d). The average LAI of lysimeter vines across all trial years exceeded that of field vines by 14%. The canopy hedging effect on lysimeters vines is reflected by a sharp decline in LAI values at 2013 DOY 205–220 (Fig. 3a) and at 2015 DOY 195 (Fig. 3c). The lifting of catch wires caused a 42% reduction in measured LAI in lysimeter vines and a 35% reduction in field vines (DOY 150, Fig. 3d). The average pruning mass of field vines was 52% lower than that of lysimeter vines (Table 2).

Stem water potential (Ψ_s) of lysimeter vines remained steady along the growing season, in the range -0.35 MPa to -0.6 MPa (Fig. 3e-h). On two exceptional occasions (Fig. 3e DOY 128, Fig. 3f DOY 142) Ψ_s of lysimeter vines declined to -0.7 MPa . The Ψ_s of the field vines was high (-0.6 MPa to -0.85 MPa) during spring and then consistently decreased until harvest, reaching -1.4 MPa to -1.6 MPa (Fig. 3e-h). During 2013 and 2015, Ψ_s of field vines resembled that of lysimeter vines until the end of stage I (DOY 170), while in 2014 and 2016 it was -0.2 MPa lower, on average, from the beginning of the growing season

(Fig. 3e-h).

3.3. Yield and must composition

The yield of the lysimeter vines (7.5 kg vine^{-1}) was 50% higher compared to that of field vines (Table 2) nevertheless it was still in the range of yields reported by local commercial vineyards ($5 - 7.8 \text{ kg vine}^{-1}$). Bunch number of lysimeter vines was 8% higher compared to that of field vines, both of them representative of vines in commercial vineyards in the region. Similarly, the berry mass of lysimeter vines was 40% higher than that of field vines (Table 2), while the number of berries per bunch was similar in lysimeter and field vines. While the TSS of field vines was adequate for production of dry red wine (24.4° Brix), the TSS of lysimeter vines was lower (20.1° Brix). Acid level was similar in both lysimeter and field vines, and was adequate for dry red wine production (Table 2).

3.4. Leaf area index and crop coefficient relationship

The multi-seasonal linear correlation between LAI and K_c was strong and significant (Fig. 4, $R^2 = 0.66$, $P < 0.0001$). Since, as described above, there is a rapid increase in leaf area followed by stabilization, most of the LAI values used in the correlation are in the range of $0.8 - 1.3 \text{ m}^2 \text{ m}^{-2}$.

3.5. Evaporation and transpiration relationship

Evaporation remained relatively stable during the growing season ($1.5 - 3.7 \text{ L day}^{-1}$), and the average percent evaporation from total water consumption was 18% (Table 3). At the beginning and end of the growing season (April, October), when evapotranspiration values were low ($7.0 - 7.5 \text{ L day}^{-1}$), the percent evaporation from total water consumption was 21–38% (Table 3), while during the main growing period (May to September), when ET was high ($9.9 - 25.5 \text{ L day}^{-1}$), the percent evaporation from total evapotranspiration was 9–15% (Table 3).

4. Discussion

This experiment was intentionally conducted in a commercial vineyard and avoiding construction of lysimeters in the first border row, even though considerable technical difficulties were expected. This approach reflected our desire to measure water consumption of wine grapevines in a way that most accurately represents water consumption of "real" vines growing in "real" commercial vineyard conditions. Similarly, canopy area and water status were always compared between lysimeter vines and field vines.

4.1. Crop and reference evapotranspiration and crop coefficient

The ET_c of $715 \text{ mm season}^{-1}$ recorded in this study was measured in a region with total ET_o of $1237 \text{ mm season}^{-1}$, thus the seasonal ET_c/ET_o ratio is 0.58. This level of water consumption is in the range reported in the literature for wine grapevines. López-Urrea et al. (2012) reported water consumption (using weighting lysimeters) of $477 \text{ mm season}^{-1}$ for "Tempranillo" grapevines grown under climatic conditions of ET_o of $895 \text{ mm season}^{-1}$ giving an ET_c/ET_o ratio of 0.53. For the same grape cultivar, Picón-Toro et al. (2012) obtained (using weighting lysimeters) water consumption of $834 \text{ mm season}^{-1}$ with ET_o of $1159 \text{ mm season}^{-1}$ giving an ET_c/ET_o ratio of 0.72. It is important to note that both López-Urrea et al. (2012) and Picón-Toro et al. (2012) measured minimal evaporation of dry soil, while in the current study the soil was always completely wet (accepted procedure for drainage lysimeters irrigated at 1-hour intervals). For comparison, Evans et al. (1993) reported seasonal water consumption (using drainage lysimeters) of 387, 431, 432 mm season⁻¹ for "White Riesling", "Chenin Blanc" and "Cabernet Sauvignon". The cumulative seasonal ET_o was

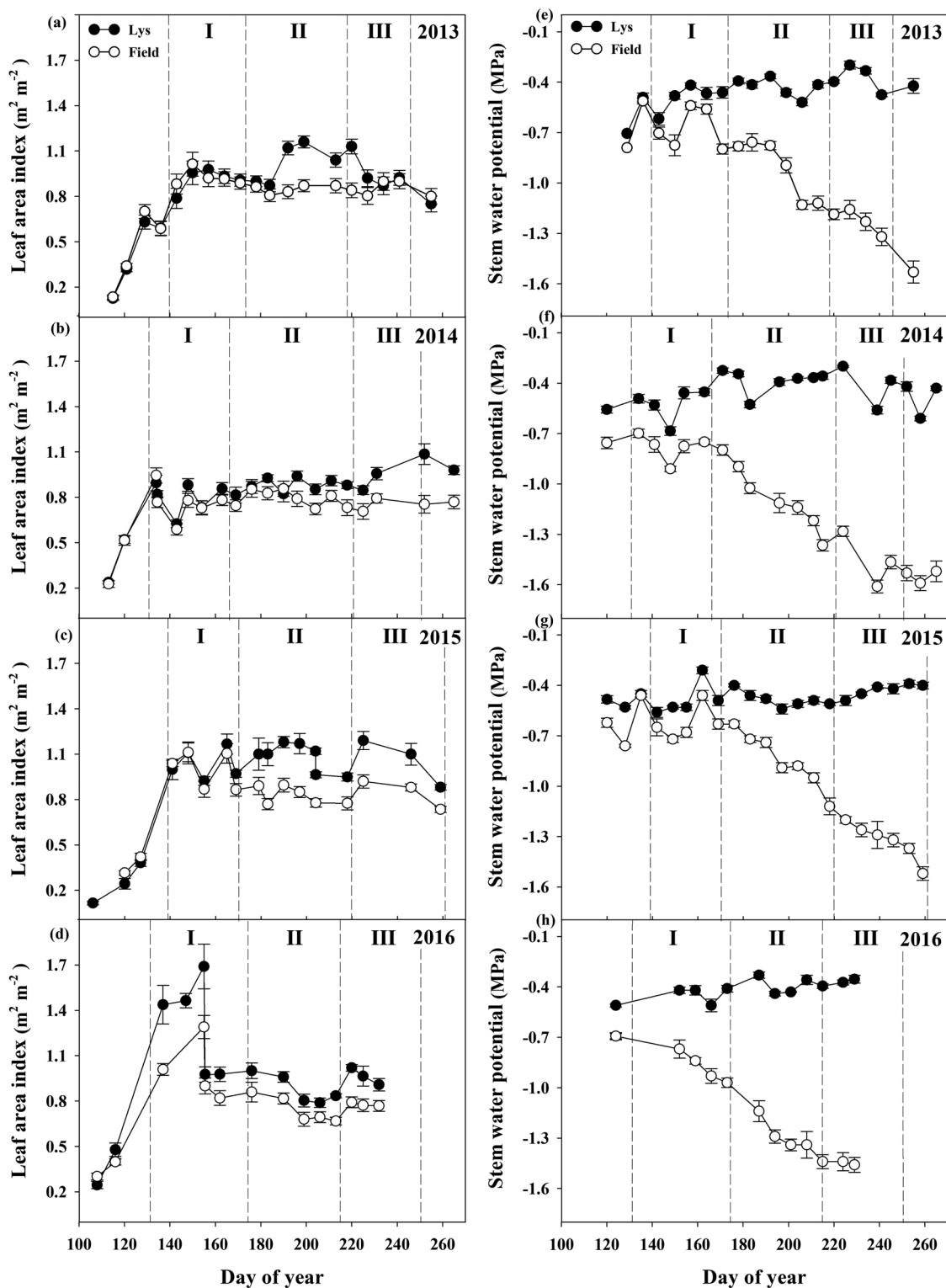


Fig. 3. (a – d) Seasonal curves of canopy development (LAI) in lysimeter vines (closed circles) and field vines (open circles). (e – f) Seasonal curves of midday stem water potential (Ψ_s) in lysimeter vines (closed circles) and field vines (open circles). Phenological stages (I, II, III) are marked by dashed lines. Each point is the mean of six vines. Vertical bar denotes one standard error. Measured from 2013 to 2016 in a 'Cabernet Sauvignon' vineyard, Kida Israel.

908 mm season⁻¹, giving ET_c/ET_0 ratios of 0.43, 0.47 and 0.48, respectively. Based primarily on the results of gravimetric soil sampling, Doorenbos and Pruitt (1977) reported that vineyard ET_c may vary from 650 to 1000 mm year⁻¹.

The maximal K_c values below 1 obtained in this study are reasonable for VSP-trained wine grapevines with limited canopy area. Our

maximal K_c values of 0.8 - 0.9 are in good agreement with other reported K_c values for wine grapevine cultivars. Picón-Toro et al. (2012) reported maximal K_{cb} (dry soil) values around 1 for "Tempranillo" (using weighting lysimeters). Intrigliolo et al. (2009) obtained maximal K_{cb} values of 0.55 for field grown "Riesling" (using a canopy chamber). Dragoni et al. (2006) calculated maximal K_{cb} values of 1–1.2 for field

Table 2
Yield components and pruning mass of lysimetres and field vines, 'Cabernet sauvignon', 'Kida' vineyard, 2013 - 2017.

pH	TSS(°Brix)	Berries(number bunch ⁻¹)	Berry mass(g)	Pruning mass(kg vine ⁻¹)	Bunch(number vine ⁻¹)	Yield(kg vine ⁻¹)
3.30 ± 0.04	20.1 ± 0.8	82.7 ± 7.5	1.67 ± 0.08	2.1 ± 0.05	72.7 ± 10.1	7.5 ± 1.9
3.35 ± 0.05	24.4 ± 0.4	86.4 ± 2.4	1.22 ± 0.13	1.0 ± 0.23	64.1 ± 7.7	5.0 ± 1.5

Values represent means (n = 30, 6 vines * 5 years), except for yield and bunch number that has missing data in 2015.

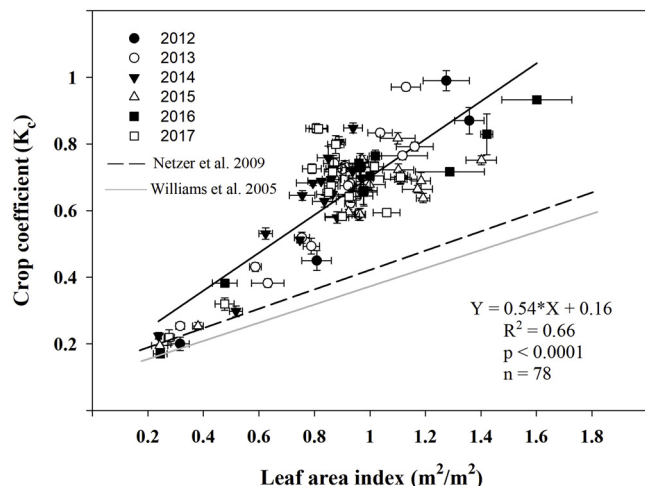


Fig. 4. Relationship between leaf area index (LAI) and crop coefficient (K_c). Each point is the mean LAI of six vines, and the mean K_c of weekly water consumption of six lysimeters. Vertical and horizontal bars denote one standard error. Measured from 2012 to 2017 in a 'Cabernet Sauvignon' vineyard, Kida Israel.

Table 3
Evapotranspiration, transpiration and calculated evaporation. 'Cabernet sauvignon', 'Kida' vineyard. 2012–2017.

E/ ET (%)	Evaporation L (day ⁻¹)	Transpiration- soil surface covered (L day ⁻¹)	Evapotranspiration- soil surface uncovered (L day ⁻¹)	Month
21	1.46 ± 0.21	5.55 ± 0.55	7.01 ± 0.56	Apr
13	1.27 ± 0.18	8.68 ± 0.86	9.95 ± 0.95	May
15	3.72 ± 0.59	21.81 ± 0.69	25.52 ± 0.83	Jun
9	2.40 ± 1.00	22.17 ± 1.49	24.58 ± 0.79	Jul
12	1.87 ± 0.50	13.31 ± 0.77	15.12 ± 0.46	Sep
38	2.88 ± 0.39	4.67 ± 0.41	7.55 ± 0.68	Oct

grown *Vitis labruscana* "Concord" vines, but their canopy was very wide (LAI = 2.5 m² m⁻²). Carrasco-Benavides et al. (2012) calculated (using eddy correlation) maximal K_c values of 0.7 for field-grown "Merlot" vines. Allen and Pereira (2009) calculated maximal K_c values of 0.7 - 0.75 for wine grapes (using a stress factor of 0.7). Higher values of K_c (above 1) have been reported for table grapes with a much wider canopy (LAI = 5 m² m⁻², Netzer et al., 2009). In "Thompson seedless", Williams et al. (2003) found maximal K_c above 1, and in "Superior Seedless", Netzer et al., (2009) and Wang et al. (2018) reported maximal K_c of 1.2 - 1.3.

4.2. Leaf area index and water potential

Grapevine canopy development, occurring mainly from bud break till the end of stage I (bunch closure), as observed in this study, is consistent with our former results (Munitz et al., 2016), and has also been reported by others (Ben-Asher et al., 2006; Edwards and Clingeleffer, 2013; Peacock et al., 1987; Picón-Toro et al., 2012; Romero et al., 2010). Similar LAI values of lysimeter and field vines indicate that the lysimeter vines are well representative of field-grown

vines. The maximal LAI values measured in this study (0.9 to 1.7 m² m⁻²) are in the range of LAI values of field-grown vines trained on a VSP trellis system reported by others, who used different measuring methods. Intrigliolo and Castel (2010) reported LAI of 0.6 to 1.6 m² m⁻² in "Tempranillo" vines. Romero et al. (2010) measured maximal LAI of 2.2 m² m⁻² in "Monastrell" vines. Edwards and Clingeleffer (2013) reported LAI in the range 1.7 to 2.9 m² m⁻² in "Cabernet Sauvignon" vines. Johnson et al. (2003) obtained LAI in the range 0.4 - 2.8 m² m⁻² in four different cultivars ("Chardonnay", "Cabernet Sauvignon", "Cabernet Franc" and "Sangiovese"). Buesa et al. (2017) measured LAI in the range 0.9 to 2.1 m² m⁻² in "Muscat of Alexandria". Intrigliolo et al. (2009) reported maximal LAI of 1.5 m² m⁻² in "Riesling". Picón-Toro et al. (2012) reported LAI values above 4 m² m⁻² in "Tempranillo" VSP-trained vines. These authors stated that the development of their vineyard is greater than in most winemaking areas, but their values are almost double those mentioned above and seem to be a bit overestimated.

The range of Ψ_s values measured in this study in the lysimeter vines (-0.3 to -0.65 MPa), are typical for non-stressed grapevines. Picón-Toro et al. (2012) reported Ψ_s of -0.35 to -0.8 MPa in non-stressed "Tempranillo" vines. Patakas et al. (2005) obtained Ψ_s of -0.4 to -0.6 MPa in non-stressed "Malagouzia" vines. Buesa et al. (2017) measured Ψ_s of -0.4 to -0.8 MPa in non-stressed "Muscat of Alexandria" vines. Picón-Toro et al. (2012) calculated that in grapevines, evapotranspiration is maximal down to Ψ_s of -0.5 to -0.6 MPa, and then begins to decrease. Our lysimeter vines maintained Ψ_s of -0.6 MPa and higher throughout all growing seasons, meaning that their evapotranspiration was kept maximal as required by FAO paper 56 for ET_c calculation (Allen et al., 1998). The seasonal curve of declining Ψ_s measured in this study in the field-grown vines is typical for deficit-irrigated vineyards located in semi-arid regions (Intrigliolo and Castel, 2010; Munitz et al., 2016; Romero et al., 2010). The similar Ψ_s of field-grown vines and lysimeter vines during the spring period demonstrates that lysimeter vines represent field-grown vines during high water availability periods.

4.3. Leaf area index and crop coefficient relationship

The linear correlation between LAI and K_c reported in this study has a steeper slope (higher K_c for similar LAI) than that of relationships reported for table grapes (Netzer et al., 2009; Williams and Ayars, 2005). This is because the VSP trellis systems used for wine grapes receive much greater sun exposure compared to the open gable / overhead trellis systems used for table grapes. As mentioned above, K_c is affected by canopy shape and trellising architecture (Williams and Ayars, 2005; Williams and Fidelibus, 2016). We converted the canopy cover percentage data of López-Urrea et al. (2012) to LAI, using correlations from Williams and Ayars (2005) and converted their basal crop coefficient (K_{cb} , only transpiration) to crop coefficient (K_c , transpiration + evaporation, using their own data). The resulting LAI / K_c relationship resembles our correlation, but with a decline in the slope. The slope of the LAI / K_{cb} relationship obtained for wine grapes by Picón-Toro et al. (2012) is quite similar to slopes reported previously for table grapes (Netzer et al., 2009; Williams and Ayars, 2005). Even after adding 18% to K_{cb} in order to transform it to K_c (18% of average evaporation from total evapotranspiration according to our data in Table 3.) the slope of the Picón-Toro et al. (2012) LAI / K_c relationship is still quite similar to that of table grapes. This shift can be caused by

overestimation of LAI, as mentioned above.

4.4. Evaporation and transpiration relationship

The average percent evaporation from total evapotranspiration measured in this study was 18%. This is in good agreement with evaporation values reported by others in vineyards. In "Tempranillo" vines, Montoro et al. (2016) calculated 26–31% evaporation (using FAO 56 methodology) from total evapotranspiration. In "Cabernet Sauvignon" vines, Kool et al. (2014) reported 8–17% evaporation (using eddy correlation) of total evapotranspiration. In table grapes with a much wider canopy that shades the soil, lower evaporation/evapotranspiration ratios were found. In "Thompson seedless", 13% was reported (Williams and Fidelibus, 2016), and in "Superior Seedless", 7% (Netzer et al., 2009). It is important to note that our evaporation results overestimate vineyard evaporation since our lysimeter soil was always wet; nevertheless, our evaporation results underestimate vineyard evaporation since our lysimeter soil surface is only 1.1 m² while the soil surface per vine in the vineyard is 4.5 m².

5. Conclusions

The water potential and all vegetative parameters measured in this study clearly show that our lysimeter vines demonstrate similar physiological performance to that of field-grown vines under high water availability conditions, and can serve as a reference model vines for field-grown grapevine irrigation. The robust multiyear relationship between LAI and K_c proves that measuring the canopy area of wine grapevines is a reliable approach for estimating their K_c. The LAI to K_c relationship established in this study can be used as a basis for developing a comprehensive irrigation model for wine grapevines that integrates both climatic conditions and canopy area. Measuring canopy area in a vineyard (and converting it to K_c) combined with meteorological data from an adjacent weather station (ET_o) will enable calculation of the ET_c of the vineyard using the equation: ET_c = ET_o * K_c. Applying this irrigation model to wine grapevines, in which a certain drought stress is desirable, requires the incorporation of a stress factor (K_s) as explained by Munitz et al. (2016).

Acknowledgments

This study was sponsored by the Ministry of Science and Technology, Israel and the Ministry of Agriculture and Rural Development, Israel and the Israeli Wine Grape Council.

The authors thank to the dedicated growers: Yoav David, Itamar Weis, Yedidia Spitz and Shlomi Choen. We particularly thank Yechezkel Harroch, Bentzi Green, Yossi Shteren, Alon Katz, Ben hazut, David Kimchi, Gilad gersman, Alon chores, Yedidia sweid, Daniel Mintz and Yair hayat for assisting in the field measurements and to Ziv Charit from Netafim for the help with the vineyard irrigation system. We thank the team of Teperberg Winery, Udi Gliksman, Shiki Rauchberger and Olivier Fratty for their collaboration.

Appendix A. Supplementary data

Supplementary material related to this article can be found, in the online version, at doi:<https://doi.org/10.1016/j.agwat.2019.03.051>.

References

Allen, R.G., Pereira, L.S., 2009. Estimating crop coefficients from fraction of ground cover and height. *Irrig. Sci.* 28, 17–34. <https://doi.org/10.1007/s00271-009-0182-z>.

Allen, R.G., Pereira, L.S., Raes, D., Smith, M., 1998. *Crop Evapotranspiration. Guidelines for Computing Crop Water Requirements*. FAO irrigation and drainage paper no. 56, FAO irrigation and drainage paper no. 56, ROME. <https://doi.org/10.1016/j.eja.2010.12.001>.

Allen, R.G., Pereira, L., Raes, D., 2006. *Crop Evapotranspiration. Guidelines for Computing*

Crop Water Requirements. FAO Irrigation and Drainage Paper, ROME.

Ben-Asher, J., Tsuyuki, I., Bravdo, B.-A., Sagih, M., 2006. Irrigation of grapevines with saline water I. Leaf area index, stomatal conductance, transpiration and photosynthesis. *Agric. Water Manag.* 83, 13–21. <https://doi.org/10.1016/j.agwat.2006.01.002>.

Ben-Gal, A., Kool, D., Agam, N., van Halsema, G.E., Yermiyahu, U., Yafe, A., Presnov, E., Erel, R., Majdop, A., Zipori, I., Segal, E., Rüter, S., Zimmermann, U., Cohen, Y., Alchanatis, V., Dag, A., 2010. Whole-tree water balance and indicators for short-term drought stress in non-bearing "Barnea" olives. *Agric. Water Manag.* 98, 124–133. <https://doi.org/10.1016/j.agwat.2010.08.008>.

Boyer, J., 1995. *Water Relations of Plants and Soils*. Academic Press, San Diego, CA, USA.

Bravdo, B., Hepner, Y., Loinger, C., Cohen, S., Tabacman, H., 1985. Effect of irrigation and crop level on growth, yield and wine quality of Cabernet Sauvignon. *Am. J. Enol. Vitic.* 36, 132–139.

Buesa, I., Pérez, D., Castel, J., Intrigliolo, D., Castel, J., 2017. Effect of deficit irrigation on vine performance and grape composition of *Vitis vinifera* L. Cv. Muscat of Alexandria. *Aust. J. Grape Wine Res.* 23, 251–259. <https://doi.org/10.1111/ajgw.12280>.

Bureau, S.M., Baumes, R.L., Razungles, A.J., 2000. Effects of vine or bunch shading on the glycosylated flavor precursors in grapes of *Vitis vinifera* L. Cv. Syrah. *J. Agric. Food Chem.* 48, 1290–1297. <https://doi.org/10.1021/jf990507x>.

Carrasco-Benavides, M., Ortega-Farías, S., Lagos, L.O., Kleissl, J., Morales, L., Poblete-Echeverría, C., Allen, R.G., 2012. Crop coefficients and actual evapotranspiration of a drip-irrigated Merlot vineyard using multispectral satellite images. *Irrig. Sci.* 30, 485–497. <https://doi.org/10.1007/s00271-012-0379-4>.

Chaves, M., Zarrouk, O., Francisco, R., Costa, J., Santos, T., Regalado, A., Rodrigues, M., Lopes, C., 2010. Grapevine under deficit irrigation: hints from physiological and molecular data. *Ann. Bot.* 105, 661–676. <https://doi.org/10.1093/aob/mcq030>.

Chorti, E., Guidoni, S., Ferrandino, A., Novello, V., 2010. Effect of different cluster sunlight exposure levels on ripening and anthocyanin accumulation in Nebbiolo grapes. *Am. J. Enol. Vitic.* 61, 23–30.

Consoli, S., D'Urso, G., Toscano, A., 2006. Remote sensing to estimate ET-fluxes and the performance of an irrigation district in southern Italy. *Agric. Water Manag.* 81, 295–314. <https://doi.org/10.1016/j.agwat.2005.04.008>.

Deidda, P., Dettori, S., Filigheddu, M., Virdis, F., Pala, M., 1990. Lysimetric analysis of water requirements for young table-olive trees. *Acta Hort.* 286, 259–261.

Di, H., Cameron, K., 2002. Nitrate leaching in temperate agroecosystems: sources, factors and mitigating strategies. *Nutr. Cycl. Agroecosystems* 64, 237–256. <https://doi.org/10.1023/A:1021471531188>.

Doorenbos, J., Pruitt, W., 1977. *Guidelines for predicting crop water requirements*. FAO Irrig. Drain. Pap. 24, 144.

Dragoni, D., Lakso, A.N., Piccioni, R.M., Tarara, J.M., 2006. Transpiration of grapevines in the humid northeastern United States. *Am. J. Enol. Vitic.* 57, 460–467.

Edwards, E.J., Clingeffer, P.R., 2013. Interseasonal effects of regulated deficit irrigation on growth, yield, water use, berry composition and wine attributes of Cabernet Sauvignon grapevines. *Aust. J. Grape Wine Res.* 19, 261–276. <https://doi.org/10.1111/ajgw.12027>.

Esteban, M.A., Villanueva, M.J., Lissarrague, J.R., 2001. Effect of irrigation on changes in the anthocyanin composition of the skin of cv Tempranillo (*Vitis vinifera* L) grape berries during ripening. *J. Sci. Food Agric.* 81, 409–420. [https://doi.org/10.1002/1097-0010\(200103\)81:4<409::AID-JSFA830>3.0.CO;2-H](https://doi.org/10.1002/1097-0010(200103)81:4<409::AID-JSFA830>3.0.CO;2-H).

Evans, R.G., Spayd, S.E., Wample, R.L., Kroeger, M.W., Mahan, M.O., 1993. Water use of *Vitis vinifera* grapes in Washington*. *Agric. Water Manag.* 23, 109–124. [https://doi.org/10.1016/0378-3774\(93\)90035-9](https://doi.org/10.1016/0378-3774(93)90035-9).

Fereres, E., Evans, R.G., 2006. Irrigation of fruit trees and vines: an introduction. *Irrig. Sci.* 24, 55–57. <https://doi.org/10.1007/s00271-005-0019-3>.

Gao, Y., Cahoon, G.A., 1994. Cluster shading effects on fruit quality, fruit skin color, and anthocyanin content and composition in Reliance (*Vitis* hybrid). *Vitis* 33, 205–209.

García-Tejero, I.F., Hernandez, A., Rodriguez, V., Ponce, J., Ramos, V., Muriel, J., Duran-Zuazo, V.H., 2015. Estimating almond crop coefficients and physiological response to water stress in semiarid environments (SW Spain). *J. Agric. Sci. Technol.* 17, 1255–1266.

Girona, J., Marsal, J., Mata, M., Del Campo, J., Basile, B., 2009. Phenological sensitivity of berry growth and composition of Tempranillo grapevines (*Vitis vinifera* L.) to water stress. *Aust. J. Grape Wine Res.* 15, 268–277. <https://doi.org/10.1111/j.1755-0238.2009.00059.x>.

Girona, J., del Campo, J., Mata, M., Lopez, G., Marsal, J., 2011. A comparative study of apple and pear tree water consumption measured with two weighing lysimeters. *Irrig. Sci.* 29, 55–63. <https://doi.org/10.1007/s00271-010-0217-5>.

Grimes, D.W., Williams, L.E., 1990. Irrigation effects on plant water relations and productivity of Thompson seedless grapevines. *Crop Sci.* 30, 255–260. <https://doi.org/10.2135/cropsci1990.0011183X003000020003x>.

Heilmeyer, H., Wartinger, A., Erhard, M., Zimmermann, R., Horn, R., Schulze, E.D., 2002. Soil drought increases leaf and whole-plant water use of *Prunus dulcis* grown in the Negev Desert. *Oecologia* 130, 329–336. <https://doi.org/10.1007/s004420100808>.

Intrigliolo, D.S., Castel, J.R., 2010. Response of grapevine cv. "Tempranillo" to timing and amount of irrigation: water relations, vine growth, yield and berry and wine composition. *Irrig. Sci.* 28, 113–125. <https://doi.org/10.1007/s00271-009-0164-1>.

Intrigliolo, D.S., Lakso, A.N., Piccioni, R.M., 2009. Grapevine cv. 'riesling' water use in the northeastern United States. *Irrig. Sci.* 27, 253–262. <https://doi.org/10.1007/s00271-008-0140-1>.

Jagtap, S., Jones, J., 1989. Stability of crop coefficients under different climate and irrigation Management Practices *. *Irrig. Sci.* 10, 231–244.

Johnson, L., Roczen, D., Youkhana, S., Nemani, R., Bosch, D., 2003. Mapping vineyard leaf area with multispectral satellite imagery. *Comput. Electron. Agric.* 38, 33–44.

Keller, M., 2005. Deficit irrigation and vine mineral nutrition. *Am. J. Enol. Vitic.* 56, 267–283.

- Keller, M., Smithyman, R., Mills, L., 2008. Interactive effects of deficit irrigation and crop load on Cabernet Sauvignon in an arid climate. *Am. J. Enol. Vitic.* 59, 221–234. <https://doi.org/10.5344/ajev.2011.10103>.
- Kool, D., Ben-Gal, A., Agam, N., Šimůnek, J., Heitman, J., Sauer, T., Lazarovitch, N., 2014. Spatial and diurnal below canopy evaporation in a desert vineyard: measurements and modeling. *Water Resour. Res.* 50, 7035–7049. <https://doi.org/10.1002/2014WR015409>.
- Lopes, C., Monteiro, A., Rückert, F.E., Gruber, B., Steinberg, B., Schultz, H.R., Braun, P., Schmid, J., Campos, I., Neale, C.M.U., Calera, A., Balbontín, C., González-Piqueras, J., Ferreyra, R., Sellés, G., Ruiz, R., Sellés, Im., 2010. Assessing satellite-based basal crop coefficients for irrigated grapes (*Vitis vinifera* L.). *Agric. Water Manag.* 98, 45–54. <https://doi.org/10.1016/j.agwat.2010.07.011>.
- López-Urrea, R., Montoro, a., Mañas, F., López-Fuster, P., Fereres, E., 2012. Evapotranspiration and crop coefficients from lysimeter measurements of mature ‘Tempranillo’ wine grapes. *Agric. Water Manag.* 112, 13–20. <https://doi.org/10.1016/j.agwat.2012.05.009>.
- Lorite, I., Santos, C., Testi, L., Fereres, E., 2012. Design and construction of a large weighing lysimeter in an almond orchard. *Span. J. Agric. Res.* 10, 238. <https://doi.org/10.5424/sjar/2012101-243-11>.
- Medrano, H., Escalona, J.M., Cifre, J., Bota, J., Flexas, J., 2003. A ten-year study on the physiology of two Spanish grapevine cultivars under field conditions: effects of water availability on leaf photosynthesis to grape yield and quality. *Funct. Plant Biol.* 30, 607–619. <https://doi.org/10.1071/FP02110>.
- Montoro, A., Mañas, F., López-Urrea, R., 2016. Transpiration and evaporation of grapevine, two components related to irrigation strategy. *Agric. Water Manag.* 177, 193–200. <https://doi.org/10.1016/j.agwat.2016.07.005>.
- Morrison, J.C., Noble, A.C., 1990. The effects of leaf and cluster shading on the composition of Cabernet Sauvignon grapes and on fruit and wine sensory properties. *Am. J. Enol. Vitic.* 41, 193–200.
- Mpelasoka, B., Behboudian, M., Green, S., 2001. Water use, yield and fruit quality of lysimeter-grown apple trees: responses to deficit irrigation and to crop load. *Irrig. Sci.* 20, 107–113. <https://doi.org/10.1007/s002710100041>.
- Munitz, S., Netzer, Y., Schwartz, A., 2016. Sustained and regulated deficit irrigation of field-grown Merlot grapevines. *Aust. J. Grape Wine Res.* 23, 87–94. <https://doi.org/10.1111/ajgw.12241>.
- Netzer, Y., Yao, C., Shenker, M., Bravdo, B.-A., Schwartz, A., 2009. Water use and the development of seasonal crop coefficients for Superior Seedless grapevines trained to an open-gable trellis system. *Irrig. Sci.* 27, 109–120. <https://doi.org/10.1007/s00271-008-0124-1>.
- Netzer, Y., Shenker, M., Schwartz, A., 2014. Effects of irrigation using treated wastewater on table grape vineyards: dynamics of sodium accumulation in soil and plant. *Irrig. Sci.* 32, 283–294. <https://doi.org/10.1007/s00271-014-0430-8>.
- Oliver, H., Sene, K., 1992. Energy and water balances of developing vines. *Agric. For. Meteorol.* 61, 167–185. [https://doi.org/10.1016/0168-1923\(92\)90048-9](https://doi.org/10.1016/0168-1923(92)90048-9).
- Patakas, A., Noitsakis, B., Chouzouri, A., 2005. Optimization of irrigation water use in grapevines using the relationship between transpiration and plant water status. *Agric. Ecosyst. Environ.* 106, 253–259. <https://doi.org/10.1016/j.agee.2004.10.013>.
- Peacock, W., Christensen, L., Andris, H., 1987. Development of a drip irrigation schedule for average canopy vineyards in the San Joaquin valley. *Am. J. Enol. Vitic.* 38, 113–119.
- Picón, J., Uriarte, D., Mancha, L.A., Blanco, J., Prieto, M.H., 2012. Seasonal crop coefficients and relationships with measures of canopy development for “Tempranillo” grapevines in south-western Spain. *Acta Hort.* 235–242.
- Picón-Toro, J., González-Dugo, V., Uriarte, D., Mancha, L., Testi, L., 2012. Effects of canopy size and water stress over the crop coefficient of a “Tempranillo” vineyard in south-western Spain. *Irrig. Sci.* 30, 419–432. <https://doi.org/10.1007/s00271-012-0351-3>.
- Prior, L.D., Grieve, A.M., 1987. Water use and irrigation requirements of grapevine. Sixth Australian Wine Industry Technical Conference. pp. 165–168.
- Ro, H.M., 2001. Water use of young “Fuji” apple trees at three soil moisture regimes in drainage lysimeters. *Agric. Water Manag.* 50, 185–196. [https://doi.org/10.1016/S0378-3774\(01\)00099-3](https://doi.org/10.1016/S0378-3774(01)00099-3).
- Romero, P., Fernández-Fernández, J.I., Martínez-Cutillas, A., 2010. Physiological thresholds for efficient regulated deficit-irrigation management in winegrapes grown under semi-arid conditions. *Am. J. Enol. Vitic.* 61, 300–312.
- Romero, P., Gil-Muñoz, R., del Amor, F.M., Valdés, E., Fernández, J.I., Martínez-Cutillas, A., 2013. Regulated Deficit Irrigation based upon optimum water status improves phenolic composition in Monastrell grapes and wines. *Agric. Water Manag.* 121, 85–101. <https://doi.org/10.1016/j.agwat.2013.01.007>.
- Rozenstein, O., Haymann, N., Kaplan, G., Tanny, J., 2018. Estimating cotton water consumption using a time series of Sentinel-2 imagery. *Agric. Water Manag.* 207, 44–52. <https://doi.org/10.1016/j.agwat.2018.05.017>.
- Trambouze, W., Voltz, M., 2001. Measurement and modelling of the transpiration of a Mediterranean vineyard. *Agric. For. Meteorol.* 107, 153–166. [https://doi.org/10.1016/S0168-1923\(00\)00226-4](https://doi.org/10.1016/S0168-1923(00)00226-4).
- Van Zyl, J., Van Huyssteen, L., 1980. Comparative studies on wine grapes on different trellising systems: I. Consumptive water use South African. *J. Enol. Vitic.* 1, 7–14.
- Vanino, S., Pulighe, G., Nino, P., De Michele, C., Bolognesi, S., D’Urso, G., 2015. Estimation of evapotranspiration and crop coefficients of tendone vineyards using multi-sensor remote sensing data in a mediterranean environment. *Remote Sens. (Basel)* 7, 14708–14730. <https://doi.org/10.3390/rs71114708>.
- Wang, S., Zhu, G., Xia, D., Ma, J., Han, T., Ma, T., Zhang, K., Shang, S., 2018. The characteristics of evapotranspiration and crop coefficients of an irrigated vineyard in arid Northwest China. *Agric. Water Manag.* 212, 388–398. <https://doi.org/10.1016/j.agwat.2018.09.023>.
- Watts, D.G., Hergert, G.W., Nichols, J.T., 1991. Plant and Environment Interactions. Nitrogen Leaching Losses from Irrigated Orchardgrass on Sandy Soils. *J. Environ. Qual.* 20, 355–362.
- Williams, L.E., Araujo, F.J., 2002. Correlations among predawn leaf, midday leaf, and midday stem water potential and their correlations with other measures of soil and plant water status in *Vitis vinifera*. *J. Am. Soc.* 127, 448–454.
- Williams, L.E., Ayars, J.E., 2005. Water use of Thompson Seedless grapevines as affected by the application of gibberellic acid (GA3) and trunk girdling - Practices to increase berry size. *Agric. For. Meteorol.* 129, 85–94. <https://doi.org/10.1016/j.agrformet.2004.11.007>.
- Williams, L.E., Fidelibus, M.W., 2016. Measured and estimated water use and crop coefficients of grapevines trained to overhead trellis systems in California’s San Joaquin Valley. *Irrig. Sci.* <https://doi.org/10.1007/s00271-016-0513-9>.
- Williams, L.E., Phene, C.J., Grimes, D.W., Trout, T.J., 2003. Water use of mature Thompson Seedless grapevines in California. *Irrig. Sci.* 22, 11–18. <https://doi.org/10.1007/s00271-003-0067-5>.
- Yunusa, I.A.M., Walker, R.R., Blackmore, D.H., 1997. Characterisation of water use by Sultana grapevines (*Vitis vinifera* L.) on their own roots or on Ramsey rootstock drip-irrigated with water of different salinities. *Irrig. Sci.* 17, 77–86. <https://doi.org/10.1007/s002710050025>.
- Yunusa, I.A.M., Walker, R.R., Lu, P., 2004. Evapotranspiration components from energy balance, sapflow and microlysimetry techniques for an irrigated vineyard in inland Australia. *Agric. For. Meteorol.* 127, 93–107. <https://doi.org/10.1016/j.agrformet.2004.07.001>.

2.2: Chapter 2:

**Evaluation of Seasonal Water Use and Crop Coefficients for Cabernet Sauvignon
Grapevines As the Base for Skilled regulated irrigation**

Sarel Munitz, Amnon Schwartz and Yishai Netzer

Published in Acta Horticulturae March 2016

Evaluation of seasonal water use and crop coefficients for 'Cabernet Sauvignon' grapevines as the base for skilled regulated deficit irrigation

S. Munitz^{1,2}, A. Schwartz² and Y. Netzer¹

¹The Shomron and Jordan rift Regional, Research and Development, Israel; ²The Robert H. Smith Institute for Plant Sciences and Genetics in Agriculture, Faculty of Agriculture, Food and Environmental Quality Science, The Hebrew University of Jerusalem, Rehovot, Israel.

Abstract

Water consumption of wine grapevines (*Vitis vinifera* 'Cabernet Sauvignon') was measured during three consecutive growing seasons (2012-2014) using 6 drainage lysimeters. The lysimeters (1.5 m³ each) were installed within a two-hectare commercial vineyard in a Mediterranean region in the central mountain region of Israel. Water consumption of the lysimeter-grown vines (ET_c) was measured daily and reference evapotranspiration (ET_o) was calculated from regional meteorological data according to the Penman Monteith equation. Seasonal curves of crop coefficient (K_c) were calculated as $K_c = ET_c/ET_o$. Maximum ET_c values (weekly average) in different seasons ranged from 7.5 to 6.64 mm day⁻¹ and seasonal ET_c (from DOY 99 through DOY 288) ranged from 746 to 780 mm over the growing seasons. Leaf area index (LAI) was measured weekly using the SunScan Canopy Analysis System. Maximum LAI ranged from 1.36 to 1.16 m² m⁻² for the 2012-2013 seasons, the seasonal LAI pattern was quite similar to control vines grown in the surrounding vineyard. A linear curve relating K_c to LAI (R² values ranged from 0.76 to 0.85) is proposed as the basis for efficient irrigation management. Some of the differences in ET_c and K_c values that were observed are different from those obtained in table grapes (Williams et al., 2003; Netzer et al., 2009) and wine grapes (Picón-Toro et al., 2012) is explained by the different canopy size and architecture.

Keywords: *Vitis vinifera*, 'Cabernet Sauvignon', wine grapes, water consumption, water use, evapotranspiration, crop coefficient, drainage lysimeters, leaf area index

INTRODUCTION

Optimizing irrigation in vineyards is an essential need given the increase in water costs and its low availability. Traditionally in table grapes the growers use large amounts of water (compared to wine grapes); this is due to a larger canopy size and wider trellis systems. In table grapes, skilled irrigation is important in order to achieve high yields and big berry size. In wine grapes, exuberant irrigation may lead to high yields with pronounced negative effects on red wine quality. On the other hand, restricted irrigation aimed to improve red wine production may lead to over stressed vines with a limited hydraulic system, poor vegetation, extremely low yields and eventually can cause vine death.

Most of the water absorbed by plant roots returns to the atmosphere by evaporation from the soil and via transpiration from the canopy. The amount of water that actually transpires via the stomata is determined by atmospheric conditions, stomatal conductance, canopy area and canopy architecture. Skilled irrigation aimed to maximize the production potential of the yield and quality. In perennial crops the constant changes in canopy size and atmospheric conditions must be an integral part in water use evaluation. In the current study, vine water use (ET_c) was measured using 6 drainage lysimeters.

The relationship between crop evapotranspiration (ET_c) and reference evapotranspiration (ET_o) is termed the crop coefficient (K_c) (Allen et al., 1998). ET_c and K_c changes during the growing season due to phenological development and agro technical practices. These factors include: canopy management treatments, trellis type, row and inter



row spacing and more factors.

The objective of the present study is to determine seasonal crop water use of *Vitis vinifera* 'Cabernet Sauvignon' (used for red wine production) grown under unlimited water supply in the central mountain region of Israel. A derivative of the objective is to correlate K_c to leaf area index (LAI).

MATERIALS AND METHODS

Experiment site

The vineyard and the lysimeters are located in the central mountain region of Israel (lat 32.2°N, long. 35°E), 759 m above sea level. *Vitis vinifera* 'Cabernet Sauvignon' vines were planted in 2007. The area is considered to be one of the premium quality wine regions in Israel. The climate is characterized as Mediterranean with relatively cool nights. Vine spacing was 1.5 m within rows and 3 m between rows i.e. 2222 vines per hectare. Rows were oriented east-west and the vines were trained to a 2-m-high vertical shoot positioning (VSP) system with 2 foliage wires. Each vine was trained to a bi-lateral cordon pruned to 16 spurs consisting of two buds each.

Lysimeters – structure and maintenance

ET_c of 'Cabernet Sauvignon' wine grapes was determined by the use of 6 drainage lysimeters. Each lysimeter tank was 1.2 m in diameter and 1.3 m deep, for a total volume of 1.50 m³. The lysimeters were filled with local soil (deep, stone free terra rossa composed of 36.4% sand, 30.6% silt and 33% clay) packed to the original bulk density. The lysimeters were installed in the ground with their top surfaces aligned with the soil surface (Figure 1). The lysimeters were located on the second row of the vineyard to avoid border row effect. To ensure drainage of water from the lysimeter into the receiver tank, the bottom of the tank was packed with 30 cm of rock wool. Two drainage pipe lines (50.8 mm in diameter) were connected to the bottom of each lysimeter. Each pipe was ~10 m long leading to an underground tunnel located 7.5 m outside the vineyard (Figure 1).

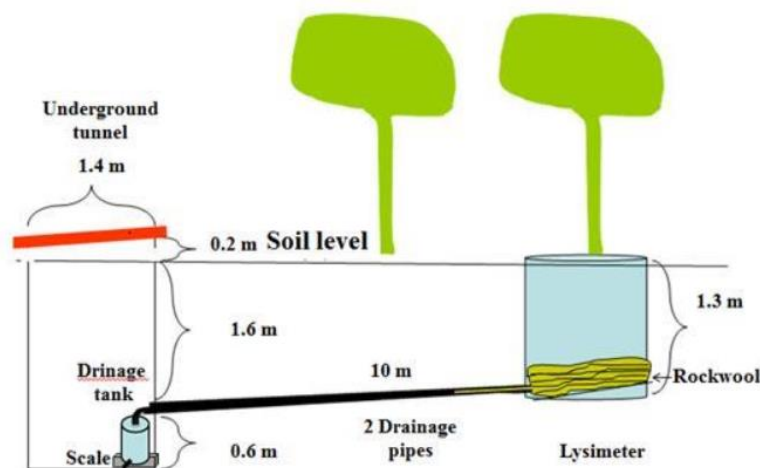


Figure 1. General scheme of one lysimeter (out of six) and the underground tunnel set up.

Each lysimeter was irrigated separately with a tailor-made computer controlled system (Crystal vision, Kibbutz Samr, Israel). The drip line that was connected to a fine water meter was equipped with four 1-L h⁻¹ drip emitters spaced 30 cm apart. Drainage water was collected in receiver tanks located in a 2.5-m deep underground tunnel that was dug parallel to the row containing the lysimeters. The drainage was collected in a tailor-made 30 L round container placed on a scale. The data were recorded on the system data logger and were downloaded on a daily basis via cellular communication. The volume of water that drained through each lysimeter was recorded every 15 min. The drainage tank was automatically

emptied between 23:46 and 23:59. The “drainage scales” and the fine water irrigation meters were calibrated manually twice a week. In order to ensure that the vines were not limited by water availability, the volume of water supplied by irrigation exceeded the vines estimated daily water consumption by 20-30%. During 2012, daily irrigation began at 6:00 am and continued for 4-8 hours depending on the amount of water that was applied. During 2013-2014, irrigation was set on an hourly basis, i.e. 24 irrigation pulses per day.

ET_c, ET_o and K_c calculation

The daily water consumption, ET_c (kg or L), was calculated by subtracting the volume of water collected as drainage (over a 24-h period) from the amount that was supplied by irrigation during the same period. ET_c (mm) was calculated by multiplying the average daily water consumption per vine as measured using the lysimeters, by 0.222 (2222 vines ha⁻¹, inter row spacing 1.5 m, row spacing 3 m). Reference evapotranspiration (ET_o) was calculated according to the Penman-Monteith equation (ASCE method). The meteorological data used for calculating ET_o were obtained from a weather station located 50 m east to the vineyard. The daily crop coefficient (K_c) was calculated by dividing daily ET_c (mm day⁻¹) by daily ET_o (mm day⁻¹) as detailed in Allen et al. (1998).

Leaf area index measurements

Leaf Area Index (LAI) of the lysimeter-grown vines and of 6 reference field-grown vines was measured weekly during the growing seasons, using a canopy analysis system (SunScan model SS1-R3-BF3; Delta-T Devices, Cambridge, UK). The canopy analysis system uses a line quantum sensor array sensitive to photosynthetic active radiation (PAR). The analyzer was operated using the standard protocol recommended by the manufacturer. Each sample consisted of equally spaced observations (10 cm apart), starting from the center of the row to half the distance between adjacent rows with the linear probe positioned parallel to the rows. The LAI values obtained by this method were correlated with destructive harvesting of leaves. After leaf defoliation, leaf area was then measured using an area meter (model 3100; Li-Cor, Lincoln, Nebraska). The leaf area of 27 vines (3 cultivars from 5 sites) was measured at different phenological stages during the growing seasons. Strong linear correlation (R²=0.921, P<0.001, n=27) was observed between Sunscan’s measured LAI and destructively obtained LAI (Figure 2).

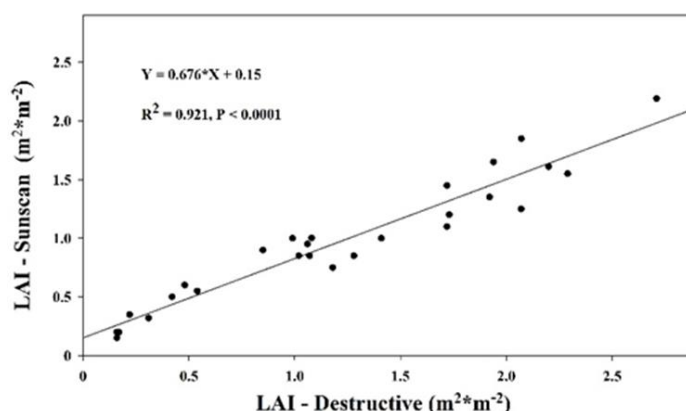


Figure 2. Correlation between Leaf Area Index (LAI) measured destructively (Li-Cor 3100) and Sunscan's estimated non-destructive measurements (n=27).

RESULTS AND DISCUSSION

In the current experiment we monitored the changes in vine water consumption, weather conditions and canopy area. In order to illustrate the changes of one full growing season, only the data of one season will be presented in detail (2013). However, important

canopy to crop coefficient correlations of the three seasons (2012-2014) are also presented. Budbreak in all three seasons occurred in the beginning of April (Table 1), phenological stages were defined according to Kennedy (2002), and the end of stage I was defined as bunch closure. At this point ET_c values were $\sim 1 \text{ mm day}^{-1}$ while ET_o values were $\sim 4 \text{ mm day}^{-1}$ in the season of 2013 (Figure 3). Since LAI reading was minimal, most of the water use was actually water evaporation from fully exposed soil. Accelerated vegetative growth was recorded from DOY 110-150 (Figure 5) and accompanied by an increase in vine water use (ET_c) from $\sim 1 \text{ mm day}^{-1}$ to $\sim 5 \text{ mm day}^{-1}$. Extreme weather conditions occurred between DOY 115-125 (ET_o above 7 mm day^{-1}), having a pronounced effect on the rapid and sharp ET_c increase.

Table 1. Phenological stages, and day of year (DOY) of *Vitis vinifera* ‘Cabernet Sauvignon’ vines, grown in lysimeters 2012-2014.

Year	Bud break (DOY)	Veraison	Harvest
2012	05 April (95)	25 July (206)	7 September (250)
2013	01 April (91)	06 August (218)	29 August (241)
2014 ¹	08 April (98)	10 August (222)	5 September (248)

¹2014 data from April 8 until September 15.

Stage II of berry development begins with bunch closure (mid-June) and ends in full veraison (end of July-beginning of August). At this stage we recorded slight changes in ET_c with close contact to ET_o changes. A sharp increase in ET_c and K_c occurred from DOY 204 until 224 (Figures 3 and 4). This can partially be explained by the exuberant canopy size in the lysimeter-grown vines, compared to the “regular” reference vines grown in the vineyard, as observed from DOY 190 to DOY 220 (Figure 5). The delay between the increase in ET_c and LAI growth can be explained by the fact that it takes about 25 days for young vine leaves to reach full maturity and to attain their maximum values of net assimilation rate and stomatal conductance (Poni et al., 1994). The hedging practice took place in DOY 226 reducing LAI by $\sim 0.2 \text{ m}^2 \text{ m}^{-2}$ followed by an immediate and sharp decrease in ET_c and K_c .

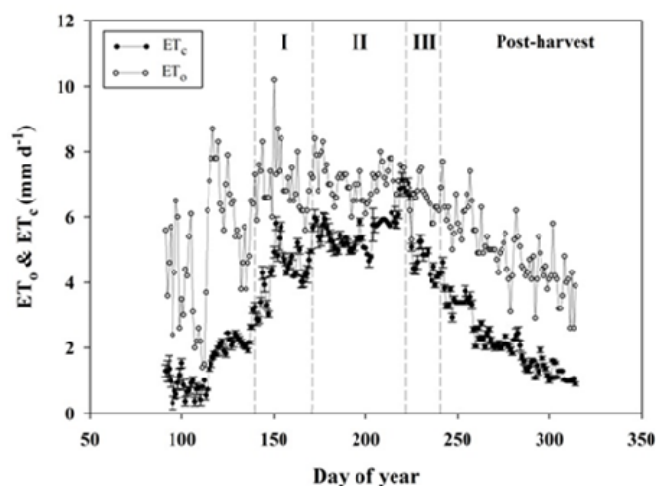


Figure 3. Seasonal curve of vine water use (ET_c) of *Vitis vinifera* ‘Cabernet Sauvignon’ vines as measured using 6 drainage lysimeters, and reference evapotranspiration (ET_o) calculated using the ASCE Penman-Montith equation. Each data point represents a daily average of six vines during 2013 season, Error bars represent \pm standard error. Roman letters indicates the three phenological stages of berry development.

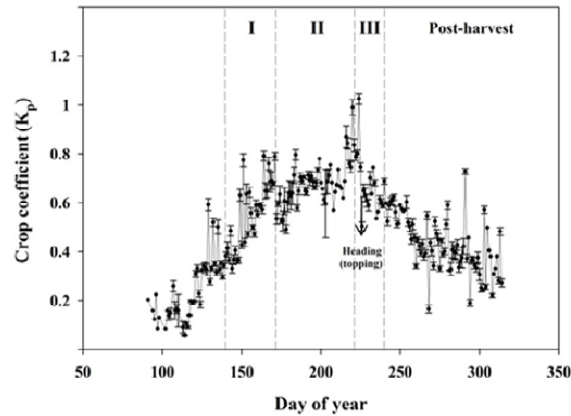


Figure 4. Seasonal curve of crop coefficient (K_c) of *Vitis vinifera* 'Cabernet Sauvignon' vines as calculated during 2013 season. Each data point represents daily average of six vines during 2013 season. Error bars represent \pm standard error. Roman letters indicate the three phenological stages of berry development.

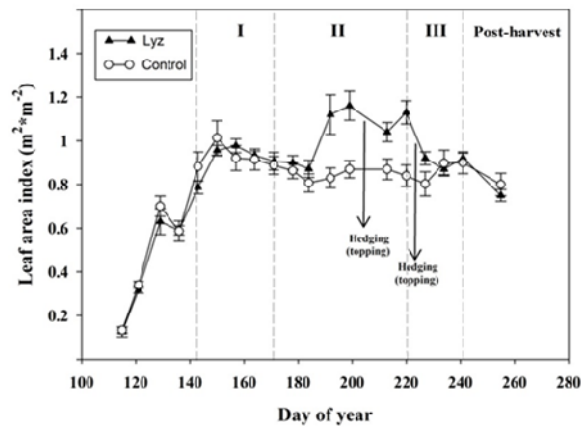


Figure 5. Seasonal course of Leaf Area Index (LAI) of *Vitis vinifera* 'Cabernet Sauvignon' vines as measured during 2013 season. Each data point represents daily average of six lysimeter-grown vines (marked as black triangles) and 6 reference vines (marked as open circles) grown in the vineyard under local agricultural standards. Error bars represent \pm standard error. Roman letters indicate the three phenological stages of berry development.

During stage III (from full veraison to harvest) and post-harvest, ET_o decreased almost linearly due to shortening of the day and temperature reduction, this in turn led to reduced ET_c and K_c results. During stage III LAI was rather stable (Figure 5), while a slight decrease was recorded in DOY 255. No further measurements were made towards the end of the season since zenith angle during mid-day was larger than 30° causing the shade beneath the vines to be too wide. Seasonal K_c curve showed a normal (Gaussian) distribution pattern which increased up until mid-season, and then decreased throughout the rest of the season. This normal distribution pattern is similar to K_c curves recorded in 'Thompson Seedless' table grapes (Williams et al., 2003) and differs from polynomial patterns observed in 'Superior Seedless' table grapes (Netzer et al., 2009). It was explained that in table grapes, post-harvest heavy infection of downy mildew may cause an increase in transpiration and a high K_c (Netzer et al., 2009). In the current research, strictly observed pest management control was maintained during all seasons.

Total seasonal ET_c for 2012-2013 was 763 mm, which is 60.4% of ET_o . Similar

relations were calculated for the 2014 season (Table 2).

Table 2. Seasonal vine water consumption (ET_c) and seasonal evapotranspiration of *Vitis vinifera* 'Cabernet Sauvignon' vines, grown in lysimeters 2012-2014.

Year	ET_c (L vine ⁻¹ season ⁻¹)	ET_c (mm season ⁻¹)	ET_o (mm season ⁻¹)
2012	3510	780	1205
2013	3357	746	1321
2014 ¹	2660	583	992

¹2014 data from April 8 until September 15.

A linear correlation was observed between LAI and K_c (Figure 6). In the first year of the experiment (2012) the R^2 value was 0.761. During this season we increased measurement accuracy by replacing the water meters with more accurate ones, and adopting a calibration protocol for water meters and drainage scales (applied twice a week). The LAI - K_c correlation improved during the 2013-2014 seasons (Figure 6) to R^2 values >0.8. The LAI - K_c correlation observed in the current study are in good agreement with similar correlations made in table grapes (Williams et al., 2003; Netzer et al., 2009). However, some differences in K_c values between table grapes and wine grapes were observed when LAI values ranged between 1-1.4 mm² mm⁻², i.e., higher K_c values in wine grapes compared to table grapes. These differences can be explained by the architecture of the canopies. While table grapes are trained to Geneva double curtain-GDC trellis system (Williams et al., 2003) or Y-shape open gable trellis system (Netzer et al., 2009), in wine grapes the VSP trellis system allows for a more effective canopy being exposed to the atmosphere, thus leading to relatively higher K_c and ET_c values. In Vegas Bajas del Guadiana, Spain, a 5-year study was conducted in order to measure ET_c and K_c of 'Tempranillo' vines while using weighing lysimeters (Picón-Toro et al., 2012). In comparison to our data the ET_c and K_c values were 20-30% higher. This can partly be explained by the planting density that was relatively high (1.2×2.5 m) in the Spanish research. This, along with vigorous vegetative growth and consequently high LAI values was similar to values previously measured in table grapes.

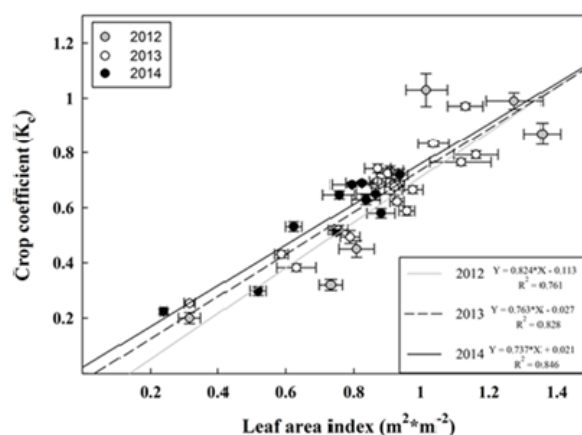


Figure 6. Correlation between Leaf Area Index (LAI) and crop coefficient (K_c) of *Vitis vinifera* 'Cabernet Sauvignon' vines grown in the lysimeters as measured during 2012-2014 seasons. Each K_c data point represents an average value of 7 days, 3-4 days before the LAI measurement and 3-4 days after the measurement. Each data point represents the average LAI value of 6 vines. Vertical and horizontal error bars represent \pm standard errors. The curves were fitted to linear equations. Roman letters indicate the three phenological stages of berry development.

CONCLUSIONS

In the current work a pronounced effect of canopy size and climatic conditions on vine water consumption was observed. The strong and repeatable relations between LAI and K_c that was found by us, is similar to other LAI- K_c relations reported in the literature. Hence, it seems that LAI- K_c relation is reliable and adequate for the use as the base of skilled regulated irrigation regime.

ACKNOWLEDGEMENTS

This project was funded by the Israeli Ministry of Science, and by the Israeli wine council. The authors would like to thank Mr. Giora Gez, Mr. Yoav David and Mr. Itamar Weiss for their assistance in the vineyard, and to Mr. Alex Gimburg, Mr. Yakov Hening and Mr. Benzi Green for their technical help in operating the lysimeters. We would also like to thank Mr. Shlomi Cohen the winegrower and Teperbrg winery for allowing us to use their vineyard for conducting this research.

Literature cited

Allen, R., Pereira, L., Raes, D. and Smith, M. (1998) Crop evapotranspiration. Guidelines for computing crop water requirements. FAO irrigation and drainage paper no. 56.

Kennedy, J. (2002). Understanding grape berry development. Pract. Winer. Vineyard.

Netzer, Y., Yao, C., Shenker, M., Bravdo, B.-A., and Schwartz, A. (2009). Water use and the development of seasonal crop coefficients for Superior Seedless grapevines trained to an open-gable trellis system. *Irrig. Sci.* 27 (2), 109–120 <http://dx.doi.org/10.1007/s00271-008-0124-1>.

Picón-Toro, J., González-Dugo, V., Uriarte, D., Mancha, L.A., and Testi, L. (2012). Effects of canopy size and water stress over the crop coefficient of a "Tempranillo" vineyard in south-western Spain. *Irrig. Sci.* 30 (5), 419–432 <http://dx.doi.org/10.1007/s00271-012-0351-3>.

Poni, S., Intrieri, C., and Silvestroni, O. (1994). Interactions of leaf age, fruiting, and exogenous cytokinins in Sangiovese grapevines under non-irrigated conditions. I. Gas exchange. *Am. J. Enol. Vitic.* 45, 71–78.

Williams, L., Phene, C., Grimes, D., and Trout, T. (2003). Water use of mature Thompson Seedless grapevines in California. *Irrig. Sci.* 22, 11–18.



2.3: Chapter 3:

The effect of irrigation initiation timing on vegetative growth, physiological parameters and yield components in 'Cabernet Sauvignon' grapevines

Unpublished

Sarel Munitz, Amnon Schwartz and Yishai Netzer

The effect of irrigation initiation timing on vegetative growth, physiology and yield parameters in 'Cabernet Sauvignon' grapevines

Sarel Munitz^{b,c}, Amnon Schwartz^b and Yishai Netzer^{a,c}

^aDepartment of Chemical engineering, Biotechnology and Materials, Ariel 40700 University.

^bR.H. Smith Institute of Plant Science and Genetics in Agriculture, Faculty of Agriculture, Food and Environment, The Hebrew University of Jerusalem, Rehovot 76100, Israel.

^cThe Eastern Regional Research and Development Center, Ariel 40700, Israel. Science Park, 40700, Ariel, Israel

Corresponding author: Yishai Netzer, email: YNetzer@gmail.com

ABSTRACT

The effect of irrigation initiation timing along the growing season on *Vitis vinifera* 'Cabernet Sauvignon' vines was investigated during five successive years. Five irrigation initiation thresholds based on measurements of midday stem water potential (SWP) were examined: at Budbreak, -0.6MPa, -0.8MPa, -1.0MPa and -1.2MPa. Midday SWP, gas exchange parameters (stomatal conductance & net assimilation rate) and leaf area index (LAI) were measured weekly in order to determine the vegetative and physiological effect of drought stress on the vines. Four electronic trunk dendrometers were installed on vines in each treatment (20 in total). During harvest, 12 vines per replicate (48 per treatment) were separately harvested, the total yield was weighted and the number of clusters per vine were recorded. During winter period, number of shoots per vine and pruning weight of 12 vines per replicate were recorded separately. Our results

show that vines in the early irrigation treatments (budbreak, -0.6MPa) displayed values of improved SWP and gas exchange parameters (g_s & A_n , respectively) accompanied by vigorous vegetative growth and high yields. The raise in the yield level was derived from enlarged berry size and increased number of clusters. Contrarily, vines in the late irrigation treatments (-1.0MPa, -1.2MPa) had low SWP values and gas exchange parameters combined with depressed vegetative growth and reduced yield. The depression effect on late irrigation vines was accumulative and was more pronounced as trial years advanced.

Our results emphasize the crucial role of water availability during springtime (vegetative growth period) on vines development, physiological performance and yield parameters.

KEYWORDS: *Vitis vinifera*; irrigation initiation; drought stress thresholds; water potential; vegetative growth.

1. Introduction

Most cultivated vineyards worldwide are located in semi-arid and arid regions, in which drought stress is prevalent during the growing season (Beis and Patakas, 2015; Chaves et al., 2007; Schultz, 2016). In those areas water shortage is likely the most dominant environmental constraint (Chaves et al., 2010; Cifre et al., 2005; Patakas et al., 2005; Schultz, 2016). In wine grapevine cultivation water has additional importance, since skilled vineyard water management is considered the main tool for controlling vegetative growth and guaranteeing grape quality (Bravdo et al., 1985; Chaves et al., 2010; Fereres and Evans, 2006; Keller et al., 2008; Munitz et al., 2016; Patakas et al., 2005; Romero et al., 2010b). At those environmental conditions skilled irrigation methods have enormous potential to maximize crop productivity without damaging vineyard sustainability, and also may save water which is a scarce resource (Beis and Patakas, 2015; Cifre et al., 2005; Munitz et al., 2019). Calculation of vines evapotranspiration is the base for development of any irrigation method.

The term evapotranspiration (ET) refers to the total amount of water that is evaporated from the soil surface and transpired through the plant canopy (Allen et al., 2006). The reference evapotranspiration (ET_o) of a well-watered 12 cm high grassy surface that fully covers the ground, is calculated from the FAO Penman-Monteith equation using meteorological data (Allen et al., 2006; Doorenbos and Pruitt, 1977). Crop evapotranspiration (ET_c) is the actual evapotranspiration of a specific crop at standard conditions (Allen et al., 1998; Munitz et al., 2019), and the ‘crop coefficient’ (K_c) is the relationship between these two parameters (ET_c / ET_o) (Allen et al., 1998). Seasonal curves of K_c for wine grapes have been calculated (Evans et al., 1993; López-Urrea et al., 2012; Munitz et al., 2019; Picón-Toro et al., 2012).

Application of water at lower amounts than the full ET_c requirement is termed ‘deficit irrigation’ (Beis and Patakas, 2015; Chaves et al., 2007; Fernandes-Silva et al., 2019). Imposing deficit irrigation is achieved by water reduction relative to the maximum crop consumption (% of ET_c), using ‘water stress coefficient’ (K_s , Allen et al., 1998; Munitz et al., 2019). In cultivation of wine vineyards, deficit irrigation is considered a common and necessary agricultural practice for inducing drought stress that is a key factor for determining wine quality (Bravdo et al., 1985; Chaves et al., 2007; Matthews et al., 1990; Munitz et al., 2016; Roby et al., 2004). In semi-arid regions such as Israel, the degree of deficit irrigation to be imposed in the vineyard depends considerably on the wine standard planned to be produced from the grapes (Munitz et al., 2016). In general, severer deficit irrigation regime is imposed at certain phenological stages for production of high-quality wines, since drought stress increases sugar accumulation and color and

aroma intensity in berries. Drought stress is considered to increase grape quality by two main mechanisms. One is increased skin-to-pulp ratio (that results from decreased berry size), raising the concentration of phenolic substances and anthocyanins that can be extracted from berries skin (Bravdo et al., 1985; Keller et al., 2008; Kennedy et al., 2002). The other is an enhancing effect on the biosynthesis of precursors in the metabolic pathway of color and aroma molecules (Castellarin et al., 2007; Chaves et al., 2010; Ollé et al., 2011; Zarrouk et al., 2012).

Inducing the proper drought stress at the suitable phenological stage may raise wine quality with almost no yield reduction (Girona et al., 2009; Intrigliolo and Castel, 2010; Munitz et al., 2016; Romero et al., 2013; Williams and Araujo, 2002). Contrariwise, inducing extreme drought stress at an unsuitable phenological stage, may result in significant yield reduction and even a decrease in sugar accumulation and color and aroma intensity in berries (Bravdo et al., 1985; Chaves et al., 2010; Cifre et al., 2005; Esteban et al., 2001; Grimes and Williams, 1990; Keller et al., 2008; Medrano et al., 2003). In the long term, prolonged severe drought stress conditions can lead to reduction in vegetative growth and may shorten the lifespan of the vineyard.

There are several methods for applying deficit irrigation, one of which is termed 'Regulated Deficit Irrigation' (RDI). The RDI method introduces alternation of water stress coefficients along the course of the irrigation period, imposing differential drought stress levels at certain periods along the growing season (Fernandes-Silva et al., 2019; Girona et al., 2009; Intrigliolo and Castel, 2010; Romero et al., 2010a; Santesteban et al., 2011). The theory behind RDI method is that vines respond differently to drought stress conditions at various phenological stages (Girona et al., 2009; Hardie and Considine, 1976; Keller et al., 2008; Munitz et al., 2016; Netzer et al., 2019; Romero et al., 2013). Inducing the precise drought stress level at the adequate phenological stage enables to achieve balanced vegetative growth, reduced berry size, and only a moderate yield loss (Chaves et al., 2010; Fernandes-Silva et al., 2019; Keller et al., 2008; Netzer et al., 2019; Romero et al., 2013).

Our previous studies showed that applying high water amounts during stage I of berry development and reducing irrigation level during stages II & III resulted in increased vegetative growth (represented by LAI and pruning weight), improved morphological and anatomical parameters (such as trunk diameter, annual ring area and calculated hydraulic conductivity) and high yields combined with improved wine quality (Munitz et al., 2018, 2016; Netzer et al., 2019).

In current study we examined a method for irrigation initiation timing in order to achieve better understanding of the effect of water availability during springtime (budbreak to bunch closure) on

canopy development and yield parameters. This is important, since there is a lack of available information in the literature in this subject. This knowledge is a key factor for developing a skilled irrigation model for vineyards, based on canopy area and meteorological parameters (Munitz et al., 2019, 2016). The physiological hypothesis of current research is that high water availability during vegetative growth period (spring time) will enhance vegetative growth and increase yield level, while withholding irrigation until drought stress levels will depress vegetative growth and reduce yield level. Since water availability is the main factor determining vegetative growth of vines (Medrano et al., 2003; Munitz et al., 2018, 2016; Padgett-Johnson et al., 2003; Pellegrino et al., 2005; Santesteban et al., 2011), the irrigation initiation thresholds were set according to different levels of midday SWP (-0.6, -0.8, -1.0, -1.2 MPa).

2. Materials and methods

2.1 Experimental site

This study was carried out during 5 successive years from 2014 to 2018 at 'Kida' vineyard, located in the central mountain region of Israel (lat 32.2°N, long. 35.1°E), at 759 m above sea level. The commercial vineyard was planted in 2007 with *Vitis vinifera* cv. 'Cabernet Sauvignon' vines grafted on 110 Richter (*V. berlandieri* × *V. rupestris*) and trained onto a two-wire vertical trellis system (VSP). The vines were designed as a bilateral cordon and pruned during winter time to 16 spurs (8 per arm), each comprised of two buds. Row direction was north-west/south-east (115°) and vine and row spacing were 1.5 and 3 m, respectively (i.e 2222 vines per hectare). The soil is deep stone free 'terra rossa' composed of 36.4% sand, 30.6% silt and 33% clay with bulk density of 1.25 g cm⁻³. The climate at the experimental site is characterized as semi-arid Mediterranean with predominant winter rainfall of 416 mm (84% winter rainfall, Table 1), with dry summers, warm days (maximum > 30°C) and relatively cool nights (minimum < 20°C) during growing season. Aside from irrigation, experimental vines were treated by following local commercial vineyard growing practices (pest control, green canopy treatments, and winter pruning). Meteorological data were obtained from an automatic weather station located inside the vineyard, for detailed specification of station sensors see Munitz et al. (2019).

2.2 Experimental design

The experimental layout was a randomized complete block design with five irrigation treatments, each replicated four times, where each block consisted of three rows (one data collection row and two border rows). In order to get optimum spatial balance of the treatment's arrangement within the replicates, treatments design was planned as suggested by van Es et al., (2007). Each replicate

plot comprised of 16 vines with the outer two vines from each side being buffer vines and the inner 12 vines being measurement vines used for yield parameters and pruning weight (a total of 240 measurement vines, i.e. 12 vines * 4 replicates * 5 treatment). At each plot, 3 grapevines, with homogeneous trunk diameter and average canopy size, were marked and used for physiological and vegetative measurements. A drip irrigation system with one line per row and in-line pressure-compensated 2.4 L h⁻¹ UniRam drippers was employed, with 0.5 m spacing between drippers (Netafim Ltd., Hatzerim, Israel). Irrigation control unit (Talgil Computing & Control Ltd., Haifa, Israel) was used to separately irrigate each of the five irrigation treatments. Irrigation was applied once a week to all treatments (similar to local agricultural practice) .

2.3 Phenological stages

The growing season was divided (following Kennedy et al., 2002) into three phenological stages according to berry development: stage I from bloom to bunch closure, stage II from bunch closure to veraison and stage III from veraison to harvest.

2.4 Irrigation treatments, calculation of evapotranspiration and stress factors

Irrigation initiation of each treatment was set according to its Ψ_s threshold (with exception of the first treatment), and then continued consecutively until the end of the growing season (Fig. 1). The irrigation in the first treatment started on a at budbreak, while in the other four treatments irrigation initiation started at values of midday stem water potential (Ψ_s) measurements of: -0.6 MPa, -0.8 MPa, -1.0 MPa and -1.2 MPa. Irrigation amounts of all irrigation treatments were calculated as percentage of ET_c . Evapotranspiration (ET_c) was calculated according to the following equation: $ET_c = ET_o * K_c$, where ET_o was calculated according to the Penman-Monteith equation (Allen et al., 1998; Munitz et al., 2016) using the data obtained by an automatic weather station. The K_c values were calculated from the LAI- K_c relationship, as previously described by Netzer et al., (2009): $K_c = 0.028 * LAI^2 + 0.355 * LAI + 0.077$. During stage I irrigated vines received 40% of ET_c , 15% of ET_c at stage II and 10% during stage III ($K_s = 0.4, 0.15, 0.1$ respectively).

2.5 Leaf area index measurements

Leaf area of 12 representative vines per treatment (3 vines per replicate * 4 replicates) was determined over the growing season once a week, using a non-destructive Sunscan canopy analysis system (model SS1- R3-BF3, Delta-T Devices, Cambridge, UK). The Sunscan system was operated using the standard protocol recommended by the manufacturer, and all measurements were conducted while the zenith angle was below 30°. Underneath each vine 8

radiation measurements were taken (spaced every 20 cm), covering the soil surface completely under a given vine (for more details, see Netzer et al., 2009). The LAI values obtained by this method were compared with measurements obtained after destructive defoliation of leaves from 39 vines (3 cultivars from 6 sites), using an area meter (model 3100; Li-Cor, Lincoln, Nebraska). The two measurement methods were found to be highly correlated with a linear relationship ($R^2 = 0.92$; $P < 0.001$, Munitz et al., 2019).

2.6 Midday stem water potential measurements

Midday stem water potential (Ψ_s) was measured weekly (before irrigation) at solar noon (12:30 – 15:00), using a pressure chamber (model Arimad 3000, MRC, Hulon, Israel) according to the procedures of Boyer et al. (1995). The calibration of the pressure chamber was validated each month using high precision external pressure sensor (Baroli 02, BD sensors, Thierstein, Germany). Twelve sunlit, mature and healthy, fully expanded leaves from each treatment (3 leaves from 3 vines per replicate * 4 replicates, one leaf per vine) were bagged 2 h prior to measurement with plastic bags covered with aluminum foil. The time elapsed between leaf excision and chamber pressurization was less than 20 s.

2.7 Gas exchange measurements

Leaf net CO₂ assimilation rate (A_n) and stomatal conductance (g_s) were measured weekly (before irrigation) at solar noon for 16 leaves per treatment (4 leaves from 4 vines per replicate * 4 replicates, one leaf per vine), using a portable infrared gas analyzer LI-6400 (Li-Cor, Lincoln, NE, USA), equipped with 6 cm² chamber. Similar leaves used for Ψ_s were chosen for gas exchange measurements. All measurements were conducted at ambient humidity and temperature, light intensity of 1000 PPFD (6400–02B led light source, 10% blue), reference CO₂ concentration of 400 $\mu\text{mol mol}^{-1}$ and an air flow rate of 500 $\mu\text{mol s}^{-1}$. Before each day of measuring, full calibration and validation procedure recommended by manufacture were conducted.

2.8 Stem width variation measurements

Before the beginning of the growing season of 2014, four electronic dendrometers (Model DE-1M, Phytech, Israel) were installed in each treatment (20 in total). Due to cable length limitation, two pairs of dendrometers (for two adjacent vines) in two replicates per treatment were installed. The dendrometers (LVDT) automatically recorded each hour the radius of the vine trunks at a height of 40 cm above ground. Data was saved in a data logger, and transmitted each 6 hours to the Phytech website.

2.9 Berry mass measurements

At several occasions during the growing season, berry mass of vines in different irrigation treatments was determined. 100 berries per treatment (25 per replicate * 4 replicate) were randomly picked and weighted.

2.10 Yield measurements

A week before harvest, 36 bunches per plot (3 bunches per vine) were randomly picked and hand-crushed for determination of must's total soluble solids and pH. Before crushing, the number of shriveled berries in 24 clusters per treatment were counted (6 per replicate). Each plot was harvested when the fruit total soluble solids (TSS) reached 23.5° Brix. Each of all 12 measurement vines within each plot were harvested separately, the total yield was weighted and the number of clusters per vine were recorded. An assessment of the average number of berries per cluster was calculated by dividing the yield by bunch number and berry mass. During winter period, the number of shoots per vine and pruning weight of all 12 measurement vines within each plot were recorded separately. An estimate of shoot mass was calculated by dividing pruning mass by the number of shoots.

2.11 Statistical analyses

The analyses included calculations of the means of samples within each replicated plot (4 plots per treatment). Additionally, Analysis of variance (ANOVA) was carried out, followed by Tukey post-hoc test (JMP Pro 14 Statistical Software; SAS Institute Inc., Cary, NC, USA) to determine the statistical significance of differences between treatment means at $\alpha = 0.05$.

3. Results

3.1 Cumulative evapotranspiration, rainfall, phenological development and water amounts

During the trial period (2014 - 2018) the values of seasonal cumulative reference evapotranspiration (ET_0) were quite stable across seasons (Table 1), with a maximal difference of 149 mm season⁻¹. Rainfall amounts varied considerably during the trial years, with 2015 experiencing the highest amounts of precipitation, 509 mm, and 2017 having the lowest rainfall amounts with 341 mm. The average annual rainfall, 416 mm, is typical for semi-arid regions. The proportion of spring rainfall from total annual rainfall was 4 – 27% over trial years (Table 1). Phenological development did not show any pronounced differences over the time course of the experiment (Fig. 2,3). Budbreak occurred from DOY 88 to 103, full bloom from DOY 128 to 139, bunch closure from DOY 161 to 173, veraison from DOY 205 to 224 and harvest from DOY 245 to 262. Due to the dynamic irrigation model implemented in this study, the amount of water

applied to vines in different irrigation treatments diverged weekly during the growing season, according to variation in canopy size, reference evapotranspiration and the change of stress factors (Fig. 1). Average daily water amounts applied to irrigated treatments were 1.3, 0.45, and 0.4 mm day⁻¹ during stages I, II and III, respectively (Fig. 1). Vines in the budbreak treatment, in which irrigation was applied throughout the entire growing season, received in average 39 mm from budbreak to full bloom, and 39, 23, 18 mm during stages I, II, III in comparison (Table 2). The vines in the -0.6 MPa treatment, received in average 21 mm from budbreak to full bloom, followed by similar water amounts as the budbreak vines. Irrigation to the vines of the -0.8 MPa treatment initiated only during stage I (20 mm in average), after which they received similar water amounts as the budbreak vines (Table 2). Vines of the -1.0 MPa & -1.2 MPa treatments received minimal irrigation during stage I (average of 2.1, 0.7 mm respectively), 16.8 & 9.8 mm (in average, respectively) during stage II, and from then on they received similar water amounts as the budbreak vines (Table 2). During the postharvest period irrigation applied to vines in all treatments was similar, with 10.5 to 11.2 mm.

3.2 stem water potential and vegetative growth.

The seasonal trend of Ψ_s in vines of all irrigation treatments was similar during all seasons; Ψ_s decreased continuously from spring period until the end of the growing season (Fig. 2a-e). During 2014 & 2016 (Fig. 2a,c) there was a stabilization in Ψ_s values during stage III, while in 2015, 2017 & 2018 (Fig. 2b,d,e) Ψ_s values continued to decline until the end of the growing season. From the middle of stage I (DOY 140 - 155) vines that received different irrigation treatments differed significantly in their Ψ_s values, whereas in 2015 they started to differ only at the beginning of stage II (DOY 180). Vines in the -0.6 MPa treatment reached their threshold in quite similar dates over the trail years, at the early period of the growing season before stage I (DOY 113 - 127). Vines in the -0.8 MPa irrigation treatment also exhibited stable pattern and reached their threshold at the middle/end of stage I (DOY 145 - 159), except for 2015 in which the -0.8 MPa threshold was crossed only in DOY 189 (Fig. 1a-e). In the late irrigation treatments, wide variation in irrigation initiation was recorded. Vines in the -1.0 MPa reached their threshold at the end of stage I in 2017 & 2018 (DOY 158 - 167, Fig. 1d,e), at the beginning of stage II during 2016 (DOY 180) and at the middle of stage II during 2014 & 2015 (DOY 182 – 203, Fig. 1a,b). Irrigation initiation in the -1.2 MPa vines was also highly diverse, occurring at the beginning of stage II during 2017 & 2018 (DOY 172 – 173, Fig. 1d,e), at the middle of stage II during 2016 (DOY 193) and at the beginning of stage III during 2014 & 2015 (DOY 203 – 231, Fig. 1a,b). Vines of the early irrigation treatments (budbreak, -0.6 MPa) had significantly less negative Ψ_s values in comparison

to vines in the late irrigation treatments (-1.0 MPa & -1.2 MPa), which had consistently lower Ψ_s values. The vines in the -0.8 MPa irrigation treatment were at intermediate level, whereas in some years their Ψ_s values resembled those of vines in the early irrigation treatments (2017 & 2018, Fig. 1d,e), while in other years they resembled those of vines in the late irrigation treatments (2014 & 2015, Fig. 1a,b). It is important to note that vines in the budbreak treatment had more negative Ψ_s values (not significant) compared to the -0.6 MPa vines in many occasions during the time course of the growing seasons (Fig. 1a-e), even though during spring time they had received only additional 18 mm in average. Some of those variations occurred during stages II & III, after more than two months of similar irrigation applied to the budbreak and -0.6 MPa vines.

The seasonal course of LAI development of vines in different irrigation treatments was similar from 2014 through 2018 (Fig. 2f-j). A rapid canopy development at the beginning of the growing season resulted in maximal LAI values at the middle/end of stage I (DOY 155 -170). During the growing season of 2014, early irrigation treatments (budbreak & -0.6 MPa) were exceptional and continued to exhibit moderate canopy development until the middle of stage II (DOY 185). During all growing seasons (except for 2016) from stage II until the end of the growing season, LAI values were stable (Fig. 2f-j). The canopy hedging effect is reflected as a sharp decline in LAI values at 2017 season during DOY 150 - 155 (Fig. 1i). The lifting of catch wires can be seen as "artificial" reductions in measured LAI during stage I in 2014 season during DOY 135 – 140 (Fig. 2f), in 2015 season during DOY 120 – 145 (Fig. 2f) and in 2016 season during DOY 155 – 160 (Fig. 2h). Vines in the early irrigation treatments (budbreak, -0.6 MPa) had significantly higher LAI values (maximal values of 0.90 to 1.45 $\text{m}^2 \text{m}^{-2}$) in comparison to vines in the late irrigation treatments (-1.0 MPa & -1.2 MPa), which had consistently lower LAI values (maximal values of 0.75 to 1.2 $\text{m}^2 \text{m}^{-2}$). In all years, irrigation was initiated in the late irrigation treatments after canopy development was ceased. The LAI values measured in vines in the -0.8 MPa treatment were similar to those of vines in late irrigation treatments (Fig. 2f-j).

Pruning mass was significantly higher in the early irrigation treatment (budbreak; 1.04 kg vine^{-1}) compared to the late irrigation treatments (-0.8 MPa, -1.0 MPa, -1.2 MPa; 0.86, 0.85, 0.80 kg vine^{-1} respectively, Table 3). Shoot number per vine was not affected significantly by irrigation initiation treatments (36 to 38 per vine in all treatments, table 3). Shoot mass was positively affected by irrigation initiation timing, i.e. the earlier the irrigation was implied- the heavier the shoot mass was (table 3). The trend in the maximal LAI was similar to that of the pruning mass, whereas Maximal LAI declined as the irrigation initiation was delayed.

Vines of all irrigation treatments had similar trends of trunk width development over the measured years (Fig. 4). The increase in trunk width commenced about 14 days after budbreak, and

continued consistently until the end of stage I. After the increase has ceased at the end of stage I, a slight decrease in trunk width was recorded, followed by a stabilization until next spring. The differences between the increase of trunk diameter in vines of different irrigation treatments were developed gradually over the experiment period, and at the end of growing season 2017 (fourth measured season) were very pronounced (Fig. 4). Vines of the early irrigation treatments had a larger trunk width increase (Budbreak & -0.6MPa; 7750, 7200 μm respectively, Fig. 4), the -0.8 MPa vines exhibited an intermediate enlargement (6800 μm), while in the late irrigation treatments vines the narrowest trunk width addition was recorded (-1.0 MPa & -1.2MPa; 5500, 4250 μm , Fig. 4). It is important to note that the late irrigation treatments received almost no irrigation (less than 2 mm) during the period of increase in trunk diameter (stage I).

3.3 Gas exchange parameters

In growing seasons 2014 & 2015 the A_n values were high and stable until the end of stage I and then started to decline until the end of the growing season (Fig. 3a,b). In growing seasons 2016 to 2018 the A_n values started to decrease already at the beginning of stage I (Fig. 3c-e). Many measurements indicated that vines of the early irrigation treatments had significantly higher A_n values, compared to vines of the late irrigation treatments that had lower A_n values (Fig. 3). These differences were obscured when the A_n values dropped and decreased beneath the threshold of 4 $\mu\text{mol CO}_2 \text{ m}^{-2} \text{ s}^{-1}$. During growing season 2015, differences between vines of different irrigation treatments were less pronounced (Fig. 3b). Vines of the -0.8 MPa treatment had high A_n values in some years (2016 – 2018) and low A_n values in other years (2014 – 2015).

The general trends of g_s values of vines in all irrigation treatments was similar to those of the A_n values (Fig. 3). During growing seasons 2014 to 2016 the variations between vines of different irrigation treatments were more pronounced in the g_s values compared to the A_n values. In the g_s values a reduction in the variation between vines of different irrigation treatments was also seen, when g_s values decreased beneath the threshold of 50 $\text{mmol H}_2\text{O m}^{-2} \text{ s}^{-1}$. Like the A_n values, in many measurements the g_s values of vines of the early irrigation treatments were significantly higher in comparison to those of vines in late irrigation treatments (Fig. 4.f-j).

3.4 Berry development and yield parameters.

Berry development occurred continuously throughout the entire growing season, except for slight lag phase which was present in the beginning of stage II in growing seasons 2017 & 2018 (Fig. 5). Berries of vines from different irrigation treatments differed significantly in their mass, whereas the earlier the irrigation was implied the heavier the berry mass had consequently become. In

growing season 2015, differences in berries masses between vines from different irrigation treatments were less pronounced (Fig. 5b). During all growing seasons, in all irrigation treatments, berry shrinkage occurred at the end of stage III.

Yield was significantly positively affected ($p < 0.05$) by irrigation initiation, i.e. earlier application of irrigation generated higher yield values (Table 4). Interestingly, addition of 18 mm at spring (3 irrigation events, Table 2) to budbreak vines resulted in significant yield increase of $0.73 \text{ kg vine}^{-1}$ compared to the -0.6 MPa vines (Table 4). The effect of irrigation initiation on bunch number was less dramatic, but still vines in the early irrigation treatments had significantly higher bunch numbers compared to vines of the late irrigation treatments (Table 4). Final berry mass had similar trend as the yield, with significant negative effect ($p < 0.05$) of irrigation withholding on berry mass. Berries number per bunch was not affected by irrigation regime, and was in average 78 – 80 berries per bunch in vines of all irrigation treatments (Table 4). As irrigation was initiated earlier during the growing season, a significant decrease in the number of shriveled berries per bunch was recorded. Acid level was significantly higher and sugar content significantly lower in the early irrigation regimes, i.e. early irrigation treatments had lower pH and higher TSS (Table 4). For all parameters, no interaction between treatments and years was found.

4. Discussion

4.1 Evapotranspiration, precipitation and water amounts.

The average cumulative ET_o ($1238 \text{ mm season}^{-1}$) and annual rainfall (416 mm) measured in this current research, are characteristics of semi-arid regions (Edwards and Clingeleffer, 2013; Esteban et al., 2001; Munitz et al., 2016; Phogat et al., 2017; Picón-Toro et al., 2012; Williams and Baeza, 2007). The combination of high seasonal evapotranspiration accompanied by moderate winter rainfall and minimal spring precipitation, led to a gradual development of drought stress conditions in the experimental vineyard. Seasonal water amounts of 37 to $131 \text{ mm season}^{-1}$ applied via the drip line to the vines in different irrigation treatments, are typical for deficit irrigated vineyards in regions with similar climate (Acevedo-Opazo et al., 2010; Buesa et al., 2017; Romero et al., 2013; Santesteban et al., 2011; Shellie, 2017; Zarrouk et al., 2012), and are also representative of local agricultural practices.

4.2 Physiological parameters

In general, the vines physiological parameters were strongly affected by the irrigation regime, e.g. irrigation initiation timing.

The seasonal trend of decreasing values of Ψ_s along the growing seasons is typical for deficit irrigated vineyards, where there is a continuous depletion of available soil water content (Intrigliolo and Castel, 2010; Munitz et al., 2016; Netzer et al., 2019; Olivo et al., 2008; Romero et al., 2010b). The vines of the early irrigation treatments (Budbreak & -0.6 MPa) had consistently significantly higher values of Ψ_s compared to those of the late irrigation treatments (-1.0 MPa & -1.2 MPa, Fig. 2), reinforcing the findings that Ψ_s is a sensitive indicator of vine water status (Acevedo-Opazo et al., 2010; Choné et al., 2001; Munitz et al., 2016; Patakas et al., 2005; Santesteban et al., 2019; Williams and Araujo, 2002). A phenomenon that had emerged over the trial years is that vines of the late irrigation treatments reached their thresholds points (that determined irrigation start point) earlier as the trial years passed, in contrast to vines of the early irrigation treatments that reached a stabilized threshold timeframe. This may imply on increased drought stress sensitivity derived from prolong exposure to a deficit irrigation regime. SWP value of -1.4 MPa is considered as an indicator of severe drought stress (Leeuwen et al., 2009; Romero et al., 2010b), and was not crossed by any of the vines in all irrigation treatments during 2014 & 2015. In contrast, the -1.4 MPa threshold was crossed by all vines in all irrigation treatments during the beginning of stage III in 2016 and during the middle of stage II in 2017 & 2018 (Fig. 2). This phenomenon cannot be explained by differences in evapotranspiration and precipitation (Table 1), neither by canopy area (Fig. 2). Severe drought stress conditions that are evident earlier along the growing season as trial year's advance, can be derived from the long-term effect of deficit irrigation.

Significant differences in values of g_s and A_n between vines of the early and the late irrigation treatments were present from DOY 140 to 180 (Fig. 3), but they were less pronounced compared to differences in the Ψ_s values. When g_s values decreased beneath the severe drought stress threshold of $50 \text{ mmol H}_2\text{O m}^{-2} \text{ s}^{-1}$ (Flexas et al., 2002; Medrano et al., 2002), the differences between vines of different irrigation treatments were obscured, even though significant differences in Ψ_s values were still present during that time (Fig. 2). When A_n values declined beneath the threshold of $4 \text{ } \mu\text{mol CO}_2 \text{ m}^{-2} \text{ s}^{-1}$, the same phenomenon was recorded, thus it can be considered as A_n severe drought stress threshold. The meaning of this, is that Ψ_s is a clearer vine water status indicator compared to gas exchange parameters, especially during periods in which severe drought stress conditions prevail. A commencement of decline in g_s and A_n values was recorded at DOY 160 - 170 during 2014 - 2015 in vines of all irrigation treatments, while during 2016 - 2018 it was present already at DOY 130 - 145 (Fig. 3). Again, this can be interpreted as long-term effect of photosynthesis downregulation caused by a prolonged deficit irrigation regime. Since in our previous works we showed that drought stress effects anatomical structure and hydraulic

conductivity (Munitz et al., 2018; Netzer et al., 2019), it can give good explanation of the long term additive effect of drought stress on physiological parameters.

4.3 Vegetative growth

In general, vegetative growth occurred mainly during springtime (stage I), in which late irrigation vines received minimal irrigation, resulting in decreased vegetative growth in those vines. As the experiment period advanced, a reduction in seasonal vegetative development was recorded in all vines, nevertheless it was more pronounced in the late irrigation vines.

The growth of vine trunk diameter occurring during the period of early season (mainly stage I, Fig 4), is also reported by others for wine grapevines (Edwards and Clingeleffer, 2013; Intrigliolo and Castel, 2007; Montoro et al., 2011; Myburgh, 1996; Ton and Kopyt, 2004) and is consistent with spring time cambium activity (Bernstein and Fahn, 1960). During the trunk widening period, the late irrigation vines received almost no irrigation, explaining the multiseasonal gradual deceleration in their trunk growth compared to the early irrigation vines. Interestingly, a sharp decrease in annual width growth in the late irrigation treatments trunks was recorded over 2017, enlarging by nearly a third compared to trunk growth of the early irrigation treatments. This also suggests a cumulative effect of drought stress conditions on vegetative growth. The fluctuations in trunk width during the dormancy period of the vines can be attributed to temperature variation effect on dendrometers and to changes in the phloem and outer bark width as a result of wetting/drying cycles. To our knowledge, this is the first multiseasonal curve of trunk's dendrometry of wine grapevines reported in the literature.

Vine canopy area (measured as LAI) development usually takes place from bud break until the end of stage I (bunch closure) as observed in this current study (Fig. 2). This is consistent with documented results (Munitz et al., 2019, 2016; Netzer et al., 2019, Ben-Asher et al., 2006; Edwards and Clingeleffer, 2013; Intrigliolo et al., 2009; Peacock et al., 1987; Romero and Martinez-Cutillas, 2012). The range of maximal LAI values (0.75 to 1.45 m² m⁻²), is in agreement with others that conducted LAI measurements (using several different methods) at deficit irrigated vineyards trained on a VSP trellis system (Buesa et al., 2017; Intrigliolo and Castel, 2010; Johnson et al., 2003; Romero et al., 2010b). LAI was shown to have a strong effect on ET_c (Munitz et al., 2019). Ohana-Levi et al. (2019) analyzed the dataset derived from the lysimeters located at the same experimental site planted with similar cultivar and related the influence of meteorological variables and LAI on ET_c. They found that LAI had a relative influence over ET_c ranging between 62 and 86% compared to the impact of the meteorological variables.

Pruning mass values recorded in this work (0.8 to 1.0 kg vine⁻¹, Table 3) are complementary to those reported by others in VSP trained vines (Bou Nader et al., 2019; Buesa et al., 2017; Edwards and Clingeleffer, 2013; Intrigliolo and Castel, 2007; Reynolds et al., 1996; Turkington et al., 1980). The vines treated with early irrigation had significantly heavier pruning mass compared to the late irrigation vines, supporting the findings that pruning mass is a well-established indicator of seasonal vegetative growth (Bravdo et al., 1984; Buesa et al., 2017; Chaves et al., 2007; Kliewer and Dokoozlian, 2005; Poni et al., 1994; Williams et al., 2003). The significantly heavier pruning mass was derived from heavier shoot mass, while there was no increase in shoot number (Table 4). Interestingly, the "Budbreak" vines had 20% heavier pruning mass compared to the -0.6 MPa vines (not significant), even though they received during springtime only an additional 18 mm in average.

4.3 Yield components

The range of yield that was recorded (4.3 to 6.1 kg vine⁻¹, Table 4) complies with values reported by other studies for high quality vineyards planted in similar densities (Guidoni et al., 2002; Keller et al., 2008; Medrano et al., 2003; Shellie and Bowen, 2014), and is also representative for local premium commercial vineyards. The crucial effect of water availability during spring time on yield levels, found in this current work, is consistent with a recent study (Munitz et al., 2016). Yield increase in early irrigation treatment vines was a result of increased berry mass and to lesser extent due to higher bunch number (Table 4). The values of berry mass obtained by us (1.20 to 0.95 gr) are typical for deficit irrigated field-grown 'Cabernet Sauvignon' vines (Bravdo et al., 1985; Chalmers et al., 2010; Edwards and Clingeleffer, 2013; Shellie and Bowen, 2014). The classical "double sigmoid" berry growth pattern reported by others (Coombe et al., 1992; Coombe and McCarthy, 2000; Hardie and Considine, 1976) was not present in current study. Interestingly, over the seasons with more extreme drought stress levels (2016 - 2018) differences in berry mass of vines that received different irrigation treatments were more pronounced compared to seasons in which higher water availability prevailed (2014 - 2015, Fig. 5). As shown in other studies (Bahar et al., 2011; Bonada et al., 2013; Fuentes et al., 2010), we found that the occurrence of shriveled berries is significantly positively affected ($p < 0.05$) by drought stress.

5. Conclusions

The current study investigated the effect of the irrigation initiation timing on vegetative growth, physiological parameters and yield components. Early irrigation initiation during springtime, in which most vegetative growth processes occur, resulted in enhancement effect on all vegetative &

physiological parameters. Initiating irrigation at budbreak resulted in an increase in all physiological & vegetative parameters, even compared to the -0.6 MPa vines. Thus, in situations where maximal yield is desirable, this practice should be taken into consideration.

However, postponing irrigation initiation until advanced periods in the growing season, was followed by diminished vegetative growth, reduced physiological performance and decreased yield. Nevertheless, it was also accompanied by higher sugar content, reduced berry size and increased wine quality (Munitz, unpublished). In a premium vineyard, in which limited vegetative growth combined with low yields is favorable, this method can be implied with precautions, since the accumulated effect of drought stress can shorten the lifespan of the vineyard and on the long run reduce considerably the yield level and even reduce grape quality.

6. Acknowledgments

The authors would like to thank to dedicated growers: Yoav David , Itamar Weis, Yedidia Maman and Shlomi Choen. We thank Yechezkel Harroch, Bentzi Green, Yossi Shteren, Alon Katz, Ben hazut, Elnatan Golan, David Kimchi, Gilad gersman, Alon chores, Yedidia sweid, Daniel Mintz and Yair hayat for assisting in the field measurements and to Ziv Charit from "Netafim" company for the help with the vineyard irrigation system. We thank the team of Teperberg Winery, Udi Gliksman, Shiki Rauchberger and Olivier Fratty for their collaboration. We thank Sarig Duek and Omer Guy from "Phytech" company for help with the trunk dendrometers.

We particularly want to thank Dr. Noa Levi for careful scientific reading and the help with more precise statistical analysis.

Source of funding

This study was sponsored by the Ministry of Science and Technology (Grant No. 6-6802), Israel, the Ministry of Agriculture and Rural Development (Grant No. 31-01-0013), Israel and the Israeli Wine Grape Council.

Literature cited

- Acevedo-Opazo, C., Ortega-Farias, S., Fuentes, S., 2010. Effects of grapevine (*Vitis vinifera* L.) water status on water consumption, vegetative growth and grape quality: An irrigation scheduling application to achieve regulated deficit irrigation. *Agric. Water Manag.* 97, 956–964. <https://doi.org/10.1016/j.agwat.2010.01.025>
- Allen, R.G., Pereira, L., Raes, D., 2006. Crop evapotranspiration. Guidelines for computing crop water requirements., in: *FAO Irrigation and Drainage Paper*. ROME.
- Allen, R.G., Pereira, L.S., Raes, D., Smith, M., 1998. Crop evapotranspiration. Guidelines for computing crop water requirements. *FAO irrigation and drainage paper no. 56*, *FAO irrigation and drainage paper no. 56*. ROME. <https://doi.org/10.1016/j.eja.2010.12.001>
- Bahar, E., Carbonneau, A., Korkutal, I., 2011. The effect of extreme water stress on leaf drying limits and possibilities of

- recovering in three grapevine (*Vitis vinifera* L.) cultivars. *Afr. J. Agric. Res.* 6, 1151–1160. <https://doi.org/10.5897/AJAR10.778>
- Beis, A., Patakas, A., 2015. Differential physiological and biochemical responses to drought in grapevines subjected to partial root drying and deficit irrigation. *Eur. J. Agron.* 62, 90–97. <https://doi.org/10.1016/j.eja.2014.10.001>
- Ben-Asher, J., Tsuyuki, I., Bravdo, B.-A., Sagih, M., 2006. Irrigation of grapevines with saline water I. Leaf area index, stomatal conductance, transpiration and photosynthesis. *Agric. Water Manag.* 83, 13–21. <https://doi.org/10.1016/j.agwat.2006.01.002>
- Bernstein, Z., Fahn, A., 1960. The Effect of Annual and Bi-annual Pruning on the Seasonal Changes in Xylem Formation in the Grapevine. *Ann. Bot.* 24, 159–171.
- Bonada, M., Sadras, V., Moran, M., Fuentes, S., 2013. Elevated temperature and water stress accelerate mesocarp cell death and shrivelling, and decouple sensory traits in Shiraz berries. *Irrig. Sci.* 31, 1317–1331. <https://doi.org/10.1007/s00271-013-0407-z>
- Bou Nader, K., Stoll, M., Rauhut, D., Patz, C.D., Jung, R., Loehnertz, O., Schultz, H.R., Hilbert, G., Renaud, C., Roby, J.P., Delrot, S., Gomès, E., 2019. Impact of grapevine age on water status and productivity of *Vitis vinifera* L. cv. Riesling. *Eur. J. Agron.* 104, 1–12. <https://doi.org/10.1016/j.eja.2018.12.009>
- Boyer, J., 1995. *Water relations of plants and soils.* Academic Press, San Diego, CA, USA.
- Bravdo, B., Hepner, Y., Loinger, C., Cohen, S., Tabacman, H., 1984. Effect of crop level on growth, yield and wine quality of a high yielding Carignane vineyard. *Am. J. Enol. Vitic.* 35, 247–252.
- Bravdo, B., Hepner, Y., Loinger, C., Cohen, S., Tabacman, H., 1985. Effect of irrigation and crop level on growth, yield and wine quality of Cabernet Sauvignon. *Am. J. Enol. Vitic.* 36, 132–139.
- Buesa, I., Pérez, D., Castel, J., Intrigliolo, D., Castel, JR, 2017. Effect of deficit irrigation on vine performance and grape composition of *Vitis vinifera* L. cv. Muscat of Alexandria. *Aust. J. Grape Wine Res.* 23, 251–259. <https://doi.org/10.1111/ajgw.12280>
- Castellarin, S.D., Matthews, M. a, Di Gaspero, G., Gambetta, G. a, 2007. Water deficits accelerate ripening and induce changes in gene expression regulating flavonoid biosynthesis in grape berries. *Planta* 227, 101–112. <https://doi.org/10.1007/s00425-007-0598-8>
- Chalmers, Y.M., Downey, M.O., Krstic, M.P., Loveys, B.R., Dry, P.R., 2010. Influence of sustained deficit irrigation on colour parameters of Cabernet Sauvignon and Shiraz microscale wine fermentations. *Aust. J. Grape Wine Res.* 16, 301–313. <https://doi.org/10.1111/j.1755-0238.2010.00093.x>
- Chaves, M., Zarrouk, O., Francisco, R., Costa, J., Santos, T., Regalado, A., Rodrigues, M., Lopes, C., 2010. Grapevine under deficit irrigation: hints from physiological and molecular data. *Ann. Bot.* 105, 661–76. <https://doi.org/10.1093/aob/mcq030>
- Chaves, M.M., Santos, T.P., Souza, C.R., Ortuño, M.F., Rodrigues, M.L., Lopes, C.M., Maroco, J.P., Pereira, J.S., 2007. Deficit irrigation in grapevine improves water-use efficiency while controlling vigour and production quality. *Ann. Appl. Biol.* 150, 237–252. <https://doi.org/10.1111/j.1744-7348.2006.00123.x>
- Choné, X., Leeuwen, C. Van, Dubourdieu, D., Gaudillere, J.P., 2001. Stem water potential is a sensitive indicator of grapevine water status. *Ann. Bot.* 87, 477–483.
- Cifre, J., Bota, J., Escalona, J.M., Medrano, H., Flexas, J., 2005. Physiological tools for irrigation scheduling in grapevine (*Vitis vinifera* L.). *Agric. Ecosyst. Environ.* 106, 159–170. <https://doi.org/10.1016/j.agee.2004.10.005>
- Coombe, B.G.G., McCarthy, M.G., Kennedy, B.Y.J., 1992. Research on Development and Ripening of the Grape Berry. *Am. J. Enol. Vitic.* 43, 101–110. <https://doi.org/10.1111/j.1755-0238.2000.tb00171.x>
- Coombe, B.G.G., McCarthy, M.G.G., 2000. Dynamics of grape berry growth and physiology of ripening. *Aust. J. Grape Wine Res.* 6, 131–135. <https://doi.org/10.1111/j.1755-0238.2000.tb00171.x>
- Doorenbos, J., Pruitt, W., 1977. Guidelines for predicting crop water requirements. *FAO Irrig. Drain. Pap.* 24, 144.
- Edwards, E.J., Clingeleffer, P.R., 2013. Interseasonal effects of regulated deficit irrigation on growth, yield, water use, berry composition and wine attributes of Cabernet Sauvignon grapevines. *Aust. J. Grape Wine Res.* 19, 261–276. <https://doi.org/10.1111/ajgw.12027>
- Esteban, M.A., Villanueva, M.J., Lissarrague, J.R., 2001. Effect of irrigation on changes in the anthocyanin composition of the skin of cv Tempranillo (*Vitis vinifera* L) grape berries during ripening. *J. Sci. Food Agric.* 81, 409–420. [https://doi.org/10.1002/1097-0010\(200103\)81:4<409::AID-JSFA830>3.0.CO;2-H](https://doi.org/10.1002/1097-0010(200103)81:4<409::AID-JSFA830>3.0.CO;2-H)
- Evans, R.G., Spayd, S.E., Wample, R.L., Kroeger, M.W., Mahan, M.O., 1993. Water use of *Vitis vinifera* grapes in Washington*. *Agric. Water Manag.* 23, 109–124. [https://doi.org/10.1016/0378-3774\(93\)90035-9](https://doi.org/10.1016/0378-3774(93)90035-9)

- Fereres, E., Evans, R.G., 2006. Irrigation of fruit trees and vines: An introduction. *Irrig. Sci.* 24, 55–57. <https://doi.org/10.1007/s00271-005-0019-3>
- Fernandes-Silva, A., Oliveira, M., A. Paço, T., Ferreira, I., 2019. Deficit Irrigation in Mediterranean Fruit Trees and Grapevines: Water Stress Indicators and Crop Responses, in: *Irrigation in Agroecosystems*. pp. 1–35. <https://doi.org/10.5772/intechopen.80365>
- Flexas, J., Escalona, J.M., Evain, S., Gulías, J., Moya, I., Osmond, C.B., Medrano, H., 2002. Steady-state chlorophyll fluorescence (Fs) measurements as a tool to follow variations of net CO₂ assimilation and stomatal conductance during water-stress in C₃ plants, in: *Phys.* pp. 231–240.
- Fuentes, S., Sullivan, W., Tilbrook, J., Tyerman, S., 2010. A novel analysis of grapevine berry tissue demonstrates a variety-dependent correlation between tissue vitality and berry shrivel. *Aust. J. Grape Wine Res.* 16, 327–336. <https://doi.org/10.1111/j.1755-0238.2010.00095.x>
- Girona, J., Marsal, J., Mata, M., Del Campo, J., Basile, B., 2009. Phenological sensitivity of berry growth and composition of Tempranillo grapevines (*Vitis vinifera* L.) to water stress. *Aust. J. Grape Wine Res.* 15, 268–277. <https://doi.org/10.1111/j.1755-0238.2009.00059.x>
- Grimes, D.W., Williams, L.E., 1990. Irrigation Effects on Plant Water Relations and Productivity of Thompson Seedless Grapevines. *Crop Sci.* 30, 255–260. <https://doi.org/10.2135/cropsci1990.0011183X003000020003x>
- Guidoni, S., Allara, P., Schubert, A., 2002. Effect of cluster thinning on berry skin anthocyanin composition of *Vitis vinifera* cv. Nebbiolo. *Am. J. Enol. Vitic.* 53, 224–226.
- Hardie, W., Considine, J., 1976. Response of grapes to water-deficit stress in particular stages of development. *Am. J. Enol. Vitic.* 27, 55–61.
- Intrigliolo, D.S., Castel, J.R., 2010. Response of grapevine cv. ‘Tempranillo’ to timing and amount of irrigation: water relations, vine growth, yield and berry and wine composition. *Irrig. Sci.* 28, 113–125. <https://doi.org/10.1007/s00271-009-0164-1>
- Intrigliolo, D.S., Castel, J.R., 2007. Evaluation of grapevine water status from trunk diameter variations. *Irrig. Sci.* 26, 49–59. <https://doi.org/10.1007/s00271-007-0071-2>
- Intrigliolo, D.S., Lakso, A.N., Piccioni, R.M., 2009. Grapevine cv. ‘Riesling’ water use in the northeastern United States. *Irrig. Sci.* 27, 253–262. <https://doi.org/10.1007/s00271-008-0140-1>
- Johnson, L., Roczen, D., Youkhana, S., Nemani, R., Bosch, D., 2003. Mapping vineyard leaf area with multispectral satellite imagery. *Comput. Electron. Agric.* 38, 33–44.
- Keller, M., Smithyman, R., Mills, L., 2008. Interactive effects of deficit irrigation and crop load on Cabernet Sauvignon in an arid climate. *Am. J. Enol. Vitic.* 59, 221–234. <https://doi.org/10.5344/ajev.2011.10103>
- Kennedy, J., Kennedy, B.Y.J., Kennedy, J., Kennedy, B.Y.J., 2002. Understanding grape berry development. *Pract. Winer. Vineyard* 4, 1–5.
- Kliwer, W., Dokoozlian, N., 2005. Leaf area/crop weight ratios of grapevines: influence on fruit composition and wine quality. *Am. J. Enol. Vitic.* 56, 170–181.
- Leeuwen, C. Van, Tregoat, O., Chon?, X., Bois, B., Pernet, D., Gaudill?re, J.P., 2009. Vine water status is a key factor in grape ripening and vintage quality for red bordeaux wine. How can it be assessed for vineyard management purposes? *J. Int. des Sci. la Vigne du Vin* 43, 121–134. <https://doi.org/10.20870/oeno-one.2009.43.3.798>
- López-Urrea, R., Montoro, a., Mañas, F., López-Fuster, P., Fereres, E., 2012. Evapotranspiration and crop coefficients from lysimeter measurements of mature ‘Tempranillo’ wine grapes. *Agric. Water Manag.* 112, 13–20. <https://doi.org/10.1016/j.agwat.2012.05.009>
- Matthews, M., Ishii, R., Anderson, M., O’Mahony, M., 1990. Dependence of wine sensory attributes on vine water status. *J. Sci. Food Agric.* 51, 321–335.
- Medrano, H., Escalona, J.M., Bota, J., Gulías, J., Flexas, J., 2002. Regulation of photosynthesis of C₃ plants in response to progressive drought: Stomatal conductance as a reference parameter. *Ann. Bot.* 89, 895–905. <https://doi.org/10.1093/aob/mcf079>
- Medrano, H., Escalona, J.M., Cifre, J., Bota, J., Flexas, J., 2003. A ten-year study on the physiology of two Spanish grapevine cultivars under field conditions: effects of water availability from leaf photosynthesis to grape yield and quality. *Funct. Plant Biol.* 30, 607–619. <https://doi.org/10.1071/FP02110>
- Montoro, A., Urrea, R.L., Manas, F., Fuster, L.L., 2011. Dendrometric measurements in grapevine (*Vitis vinifera* L. ‘Tempranillo’ and ‘Cabernet sauvignon’) under regulated deficit irrigation. *Acta Hort* 113–122.
- Munitz, S., Netzer, Y., Schwartz, A., 2016. Sustained and regulated deficit irrigation of field-grown Merlot grapevines. *Aust. J.*

- Munitz, S., Netzer, Y., Shetin, I., Schwartz, A., 2018. Water availability dynamics have long-term effects on mature stem structure in *Vitis vinifera*. *Am. J. Bot.* 105, 1–10. <https://doi.org/10.1111/ijlh.12426>
- Munitz, S., Schwartz, A., Netzer, Y., 2019. Water consumption, crop coefficient and leaf area relations of a *Vitis vinifera* cv. “Cabernet Sauvignon” vineyard. *Agric. Water Manag.* 219, 86–94. <https://doi.org/10.1016/j.agwat.2019.03.051>
- Myburgh, P.A., 1996. Response of *Vitis vinifera* L. cv. Barlinka/Ramsey to soil water depletion levels with particular reference to trunk growth parameters. *South African J. Enol. Vitic.* 17.
- Netzer, Y., Munitz, S., Shtein, I., Schwartz, A., 2019. Structural memory in grapevines : Early season water availability affects late season drought stress severity. *Eur. J. Agron.* 105, 96–103. <https://doi.org/10.1016/j.eja.2019.02.008>
- Ohana-Levi, N., Munitz, S., Ben-Gal, A., Schwarz, A., Peeters, A., Netzer, Y., 2019. Multiseasonal grapevine water consumption – drivers and forecasting. *Agric. For. Meteorol.* accepted.
- Olivo, N., Girona, J., Marsal, J., 2008. Seasonal sensitivity of stem water potential to vapour pressure deficit in grapevine. *Irrig. Sci.* 27, 175–182. <https://doi.org/10.1007/s00271-008-0134-z>
- Ollé, D., Guiraud, J.L., Souquet, J.M., Terrier, N., AgeorgeS, a., Cheyner, V., Verries, C., 2011. Effect of pre- and post-veraison water deficit on proanthocyanidin and anthocyanin accumulation during Shiraz berry development. *Aust. J. Grape Wine Res.* 17, 90–100. <https://doi.org/10.1111/j.1755-0238.2010.00121.x>
- Padgett-Johnson, M., Williams, L., Walker, M., 2003. Vine water relations, gas exchange, and vegetative growth of seventeen *Vitis* species grown under irrigated and nonirrigated conditions in California. *J. Am. Soc.* 128, 269–276.
- Patakas, A., Noitsakis, B., Chouzouri, A., 2005. Optimization of irrigation water use in grapevines using the relationship between transpiration and plant water status. *Agric. Ecosyst. Environ.* 106, 253–259. <https://doi.org/10.1016/j.agee.2004.10.013>
- Peacock, W., Christensen, L., Andris, H., 1987. Development of a drip irrigation schedule for average canopy vineyards in the San Joaquin valley. *Am. J. Enol. Vitic.* 38, 113–119.
- Pellegrino, A., Lebon, E., Simonneau, T., Wery, J., 2005. Towards a simple indicator of water stress in grapevine (*Vitis vinifera* L.) based on the differential sensitivities of vegetative growth components. *Aust. J. Grape Wine Res.* 11, 306–315.
- Phogat, V., Skewes, M.A., McCarthy, M.G., Cox, J.W., simunek, J., Petrie, P.R., 2017. Evaluation of crop coefficients, water productivity, and water balance components for wine grapes irrigated at different deficit levels by a sub-surface drip. *Agric. Water Manag.* 180, 22–34. <https://doi.org/10.1016/j.agwat.2016.10.016>
- Picón-Toro, J., González-Dugo, V., Uriarte, D., Mancha, L., Testi, L., 2012. Effects of canopy size and water stress over the crop coefficient of a “Tempranillo” vineyard in south-western Spain. *Irrig. Sci.* 30, 419–432. <https://doi.org/10.1007/s00271-012-0351-3>
- Poni, S., Lakso, A., Turner, J., Melious, R.E., 1994. Interactions of crop level and late season water stress on growth and physiology of field-grown Concord grapevines. *Am. J. Enol. Vitic.* 45, 252–258.
- Reynolds, A.G., Wardle, D.A., Naylor, A.P., 1996. Impact of training system, vine spacing, and basal leaf removal on riesling. Vine performance, berry composition, canopy microclimate, and vineyard labor requirements. *Am. J. Enol. Vitic.* 47, 63–76. <https://doi.org/10.1071/PP9960115>
- Roby, G., Harbertson, J.F., Adams, D. a., Matthews, M. a., 2004. Berry size and vine water deficits as factors in winegrape composition: Anthocyanins and tannins. *Aust. J. Grape Wine Res.* 10, 100–107. <https://doi.org/10.1111/j.1755-0238.2004.tb00012.x>
- Romero, P., Fernández-Fernández, J.I., Martínez-Cutillas, A., 2010a. Physiological Thresholds for Efficient Regulated Deficit-Irrigation. *Am. J. Enol. Vitic.* 61, 400–401.
- Romero, P., Fernández-Fernández, J.I., Martínez-Cutillas, A., Ignacio, F., Fernández-Fernández, J.I., Martínez-Cutillas, A., 2010b. Physiological thresholds for efficient regulated deficit-irrigation management in winegrapes grown under semiarid conditions. *Am. J. Enol. Vitic.* 61, 300–312.
- Romero, P., Gil-Muñoz, R., del Amor, F.M., Valdés, E., Fernández, J.I., Martínez-Cutillas, A., 2013. Regulated Deficit Irrigation based upon optimum water status improves phenolic composition in Monastrell grapes and wines. *Agric. Water Manag.* 121, 85–101. <https://doi.org/10.1016/j.agwat.2013.01.007>
- Romero, P., Martínez-Cutillas, A., 2012. The effects of partial root-zone irrigation and regulated deficit irrigation on the vegetative and reproductive development of field-grown Monastrell grapevines. *Irrig. Sci.* 30, 377–396. <https://doi.org/10.1007/s00271-012-0347-z>
- Santesteban, L.G., Miranda, C., Marín, D., Sesma, B., Intrigliolo, D.S., Mirás-Avalos, J.M., Escalona, J.M., Montoro, A., de Herralde, F., Baeza, P., Romero, P., Yuste, J., Uriarte, D., Martínez-Gascuña, J., Cancela, J.J., Pinillos, V., Loidi, M.,

Urrestarazu, J., Royo, J.B., 2019. Discrimination ability of leaf and stem water potential at different times of the day through a meta-analysis in grapevine (*Vitis vinifera* L.). *Agric. Water Manag.* 221, 202–210. <https://doi.org/10.1016/j.agwat.2019.04.020>

Santesteban, L.G., Miranda, C., Royo, J.B., 2011. Regulated deficit irrigation effects on growth, yield, grape quality and individual anthocyanin composition in *Vitis vinifera* L. cv. “Tempranillo.” *Agric. Water Manag.* 98, 1171–1179. <https://doi.org/10.1016/j.agwat.2011.02.011>

Schultz, H.R., 2016. Global Climate Change, Sustainability, and Some Challenges for Grape and Wine Production. *J. Wine Econ.* 11, 181–200. <https://doi.org/10.1017/jwe.2015.31>

Shellie, K., 2017. Above Ground Drip Application Practices Alter Water Productivity of Malbec Grapevines under Sustained Deficit. *J. Agric. Sci.* 9, 1. <https://doi.org/10.5539/jas.v9n6p1>

Shellie, K.C., Bowen, P., 2014. Isohydrodynamic behavior in deficit-irrigated Cabernet Sauvignon and Malbec and its relationship between yield and berry composition. *Irrig. Sci.* 32, 87–97. <https://doi.org/10.1007/s00271-013-0416-y>

Ton, Y., Kopyt, M., 2004. Phytomonitoring in realization of irrigation strategies for wine grapes. *Acta Hort.* 652, 167–173.

Turkington, C.R., Peterson, J.R., Evans, J.C., 1980. A Spacing, Trellising, and Pruning Experiment with Muscat Gordo Blanco Grapevines. *Am. J. Enol. Vitic.* 31, 298–302.

Williams, L.E., Araujo, F.J., 2002. Correlations among predawn leaf, midday leaf, and midday stem water potential and their correlations with other measures of soil and plant water status in *Vitis vinifera*. *J. Am. Soc.* 127, 448–454.

Williams, L.E., Baeza, P., 2007. Relationships among ambient temperature and vapor pressure deficit and leaf and stem water potentials of fully irrigated, field-grown grapevines. *Am. J. Enol. Vitic.* 58, 173–181.

Williams, L.E., Phene, C.J., Grimes, D.W., Trout, T.J., 2003. Water use of mature Thompson Seedless grapevines in California. *Irrig. Sci.* 22, 11–18. <https://doi.org/10.1007/s00271-003-0067-5>

Zarrouk, O., Francisco, R., Pinto-Marijuan, M., Brossa, R., Santos, R.R., Pinheiro, C., Costa, J.M., Lopes, C., Chaves, M.M., 2012. Impact of irrigation regime on berry development and flavonoids composition in Aragonez (Syn. Tempranillo) grapevine. *Agric. Water Manag.* 114, 18–29. <https://doi.org/10.1016/j.agwat.2012.06.018>

Figures

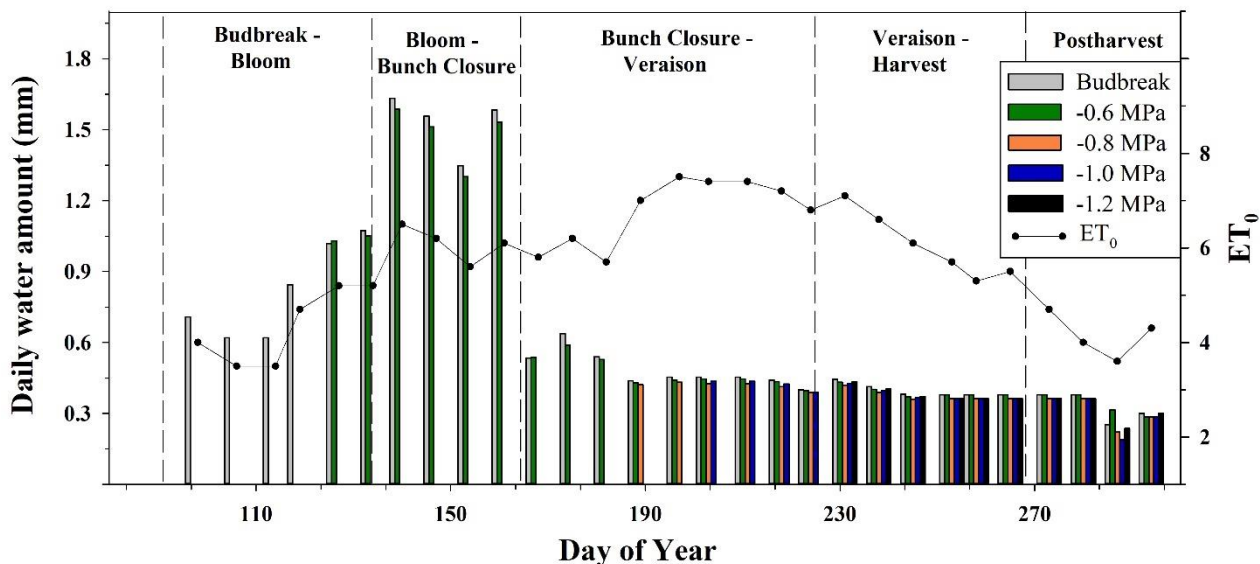


Fig. 1 Seasonal pattern of water amounts applied to different irrigation treatments and ET_0 . Each bar represents one irrigation (once a week) expressed as daily water amount. Each treatment initiated to receive irrigation according to his threshold, then irrigated continuously until the end of growing season. 'Cabernet Sauvignon' vineyard 2016, Kida Israel.

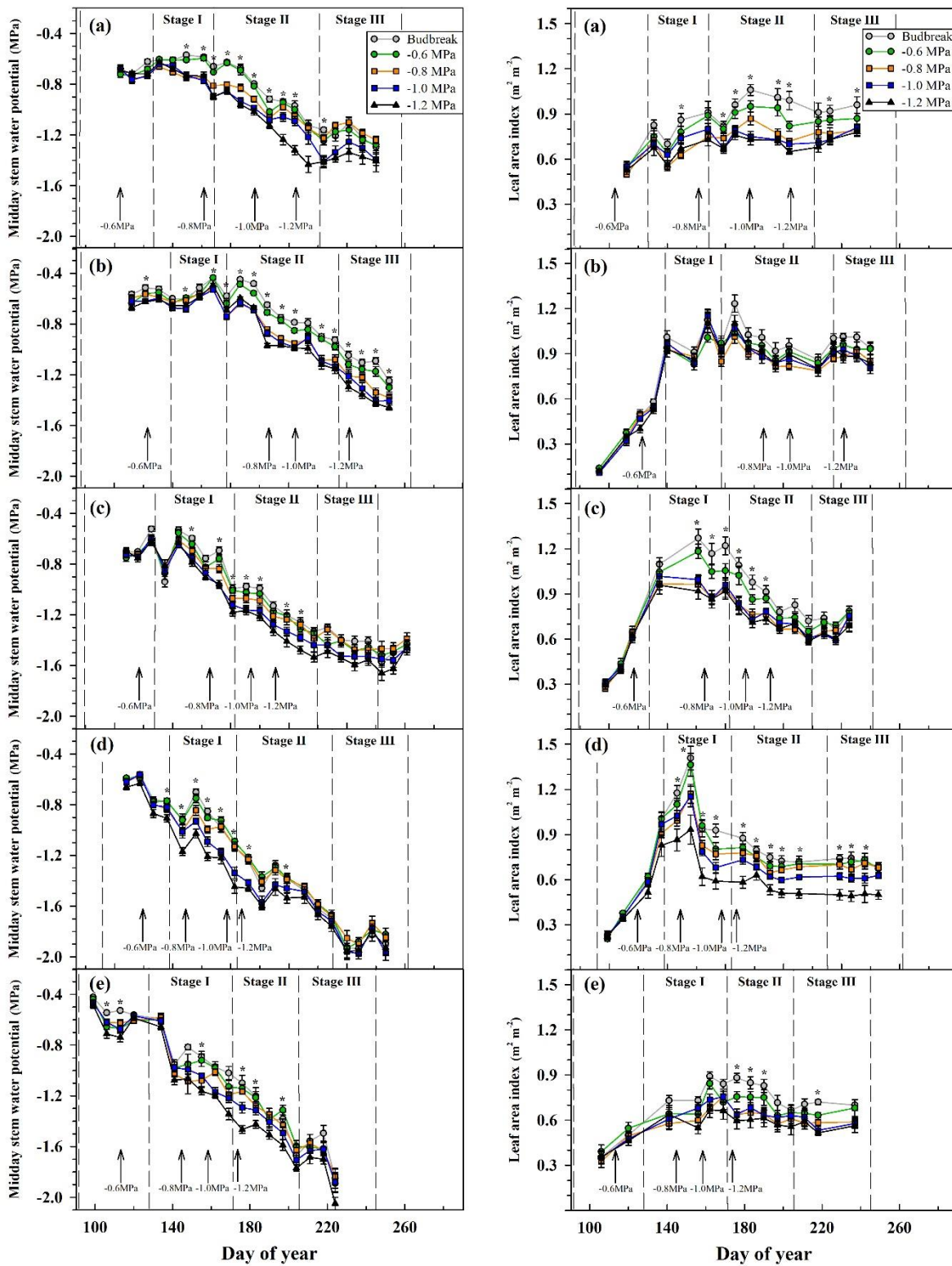


Fig. 2 (a – e) seasonal curves of midday stem water potential of grapevines from different irrigation treatments. (a) 2014, (b) 2015, (c) 2016, (d) 2017, (e) 2018. (f – j) seasonal curves of Leaf area index of grapevines from different irrigation treatment. (f) 2014, (g) 2015, (h) 2016, (i) 2017, (j) 2018. Each value is the mean of 12 leaves/vines (3 leaves/vines per replicate). The bars denote one standard error. Asterisks indicate significant difference ($P < 0.05$) between irrigation treatments according to Tukey's test. Measurements were taken at midday a day before irrigation was applied. 'Cabernet Sauvignon' vineyard, Kida Israel.

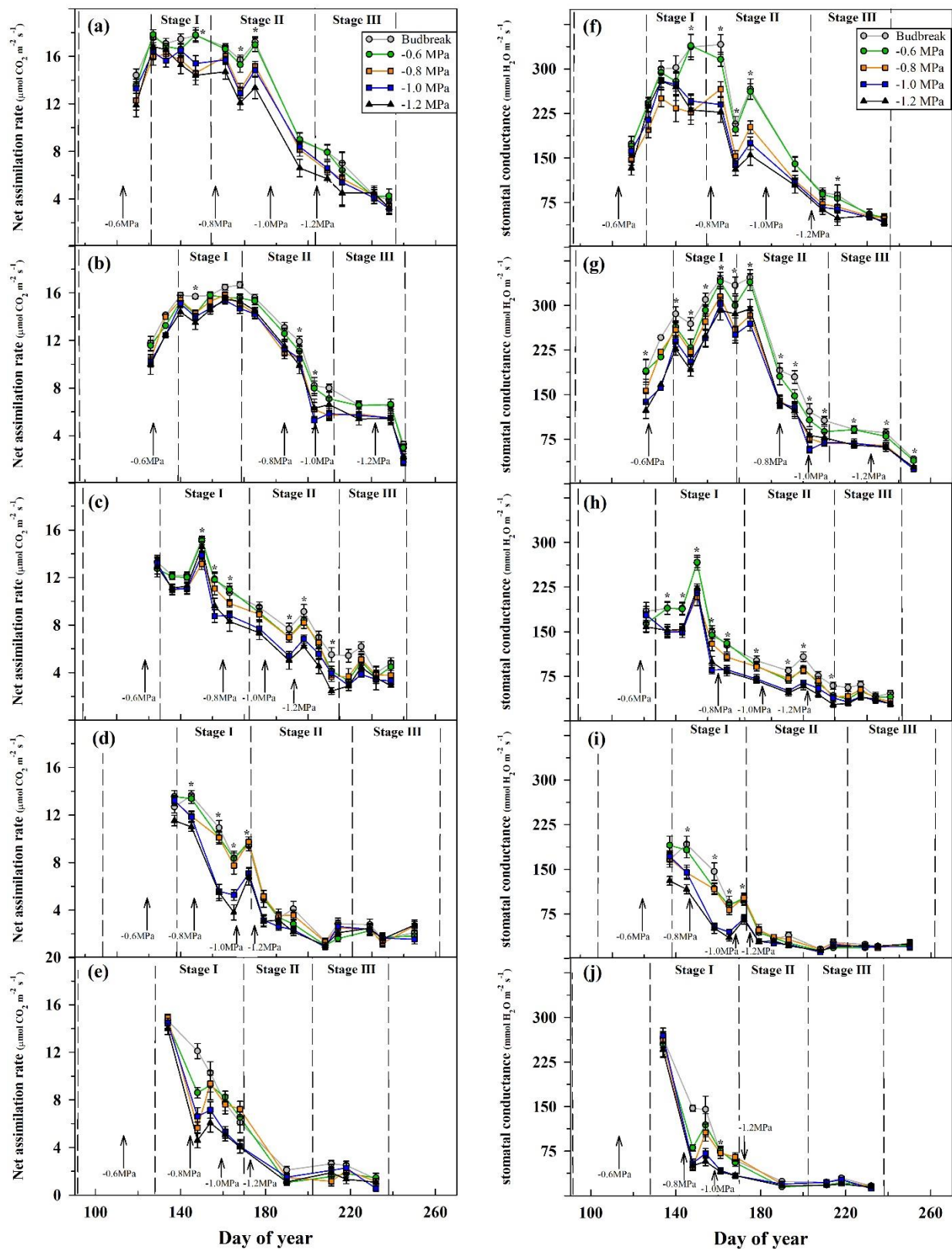


Fig. 3 (a – d) Seasonal curves of net assimilation rate (A_n) of grapevines from different irrigation treatments. (a) 2014, (b) 2015, (c) 2016, (d) 2017, (e) 2018. (e – f) Seasonal curves of stomatal conductance (g_s) of grapevines from different irrigation treatments. (a) 2014, (b) 2015, (c) 2016, (d) 2017, (e) 2018. Each value is the mean of 16 leaves (4 leaves per replicate). The bars denote one standard error. Asterisks indicate significant difference ($P < 0.05$) between irrigation treatments according to Tukey's test. Measurement were taken at midday a day before irrigation was applied. 'Cabernet Sauvignon' vineyard, Kida Israel.

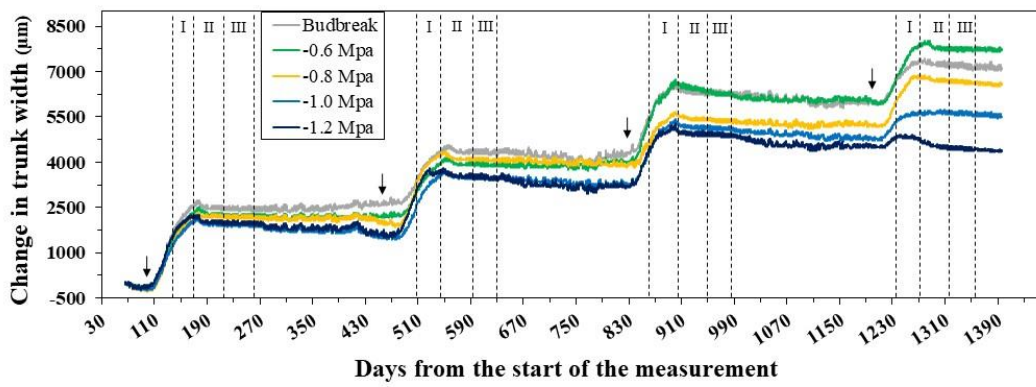


Fig 4. Multi seasonal (2014 – 2017) curve of the change in the trunk width of grapevines from different irrigation treatments. Budbreak at each year is marked by an arrow. Each line represents an average of 4 dendrometers. 'Cabernet Sauvignon' vineyard, Kida Israel.

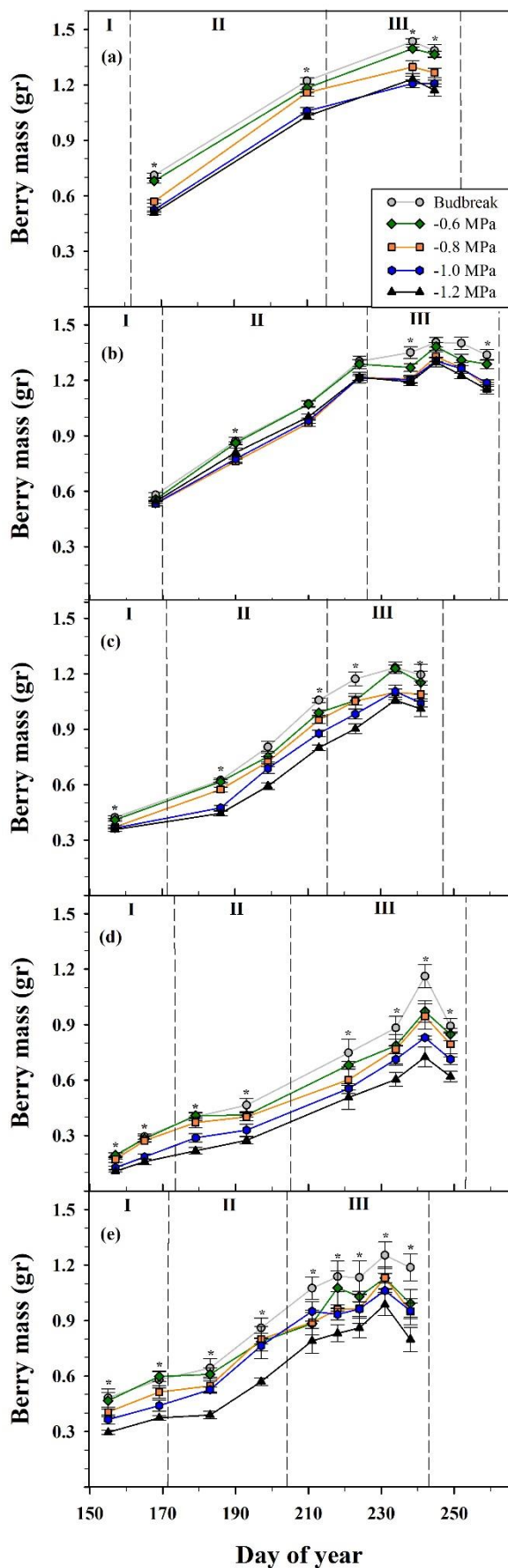


Fig. 5 (a – e) Seasonal accumulation of berry mass of grapevines from different irrigation treatments. (a) 2014, (b) 2015, (c) 2016, (d) 2017, (e) 2018. Each point is the mean of 100 berries (25 berries per replicate). Asterisks indicate significant difference ($P < 0.05$) between irrigation treatments according to Tukey's test. The bars denote one standard error. 'Cabernet Sauvignon' vineyard, Kida Israel.

Table 1. Cumulative Evapotranspiration (mm season⁻¹) and rainfall (mm). Data obtained from meteorological station located at ‘Kida’ Cabernet Sauvignon vineyard, over the years 2014 - 2018.

Year	ET _o (mm season ⁻¹)	*Annual rainfall (mm)	**Spring rain (mm)
2014	1203	416	108
2015	1197	509	68
2016	1322	390	40
2017	1173	341	15
2018	1294	422	116

* Annual rainfall was defined as rain events occurred from 01/10 to 01/06.

** Spring rainfall was defined as rain events occurred from 01/3 to 01/06.

No rain events were recorded from 01/06 to 01/10.

Table 2. Water amounts (mm) applied at different phenological stages. ‘Kida’ Cabernet Sauvignon vineyard, 2014 - 2018.

Irrigation treatment	Budbreak - Full bloom	Full bloom - Bunch closure	Bunch closure - Veraison	Veraison - Harvest	Postharvest
Budbreak	39.2	39.9	23.1	18.2	11.2
-0.6 MPa	21.0	38.5	22.4	17.5	10.5
-0.8 MPa	0	20.3	19.6	17.5	10.5
-1.0 MPa	0	2.1	16.8	16.8	10.5
-1.2 MPa	0	0.7	9.8	16.1	10.5

Table 3. Vegetative parameters. ‘Kida’ Cabernet Sauvignon vineyard, 2014 - 2018.

Irrigation treatment	pruning mass (kg vine ⁻¹)	Shoot (number vine ⁻¹)	Shoot mass (gr)	Maximal LAI (m ² m ⁻²)
Budbreak	1.04 ^a	38.4	27.3 ^a	1.20 ^a
-0.6 MPa	0.95 ^{ab}	37.4	25.1 ^{ab}	1.12 ^a
-0.8 MPa	0.86 ^{bc}	36.6	22.8 ^{bc}	1.03 ^{ab}
-1.0 MPa	0.85 ^{bc}	36.7	23.1 ^{bc}	1.02 ^{ab}
-1.2 MPa	0.80 ^c	37.7	21.6 ^c	0.90 ^b

Values represent means (n = 20). Within each column, means followed by different letters are significantly different ($P < 0.05$) according to Tukey’s test.

Table 4. Yield components and water amounts. ‘Kida’ Cabernet Sauvignon vineyard, 2014 - 2018.

Irrigation treatment	Water amount (mm season ⁻¹)	Yield (kg vine ⁻¹)	Bunch (number vine ⁻¹)	Berry mass (gr)	Berries (number bunch ⁻¹)	Shrivelled berries (number bunch ⁻¹)	pH	TSS (°Brix)
Budbreak	131	6.14 ^a	66.9 ^a	1.20 ^a	79.7	0.6 ^b	3.48 ^b	22.9 ^{cd}
-0.6 MPa	110	5.41 ^b	62.5 ^{ab}	1.13 ^a	78.8	0.9 ^{ab}	3.51 ^b	22.8 ^d
-0.8 MPa	67	5.03 ^{bc}	62.3 ^{ab}	1.05 ^b	79.2	0.8 ^{ab}	3.51 ^b	23.7 ^{bc}
-1.0 MPa	46	4.57 ^{cd}	58.9 ^b	1.02 ^b	77.6	1.0 ^{ab}	3.58 ^a	24.0 ^{ab}
-1.2 MPa	37	4.30 ^d	59.0 ^b	0.95 ^c	77.5	1.5 ^a	3.61 ^a	24.5 ^a

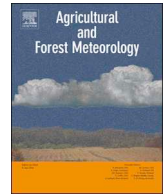
Values represent means (n = 20). Within each column, means followed by different letters are significantly different ($P < 0.05$) according to Tukey’s test.

2.4: Chapter 4:

Multiseasonal grapevine water consumption - drivers and forecasting

Noa Ohana-Levi, Sarel Munitz, Alon Ben-Gal, Amnon Schwartz, Aviva Peeters and Yishai Netzer

Published in Agricultural and Forest Meteorology January 2020



Multiseasonal grapevine water consumption – Drivers and forecasting

Noa Ohana-Levi^c, Sarel Munitz^{b,d}, Alon Ben-Gal^c, Amnon Schwartz^d, Aviva Peeters^e,
Yishai Netzer^{a,b,*}

^a Department of Chemical engineering, Biotechnology and Materials, Ariel University, Ariel 40700, Israel

^b Department of Agriculture and Oenology, Eastern R&D Center, Israel

^c Department of Soil, Water and Environmental Sciences, Agricultural Research Organization, Gilat Research Center, Mobile post Negev 2, 85280, Israel

^d R.H. Smith Institute of Plant Science and Genetics in Agriculture, Faculty of Agriculture, Food and Environment, The Hebrew University of Jerusalem, Rehovot 76100, Israel

^e TerraVision Lab, Midreshet Ben-Gurion 8499000, Israel

ARTICLE INFO

Keywords:

Time series analysis
Machine learning
Evapotranspiration
Vitis vinifera
Agricultural meteorology
Drainage lysimeters

ABSTRACT

The interactions between temperature, relative humidity, radiation, wind speed and their effect on plant transpiration in the context of water consumption for irrigation purposes have been studied for over a century. Leaf area has also been established as an important factor affecting water consumption. We analyzed a multivariable time series composed of both meteorological and vegetative variables with a daily temporal resolution for the growing seasons of 2013–2016 for *Vitis vinifera* ‘Cabernet Sauvignon’ vineyards in the mountainous region in Israel. Time-series analysis of this data was used to characterize seasonal patterns affecting water consumption (ET_c) of vines and to quantify interrelations between meteorological and vegetative factors affecting vine water consumption. Moreover, we applied a machine learning regression model to determine the relative influence of meteorological and vegetative factors on ET_c during four growing seasons. Finally, we developed an ensemble model for temporally forecasting vine ET_c for an additional season using a training dataset of multiple variables. Our findings show that decomposing the time-series dataset uncovered a wider variety of underlying temporal patterns, and enabled quantification of seasonal and daily relationships. Leaf area had a substantial impact on ET_c and was found to have a relative influence ranging between 62 and 86% for the different growing seasons. Mean temperature was ranked second followed by minor effects of relative humidity, solar radiation and wind speed that were interchangeably ordered. The ensemble model produced reliable results, with cross validation coefficients ~ 0.9 . Incorporating leaf area measurements into the regression model improved both the performance of the model and the training data correlation. Using time-series statistics to explore meteorological and vegetative temporal characteristics, patterns, interrelations and relative effect on evapotranspiration may facilitate the understanding of water consumption processes and assist in generating more effective and skillful irrigation models.

1. Introduction

During the past century, studies have been conducted to determine the role of meteorological factors in generating transpiration from agricultural fields (Allen et al., 1998; Briggs and Shantz, 1916; Fuchs et al., 1987; Pierce, 1958; Tao et al., 2009; Widstoe, 1909). In 1948 Howard Penman published the equation that describes the standard climatological factors affecting evaporation from an open water source (Penman, 1948). Later on, the Penman–Monteith equation was developed to approximate plant evapotranspiration (ET) based on temperature, relative humidity, radiation, and wind speed (Monteith, 1965). The United Nations Food and Agriculture

Organization (FAO) adopted the Penman–Monteith equation as the standard methods for ET modeling. ET refers to processes of water loss to the atmosphere from irrigated plots or rainfed ecosystems, with E representing the physical evaporation from the surfaces and T denoting the transpiration from the plant canopy. The term ET_c refers to transpiration by a specific crop. The FAO Irrigation and drainage paper 56 defines this as “...crop evapotranspiration under standard conditions (ET_c), from disease-free, well-fertilized crops, grown in large fields, under optimum soil water conditions, and achieving full production under the given climatic conditions” (Allen et al., 1998).

There are several methods for whole-tree-scale ET_c assessment (Rana and Katerji, 2000), the most common of which is via lysimeters

* Corresponding author at: Department of Chemical engineering, Biotechnology and Materials, Ariel University, Ariel 40700, Israel.
E-mail address: yishaine@ariel.ac.il (Y. Netzer).

<https://doi.org/10.1016/j.agrformet.2019.107796>

Received 27 March 2019; Received in revised form 6 October 2019; Accepted 10 October 2019

0168-1923/ © 2019 Elsevier B.V. All rights reserved.

where the tree is planted in a container filled with natural soil. Two types of lysimeters have been reported in studies assessing ET_c in vines. The first are drainage lysimeters (Munitz et al., 2019; Netzer et al., 2008), from which leachate from below the root zone is collected and measured; and the second are weighing lysimeters, in which the plant and soil are placed in a storage tank on top of a system of scales (López-Urrea et al., 2012; Picón-Toro et al., 2012; Williams et al., 2003). Measurement of water consumption under field conditions, using vines that are similar in their dimensions and physiological performance to those grown in a commercial vineyard, is beneficial for assessing the actual ET_c dynamics of crops. Currently, the recommended technique for modeling the relationship between various weather conditions and crop characteristics for irrigation purposes is by deriving the ratio between ET_c and the Penman–Monteith reference evapotranspiration (ET_0), namely the crop coefficient (K_c) (Allen et al., 1998).

Leaf area has a substantial effect on plant water consumption, due to stomatal response to meteorological conditions. A larger leaf area signifies a larger transpiring surface. Conversely, a larger leaf area generates a wider shaded ground area and a reduction in the relative portion of evaporation from the ground. Leaf area is typically measured using leaf area index (LAI) which is defined as one-sided green leaf area per unit ground surface area ($m^2 m^{-2}$) allocated to a single plant. This ratio standardizes the canopy area to the ground surface allocated to the plant, which enables to compare leaf area among different crops and between various plots that differ in their planting density or other characteristics (Watson, 1947). Studies on water consumption in vineyards have established leaf area as a driver of water consumption, mostly due to its effect on K_c . In a study on table grape vines in Israel, Netzer et al. (2019) found a second-degree polynomial correlation between LAI and both ET_c and K_c . In a table grape vineyard in California a linear correlation was found between leaf area and water consumption (Williams and Ayars, 2005). For “Tempranillo” wine grapes, a linear relationship was found between canopy cover and crop coefficient (López-Urrea et al., 2012). An additional study dealing with the same cultivar found a linear relationship between ground cover fraction and basal crop coefficient (K_{cb}) (Picón-Toro et al., 2012), which is defined as K_c when the soil surface is dry but transpiration is occurring while water supply does not limit transpiration (Allen et al., 1998). Quantification of leaf area and water consumption relations, when using continuous measurements through time, may benefit from statistical techniques designed for time-series analysis (Palumbo et al., 2011). Underlying patterns within multi-seasonal datasets may be extracted using complex modeling, as well as the interrelations of multiple meteorological variables (MV) measured throughout several consecutive seasons.

Machine learning (ML) techniques have been increasingly used in various agricultural applications, especially for spatial analysis and classification purposes (Behmann et al., 2015; Kamilaris and Prenafeta-Boldú, 2018). ML is used to autonomously solve large non-linear problems using multiple sources of data in order to provide information based on these large datasets and enable better management and decision-making across space and time (Chlingaryan et al., 2018). Studies regarding space-time processes in agriculture are commonly conducted (e.g. Waldner et al., 2015; Jin et al., 2016), especially using datasets collected using remote sensing. High-resolution time-series analysis of agricultural dynamics is typically conducted based on meteorological datasets relating to the global trend (Palumbo et al., 2011; Tabari et al., 2011) or forecasting methods such as autoregressive models and artificial neural networks (ANN) ML techniques (Landeras et al., 2009; Valipour, 2012). The gradient boosted regression trees (BRT) algorithm uses regression trees to study complex relationships between variables to generate a regression model. It is a robust method that is widely used for non-linear quantification, while dealing with different types of

predictor variables (continuous, thematic, binary) for projection of a response variable (Elith et al., 2008; Ohana-Levi et al., 2019a). BRT enables evaluation of the relative importance of predictor variables for forecasting and model interaction effects (Döpke et al., 2017) with very high accuracy and is suitable for dealing with seasonal meteorological datasets (Gu et al., 2019). Regression methods used for multivariable time-series analysis and forecasting are common in disciplines such as econometrics (Chen et al., 2014; Park and Phillips, 2001), public health (Elgar et al., 2015; Imai et al., 2015; Wu et al., 2017), and human behavior (Kaytez et al., 2015). To our knowledge, no study has incorporated LAI measurements into time-series models in order to define the interrelations between the meteorological and LAI variables and their effect on ET_c or for forecasting purposes. In this study, we propose a novel framework to analyze basic MV, LAI and ET_c interrelations while taking the temporal patterns of a multi-seasonal dataset into account. Moreover, we suggest an ensemble ML model to quantify the seasonal effects of MV and LAI on ET_c , and further use these interrelations to forecast ET_c for an entire growing season.

The purpose of this study was to analyze a multivariable time series to characterize seasonal patterns affecting water consumption (ET_c) of vines. The specific objectives were (1) to characterize the time-series interrelations between meteorological and vegetative factors affecting vine water consumption; (2) to determine the relative influence of meteorological and vegetative factors on ET_c ; and (3) to develop a temporal forecasting model for vine ET_c .

2. Materials and methods

2.1. Study site and experimental data

The Kida vineyard was selected for this experiment and is located in the central mountain region of Israel (lat 32.2°N, long. 35°E), at an altitude of 759 m above sea level. The *Vitis vinifera* ‘Cabernet Sauvignon’ vines in this vineyard were planted in 2007. Row orientation is east/west and the vines were trained to a vertical shoot positioning (VSP) trellis system with two foliage wires. The vines were designed as a bilateral cordon and pruned during the winter to 16 spurs, each comprising two buds (see Munitz et al. (2016b) for more detail on the structure and characteristics of the vineyard).

2.1.1. Study site – lysimeters and drainage collection system

The experiment included six drainage lysimeters (Fig. 1b), constructed in the second row of a commercial vineyard in order to avoid boundary effects. Each lysimeter was constructed from a tailor-made polypropylene tank (Fig. 1c) with a total volume of 1.47 m³, filled with local Terra Rossa soil (36.4% sand, 30.6% silt and 33% clay) aligned parallel to the soil surface (Fig. 1c). A local four-year-old vine was uprooted and replanted in each lysimeter tank, to simulate the vineyard conditions as accurately as possible. Two pipes (10 m long) were connected to the bottom of each lysimeter, draining the accumulated leachate water to a scaling system (Fig. 1a) placed in an underground, 2.5 m deep tunnel outside the vineyard (Fig. 1b and c). The volume of collected drainage water was weighed and recorded at 15 min intervals. The scaling system was calibrated manually twice a week. The lysimeters were irrigated via a computer-controlled system (Crystal Vision, Kibbutz Samar, Israel). The irrigation amounts provided to the lysimeter vines were designed to ensure ‘optimum soil water conditions’ (Allen et al., 1998). Irrigation was set on an hourly basis, i.e. 24 irrigation pulses per day. Irrigation initiated at a rate of 15 l day⁻¹ per vine, and when hourly drainage was lower than 200 ml the irrigation was increased by additional 5 l day⁻¹ (maximum values reached 45 l day⁻¹), thus exceeding the estimated amount of daily water consumption by 20–30%. During the 2013–2017 seasons the drip line of

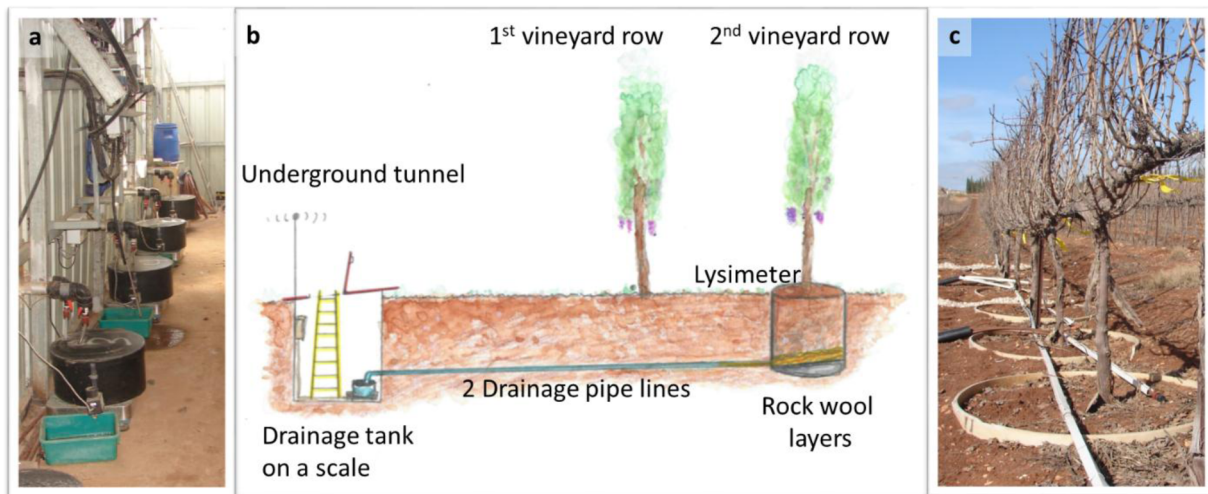


Fig. 1. General scheme of the lysimeter plot illustrating (a) drainage collection underground tunnel, the 30 l drainage collection tanks (black) mounted on scales in the underground tunnel; (b) a schematic side view of the system; and (c) an aboveground view of the six vines planted in the lysimeter tanks in the 2nd row of the vineyard.

each lysimeter was connected to a high-precision flowmeter (RS Pro Turbine Flow Meter, RS Components Ltd., Birchington Road, Corby, Northants, NN17 9RS, UK) and equipped with one compensated non-leakage 4 L h^{-1} drip emitter with 4 Split Curved Arrow Dripper emitters (Netafim, Israel) spaced 30 cm apart. The entire automated system was built and programmed by "Crystal Vision" company, Kibbutz Samar, Israel. For further detail regarding the lysimeter system functionality and design, see Munitz et al. (2019).

2.1.2. Acquisition and processing of crop evapotranspiration, leaf area index and meteorological datasets

Daily volumetric water consumption, ET_c , was calculated by subtracting the volume of collected water, over a 24 h period, from the irrigation amount supplied to each vine. The measure was then transformed to mm by multiplying the daily water volume per vine by 0.222, since vine spacing was $1.5 \times 3\text{ m}$, i.e. vine/area ratio is $2222\text{ vines ha}^{-1}$.

LAI of the lysimeter-grown vines was measured once a week during the growing seasons, using a canopy analysis system (SunScan model SS1-R3-BF3; Delta-T Devices, Cambridge, UK). The system uses a line-quantum sensor-array sensitive to photosynthetic active radiation (PAR). Each sample used observations of equal spacing (10 cm). The LAI non-destructive values obtained by this method were compared to destructive measurements collected after defoliation of 39 vines (different cultivars and sites) using an area meter (model 3100; Li-Cor, Lincoln, Nebraska). The measures of these two methods were found to be linearly and highly related ($R^2 = 0.922$; $P < 0.001$, (Netzer et al., 2019)).

Both ET_c and LAI measurements were averaged for the six lysimeter-grown vines to receive one representative time-series for each variable. For certain time periods, some values were missing from one or more lysimeters due to malfunction, and the average included the remaining data.

Vine LAI is known to increase until the canopy reaches a maximum values (Sarel Munitz et al., 2016a; Netzer et al., 2019). Therefore, values between each LAI measurement were linearly interpolated to determine a daily LAI value, using "zoo" package in R (Zeileis and Grothendieck, 2005). The ET_c series included several missing values that were interpolated using a weighted moving average algorithm, using a simple moving average window with a size of 4, applied with

the "imputeTS" package in R (Moritz and Bartz-Beielstein, 2017).

Meteorological data were obtained from a meteorological station located 50 m east of the lysimeters. The station was equipped with a combined temperature and humidity sensor at 2 m height (HMP155, Vaisala, Helsinki, Finland), wind speed and direction sensor at 10 m height (05103LM, Young, Traverse City, MI, USA), solar radiation pyranometer sensor at 2 m height (CM11, Kipp & Zonen, Delft, The Netherlands), and a data logger (CR1000, Campbell Science, Logan, UT, USA). The data were available at a one-hour temporal resolution in the Israeli Ministry of Agriculture agrometeorological web site (<http://www.meteo.co.il/home/map?TargetIds=9,3,0,1>). The MV in the dataset (Fig. 2) included mean daily values of meteorological data for temperature (T_{mean}), wind speed at 10 m (U_{10}) and relative humidity (RH_{mean}). Wind speed values were measured at an altitude of 10 m and were not transformed to values at an altitude of 2 m using $U_2 = 0.75 \cdot U_{10}$ (Eq. 47 in Allen et al. (1998), corresponding to a short-grassed surface), since this transformation is linear and would not have changed the distribution of the data. In addition, the surface roughness at the vineyard was not available, therefore a precise transformation of wind speed at 2 m was prone to errors. The active hours of transpiration were defined between 06:00 and 18:00 and the mean daily values for these variables were calculated for the 13 daytime hours. Missing values were completed from Talmon regional meteorological station, located 20 km from Kida vineyard at an altitude of 638 m above sea level and with a consistent similarity of meteorological conditions to the study site. Additionally, daily global solar radiation (R_n) was measured at 10 min intervals, and the accumulated daily sum of radiation was used for the time series dataset.

2.2. Time series decomposition

A time series may be analyzed for its underlying patterns of change over time by decomposing it into three latent sub-series (West, 1997) components: the trend, seasonality and remainder (see Appendix A for illustration). The decomposition procedure assumes that trend and seasonal components are smooth and change gradually. The trend represents the low frequency variation in the data along with nonstationary, long-term changes. The seasonal component captures the seasonal frequency and cycle of the data. The remainder component is the remaining random variation in the data after removal of the trend and

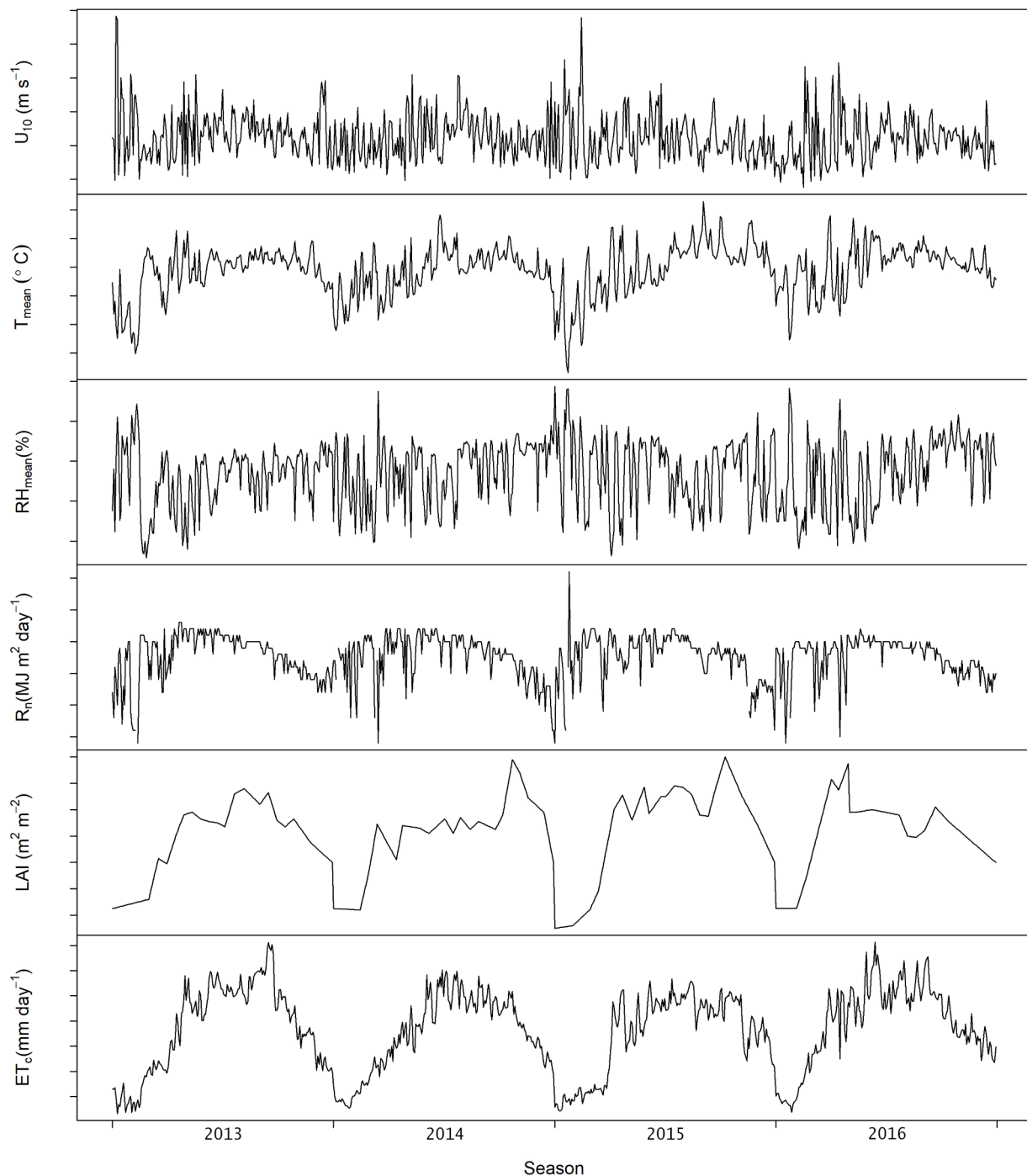


Fig. 2. Time-series illustration for the 2013–2016 growing seasons. The factors implemented to the forecasting model include the meteorological variables – mean daily wind speed (U_{10}), mean daily temperature (T_{mean}), mean daily relative humidity (RH_{mean}), and global daily solar radiation (R_n), as well as the vegetative factor leaf area index (LAI) and the response variable, crop evapotranspiration (ET_c). All variables were measured in a *Vitis vinifera* ‘Cabernet Sauvignon’ vineyard in Kida. The time-scale was between April 1st and September 30th (a total of 183 days per season) for each of the four seasons.

seasonality (Cleveland et al., 1990). Therefore, the time series may be represented as:

$$Y_t = T_t + S_t + R_t \tag{1}$$

where Y_t is the time series dataset, and T_t , S_t , and R_t are the trend, seasonal and remainder components, respectively. Decomposing the data promotes understanding of the underlying structure of the time series, and allows conducting of various manipulations while excluding specific components. The entire dataset was decomposed for modeling purposes described in Sections 2.3–2.5, using seasonal decomposition

of time series by Loess (STL) filtering procedure with the R package “stats” (R Core Team, 2018).

2.3. Interrelation of multiple variables affecting vine water consumption

The characterization of interrelations between the factors that affect vine water consumption (objective 2) was conducted by removing the time-based effects of temporal-related components from the data (Fig. 3a). The remainder components of the different variables were used to derive a matrix to calculate correlations between the

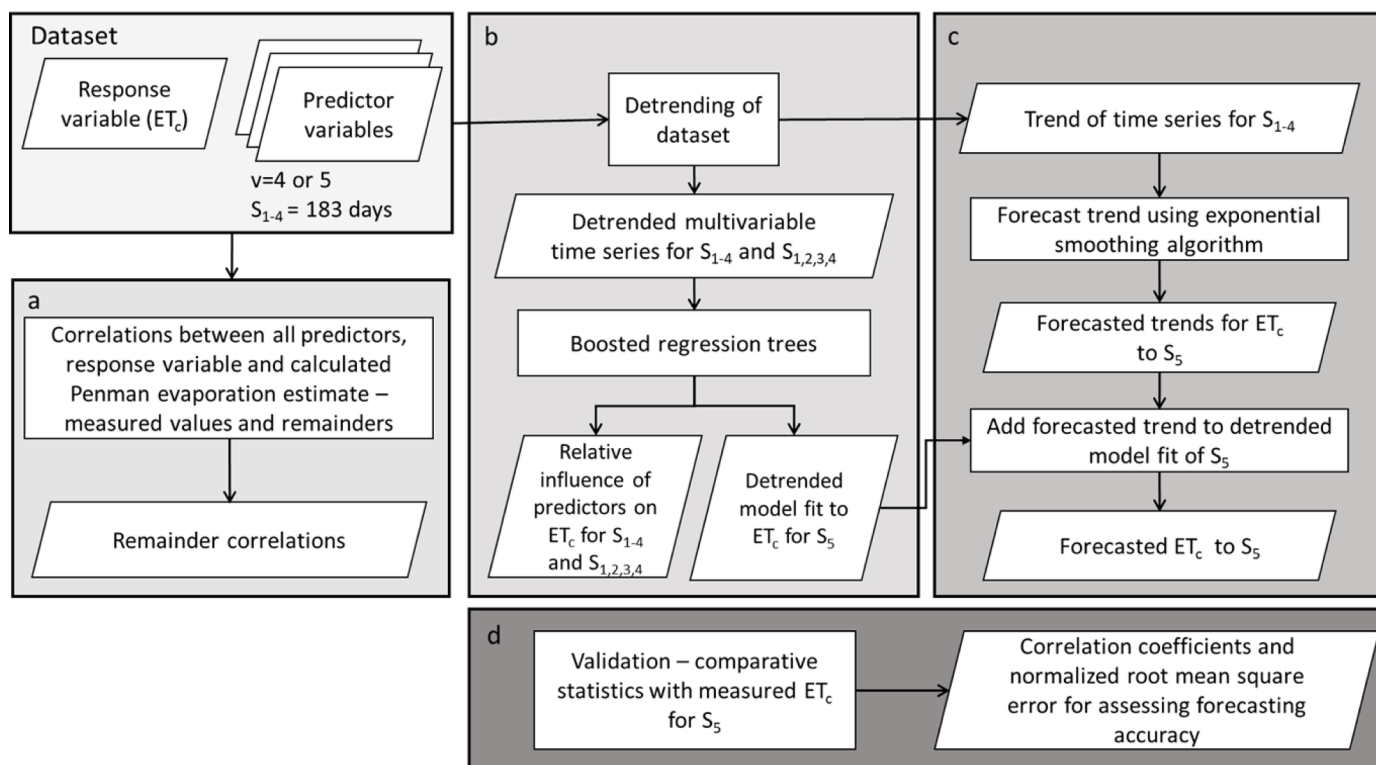


Fig. 3. A general description of the framework and analyses conducted for (a) defining the temporal interrelations between the different variables that were included in the forecast model for the training seasons (2013–2017, S_{1-4}); (b) fitting a forecast model for detrended crop evapotranspiration (dET_c), using two sets of predictors (meteorological with and without a detrended leaf area index variable) and analyzing multivariable effects for S_{1-4} and for each season separately ($S_{1,2,3,4} = 2013, 2014, 2015, 2016$); (c) fitting an ensemble of two models to forecast ET_c for the 2017 season (S_5); and (d) validation statistics to evaluate and compare model performance.

remainders of the variables specified in Section 2.1.2 (Fig. 2) (Gruber et al., 2002). Moreover, we provided the correlation coefficients between these factors and the remainder of ET_o . ET_o was calculated from the measured meteorological data, according to the Penman Monteith equation, and was added in order to quantify the relationship between this integrative measure and the variables used to build the model. Correlations were also calculated for the original set of data, in order to address the incorporated temporal effects of the time series on the interrelations between variables. Visualization of the correlation matrix was conducted using package “corrplot” in R (Taiyun Wei et al., 2017). Appendix B introduces additional analyses of time-series interrelations, namely the distance correlation matrix, that enables examination of the non-linear, serial dependencies between the variables, including all components, and accounts for the temporal nature of the multiple time-series by using a fixed lag (Edelmann et al., 2018; Fokianos and Pitsillou, 2018).

2.4. Model fitting and inter-seasonal comparison of factors affecting crop evapotranspiration and transpiration

In order to comply with objective (2) and determine the relative contribution of meteorological and vegetative predictors to ET_c variability, we applied the boosted regression trees (BRT) machine learning algorithm, using the extended “gbm” R package - “dismo” in R (Elith and Leathwick, 2015). BRT is a regression model consisting of one random response variable and a set of predictor variables, altogether composing a training sample. The model determines a function that calculates fitted values of the response variable based on the predictors, such that the expected value of a specified loss function is minimized (Friedman, 2002). A measure, in this case deviance, represents the loss in predictive performance. A series of trees is generated, where the predictor variables undergo a binary split that

generates a model fit to each section of the tree sequentially, such that each split point achieves the best model fit, and the best partitioning of the data is determined at each step. This process is repetitive until a stopping criterion for a minimized prediction error is reached, in order to avoid model overfitting. Boosting is a numerical optimization technique that minimizes the loss function by adding a new tree each step, which optimally reduces the loss function. Each additional tree is fitted to the residuals of the former tree, thus minimizing the deviance in each step. The values for each observation are re-estimated with each step and account for the contribution of the newly added tree (Elith et al., 2008). The final predicted value of an observation is formed by adding the weighted contribution of each tree.

The BRT model accounts for complex, non-linear relations between the response and predictor variables, and handles interaction effects between predictors. It is insensitive to outliers and unaffected by transformation. It handles different types of variables and accommodates missing data (Elith et al., 2008). Regression trees for multivariable time series analysis have been used for over a decade, mainly in the fields of econometrics and human behavior (Makridakis et al., 2018; Tso and Yau, 2007).

Regression trees models are limited in their ability to predict trend. These models forecast future values by incorporating rules derived from the training set. Therefore, the trend components of the variables that were used for this model were removed for this analysis, to eliminate using any long-term temporal patterns (Gu et al., 2019). The detrended ET_c (dET_c) was first modeled against four detrended predictor variables that included the meteorological variables (dMV) (i.e. dT_{mean} , dR_n , dRH_{mean} and dU_{10}), and then using the detrended LAI ($dLAI$) in addition to the dMV , to ascertain their extent and rank of influence. The model was performed for the entire time-series ($S_{1-4} = 2013-2016$) and then for each season separately ($S_{1-4} = 2013, 2014, 2015, 2016$), in order to analyze the inter-seasonal variability of the affecting

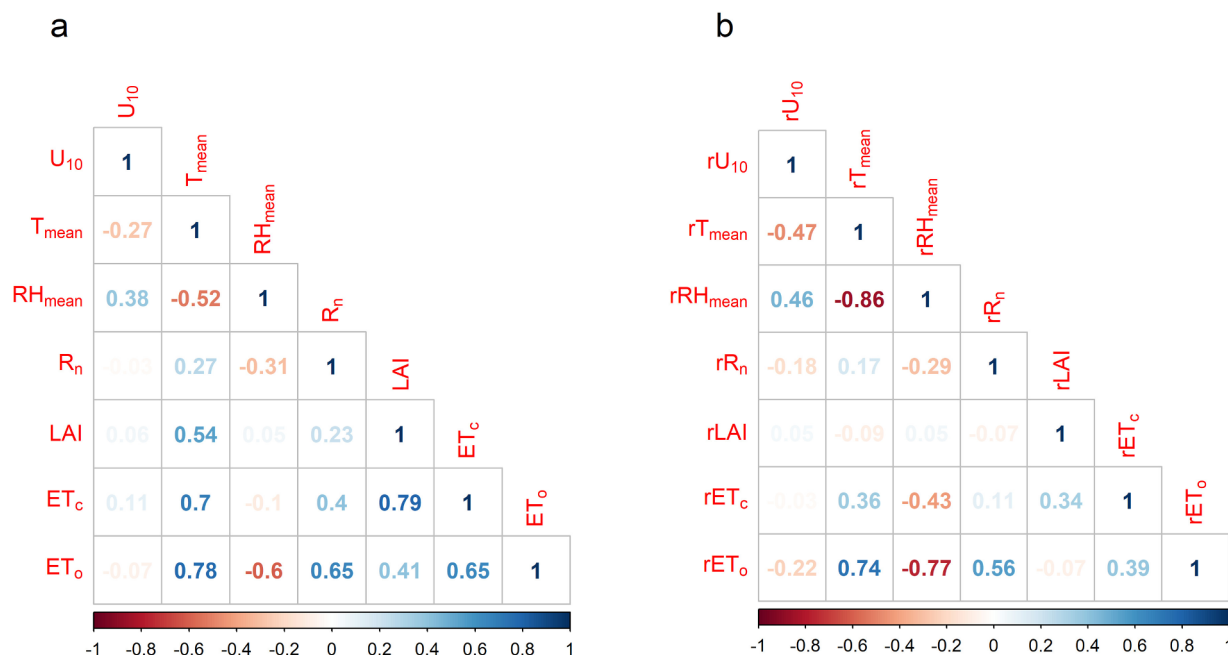


Fig. 4. Correlation matrix between all variables of interest for the 2013–2016 time-period, in a *Vitis vinifera* ‘Cabernet Sauvignon’ vineyard (Kida). In panel (a) the measured values of the variables were correlated. In panel (b) the temporal trend and seasonal components were removed from all variables and the correlations were calculated only for the remainders. The variables included the remainders of the meteorological variables mean daily wind speed (rU_{10}), mean daily temperature (rT_{mean}), mean daily relative humidity (rRH_{mean}), and total daily solar radiation (rR_n); the remainder of vegetative variable leaf area index ($rLAI$); the remainder of the response variable crop evapotranspiration (rET_c); and that of reference evapotranspiration (rET_o), according to the Penman Monteith equation.

predictors (Fig. 3b). In addition, a detrended prediction of ET_c for a test season ($S_5 = 2017$) was conducted using BRT as a part of a model ensemble (detailed in Section 2.5). The model performance was assessed by the training data correlation and cross-validation correlation using k-fold cross validation applied on the training set (Hastie et al., 2001) and provided by the BRT model.

2.5. Time-series analysis and ensemble method for forecasting – model description

Ensemble learning method for time-series forecasting are used to overcome specific limitations of forecasting models (Laurinec, 2018). In order to forecast ET_c to S_5 , we used a combination of forecasts from two different models resulting in a multivariable, unsupervised ensemble of two models. Section 2.4 described the first model of the ensemble, the BRT model, which incorporated a set of predictors (dMV and dMV + dLAI) in order to forecast d ET_c . The second model was selected to forecast only the trend component and add it to the d ET_c in order to derive a forecasted ET_c for S_5 (Fig. 3c) (Laurinec and Lucká, 2018). After testing several forecasting models, we used the exponential smoothing algorithm for trend forecasting (Hyndman et al., 2002), with the “forecast” package in R (Hyndman and Khandakar, 2008). The resulting forecasted trend was added to the d ET_c fitted values for S_5 , to generate a final projection for the 2017 growing season.

3. Results

3.1. Interrelations of multiple variables

The model variables together with ET_o were correlated to determine the interrelations of the variables including the time-related effects

(U_{10} , T_{mean} , RH_{mean} , R_n , LAI, ET_c , ET_o) (Fig. 4a). The strongest correlation among the MV was between T_{mean} and RH_{mean} (-0.52). ET_c showed the highest correlations to LAI (0.79) and T_{mean} (0.7). ET_o was positively correlated to T_{mean} (0.78), R_n (0.65) and ET_c (0.65), with a weaker negative correlation to RH_{mean} (-0.65). The variables were then cleaned from their temporal components and a correlation matrix was applied to determine the relations between their remainder (rU_{10} , rT_{mean} , rRH_{mean} , rR_n , $rLAI$, rET_c , rET_o) (Fig. 4b). The rT_{mean} was negatively linked to rRH_{mean} (-0.86), while the other relations between the remainders of the meteorological variables (rMV) were quite weak. rET_o was highly correlated with rT_{mean} (0.74) and rRH_{mean} (-0.77). The vegetative variable, $rLAI$, was found to be non-correlated to any of the variables, while rET_c experienced weak correlations (highest correlation was -0.43 with rRH_{mean}).

3.2. Inter-seasonal comparison of factors affecting evapotranspiration and transpiration

In order to determine the relative influence of meteorological and vegetative factors on ET_c , we used the BRT fitted model to quantify these contributions (Fig. 5). Table 1 summarizes the model performance statistics. For all models, using dMV + dLAI proved to enhance model performance. The models that fitted ET_c with dMV for S_{1-4} and $S_{1,2,3,4}$ (Fig. 5a) were characterized by an overall higher contribution of d T_{mean} to ET_c , ranging between 50.6 and 60.4%. d RH_{mean} , d U_{10} and d R_n were ranked differently for every season, with d RH_{mean} ranking second for S_{1-4} , S_3 and S_4 . The mean relative contribution of d T_{mean} , d R_n , d RH_{mean} and d U_{10} were 54, 17.3, 17.3 and 11.3%, respectively, with corresponding coefficients of variation of 0.06, 0.14, 0.11 and 0.31.

The model results for relative influence when including both dMV + dLAI showed a significant influence of dLAI compared to all

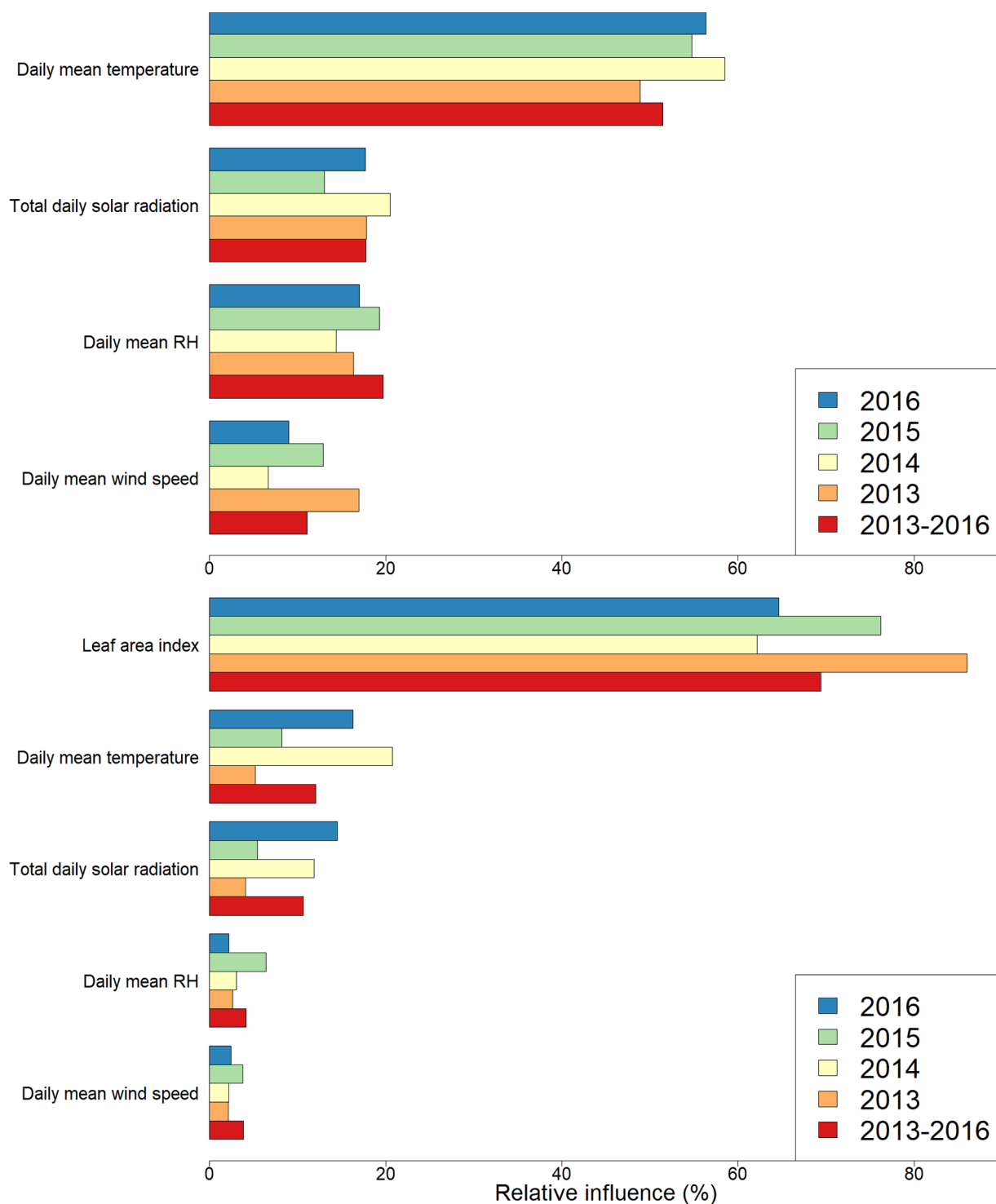


Fig. 5. The relative influence of (a) the four detrended meteorological variables (dMV); and (b) the dMV along with detrended leaf area index as predictors, on detrended vine evapotranspiration for the entire 2013–2016 time-period and for each of the seasons, in *Vitis vinifera* ‘Cabernet Sauvignon’ Kida vineyard.

dMV (Fig. 5b), with a contribution ranging between 62.1 and 86%. dT_{mean} was ranked second for all seasons, and R_n was the third influential variable for all seasons, aside from S₃ (2015). Analyzing the predictors mean relative influence on ET_c revealed that dLAI, dT_{mean}, dR_n, dRH_{mean} and dU₁₀ contributed 71.7, 12.5, 9.3, 3.7 and 2.9% to the model fitting, respectively, with corresponding coefficients of variation of 0.12, 0.44, 0.42, 0.41, and 0.27.

3.3. Time-series analysis and forecasting

The ensemble model for temporal forecasting of ET_c to S₅ was applied using the set of MV and again using MV + LAI. Fig. 6 shows the results for the forecasted ET_c using the different sets of predictors, compared to the measured reference values.

Table 2 summarizes the ensemble model performance for both fitted values (ET_c forecasting using MV and MV+LAI). Overall, the ET_c forecast using MV + LAI showed slightly better performance, with a

Table 1

Evaluation of model performance with training data correlation and cross validation correlation statistics. The model performance measures were compared between model fitting for detrended vine evapotranspiration (dET_c) using the four detrended meteorological variables (dMV) and the dMV along with the detrended leaf area index as predictors (dMV + dLAI). The comparison was conducted for the models of the entire 2013–2016 time period (S₁₋₄) and for each of the seasons (S_{1,2,3,4}), in *Vitis vinifera* ‘Cabernet Sauvignon’ Kida vineyard.

Model fitting	Training data	Correlation	Cross validation correlation	
	dMV	dMV + dLAI	dMV	dMV + dLAI
(2013–2016)	0.97	0.98	0.89	0.95
S ₁ (2013)	0.99	0.99	0.91	0.97
S ₂ (2014)	0.96	0.98	0.91	0.94
S ₃ (2015)	0.95	0.99	0.85	0.94
S ₄ (2016)	0.93	0.98	0.81	0.95

correlation of 0.9 between the fitted values and the measured ET_c for S₅, and nRMSE_{range} of 0.12. The range for both model approaches was smaller than the reference. Both forecasts were unable to capture large deviations from the seasonal component (clearly apparent in Fig. 6) and values larger than 6 mm day⁻¹ were not represented at all. However, the ensemble model accurately forecasted the overall seasonal nature of ET_c. For the first 90 days of S₅, the ET_c forecast using MV and MV + LAI resulted in correlation coefficients of 0.86 and 0.92, respectively, and corresponding nRMSE_{range} measures of 0.15 and 0.11.

4. Discussion

4.1. Interrelations of multiple variables

The relationship between various time-dependent variables may be derived at different temporal resolutions. If the focus is gathering information on seasonal-scale relations, then time components should be incorporated in the analysis, as Fig. 4a suggests. Nonetheless, multiple interrelations for short time intervals (daily, weekly) may require the removal of the general trend and the seasonal component to discard long-term trend effects, and apply correlation on the remainders (Fig. 4b). Alternatively, it is also appropriate to use the distance correlation matrix to incorporate the temporal autocorrelation into the

analysis (Table B1). Some of the correlation coefficients between certain variables changed considerably after detrending and deseasonalizing of the time series dataset. RH_{mean} and T_{mean} were poorly correlated ($r = -0.52$) when the measured time-series data was considered. The remainder correlation for this pair of variables, however, showed a major increase in the strength of their relationship ($r = -0.86$) after removing the seasonality and trend effects. Fig. 2 shows the distinct temporal pattern of RH_{mean}, which shows high variability between consecutive time steps. RH_{mean} does not capture a seasonal pattern, while T_{mean} is seasonally stationary. Therefore, once removing the seasonal component from the analysis, rT_{mean} and rRH_{mean} uncovered a much stronger relationship. Contrarily, ET_c and LAI showed a strong correlation ($r = 0.79$) due to a seasonal pattern, during which vines with more transpiring canopy essentially consume more water (Sarel Munitz et al., 2016b; Netzer et al., 2008). The ET_c-LAI correlation was especially strong in the early part of the season, a period characterized by rapid growth and frequent agro-technical interventions (shoot removal, hedging and wire lifting).

Meanwhile, the correlation coefficient for rET_c and rLAI dropped to 0.34. LAI was generated using interpolation between weekly measurements, therefore its remainders were not random as for ET_c. It is expected that actual daily LAI values change seasonally over time as a function of the nature of vine leaf development as well as temperature and solar radiation. Consequently, rET_c and rLAI were not strongly linked. Leaf area develops as a function of solar radiation and temperature levels (Menzel et al., 1987), serving as an intermediate variable, which acts as both a responder and a predictor. Leaf area is affected by some of the MVs, R_n and T_{mean}, while causally affecting ET_c. Similar to LAI-ET_c relations, T_{mean} and ET_c were also highly correlated at the seasonal scale, and their correlation coefficient was also found to be low in the remainder analysis.

ET_o (calculated according to Penman–Monteith equation) showed strong correlations with T_{mean} before and after removal of trend and seasonality effects (0.78 vs 0.74), since both display a very clear seasonal cycle and similar remainder patterns, meaning that they are interrelated in multiple temporal scales. ET_o and R_n also had quite similar seasonal patterns, and removing seasonal effects caused a decrease in their correlation strength (0.65 vs. 0.56). rET_o correlation with rRH_{mean} was stronger than ET_o against RH_{mean} (-0.77 vs -0.6, respectively), due to incompatible seasonal effects. ET_o and ET_c were moderately

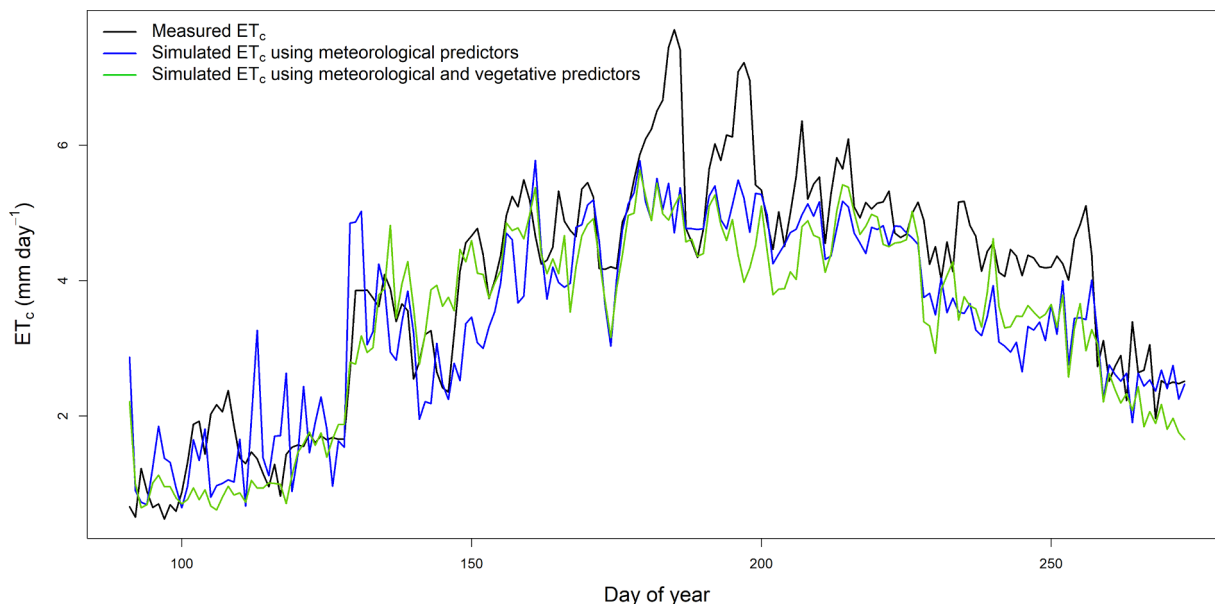


Fig. 6. Illustration of the multi-seasonal measured ET_c values (black line) and ET_c forecasts for the 2017 season. using only meteorological variables (MV) (blue line) and using the MV + leaf area index (LAI) (green line), in the *Vitis vinifera* ‘Cabernet Sauvignon’ Kida vineyard.

Table 2

Evaluation of model performance, using comparison between reference and forecasted values of ET_c with meteorological values (MV) as predictors, and MV + leaf area index (LAI). Comparison was applied for values of range, correlation coefficient, root mean squared error (RMSE) and normalized RMSE to range (nRMSE_{range}).

	ET_c simulation using meteorological predictors	ET_c simulation using meteorological and vegetative predictors
Range of measured values (mm day ⁻¹)	0.47–7.71	
Range of forecasted values (mm day ⁻¹)	0.59–5.79	0.61–5.61
Correlation	0.88	0.90
Root mean square errors (RMSE) (mm day ⁻¹)	0.92	0.90
Normalized RMSE (nRMSE _{range})	0.13	0.12

correlated ($r = 0.65$). ET_o was originally developed to be a reference for crop ET similar to a well irrigated hypothetical grass with an assumed canopy height of 0.12 m (Allen et al., 1998). ET_c , however, was measured for vines, a deciduous plant with a constantly changing leaf area that is expected to demonstrate more dynamic and diverse ET_c patterns throughout the season. The seasonal and trend components of ET_o and ET_c revealed similar patterns, although their remainders displayed much weaker relations ($r = 0.39$). By definition, ET_o was composed of the MV and therefore corresponded to their temporal and non-temporal components.

Analyzing time-series data may be more effective and definite when accounting for the different temporal components. We suggest that agricultural datasets, which are commonly collected at high temporal resolutions (hours/days), should be interpreted with regard to their seasonal trends, as well as the periodic temporal patterns. In many cases, the seasonality effect masks the true nature of higher-resolution interrelations between variables, and therefore decomposing the time-series to remove long-term trends and seasonal patterns is likely to highlight the underlying variability of the data (Gruber et al., 2002).

4.2. Leaf area-meteorology-evapotranspiration interactions

ET_c serves as the foundation for a skilled, knowledge-based, irrigation method (Allen et al., 2006, 1998). However, ET_c measurements of a specific crop are not independent of interaction effects. The FAO suggests using the standard crop coefficient method to account for these interactions. The daily crop coefficient (K_c) is calculated by dividing the ET_c by the daily ET_o . The K_c method aims to fit the ET_c to different climatic zones or different meteorological conditions during different seasons. Perennial deciduous trees typically display distinct rapid changes in canopy dimensions. Since leaves transpire water through their stomata, more leaves generate higher transpiration rates. In vines that are characterized by rapid canopy growth, ET_c and K_c are considerably affected by the leaf area (López-Urrea et al., 2012; Munitz et al., 2016b; Netzer et al., 2008; Williams and Ayars, 2005). This study demonstrates the extent of impact that LAI has on ET_c compared to MV (Fig. 5). Relative influence analysis was conducted through four seasons of training data, making the results reliable and accountable. Nevertheless, LAI relative influence on ET_c varied greatly between the different seasons. These discrepancies were likely due to differences in timing and extent of canopy agro-technical management between the seasons.

The first 90 days of S_5 were fitted less accurately using the ensemble model of MV and showed a stronger relationship when LAI was incorporated to MV. The first 90 days following budbreak occur within the spring season. In a Mediterranean climate, this season is characterized by high fluctuation of the MV, mainly temperature and radiation, which reduces the explanatory power of the regression model. Meanwhile, vine canopy development features a distinct and sharp increasing trend with a smoother pattern over time, due to minimal agro technical intervention.

4.3. Time series analysis and forecasting using model ensemble

The model ensemble that integrated both BRT for the detrended set of variables and an exponential smoothing algorithm for the ET_c trend was successful in forecasting the response variable for an entire growing season. Using LAI as an additional variable to the MV proved to enhance forecasting accuracy ($r = 0.9$), and improve model performance. Some of the cross validation correlation coefficients (Table 1) improved substantially with the addition of LAI to the model fitting. This addition increased reliability of the model ensemble for forecasting purposes. Forecasting may be applicable in scenario modeling, interpolation of missing data and generating projections for the future. A reliable model is therefore imperative to produce a dependable forecast. The weakness of the model in our study lies in its inability to project events that were not introduced to the learning process in the training data. Therefore, extreme values of ET_c were not forecasted (Fig. 6). The second part of the season was forecasted with less accuracy. This may be explained by various physiological processes that occur towards the end of the growing season, are not strongly affected by the MVs, and thus are underrepresented in the model. Water consumption decreases due to physiological deterioration and low stomatal conductivity in senescing leaves. LAI may still be at medium-high levels, however older leaves generate lower transpiration rates (Ohana-Levi et al., 2019b).

Forecasting ET_o time series has become common and is conducted using various time-series forecasting models such as autoregressive models (e.g. ARMA, ARIMA, SARIMA), Winter's model, and artificial neural networks (ANN) (Alves et al., 2017; Mohan and Arumugam, 1995; Valipour, 2012) with high success rates. However, using a multivariable model to forecast ET_c with a multiseasonal training set while incorporating LAI is a novel framework. Regression trees modeling is an appropriate choice for time-series forecasting when dealing with multivariable datasets (Laurinec, 2018), which enabled the integration of LAI into the forecasting procedure. The digital revolution in farming induces an increasingly growing number of variables that are routinely monitored across agricultural fields (Bronson and Knezevic, 2016). Availability and excess information of non-homogeneous and non-linear data necessitates the incorporation of data mining and automation techniques for identifying trends and patterns (Sharma and Mehta, 2012). This, however, requires a careful process of variable selection. The predictors that are included in regression trees models should be considered carefully and selected after accounting for their actual contribution to the response variable.

5. Conclusions

Leaf area has a pronounced effect on water consumption in vines and is worth further attention and investigation. The findings of this study demonstrate both the high extent and acute strength of the effect that a rapidly changing canopy in vines has on transpiration rates. Uncovering meteorological and vegetative temporal characteristics, patterns, interrelations and their relative contribution on

evapotranspiration may lead to a better understanding of water consumption processes and induce irrigation models that are more efficient.

When studying high-resolution sequential data that are temporally autoregressive, time series methods are highly useful. These statistical analyses may contribute to the decomposition of the data and exploration of seasonal and periodic patterns, and provide additional aspects of interrelations between temporally varying phenomena. In this study, we demonstrated an ensemble model for forecasting purposes. Ensemble models are advantageous for forecasting when dealing with complex datasets, though the specific models that compose the ensembles may be substituted by others, depending on the dataset and research objectives. Our proposed framework may be applied to other forms of agriculture, in other climatic regions and cultivars, and forecasting may be conducted for different time periods (e.g. daily, weekly, seasonally) or for various purposes (e.g. simulation of scenarios, interpolation for large amounts of missing data, etc.).

Declaration of Competing Interest

The authors declare that they have no known competing financial

Appendix A. decomposition example of ET_c

Fig. A1

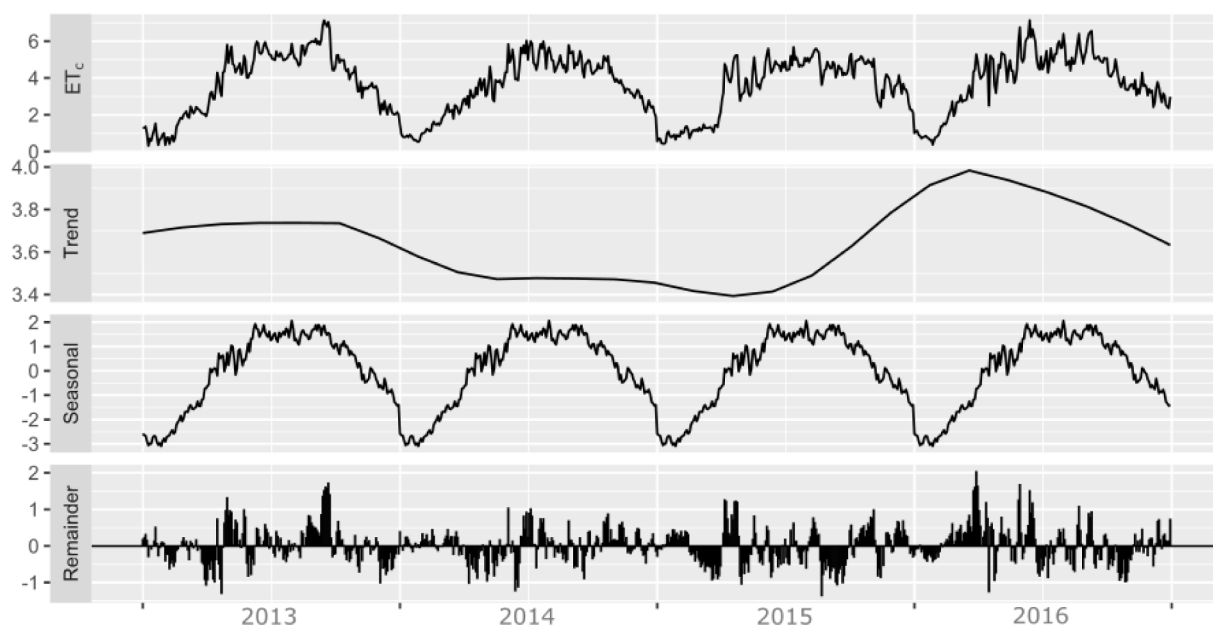


Fig. A1. An example of time-series decomposition, where the top panel illustrates crop evapotranspiration (ET_c) seasonal time-series, and the remaining panels include the three time-series components: trend, seasonal and remainder, for a four-season time period.

Appendix B. Time series distance correlation

Distance correlation is designed to characterize dependence among vectors of random variables and is used for analyzing multiple time series interrelations. The auto-distance correlation function enables identification of non-linear relationships between multivariate time series (Edelmann et al., 2018). This analysis tests whether a multiple time series is independent or similarly distributed regardless of possible dependence of its underlying components. The autodistance correlations are computed for a fixed lag that is predefined and checks the extent of multivariate interrelations for the specific time lag (Fokianos and Pitsillou, 2018). In this case, we examined the auto-distance correlation matrix for lag 2. This means that the dependencies between the different variables were examined for a two-day lag, to check the interrelations within this time lag. The analysis was applied using the R package dCovTS (Pitsillou and Fokianos, 2016).

Table B1 summarizes the results for the auto-distance correlation matrix for lag 2. Leaf area index (LAI) showed the strongest distance correlation with itself for lag=2, possibly since it is an interpolated measure with a low changing rate between consecutive days. Therefore, values between two specific days are likely to show similar values. In measured variables that have strong shifts in their values from one day to the next, such as mean daily wind speed (U_{10}), no dependencies were found. The strongest distance interrelation was found between LAI and crop evapotranspiration (ET_c), with a correlation of 0.69. This finding further confirms the boosted regression tree (BRT) model's findings that place LAI as a strong contributing factor to ET_c prediction and forecasting.

Table B1

Auto-distance correlation matrix of the meteorological variables mean daily wind speed (U_{10}), mean daily temperature (T_{mean}), mean daily relative humidity (RH_{mean}), total daily solar radiation (R_n), leaf area index (LAI), crop evapotranspiration (ET_c) and reference evapotranspiration (ET_o), according to the Penman Monteith equation, for lag = 2. All variables represent a four-season time series, measured in a *Vitis vinifera* 'Cabernet Sauvignon' vineyard in Kida.

	U_{10}	T_{mean}	RH_{mean}	R_n	LAI	ET_c	ET_o
U_{10}	0.01	0.04	0.01	0.01	0.03	0.06	0.05
T_{mean}	0.03	0.37	0.02	0.09	0.29	0.34	0.24
RH_{mean}	0.03	0.01	0.07	0.05	0.02	0.03	0.02
R_n	0.02	0.02	0.01	0.31	0.04	0.12	0.13
LAI	0.03	0.30	0.02	0.09	0.96	0.68	0.21
ET_c	0.03	0.39	0.02	0.20	0.69	0.84	0.36
ET_o	0.01	0.19	0.05	0.24	0.16	0.26	0.27

References

- Allen, R.G., Pereira, L.S., Raes, D., Smith, M., 1998. Crop Evapotranspiration-Guidelines for Computing Crop Water Requirements-FAO Irrigation and Drainage Paper 56. Food and Agriculture Organization, Rome.
- Allen, R.G., Pruitt, W.O., Wright, J.L., Howell, T.A., Ventura, F., Snyder, R., Itenfisu, D., Steduto, P., Berengena, J., Yrisarry, J.B., Smith, M., Pereira, L.S., Raes, D., Perrier, A., Alves, I., Walter, I., Elliott, R., 2006. A recommendation on standardized surface resistance for hourly calculation of reference ET_o by the FAO56 Penman-Monteith method. *Agric. Water Manag.* 81, 1–22. <https://doi.org/10.1016/J.AGWAT.2005.03.007>.
- Alves, W.B., Rolim, G., de, S., Aparecido, L.E., de, O., Alves, W.B., Rolim, G., de, S., Aparecido, L.E., de, O., 2017. Reference evapotranspiration forecasting by artificial neural networks. *Eng. Agrícola* 37, 1116–1125. <https://doi.org/10.1590/1809-4430-eng.agric.v37n6p1116-1125/2017>.
- Behmann, J., Mahlein, A.-K., Rumpf, T., Römer, C., Plümer, L., 2015. A review of advanced machine learning methods for the detection of biotic stress in precision crop protection. *Precis. Agric.* 16, 239–260. <https://doi.org/10.1007/s11199-014-9372-7>.
- Briggs, L.J., Shantz, H.L., 1916. Daily transpiration during normal growth period and its correlation with the weather. *J. Agric. Res.* 7.
- Bronson, K., Knezevic, I., 2016. Big data in food and agriculture. *Big Data Soc.* 3. <https://doi.org/10.1177/2053951716648174>.
- Chen, H., Cummins, J.D., Viswanathan, K.S., Weiss, M.A., 2014. Systemic risk and the interconnectedness between banks and insurers: an econometric analysis. *J. Risk Insur.* 81, 623–652. <https://doi.org/10.1111/j.1539-6975.2012.01503.x>.
- Chlingaryan, A., Sukkarieh, S., Whelan, B., 2018. Machine learning approaches for crop yield prediction and nitrogen status estimation in precision agriculture: a review. *Comput. Electron. Agric.* 151, 61–69. <https://doi.org/10.1016/J.COMPAE.2018.05.012>.
- Cleveland, R.B., Cleveland, W.S., McRae, J.E., Terpenning, I., 1990. STL: a seasonal-trend decomposition procedure based on loess. *J. Off. Stat.* 6, 3–33.
- Döpke, J., Fritsche, U., Pierdzioch, C., 2017. Predicting recessions with boosted regression trees. *Int. J. Forecast.* 33, 745–759. <https://doi.org/10.1016/J.IJFORECAST.2017.02.003>.
- Edelmann, D., Fokianos, K., Pitsillou, M., 2018. An updated literature review of distance correlation and its applications to time series. *Int. Stat. Rev.* <https://doi.org/10.1111/insr.12294>.
- Elgar, F.J., Pfortner, T.-K., Moor, I., De Clercq, B., Stevens, G.W.J.M., Currie, C., 2015. Socioeconomic inequalities in adolescent health 2002–2010: a time-series analysis of 34 countries participating in the Health Behaviour in School-Aged Children study. *Lancet* 385, 2088–2095. [https://doi.org/10.1016/S0140-6736\(14\)61460-4](https://doi.org/10.1016/S0140-6736(14)61460-4).
- Elith, J., Leathwick, J., 2015. Boosted Regression Trees for ecological modeling. *Ecol. Appl.* 25, 802–813. <https://doi.org/10.1111/j.1365-2656.2008.01390.x>.
- Elith, J., Leathwick, J.R., Hastie, T., 2008. A working guide to boosted regression trees. *J. Anim. Ecol.* 77, 802–813. <https://doi.org/10.1111/j.1365-2656.2008.01390.x>.
- Fokianos, K., Pitsillou, M., 2018. Testing independence for multivariate time series via the auto-distance correlation matrix. *Biometrika* 105, 337–352. <https://doi.org/10.1093/biomet/asx082>.
- Friedman, J.H., 2002. Stochastic gradient boosting. *Comput. Stat. Data Anal.* 38, 367–378. [https://doi.org/10.1016/S0167-9473\(01\)00065-2](https://doi.org/10.1016/S0167-9473(01)00065-2).
- Fuchs, M., Cohen, Y., Moreshet, S., 1987. Determining transpiration from meteorological data and crop characteristics for irrigation management. *Irrig. Sci.* 8, 91–99. <https://doi.org/10.1007/BF00259474>.
- Gruber, N., Keeling, C.D., Bates, N.R., 2002. Interannual variability in the North Atlantic ocean carbon sink. *Science* 298, 2374–2378. <https://doi.org/10.1126/science.1077077> (80-).
- Gu, H., Wang, J., Ma, L., Shang, Z., Zhang, Q., 2019. Insights into the BRT (Boosted regression trees) method in the study of the climate-growth relationship of Masson pine in Subtropical China. *Forests* 10, 228. <https://doi.org/10.3390/f10030228>.
- Hastie, T., Tibshirani, R., Friedman, J.H., Jerome, H., 2001. *The Elements of Statistical Learning: Data Mining, Inference, and Prediction*. Springer.
- Hyndman, R.J., Khandakar, Y., 2008. Automatic time series forecasting: the forecast package for R. *J. Stat. Softw.* 27, 1–22. <https://doi.org/10.18637/jss.v027.i03>.
- Hyndman, R.J., Koehler, A.B., Snyder, R.D., Grose, S., 2002. A state space framework for automatic forecasting using exponential smoothing methods. *Int. J. Forecast.* 18, 439–454. [https://doi.org/10.1016/S0169-2070\(01\)00110-8](https://doi.org/10.1016/S0169-2070(01)00110-8).
- Imai, C., Armstrong, B., Chalabi, Z., Mangtani, P., Hashizume, M., 2015. Time series regression model for infectious disease and weather. *Environ. Res.* 142, 319–327. <https://doi.org/10.1016/J.ENVRES.2015.06.040>.
- Jin, N., Tao, B., Ren, W., Feng, M., Sun, R., He, L., Zhuang, W., Yu, Q., 2016. Mapping irrigated and rainfed wheat areas using multi-temporal satellite data. *Remote Sens.* 8, 207. <https://doi.org/10.3390/rs8030207>.
- Kamilaris, A., Prenafeta-Boldú, F.X., 2018. Deep learning in agriculture: a survey. *Comput. Electron. Agric.* 147, 70–90. <https://doi.org/10.1016/J.COMPAE.2018.02.016>.
- Kaytez, F., Taplamacioglu, M.C., Cam, E., Hardalac, F., 2015. Forecasting electricity consumption: a comparison of regression analysis, neural networks and least squares support vector machines. *Int. J. Electr. Power Energy Syst.* 67, 431–438. <https://doi.org/10.1016/J.IJEPES.2014.12.036>.
- Landeras, G., Ortiz-Barredo, A., López, J.J., 2009. Forecasting weekly evapotranspiration with arima and artificial neural network models. *J. Irrig. Drain. Eng.* 135, 323–334. [https://doi.org/10.1061/\(ASCE\)IR.1943-4774.0000008](https://doi.org/10.1061/(ASCE)IR.1943-4774.0000008).
- Laurinec, P., 2018. Improving forecasting accuracy through the influence of time series representations and clustering. *Inf. Sci. Technol. Bull. ACM Slovak.* 10, 6–10.
- Laurinec, P., Lucká, M., 2018. Usefulness of unsupervised ensemble learning methods for time series forecasting of aggregated or clustered load. In: Appice, A., Loglisci, C., Manco, G., Masciari, E., Ras, Z. (Eds.), *New Frontiers in Mining Complex Patterns*, Eds. Springer, Cham, pp. 122–137. https://doi.org/10.1007/978-3-319-78680-3_9.
- López-Urrea, R., Montoro, a., Mañas, F., López-Fuster, P., Fereres, E., 2012. Evapotranspiration and crop coefficients from lysimeter measurements of mature 'Tempranillo' wine grapes. *Agric. Water Manag.* 112, 13–20. <https://doi.org/10.1016/j.agwat.2012.05.009>.
- Makridakis, S., Spiliotis, E., Assimakopoulos, V., 2018. Statistical and Machine Learning forecasting methods: concerns and ways forward. *PLoS One* 13, e0194889. <https://doi.org/10.1371/journal.pone.0194889>.
- Menzel, C.M., Simpson, D.R., Winks, C.W., 1987. Effect of temperature on growth, flowering and nutrient uptake of three passionfruit cultivars under low irradiance. *Sci. Hortic.* 31, 259–268. [https://doi.org/10.1016/0304-4238\(87\)90051-3](https://doi.org/10.1016/0304-4238(87)90051-3).
- Mohan, S., Arumugam, N., 1995. Forecasting weekly reference crop evapotranspiration series. *Hydrol. Sci. J.* 40, 689–702. <https://doi.org/10.1080/02626669509491459>.
- Monteith, J.L., 1965. Evaporation and environment. *Symp. Soc. Exp. Biol.* 19, 205–234.
- Moritz, S., Bartz-Beielstein, T., 2017. imputeTS: time series missing value imputation in R. *J. R. Stat. Soc. Ser. B* 79, 207–218. <https://doi.org/10.32614/RJ-2017-009>.
- Munitz, S., Schwartz, A., Netzer, Y., 2016a. Sustained and regulated deficit irrigation of field grown Merlot grapevines. *Aust. J. Grape Wine Res.* 23, 87–94. <https://doi.org/10.1111/ajgw.12241>.
- Munitz, S., Schwartz, A., Netzer, Y., 2019. Water consumption, crop coefficient and leaf area relations of a *Vitis vinifera* cv. "Cabernet Sauvignon" vineyard. *Agric. Water Manag.* 219, 86–94. <https://doi.org/10.1016/J.AGWAT.2019.03.051>.
- Munitz, S., Schwartz, A., Netzer, Y., 2016b. Evaluation of seasonal water use and crop coefficients for 'Cabernet Sauvignon' grapevines as the base for skilled regulated deficit irrigation. *Acta Hortic.* 33–40. <https://doi.org/10.17660/ActaHortic.2016.1115.6>.
- Netzer, Y., Munitz, S., Shtein, I., Schwartz, A., 2019. Structural memory in grapevines: early season water availability affects late season drought stress severity. *Eur. J. Agron.* 105, 96–103. <https://doi.org/10.1016/J.EJA.2019.02.008>.
- Netzer, Y., Yao, C., Shenker, M., Bravdo, B., Schwartz, A., 2008. Water use and the development of seasonal crop coefficients for Superior Seedless grapevines trained to an open-gable trellis system. *Irrig. Sci.* 27, 109–120. <https://doi.org/10.1007/s00271-008-0124-1>.
- Ohana-Levi, N., Bahat, I., Peeters, A., Shtein, A., Netzer, Y., Cohen, Y., Ben-Gal, A., 2019a. A weighted multivariate spatial clustering model to determine irrigation management zones. *Comput. Electron. Agric.* 162, 719–731. <https://doi.org/10.1016/J.COMPAE.2019.05.012>.
- Ohana-Levi, N., Munitz, S., Ben-Gal, A., Netzer, Y., 2019b. Evaluation of within-season grapevine evapotranspiration patterns and drivers using generalized additive models. *Agric. Water Manag.* accepted f.
- Palumbo, A.D., Vitale, D., Campi, P., Mastrorilli, M., 2011. Time trend in reference evapotranspiration: analysis of a long series of agrometeorological measurements in southern Italy. *Irrig. Drain. Syst.* 25, 395–411. <https://doi.org/10.1007/s10795-012-9132-7>.
- Park, J.Y., Phillips, P.C.B., 2001. Nonlinear regressions with integrated time series.

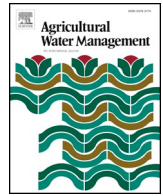
- Econometrica 69, 117–161. <https://doi.org/10.1111/1468-0262.00180>.
- Penman, H.L., 1948. Natural evaporation from open water, bare soil and grass. *Proc. R. Soc. Lond. Ser. A Math. Phys. Sci.* 193, 120–145. <https://doi.org/10.1098/rspa.1948.0037>.
- Picón-Toro, J., González-Dugo, V., Uriarte, D., Mancha, L.A., Testi, L., 2012. Effects of canopy size and water stress over the crop coefficient of a “Tempranillo” vineyard in south-western Spain. *Irrig. Sci.* 30, 419–432. <https://doi.org/10.1007/s00271-012-0351-3>.
- Pierce, L.T., 1958. Estimating seasonal and short-term fluctuations in evapo-transpiration from meadow crops. *Bull. Am. Meteorol. Soc.* 39, 73–78. <https://doi.org/10.1175/1520-0477-39.2.73>.
- Pitsillou, M., Fokianos, K., 2016. dCovTS: distance covariance and correlation for time series analysis. *R J.* 8, 324–340.
- R Core Team, 2018. R: a language and environment for statistical computing.
- Rana, G., Katerji, N., 2000. Measurement and estimation of actual evapotranspiration in the field under Mediterranean climate: a review. *Eur. J. Agron.* 13, 125–153. [https://doi.org/10.1016/S1161-0301\(00\)00070-8](https://doi.org/10.1016/S1161-0301(00)00070-8).
- Sharma, L., Mehta, N., 2012. Data mining techniques: a tool for knowledge management system in agriculture. *Int. J. Sci. Technol. Res.* 1, 67–73.
- Tabari, H., Marofi, S., Aeini, A., Talae, P.H., Mohammadi, K., 2011. Trend analysis of reference evapotranspiration in the western half of Iran. *Agric. For. Meteorol.* 151, 128–136. <https://doi.org/10.1016/J.AGRFORMET.2010.09.009>.
- Taiyun Wei, M., Taiyun Wei cre, A., Simko aut, V., Levy ctb, M., Xie ctb, Y., Jin ctb, Y., Zemla ctb, J., 2017. Package “corrplot”: visualization of a Correlation Matrix.
- Tao, F., Yokozawa, M., Zhang, Z., 2009. Modelling the impacts of weather and climate variability on crop productivity over a large area: a new process-based model development, optimization, and uncertainties analysis. *Agric. For. Meteorol.* 149, 831–850. <https://doi.org/10.1016/J.AGRFORMET.2008.11.004>.
- Tso, G.K.F., Yau, K.K.W., 2007. Predicting electricity energy consumption: a comparison of regression analysis, decision tree and neural networks. *Energy* 32, 1761–1768. <https://doi.org/10.1016/J.ENERGY.2006.11.010>.
- Valipour, M., 2012. Ability of box-jenkins models to estimate of reference potential evapotranspiration (A case study: mehrabad synoptic station, Tehran, Iran). *IOSR J. Agric. Vet. Sci.* 1, 1–11.
- Waldner, F., Canto, G.S., Defourny, P., 2015. Automated annual cropland mapping using knowledge-based temporal features. *ISPRS J. Photogramm. Remote Sens.* 110, 1–13. <https://doi.org/10.1016/J.ISPRSJPRS.2015.09.013>.
- Watson, D.J., 1947. Comparative physiological studies on the growth of field crops: I. Variation in net assimilation rate and leaf area between species and varieties, and within and between years. *Ann. Bot.* 11, 41–76. <https://doi.org/10.1093/oxfordjournals.aob.a083148>.
- West, M., 1997. Time series decomposition. *Biometrika* 84, 489–494. <https://doi.org/10.1093/biomet/84.2.489>.
- Widstoe, J.A., 1909. Irrigation investigations: factors influencing evaporation and transpiration. *Utah Agric. Exp. Stn. Bull.* 105.
- Williams, L.E., Ayars, J.E., 2005. Grapevine water use and the crop coefficient are linear functions of the shaded area measured beneath the canopy. *Agric. For. Meteorol.* 132, 201–211. <https://doi.org/10.1016/j.agrformet.2005.07.010>.
- Williams, L.E., Phene, C.J., Grimes, D.W., Trout, T.J., 2003. Water use of mature Thompson Seedless grapevines in California. *Irrig. Sci.* 22, 11–18. <https://doi.org/10.1007/s00271-003-0067-5>.
- Wu, H., Cai, Y., Wu, Y., Zhong, R., Li, Q., Zheng, J., Lin, D., Li, Y., 2017. Time series analysis of weekly influenza-like illness rate using a one-year period of factors in random forest regression. *Biosci. Trends* 11, 292–296. <https://doi.org/10.5582/bst.2017.01035>.
- Zeileis, A., Grothendieck, G., 2005. zoo: S3 infrastructure for regular and irregular time series. *J. Stat. Softw.* 14, 1–27. <https://doi.org/10.18637/jss.v014.i06>.

2.5: Chapter 5:

Evaluation of within-season grapevine evapotranspiration patterns and drivers using generalized additive models

Noa Ohana-Levi, Sarel Munitz, Alon Ben-Gal and Yishai Netzer

Published in Agricultural Water management November 2019



Evaluation of within-season grapevine evapotranspiration patterns and drivers using generalized additive models

Noa Ohana-Levi^c, Sarel Munitz^{b,d}, Alon Ben-Gal^c, Yishai Netzer^{a,b,*}

^a Department of Chemical Engineering, Biotechnology and Materials, Ariel University, Ariel, 40700, Israel

^b Department of Agriculture and Oenology, Eastern R&D Center, Israel

^c Department of Soil, Water and Environmental Sciences, Agricultural Research Organization, Gilat Research Center, Mobile post Negev 2, 85280, Israel

^d R.H. Smith Institute of Plant Science and Genetics in Agriculture, Faculty of Agriculture, Food and Environment, The Hebrew University of Jerusalem, Rehovot, 76100, Israel

ARTICLE INFO

Keywords:

Phenological growth stages
Drainage lysimeters
Leaf area index
Multivariable non-linear regression
Time-series analysis
Temporal autocorrelation

ABSTRACT

Evapotranspiration (ET_c) levels are influenced by the area of plant canopy, atmospheric conditions, plant physiology, and soil-water relations, which are all subjected to changes throughout the growing season. Understanding temporal trends, variability, and interactions between ET_c and its governing factors is valuable for modeling, predictions and vineyard water management. Our research objective was to quantify temporal patterns of ET_c of 'Cabernet Sauvignon' grapevines and affecting meteorological (temperature, relative humidity, radiation, wind speed) and vegetative (leaf area) factors during the growing season and within five phenological growth stages (0–4). Temporal variability of ET_c was modeled using five consecutive seasons of lysimeter time-series data, capturing the non-stationary nature of the data in terms of seasonality, trends and within-seasonal patterns. The temporal dependence of ET_c and its drivers throughout growing seasons was evaluated using the Box-Pierce test, autocorrelation function (ACF) and partial ACF. Patterns of the relations between ET_c and its covariates were quantified using multiple nonlinear regression, the generalized additive model (GAM), at the full growing season scale and for each phenological stage. Further examination on the effect of leaf area on ET_c was conducted using area under curve calculations and ET_c -leaf area ratio. The results demonstrate temporal autocorrelation structure of the data, supporting the incorporation of time variables in the GAM. Each phenological stage had a unique composition of relative importance of the covariates, with variation in ET_c being largely explained by time variables. Ordinarily, ET_c in early season (Stage 0) and at late season (Stage 3, approaching harvest) was mostly influenced by leaf area dynamics, while in mid-season it was highly affected by temperature. The GAM enabled quantification of within-seasonal patterns of interrelations between covariates and their effects on ET_c , and revealed inter-seasonal variability due to dissimilar meteorological conditions. Agro-technical management affects canopy dimensions and structure, thus influencing ET_c -leaf area relations.

1. Introduction

Evapotranspiration (ET) in agricultural crops refers to water loss to the atmosphere by evaporation (E) from the soil surface and transpiration (T) from the plant canopy via the stomata in the leaves (Allen et al., 1998). Crop evapotranspiration (ET_c) levels are affected by the structure and area of the plant canopy, atmospheric conditions, plant physiology (e.g. stomatal response to various processes including canopy senescence, atmospheric evaporation rates, and biotic factors), and soil-related conditions (Allen et al., 1998; Munitz et al., 2019). Numerous techniques have been suggested to determine ET_c , including in-situ or lysimeter based measurements of water balance,

micrometeorological-based energy balance measurements including eddy covariance, and plant-based measurements, such as sap flow (Rana and Katerji, 2000). For decades, lysimeter systems set in the true context of growing vegetation (Pereira et al., 2015) have been established as an accurate source of water consumption data (Hargreaves, 1974; Wright, 1990). ET_c measurements in vines are documented by using either drainage lysimeters (Evans et al., 1993; Netzer et al., 2009; Munitz et al., 2019) or weighing lysimeters (Williams et al., 2003; López-Urrea et al., 2012).

Irrigation management in agricultural crops often aspires to decrease water input and provide more efficient water use practices, as a method to increase crop profitability. In wine grape cultivation, there is

* Corresponding author at: Department of Chemical Engineering, Biotechnology and Materials, Ariel University, Ariel, 40700, Israel.
E-mail address: yishaine@ariel.ac.il (Y. Netzer).

<https://doi.org/10.1016/j.agwat.2019.105808>

Received 7 June 2019; Received in revised form 26 August 2019; Accepted 19 September 2019
0378-3774/ © 2019 Elsevier B.V. All rights reserved.

a paramount demand to acquire accurate ET_c data to support deficit irrigation modeling, which, in red wine grapes, is fundamental for determining the amount of grapes and their quality and thus wine value (Van Leeuwen et al., 2009; Munitz et al., 2016; Shtein et al., 2017; Netzer et al., 2019). Quantification of ET_c is widely used to assess the amount of water consumed by the plant, where it is imperative to assess crop water demand to design irrigation systems (López-Urrea et al., 2006), develop irrigation models (Munitz et al., 2016, 2019, Netzer et al., 2019) and increase efficiency in vineyard management. Multiple factors and drivers affect ET_c patterns throughout the growing season. Weather parameters, crop characteristics and environmental conditions (Allen et al., 1998), including their temporal variability, dynamics and interrelations are all expected to influence ET_c variability. Defining the factors that affect dynamics throughout the season and evaluating expected physiological and vegetative performance may assist in understanding ET_c patterns and provide projection models for vineyards with no direct ET_c measurements. Lopez-Urrea et al (2012) used weighing lysimeters in a *Vitis vinifera* cv. Tempranillo vineyard to quantify ET_c variability and related processes that effected it, including canopy cover. Picón-Toro et al (2012) also studied Tempranillo grapevines by using a long-term lysimeteric-derived dataset to assess the relationship between water consumption, canopy size and associated thermal time. Williams et al (2003) studied the relationships between ET_c associated factors such as leaf area, net radiation, and temperature in Thompson Seedless grapevines in California. The same experiment also recognized the association between leaf area and vine water consumption (Johnson et al., 2005). In a study conducted in Spain, Montoro et al. (2017) fitted several linear regression models to evaluate the strengths of relations between Tempranillo grapevine transpiration derived from lysimeters and several meteorological variables acquired from a weather station. These included relative humidity, global solar radiation, air temperature, wind speed, vapour pressure deficit and nocturnal CO_2 flux. Their findings show a strong relationship between transpiration and air temperature ($R^2 = 0.85$) followed by wind speed ($R^2 = 0.73$).

ET_c drivers frequently feature non-linear relationships that should be considered while modeling these impacts. Furthermore, as ET_c time-series, as well as most of its drivers, are measured at a high temporal resolution, the temporal variability and autocorrelation of datasets are critical for understanding processes and their interactions. The temporal pattern of ET_c and its associated affecting factors should be accounted for using a regression model while capturing the non-stationarity of the data, in terms of seasonality, long-term trends, daily variations and within-seasonal patterns. Other disciplines have successfully incorporated such an approach with non-stationary meteorological data. For example, urban ozone levels were associated with various non-stationary, meteorological predictors, accounting for temporal effects using seasonal terms in a regression model (Bloomfield et al., 1996). In a regression analysis of atmospheric conditions affecting human mortality in Alabama and Pennsylvania, time of season was incorporated as a predictor to account for intra-seasonal timing of mortality events and consecutive days was an additional input that controlled for temporal variations of the data (Smoyer et al., 2000). In a study conducted in Oslo, a set of meteorological predictors along with traffic volume were chosen to analyze air pollution, applying a generalized additive model (GAM) with two time variables, day number, which controlled for long-term seasonal variation in the dataset, and hour of day, accounting for diurnal time-dependencies of the covariates (Aldrin and Haff, 2005).

At a given location, grapevine ET_c variability is usually similar over different seasons, aside from specific variations due to particular, distinct meteorological events (e.g. Montoro et al., 2008). Along each season, there is high variability in vine water consumption as the crop growth cycle progresses (Evans et al., 1993; Zhang et al., 2010; López-Urrea et al., 2012; Munitz et al., 2019). Commonly, studies classify within-seasonal sub-periods, such as phenological growth stages or months, for specific definition of intra-seasonal variation in crop-

related dynamics (Azevedo et al., 2008; Zhang et al., 2010; López-Urrea et al., 2012). While some studies have dealt with the impact of meteorological and vegetative factors on vine water consumption (López-Urrea et al., 2012; Montoro et al., 2017; Wang et al., 2019), there is still a lack of information on relative importance (RI) of each predictor on water consumption. To the best of our knowledge, no work has dealt with quantifying the intra-seasonal variability of the interrelations of meteorological and vegetative factors affecting water consumption in grapevines.

The objective of this study was to quantify the temporal patterns of ET_c and its drivers for 'Cabernet Sauvignon' vines during the growing season. Specific objectives were (1) to examine temporal autoregressive features of ET_c and its drivers throughout the growing season; (2) to identify temporal patterns of the relations between ET_c and meteorological covariates as well as a vegetative predictor at the full-season scale and for each phenological growth stage; and (3) to quantify the relationship between LAI and ET_c for the entire growing season and for each growth stage.

2. Methodology

2.1. Study site

This study was based on experimental data collected by and specified in Munitz et al. (2019). The vineyard is located in the central mountain region of Israel (lat 32.2°N, long. 35°E), at an altitude of 759 m above sea level. The climate is semi-arid Mediterranean with rainfall events commonly occurring during winter (multiannual average of 415 mm), and warm, dry summers. The experiment was conducted in the Kida commercial vineyard, planted in 2007 with *Vitis vinifera* 'Cabernet Sauvignon' vines, and trained to a 2-m-high vertical shoot positioning (VSP) trellis system with two foliage wires. Vine spacing was 3 m between rows and 1.5 m between neighboring vines, with a density of 2222 vines per hectare and rows oriented east-west.

2.2. Data collection

2.2.1. Monitoring crop evapotranspiration, leaf area index and meteorological factors

The ET_c dataset was acquired from six drainage lysimeters (Fig. 1) located in the second row of the Kida vineyard. The system included six polyethylene 1.47 m³ containers (1.3 m high X1.2 m diameter), filled with local Terra Rossa soil (36.4% sand, 30.6% silt and 33% clay with bulk density of 1.25 g cm⁻³) buried in the ground, with their surfaces aligned with the soil surface. The lysimeters each included a bottom layer of highly conductive porous rockwool media in contact with the soil, and two drainage pipes, connected to the base of each tank, extending the rockwool downward 40 cm from the bottom soil boundary. The rockwool layer and extension disallowed saturation at the lower soil boundary while permitting movement of water out of the soil and leachate collection (Ben-Gal and Shani, 2002). The leachate was further drained to a scaling system, placed in a 2.5-m-deep underground tunnel located 7 m outside the vineyard (Fig. 1a). During the winter of 2011, a four-year-old vine was replanted in each tank. The lysimeter vines were treated with the same growing practices as the local commercial vineyard, except for irrigation. Each lysimeter was irrigated with a tailor-made computer controlled system (Crystal Vision, Kibbutz Samar, Israel), with irrigation amounts that exceeded the estimated daily water consumption of vines by 20–30%, thus ensuring 'optimum soil water conditions' (Allen et al., 1998).

In this paper, we considered the data of five growing seasons, between 2013 and 2017. The time series data from the six lysimeters were averaged and occasional missing values were determined using a weighted moving average algorithm with a simple moving average window ($= 4$ days), applied with the "imputeTS" package in R (Moritz and Bartz-Beielstein, 2017).



Fig. 1. The lysimeter system (a) Below-ground drainage collection tanks on scales; and (b) *Vitis vinifera* cv. 'Cabernet Sauvignon' vines planted in lysimeters during mechanical hedging. Kida Vineyard, 2014.

Whole plant leaf area of each lysimeter-grown vine was quantified using leaf area index (LAI) indirect measurements with a canopy analysis system (SunScan model SS1-R3-BF3; Delta-T Devices, Cambridge, U). LAI was measured once a week close to midday with zenith angle under 30° . The LAI for each vine (one in each lysimeter) was calculated from 31 observations of equal spacing (10 cm). For further information on LAI measurement techniques and validation, see Netzer et al (2009) and Munitz et al. (2019). The six values (one for each lysimeter-grown vine) were averaged. A linear interpolation between each consecutive pair of mean LAI values was performed to generate daily LAI values, using "zoo" package in R (Zeileis and Grothendieck, 2005).

Weather data were obtained from a meteorological station located in the vineyard. For further details regarding the sensors and equipment, see Munitz et al. (2019). The meteorological data included hourly measurements, from which only the data gathered between 06:00 and 18:00¹, defined as active hours of transpiration (Dragoni et al., 2006), were selected and averaged. Daily mean values of meteorological data were acquired for temperature (T_{mean}), wind speed measured at 10 m height (U_{10}) and relative humidity (RH_{mean}). Daily total solar radiation (R_n) was an accumulation of 10-min solar radiation measures. Missing values were filled based on measurements from Talmon regional meteorological station, located 20 km from Kida vineyard at an altitude of 638 m above sea level.

2.2.2. Determining phenological growth stages in the vineyard

The growing season was segmented into five phenological stages (Munitz et al., 2019; Rogiers et al., 2017): Stage 0 – from bud-break to bloom, Stage 1 – from full bloom to bunch closure, Stage 2 – from bunch closure to veraison, Stage 3 – from veraison to harvest, and Stage 4 – post-harvest until leaf defoliation (Table 1). Whole seasons were defined as beginning on April 1 and ending on September 30 each year, while specific start dates of each stage varied between seasons. Analyzing within-seasonal patterns of water consumption with regard to the growth stages required uniform start-dates for the different stages for all five seasons. Therefore, the data is presented according to averaged start date for the five growing seasons.

2.3. Temporal dependence of crop evapotranspiration and its drivers

Temporal patterns analyses of vine ET_c and its drivers throughout growing seasons and phenological stages may benefit from higher accuracy levels when the time-dependent structure (i.e. is non-stationarity) and the strong seasonal component of the time series dataset are

considered. Moreover, if the dataset is indeed temporally auto-correlated, then the relationships between the response and predictor variables should incorporate temporal components in order to account for variability in time. A time-series is considered non-stationary when its statistical properties (i.e. mean, variance, and covariance) are not constant over time. This may be evaluated using a statistical test for checking independence in a time series. In this study, we used the Box-Pierce test to check for non-stationarity of ET_c , the meteorological variables and LAI. Additionally, we applied the autocorrelation function (ACF) to the ET_c time series to check for correlations between different lags (k), where $k = 183$, since each season has 183 observations (days). In addition, we applied the partial ACF (PACF) to check the correlation at a certain lag after removing the effect of any correlations at shorter lags (Cowpertwait and Metcalfe, 2009). The autocorrelation for a specific lag is comprised of both the direct and indirect correlations between observations, where indirect correlations are a linear function of the correlation of a certain lag with lags at intervening time-steps. The PACF seeks to remove these effects and define only the direct temporal correlations between observations at any lag. The significant lags indicated the extent of dependence of the time series, or its autocorrelation. The Box-Pierce test, ACF and PACF were carried out using "stats" package in R (R Core Team, 2013).

2.4. Multiple nonlinear regression using generalized additive models

In order to fulfill specific objective (2) and characterize the response of ET_c to its predicting variables throughout the growing season and for each phenological stage, a regression model was required. The relationships between ET_c and the meteorological variables as well as the vegetative predictor, LAI, were not linear, therefore a non-linear, multiple regression model was selected. The generalized additive model (GAM) is an additive model technique where the influence of each covariate is captured through a smooth function (Hastie and Tibshirani, 1986) and the smoothness estimation integrated into the model (Wood, 2012). These non-parametric scatterplot smoothers can be applied to the covariates to maximize the association to the dependent variable. The smooth patterns of the covariates can be either linear or non-linear, which provides high flexibility to GAM. In this study, we used the spline function for smoothing the covariates (see Appendix A). GAM allows control of the smoothness of the predictor functions and their wiggleness to penalize models with overly complicated component functions and to avoid overfitting (Wood, 2012). The dataset that was used was time-dependent, meaning that both the dependent variable (i.e. ET_c) and the independent variables did not change at a constant rate over time. Therefore, two additional predictors were added to the model, to

¹ During the growing season sunset occurs after 19:00

Table 1

Description of the *Vitis vinifera* ‘Cabernet Sauvignon’ phenological growth stages timing within the growing season and their duration. The dates were averaged from data collected during 5 successive growing seasons (2013–2017) in Kida vineyard. Each growing season was defined from April 1 to September 30 (a total of 183 days). Illustrations of bud and cluster development for each stage are also provided.

	Stage 0 Budbreak-Flowering	Stage 1 Flowering-Bunch closure	Stage 2 Bunch closure-Veraison	Stage 3 Veraison-Harvest	Stage 4 Post Harvest
Range of start dates	March 25 – April 12	May 03 – May 21	June 12 – June 20	August 05 – August 13	August 29 – September 17
Mean start date and range	April 03 (± 9)	May 14 (-11/+7)	June 17 (± 6)	August 08 (± 5)	September 05 (-7/+12)
Duration	42 days	24 days	52 days	28 days	27 days
Illustration of grapevine growth stages					

control for temporal variability and trend (Ramsay et al., 2003) – Days of season (1–183, beginning April 1 and ending September 30) and Seasons (1–5, categorizing the growing seasons between 2013 and 2017, respectively). This was done to quantify the extent of influence that time had on the relationship between ET_c and its covariates and control for the variation explained by time-dependent predictors. The model included seven predictor variables: U_{10} , R_n , T_{mean} , RH_{mean} , LAI, days of season (Days), and Seasons. GAM was applied to the entire dataset and then to each of the growth stages, for the five consecutive growing seasons using “mgcv” package in R (Wood, 2017). The following formula (Eq. 1) schematically represents the GAM model:

$$ET_c = f_1(LAI) + f_2(T_{mean}) + f_3(RH_{mean}) + f_4(R_n) + f_5(U_{10}) + f_6(Days) + f_7(Seasons) + \epsilon \tag{1}$$

Where $f_1, f_2, f_3, f_4, f_5,$ and f_6 are the smooth functions estimated by the model for each of the predictor variables, and ϵ is the error term.

The formula for all of the six models (entire seasons + five growth stages) was calculated using the same parameters, and specified penalized cubic regression spline smoothing functions for all seven covariates, each receiving a different number of degrees of freedom associated with the spline smooth (see Appendix A for further details on spline smoothing function). The distribution of the response variable was defined as Gaussian.

The association between the predictors and the response variable was evaluated using several statistics provided by the model. The first is the pseudo adjusted R^2 that defines the extent of variability of the response variable explained by the smooth terms (i.e. the spline function of the predictors), penalized according to the number of predictors in the model. Moreover, an approximate significance (*p-value*) for each smooth term enabled us to determine which smooth terms were significantly different from zero, indicating a certain contribution to the model and an association to the response variable.

The model performance was evaluated using root mean squared error (RMSE) between measured and fitted values of ET_c , using “Metrics” package in R (Hamner et al., 2018). Additionally, a normalized root mean squared error to the range of the measured values of the response variable ($NRMSE_{range}$) was calculated so that the model performance could be compared between the six different analyses. The GAM output provides a generalized cross validation (GCV) score, which estimates the model prediction error.

The GAM results allowed for retrieving the RI of the different smooth terms on ET_c , which provided an indication regarding the rank and the extent of influence that each predictor variable had on water consumption during each phenological stage. We used “caret” package in R (Kuhn, 2008) to derive the relative variable importance for each of the six growth stages examined.

Finally, a pattern of the response of ET_c to the **two most influential variables** of the model was extracted, excluding the Seasons covariate.

This was performed using either a contour plot or a 3-dimensional grid plot that enabled viewing the combined effect between two covariates on ET_c .

2.5. Integration of crop evapotranspiration and leaf area index and their relationships

In accordance with specific objective number 3, the relationship between the LAI and ET_c throughout the growing season and for each phenological growth stage was quantified. This was done by computing the area under the curve (AUC) for both LAI and ET_c against days of season on a whole season scale (seasons 2013–2017) and for each phenological stage. This analysis was conducted using “DescTools” package in R (Signorell et al., 2019). The resulting values were divided by 5 seasons, in order to get the mean AUC per stage (or entire season), and divided again by the duration of each stage (and by 183 days for the entire season) to determine the daily mean AUC values of ET_c and LAI for each stage and the entire season. Maximum LAI values for the mean seasonal and phenological stage profiles of LAI values were extracted, using “TSrepr” package in R (Laurinec, 2018). Finally, the ET_c AUC value was divided by the LAI AUC value for each stage and for the entire season, in order to determine the ratio between ET_c and LAI for these periods.

3. Results

3.1. Temporal dependence of ET_c

The non-stationary structure of the time series of ET_c and its predictors was evaluated using the Box-Pierce test, which resulted in a significant autocorrelation structure of the ET_c time series at $k = 183$ days ($\chi = 48,702, df = 183, p < .01$). The five predictors (U_{10} , T_{mean} , RH_{mean} , R_n , and LAI) were all temporally autocorrelated as well ($p < .01$ for all cases). Fig. 2(a) shows the seasonal structure of the measured ET_c data across five growing seasons, while the inter-seasonal variation was quantified according to the growth stages. Fig. 2(b) shows the ACF plot for $k = 183$, with Y axis having correlation (r) values ranging between -0.63 and 1. The plot demonstrates strong dependencies between smaller lags, with $k < 9$ having $r > 0.8$. Negative correlations were determined for $46 < k < 140$. The PACF (Fig. 2(c)) indicates significant temporal dependencies at $k < 5$. LAI, T_{mean} and R_n had significant autocorrelations at $k \leq 4$, RH_{mean} had significant autocorrelations at $k \leq 3$, and U_{10} did not show temporal autocorrelations in PACF.

3.2. Multiple nonlinear regression using generalized additive models

The GAMs for each phenological stage and the entire season resulted in medium-high adjusted R^2 values and low $NRMSE_{range}$ values

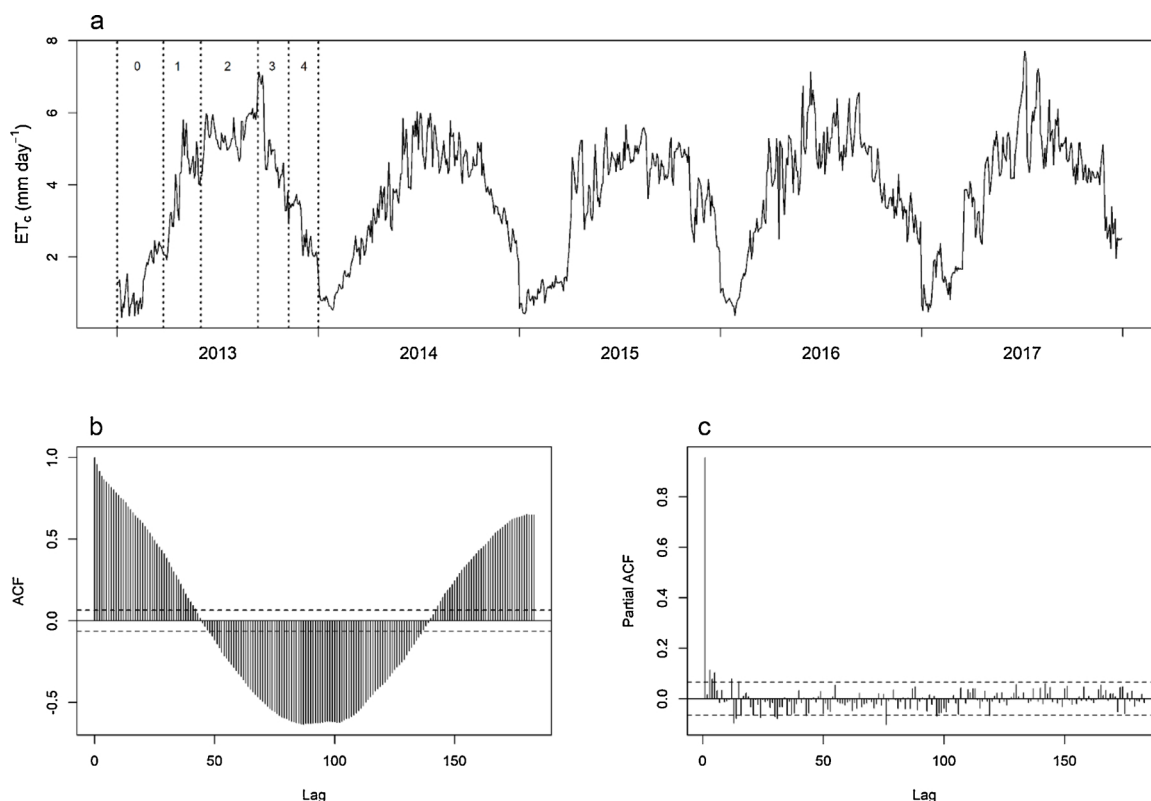


Fig. 2. Crop evapotranspiration (ET_c) time series of *Vitis vinifera* cv. ‘Cabernet Sauvignon’ vines for five consecutive growing seasons between 2013 and 2017, represented as (a) measured values, along with phenological growth stages 0–4 marked in dotted lines on top of growing season 2013 plot; (b) autocorrelation function (ACF); and (c) partial ACF. In panels (b) and (c) the dotted horizontal lines define the 95% confidence interval, below which there is no significant temporal autocorrelation.

Table 2

The generalized additive models performance statistics that include the adjusted R^2 , root mean squared error (RMSE), normalized RMSE to the range of the measured values of the response variable ($NRMSE_{range}$) and the minimized generalized cross-validation (GCV) score. *Vitis vinifera* cv. ‘Cabernet Sauvignon’, Kida.2013–2017.

Stage	Adjusted R^2	RMSE	$NRMSE_{range}$	GCV
Entire season	0.92	0.45	0.06	0.24
Stage 0	0.87	0.22	0.06	0.1
Stage 1	0.75	0.47	0.09	0.26
Stage 2	0.64	0.39	0.09	0.2
Stage 3	0.70	0.33	0.08	0.2
Stage 4	0.79	0.28	0.09	0.12

and GCV scores (Table 2). Higher GCV scores were determined for the entire season period and Stage 1, indicating a slightly lower performance of these models.

Fig. 3 shows the RI of each predictor of vine ET_c per stage and for the entire season. Overall, the temporal variables Seasons and Days, were highly dominant in explaining ET_c variance, with RI percentage ranges of 10.58–33.03% and 10.58–44.81%, respectively. Among the meteorological and LAI covariates, there was a high shift of importance percentages across the different stages, while LAI was the strongest driver for the entire season and during Stages 0 and 3 (44.81, 59.57, and 33.54%, respectively). T_{mean} had the highest influence during Stages 1 and 2 (48.14 and 23.36%, respectively). Stage 4 was most influenced by Seasons (32.58%) followed by RH_{mean} (20.42%). R_n and U_{10} consistently had the lowest impact on ET_c throughout the growing season. The GAM analyses showed that several smoothed covariates did not significantly impact the model: the smooth terms for R_n for the

entire season analysis, RH_{mean} , U_{10} , and R_n for Stage 0, R_n for Stage 1, and T_{mean} for Stage 4 analyses.

The relationships between the the smooth terms of the covariates that were included in the GAM analyses and ET_c are illustrated in Figs. 4 and 5. Fig. 4 is a contour diagram that shows the daily relationship between the smooth terms of LAI and ET_c and identifies temporal patterns associated with this relationship. The main patterns are defined in Fig. 4 as follows:

- a During stage 0, ET_c was highly variable and the amount of leaf area had varying influence on ET_c depending on the day of season. Within the stage, ET_c values increased over time.
- b During Stage 1 the same portion of leaf area as in Stage 0 generated higher rates of evapotranspiration, however this trend was unstable and shifted sharply.
- c Stage 2, which had the longest duration (52 days), was characterized by the highest ET_c values for any specific LAI value. Actual LAI values during this stage ranged between 0.79 and 1.18.
- d ET_c dynamics during Stage 3 had similar features as in Stage 1, only with a reversed direction. High variability of LAI as this stage progressed and influenced the patterns of ET_c .
- e The post-harvest Stage (4) showed patterns of lower ET_c rates, however these were still higher values than during Stage 0, for similar levels of leaf coverage.

Water consumption during different stages was unequally affected by the various predictors. Fig. 5 presents the relationships between the two most affecting covariates (smooth terms in GAM), excluding Seasons. Fig. 5a is a 3-dimensional representation of the two most influencing covariates during the entire season as presented in Fig. 4. Fig. 5b illustrates the low ET_c values that corresponded to Stage 0, with

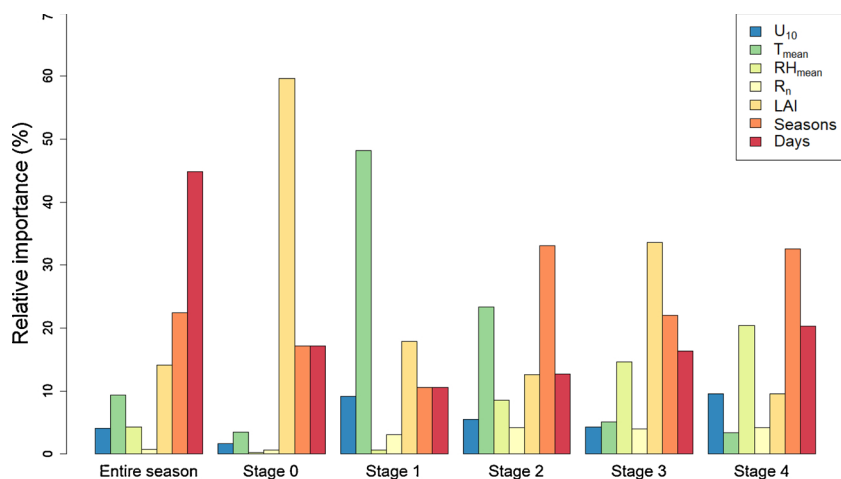


Fig. 3. Relative importance (%) of each variable on crop evapotranspiration for each phenological growth stage and for the entire season. The variables that were considered in the models were daily mean wind speed (U_{10}), daily mean temperature (T_{mean}), daily mean relative humidity (RH_{mean}), total daily radiation (R_n), leaf area index (LAI), Seasons (between 2013 and 2017), and Days (183 per growing season). *Vitis vinifera* cv. ‘Cabernet Sauvignon’, Kida.2013–2017.

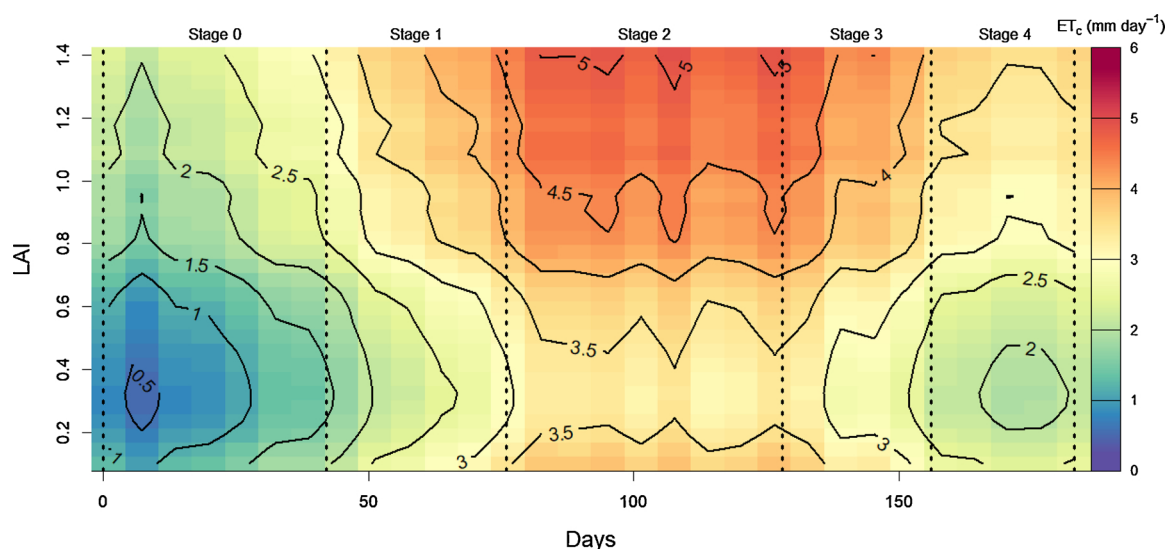


Fig. 4. Representation of the relationship between the smooth terms of days of season (Days) and leaf area index (LAI) to crop evapotranspiration (ET_c) as modeled using a generalized additive model and accounting for five consecutive growing seasons. The dotted vertical lines define the segmentation of the vines’ phenological growth stages (0–4). *Vitis vinifera* cv. ‘Cabernet Sauvignon’, Kida.2013–2017.

increasing values as time advanced. At this stage, lower LAI values affected ET_c as much as higher LAI values (ranges of 0-0.4 and 0.8–1). During Stage 1 (Fig. 5c) temperature (RI = 48.14%) was plotted against LAI (RI = 17.84%) to examine their combined effect on water consumption. Higher temperature along with larger canopy cover were related to higher values of ET_c . During Stage 2, T_{mean} was again a strong driver, and was plotted against Days (Fig. 5d), generating fluctuations in water consumption throughout this stage. ET_c increased with higher T_{mean} values, while values of $T_{mean} > 35^\circ C$ for all days were characterized by decreased ET_c rates. During Stage 3 (Fig. 5e) ET_c progressively decreased with time, with larger values of LAI having more impact on ET_c at the beginning of this stage. In the beginning of Stage 4 (Fig. 5f) RH_{mean} had a strong, negative influence on water consumption, while the second half of this stage was characterized by a moderate decrease in ET_c as RH_{mean} increased. During this stage, ET_c continued to steadily decrease with time.

3.3. Integration of crop evapotranspiration and leaf area index and their relationships

The daily mean ET_c that was calculated for the entire season using the AUC analysis was 3.7 mm day^{-1} (Table 3). Stage 0 and Stage 4 had

lower daily means, while Stage 2 had the highest daily mean of water consumption. Daily mean LAI was 0.81 for the entire season, while Stage 3 had the highest daily mean value. Daily mean ET_c values were highly variable during Stages 1–3, ranging between 3.87 and 5.22 mm day^{-1} , while LAI values were quite constant, ranging between 0.95 and 1.01. Maximum LAI for seasonal means of each stage was similar during stages 1–4 (range = 0.98–1.08), while the value for stage 0 was 0.77. The ratio between water consumption and leaf area ($1 \text{ day}^{-1} \text{ m}^{-2}$) was highest during Stage 2 and lowest during Stage 0. The value of the ratio between ET_c and LAI integrations were similar for Stages 0 and 4.

4. Discussion

The structure of ET_c throughout the growing seasons was time-dependent and influenced by meteorological and physiological processes. To quantify ET_c patterns based on data collected during five consecutive growing seasons, we chose a non-linear regression model that enabled identifying the relative influence and pattern of each covariate on water consumption. LAI was found to have the strongest impact on ET_c among the meteorological and vegetative covariates and therefore was more thoroughly analyzed for patterns and variations during the different phenological stages.

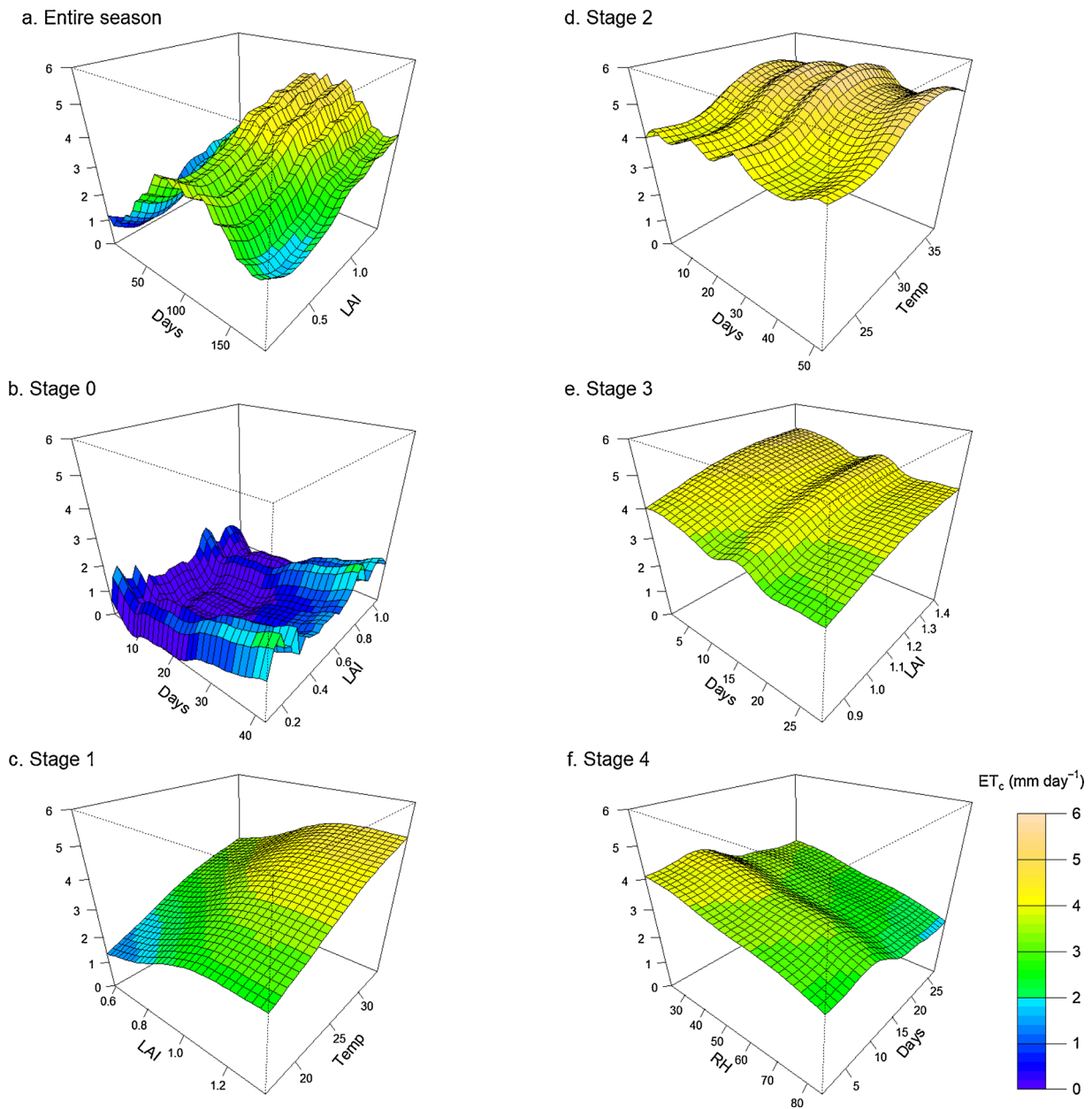


Fig. 5. The joint effect of paired predictors on vine evapotranspiration for (a) the entire season; and (b)-(f) growth stages 0–4. Z-axes are ET_c values, as well as the range of colors denoted by the color bar. The pairs were based on the smooth terms of the two covariates with the highest rank of relative importance, excluding the “Seasons” covariate. *Vitis vinifera* cv. ‘Cabernet Sauvignon’, Kida.2013–2017.

Table 3

Areas under the curves for leaf area index (LAI) and crop evapotranspiration (ET_c) for the entire season, and for the phenological stages (0–4). The values in parentheses represent the mean seasonal integration, which is the entire area under curve (AUC) divided by 5 seasons (mean seasonal AUC). The values outside the parentheses, are AUC divided by 183 days, representing the mean daily value of ET_c or LAI. Mean seasonal maximum LAI was calculated as the maximum value of the mean seasonal LAI values for each phenological stage. The last column provides the ratio between ET_c and LAI integrations.

Phenological stage (duration)	Daily (and mean seasonal/stage) integration of ET_c for 5 seasons ($mm\ day^{-1}$)	Daily (and mean seasonal/stage) integration of LAI for 5 seasons ($m^2\ m^{-2}$)	Mean seasonal/stage maximum LAI ($m^2\ m^{-2}$)	Ratio between ET_c and LAI integration ($mm\ day^{-1}$ per $m^2\ m^{-2}$)
Entire season (183 days)	3.7 (676.52)	0.81 (147.64)	1.08	4.58
Stage 0 (42 days)	1.38 (58.11)	0.36 (15.29)	0.77	3.8
Stage 1 (24 days)	3.87 (131.58)	0.96 (32.54)	1	4.04
Stage 2 (52 days)	5.22 (271.41)	0.95 (49.21)	0.99	5.52
Stage 3 (28 days)	4.59 (128.47)	1.01 (28.37)	1.08	4.53
Stage 4 (27 days)	3.09 (83.51)	0.8 (21.53)	0.98	3.88

4.1. Temporal autocorrelation

The choice of a regression model used for analyzing relations between variables determines the success of the model performance, the information that is extracted from the data and the interpretation of patterns and relationships between covariates. Therefore, a regression model should be chosen based on the dataset, its structure, the number of observations and multiple variables, and statistical parameters associated with these variables. The presence of temporal autocorrelation in time series datasets should be acknowledged and considered in the process of modeling. Lag models, such as ACF and PACF, are effective in defining the structure of the dataset and selecting the suitable model for analysis of the data (Bhaskaran et al., 2013). The Box-Pierce test results indicated that all of the variables constructing this study's dataset, aside from U_{10} , were non-stationary and therefore the analysis of ET_c and its drivers should control for time-dependency. There are numerous techniques to model autocorrelated time series, including transformation of the data to obtain stationarity using logarithms (Brockwell and Davis, 2002), differencing (Box and Pierce, 1970), Box-Cox transformation (Box and Cox, 1964) and others. However, in our current study, the ET_c variable, as well as most of its predictors, displayed a seasonal, recursive structure that was time-dependent and the autocorrelated structure of the data was important for the detection of patterns for the entire season and the growth stages that composed it. Accounting for the temporally-varying response variable was done in this case by incorporating time variables (i.e. Days and Season) (Dominici et al., 2002). The time variables, which are associated with temporal dynamics, enabled capture, rather than elimination, of the seasonal and within-seasonal patterns of the data.

4.2. Within-season temporal patterns of ET_c and its drivers

The patterns that were defined for ET_c and the multiple factors that influenced its intra-seasonal characteristics were quantified and analyzed using three techniques. First, RI of each of the meteorological and canopy covariates, as well as the time components, on ET_c were computed at the whole-season scale and during each growth stage. Second, the pattern of the relationships between ET_c and its drivers was defined throughout the season at unit resolution (i.e. days, °C, etc.). Third, the interrelations of the covariates and their effect on ET_c were quantified at the phenological stage scale. Seven covariates were considered and only the most influential ones for each growth stage are presented and discussed.

The time covariates, Days and Seasons, had pronounced effects on ET_c variability. Days was highly dominant for the entire season (Fig. 3) because of the seasonal structure of the data (Fig. 2a). During Stage 0, when vegetative growth was rapid and demonstrated a steep increase in values (Munitz et al., 2019), LAI was found to have a very strong effect on ET_c (nearly 60%). This corresponds to the findings of Williams and Ayars (2005) and Ohana-Levi et al. (2019) that showed a high impact of LAI on ET_c throughout the season. Canopy area (LAI) in vineyards for wine production undergo considerable agro-technical management (hedging, topping, unfertile shoot removal and wire lifting) throughout the growing season, subsequently affecting water consumption levels. Stages 1 and 2 were characterized by stabilization of leaf area development (Table 3), and further increase in ET_c values, especially during Stage 1. During Stage 2, ET_c reached its highest values. T_{mean} was a strong driver during these stages, since June, July and August (corresponding to Stages 1 and 2) are characterized by constant, high temperatures that generated higher evapotranspiration rates. Stage 3 marked a rapid decrease in ET_c values, due to physiological deterioration and stomatal closure, as well as a decrease in solar radiation hours. Therefore, during this stage, LAI was again the most influential covariate (RI = 33.54%). The post-harvest period (Stage 4) was highly influenced by RH_{mean} . This was due to lack of influence of the other covariates; temperature was still high and constant during Stage 4 and

had a non-significant effect on the regression model, while water consumption sharply decreased due to low stomatal conductivity in senescing leaves (Ben-Asher et al., 2006; Netzer et al., 2009) (Fig. B1). Therefore, the time covariates, Days and Seasons, as well as RH_{mean} provided the majority of RI, summing up to 73.29%.

The Seasons covariate was found to highly affect ET_c . The 2015 growing season was characterized by lower ET_c values relative to the other seasons (Fig. 2), owing to two major phenomena. The first had to do with late leaf emergence during Stage 0 that year, generating lower ET_c rates than usual. Stage 0 during 2013, 2014, 2016, and 2017 growing seasons displayed mean ET_c values ranging between 1.34–1.69 mm day⁻¹, while during Stage 0 of 2015 the mean ET_c was 1.01 mm day⁻¹. This corresponds to lower T_{mean} values during this period in 2015 (mean temperatures of 17.93 °C in 2015 compared to a range of 19.7–21.29 °C for all other seasons), which most likely affected the normal vegetative development of the canopy, while also generating low ET_c values. The rest of the season was characterized by lower ET_c values, although neither LAI nor T_{mean} were statistically different from the other growing seasons. In an attempt to understand the reasons for this exceptional phenomenon, we checked stomatal conductance (g_s) data. Stomata control the gas fluxes from and into the leaves. g_s represents the rate of passage of water vapor from the leaf to the atmosphere. Stomatal conductivity values are useful indicators for physiological functionality and viability. Abiotic stress-causing factors like salinity or drought as well as biotic stressors lead to decrease in stomatal function. Midday g_s measurements available for the 2013, 2014 and 2015 growing seasons (see Appendix B for further detail) at one-week interval measures were coupled into two-week intervals to generate a larger number of observations for higher statistical accuracy. The findings show that 50% of the measures of g_s during 2015 were significantly lower than g_s values measured in 2013 and 2014 growing seasons, mostly during Stages 2 and 3, while g_s values for 2013 and 2014 were similar (Fig. B1, Table B1). Equivalent trends were found for non-lysimeter commercial vines in the field, indicating an environmental effect during 2015, which limited stomatal conductivity during the second half of Stage 2 and in Stages 3–4. We then examined vapor pressure deficit (VPD) for the five seasons, as a function of T_{mean} and RH_{mean} , which also indicated statistically different values for 2015 compared to the other seasons during Stage 4 (Table B3). Furthermore, the standard deviation for g_s in 2015 was much higher, with 1494.5 kPa compared to a range of 1201.1–1365.9 kPa during the other four growing seasons (Table B2). This corresponds to previous knowledge regarding stomatal response in grapevines to increasing VPD (Zhang et al., 2011; Rogiers et al., 2017). Stomatal conductivity affects water consumption, thus the unusual g_s values during the second half of the 2015 growing season could explain the lower-than-normal ET_c values. Although seasonal ET_c trends are usually similar among seasons, handling of these datasets should carefully consider environmental impacts that might cause specific or seasonal deviations (e.g. Williams et al., 2003).

The seasonal pattern of ET_c and its drivers was quantified using GAM, based on the dataset of five consecutive growing seasons. We provided the pattern of the most influential variables, LAI and Days, which together provided RI of 67.28% to ET_c variability. Leaf area response to time affects ET_c in an inconsistent fashion along the season. Generally, higher ET_c values corresponded to higher LAI values throughout the season, since a larger area of leaves generates more transpiration. However, this gradient in ET_c increase together with LAI showed a non-linear pattern and high variability of change in water consumption along the LAI scale.

From our data analysis, it is clear that at each stage, ET_c dynamics and patterns were affected by different processes occurring at the plant level and associated with the meteorological drivers, along with temporal effects. The results also demonstrate an association between the starting and ending days of the phenological stages and the dynamics of ET_c . In Fig. 4, for example, large shifts in ET_c levels and accompanying

response to LAI, occur in proximity to the division between phenological stages (black dotted lines) defined according to flowering and berry development. Similar to ET_c , the developmental stages of grapevine are affected by meteorological conditions and leaf area status (Greer and Weedon, 2013; Martínez-Lüscher et al., 2016; Verdenal et al., 2017). Therefore, the seasonal dynamics of the phenological stages may serve as a proxy for ET_c levels.

During Stage 0 young leaves generated lower ET_c rates due to lower stomatal activity (Kriedemann et al., 1970; Petrie et al., 2000; Munitz et al., 2016) (Fig. B1). The effect of LAI on ET_c during this stage was highly variable (Figs. 4, 5b), due to several processes occurring concurrently. The ratio between evaporation and transpiration changes as the canopy develops, shading more soil surface area, and altering the total effect on water consumption (Montoro et al., 2016; Munitz et al., 2019). Additionally, as leaf area develops, the variability of age among the leaves increases, with leaves of different ages producing different rates of transpiration due to varying stomatal conductivity (Greer, 2012).

In Stage 1 there was an increase in the number of new leaves, more frequent mechanical interventions in controlling the canopy size, as well as high variability in most of the meteorological drivers. Therefore, the changes in vine water consumption were inconsistent over this stage (Fig. 4), with T_{mean} being the most dominant driver, generating higher ET_c values with increases in temperature. Moreover, high temperatures may accelerate vegetative growth affecting ET_c . The last few days in Stage 1 were characterized by a more moderate effect on ET_c due to the decrease in stomatal conductivity as a response to higher VPD values associated with higher temperatures (Syvertsen and Levy, 1982).

Stage 2, with a duration of 52 days, was characterized by higher stability of ET_c values (Fig. 4). T_{mean} was the most influential covariate, with higher values producing increased water consumption (Fig. 5d). However, once temperature increased above the optimal conditions, photosynthetic activity became less efficient, while transpiration was still high. The consequent response of stomatal closure to regulate transpiration, causing ET_c to decrease at temperatures higher than 35 °C, was similarly reported in studies conducted on other plants including cotton, wheat and red spruce (Lu et al., 1998; Day, 2000). The large variability in ET_c response to time may be attributed to shifts in canopy structure due to management processes such as wire lifting and hedging conducted during this stage (Williams and Ayars, 2005). Whole-plant water consumption is driven by stomatal conductivity of a large variation of leaves of different phenological ages, each transpiring different amounts of water. This variation depends on the leaves' physiological age, position (e.g. exposed to the sun, shaded by canopy, etc.), and agro-technical leaf treatment (removal of leaves, leaves moved from shaded to exposed positions, etc.). The interventions may have caused the resulting fluctuations of ET_c as a function of Days.

There was a gradual decrease in ET_c during Stage 3. Lower stomatal conductivity during this stage (Fig. B1) was associated with shorter days with less day light hours and lower solar radiation load (Pieruschka et al., 2010; Williams et al., 2012). Evapotranspiration decreased as Stage 3 progressed, due to lower transpiration rates and physiological deterioration (Hunter and Visser, 2017).

Stage 4 was characterized by lower levels of water consumption, corresponding to decrease in g_s values. Processes associated with canopy aging occurred in the post-harvest stage. The vines became increasingly subjected to physical and environmental drivers effects, with higher RH_{mean} values ($RI = 20.42\%$) negatively affecting ET_c values (Pereira et al., 2011).

4.3. Crop evapotranspiration – leaf area index relations

The relationship between LAI and ET_c was quantified for each phenological stage as another approach to determine the intra-seasonal dynamics of water consumption and its most dominant driver (Table 3).

Our findings of ET_c dynamics throughout the growing season correspond to other works that considered phenological growth stage analyses in vines (López-Urrea et al., 2012). The highest change in LAI occurred in the spring, between Stages 0 and 1, due to rapid leaf growth during Stage 0. During this stage, the difference between daily mean LAI and maximum LAI for seasonal means was also maximal, indicating a steep growing curve. Correspondingly, ET_c showed an accelerated increase in values between these stages. During Stages 1–3, canopy manipulations were conducted, resulting in a very low variability of LAI values, with very low differences between daily LAI means and maximum LAI. Additionally, Stages 1 and 2 represented 60–120 days since bud-break, during which new leaves emerge continuously, creating a consistent presence of 50-60-day-old leaves characterized by high photosynthetic rates and high stomatal conductivity (Schubert et al., 1996). ET_c during these periods, therefore, was highly variable due to successive development of new leaves along with higher temperature levels as the growing seasons progressed. The ET_c -LAI ratio provided daily mean water consumption as $mm\ day^{-1}$ per unit ($1\ m^2\ m^{-2}$) leaf area during one day for each phenological stage and for the entire period (Table 3). These dynamics are associated with the highest difference in ratios between Stages 1 and 2 (difference of $1.48\ mm\ day^{-1}$ of water consumption per unit leaf area).

LAI values were at their peak during Stage 3, while ET_c was found to decrease due to leaf-aging and decreased stomatal conductivity, as well as meteorological effects, mainly increase in RH_{mean} values and possibly due to decrease in daylight hours, which directly affect stomatal activity (Fig. B1). During Stage 4, mean seasonal maximum LAI deviated from daily mean LAI, but not as much as during Stage 0.

The effect of the presence of fruit on ET_c requires scientific attention. While some have reported that stomatal conductance was not affected by the presence or absence of fruit (Petrie et al., 2000), others reported higher stomatal conductance when fruit load is higher (Naor et al., 1997). The lysimeter system provides accurate means to measure the effect of fruit load on ET_c at the whole-plant level. During all the years of this study we did not record any significant differences in water consumption levels before and immediately after harvest. During 2017 all the clusters were removed from the grapevines in three of the six lysimeters at the bloom time. No significant differences were found between ET_c levels of the vines with and without clusters, signifying that the ET_c -LAI ratio is a representative measure of vine transpiration rate per leaf area.

5. Summary and conclusions

Water consumption throughout the grapevine growing seasons is highly variable. This study used non-linear modeling techniques to quantify ET_c temporal patterns as well as the dynamics and interrelations among the factors affecting ET_c during the growing season. The analyses were performed at the phenological stage scale, as commonly shown in studies that explore various types of within-seasonal dynamics, and used a long-term dataset composed of five consecutive growing seasons, which is sufficient to infer patterns of evapotranspiration and its drivers for 'Cabernet Sauvignon' vines grown in similar conditions.

The dataset was treated as time series, acknowledging its temporal autocorrelation and accounting for time-dependencies and effects. A non-linear regression model that accounted for temporal variations, both daily and seasonally, produced highly-accurate fitted values and enabled reliable quantification of the RI and dynamics of each covariate for each growth stage. Temporal variations of meteorological variables as well as vegetative patterns were found to have a strong, interchangeable influence on water consumption. With growing amounts of data that are time-dependent from agricultural fields, complex modeling techniques that can account for temporal non-stationarity and non-linear distributions should be developed and applied to studies that involve inter and intra-seasonal pattern analysis. Moreover, the

modeling process of temporal patterns and relations between different covariates and water consumption may be further developed and used for ET_c prediction and may facilitate wine grape production while assessing ET_c as the basis for applying deficit irrigation. Phenological growth stages are linked to water consumption dynamics since these two factors are affected by similar drivers. Predictions of ET_c may also make use of these interactions, and phenological stages may be incorporated as an additional predictor variable.

This study focused on ET_c -LAI relations since water consumption is highly affected by leaf area, but also due to the high potential of intervention and management effects on vineyard canopy properties. While environmental, meteorological factors may not be controlled and altered, leaf area may be easily modified and changed, its structure can be reshaped and its development partially constrained. Therefore, it is imperative to deepen research regarding the interrelations between leaf area and meteorological factors, as well as the effect of these non-linear relations on water consumption, both inter- and intra-seasonally, to enhance knowledge and implications for vineyard water management.

Appendix A

Generalized additive models (GAMs) extend the approach of generalized linear models by including smooth functions of the covariates in order to address non-linear relationships between response and explanatory variables (Mairdonald, 2010). In this study, the smoothing of the covariates was accomplished with spline functions. A spline curve is a piecewise polynomial curve that joins two or more polynomial curves, where the locations of the joints are defined as knots (Durrleman and Simon, 1989; Eilers and Marx, 2002). The shape of the spline can be controlled through the choice of number of knots and their exact location to allow flexibility where the trend shifts rapidly, and at the same time avoid overfitting where the trend does not fluctuate much. Another choice that must be made is the degree of polynomials to be used between knots (for example, polynomial of degree 1 is a straight line). The individual curves for each segment need to meet at the knots in a smooth fashion to create a continuous curve. For polynomials of degree n , both the spline function and the first $n-1$ derivatives are continuous at the knots. Cubic splines, as used in this study, are simply splines with polynomial degree of 3. If k knots are used, fitting a polynomial of degree n (in cubic regression spline $n = 3$) requires $k + n + 1$ regression parameters, which includes the intercept; in our case $-k + 3 + 1$. Higher order splines require more degrees of freedom as the order of splines increase (Durrleman and Simon, 1989; Croxford, 2016).

Higher number of knots might result in overfitting of the model. If the sample size is small, a small number of observations should be used in order to ensure that there are some observations between two knots, representing the variability of the covariate and fitting the polynomial. If the sample size is large and the covariate changes rapidly, it is appropriate to use a large number of knots. The locations of the knots are spaced by the model so that there is a sufficient number of observations between two consecutive knots (Durrleman and Simon, 1989). An optimal number of knots will lead to an intermediate amount of smoothing that does not cause under- or overfitting of the data. In penalized splines the coefficients, or weights, of the regression model are constrained in order to optimize the fit and avoid overfitting by the model. Weights are assigned to the splines to penalize overfitting, and at the same time allow the splines to fit the data (Griggs, 2013).

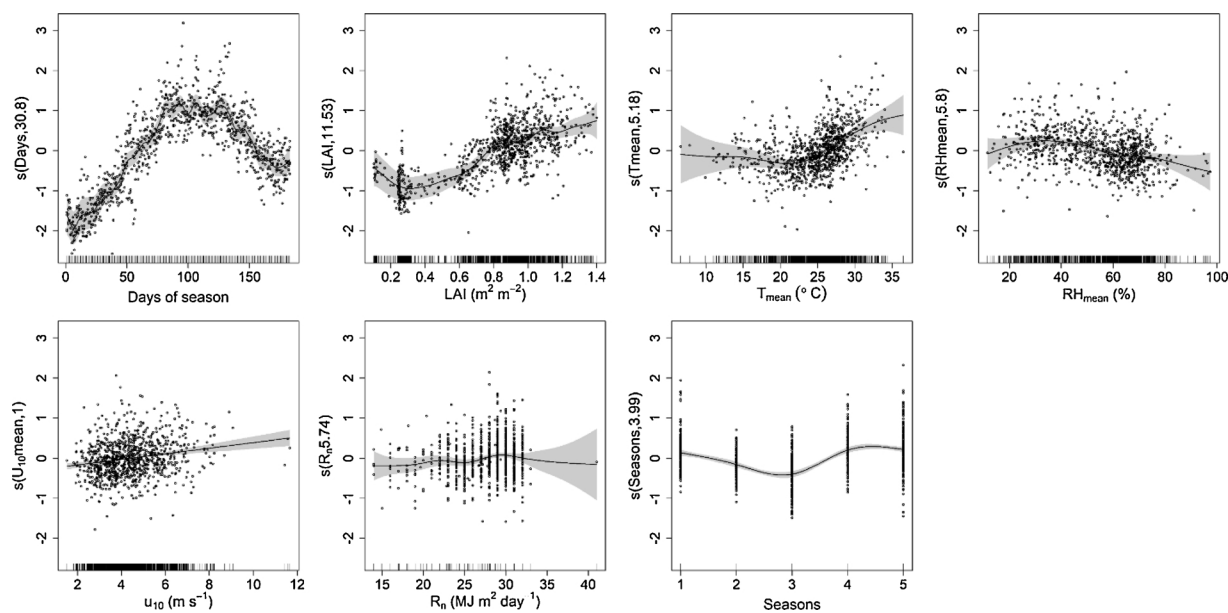


Fig. A1. The component smooth functions (black line) that construct the generalized additive model (GAM) and their estimated contribution to crop evapotranspiration (ET_c). Each panel relates to a smooth function of a specific covariate that was introduced to the GAM. The Y-axis of each plot is labelled by the covariate name and the estimated degrees of freedom for the spline-based smooths. The grey shade defines a 2 standard-error envelope above and below the estimate of the smooth terms.

The regression model treats the smoothed covariates as variables in the model, thus enabling use of any regression model, with associated outputs such as significance levels of the covariates, their RI, model performance, etc (Durrleman and Simon, 1989). Fig. A1 shows the outputs of the smooth functions generated by the GAM model applied for the entire season scale. The smooth function (Y-axis) is centered to a mean of 0. The number in parentheses signifies the estimated degrees of freedom (edf) attributed to each smoothed covariate. The maximum $edf = k-1$. edf values that are much smaller than $k-1$ are not effective and will not smooth the covariate with a sufficient amount of knots (Wood, 2017). The edf value reflects an estimate of the number of parameters that are needed to represent the smooth function and is an indication of the amount of non-linearity of the smooth term. For example, U_{10} (daily mean wind speed) has an edf value of 1, meaning that the model penalized the smooth term to a simple linear relationship. An edf larger than 1 defines a more complex, non-linear pattern (Wieling, 2018).

Appendix B

During the growing seasons of 2013–2015 stomatal conductance (g_s) of the six lysimeter-grown vines was measured on a weekly basis. Measurements were conducted each season between the second week of May and the second week of September. Three leaves from each of the vines

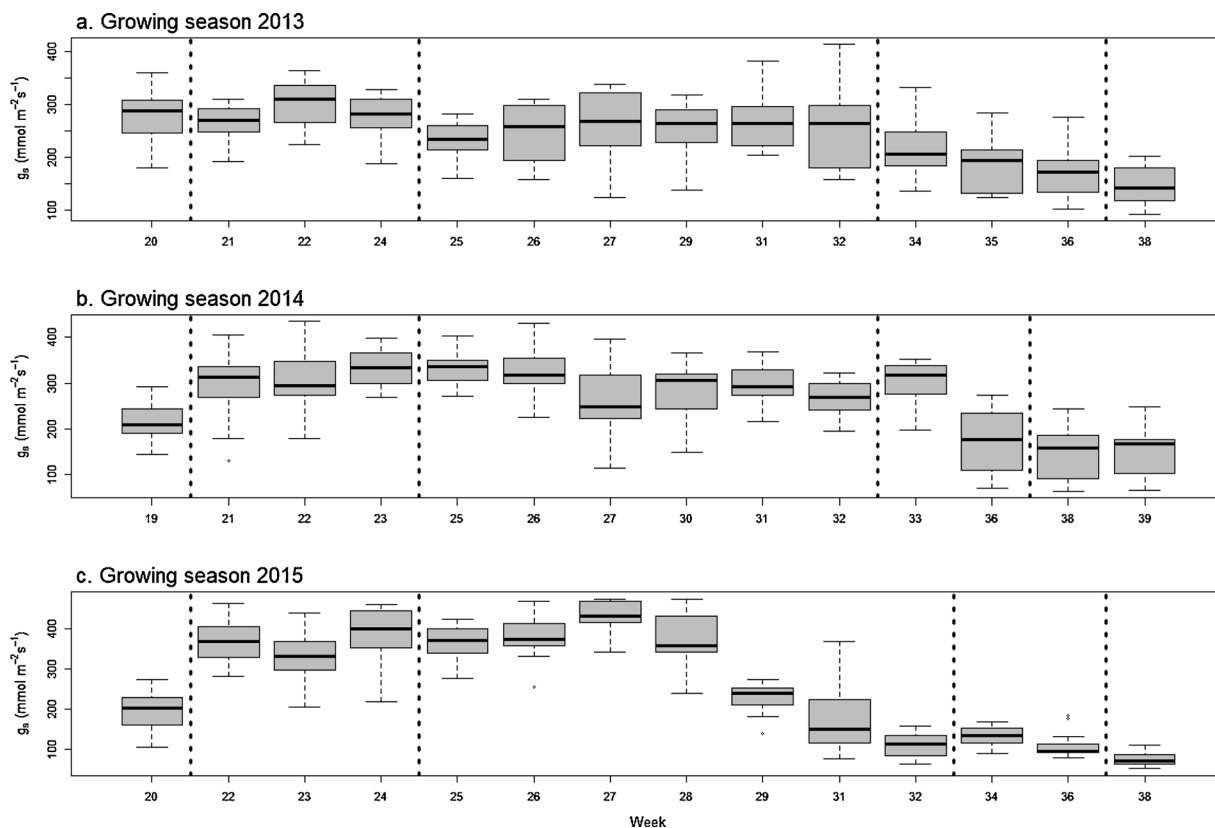


Fig. B1. Stomatal conductance (g_s) measurements in *Vitis vinifera* cv. ‘Cabernet Sauvignon’ in weekly intervals, during three growing seasons (a) 2013, (b) 2014, (c) 2015 in Kida vineyard. The data is represented in boxplots, denoting the median (black lines) and upper and lower quartiles shown in the upper and lower whiskers, respectively, with the inter-quantile range (the middle 50% measured values) marked inside the grey area within the boxes. The vertical dotted lines represent barriers between the growth stages (0–4) during each growing season, Kida vineyard.

Table B1

Differences between stomatal conductance (g_s) values measured during the 2013, 2014 and 2015 growing seasons in *Vitis vinifera* cv. ‘Cabernet Sauvignon’ in Kida vineyard, in two-weeks intervals, analyzed using one-way ANOVA, post-hoc TukeyHSD test at $\alpha = 0.05$. The values in the columns comparing paired seasonal measurements denote p -values, while the rows marked in bold indicate the periods within the seasons where g_s was similar among 2013 and 2014 and significantly different for 2015 growing season.

Weeks	Stage	Seasons 2013-2014	Seasons 2013-2015	Seasons 2014-2015
Weeks 19-20	0	0.00	0.00	0.41
Weeks 21-22	1	0.20	0.00	0.00
Weeks 23-24	1	0.04	0.00	0.46
Weeks 25-26	2	0.00	0.00	0.00
Weeks 27-28	2	0.98	0.00	0.00
Weeks 29-30	2	0.24	0.23	0.01
Weeks 31-32	2	0.26	0.00	0.00
Weeks 33-34	3	0.00	0.00	0.00
Weeks 35-36	3	0.99	0.00	0.00
Weeks 38-39	4	0.98	0.00	0.00

Table B2

Vapor pressure deficit (VPD) standard deviations (in kPa) for each growing season between 2013 and 2017. The standard deviation of 2015 is marked in bold.

Growing season	VPD standard deviation (kPa)
2013	1201.06
2014	1166.68
2015	1494.67
2016	1364.88
2017	1365.93

Table B3

Vapor pressure deficit (VPD) comparison among growing seasons 2013–2017, for Stage 4, providing the results of a one-way ANOVA, post-hoc TukeyHSD test at $\alpha = 0.05$, including difference in VPD values among each pair of seasons and the *p-value*. Rows marked in bold point to paired seasons that were found to have statistically different VPD values ($\alpha = 0.05$).

Seasonal comparison	VPD difference (kPa)	<i>p-value</i>
2014-2013	−501.82	0.41
2015-2013	619.28	0.21
2016-2013	−255.08	0.90
2017-2013	−241.64	0.92
2015-2014	1121.10	0.00
2016-2014	246.75	0.91
2017-2014	260.18	0.90
2016-2015	−874.36	0.02
2017-2015	−860.92	0.03
2017-2016	13.44	1.00

were measured each week, summing up to 18 measured leaves. g_s was measured at solar noon using a portable gas analyzer LI-6400 (Li-Cor, Lincoln, NE, USA), equipped with a 6 cm² chamber. Measurements were conducted at light intensity of 1000 PPFD (6400–02B led light source, 10% blue), ambient humidity and temperature, reference CO₂ concentration of 400 $\mu\text{mol mol}^{-1}$ and air flow rate of 500 $\mu\text{mol s}^{-1}$. At the beginning of each measurements day, a full calibration procedure recommended by the manufacturer was conducted.

Sampling measurements during week 23 in 2013 were discarded due to malfunction of the device that resulted in outlier values. Occasional measurements were also eliminated due to outliers and inconsistencies with the general levels of stomatal conductance during specific sampling days.

The measured g_s values are represented in Fig. B1. Stomatal conductance levels during the first week of the sampled seasons were usually low (in this case, excluding the 2013 growing season), followed by quite stable values until Stage 3 (week 32). Then, a gradual decrease in g_s continues until the end of the growing seasons (e.g. Williams et al., 2012).

In 2015, g_s values were found to decrease during the second half of Stage 2 (week 29), with smaller ranges of values concentrated around the median. Table B1 summarizes the differences between the unusual values measured in 2015 and those of 2013 and 2014.

To understand the differences between g_s values during 2015 and the other two growing seasons, vapor pressure deficit (VPD) was calculated as a function of T_{mean} and RH_{mean} for the growing seasons that were studied (2013–2017). The results (Tables B2 and B3) show that the VPD values for 2015 were found to vary considerably more than for the rest of the seasons, with higher standard deviation values. In addition, inter-seasonal comparison revealed that for Stage 4, 2015 had significantly different VPD values than for the other growing seasons during Stage 4, aside from 2013 (Table B3).

References

- Aldrin, M., Haff, I.H., 2005. Generalised additive modelling of air pollution, traffic volume and meteorology. *Atmos. Environ.* 39, 2145–2155.
- Allen, R.G., Pereira, L.S., Raes, D., Smith, M., 1998. Crop Evapotranspiration-Guidelines for Computing Crop Water Requirements-FAO Irrigation and Drainage Paper 56. Food and Agriculture Organization, Rome.
- Azevedo, P.Vde, Soares, J.M., Silva, V.de, da Silva, P.R., da, B.B., Nascimento, T., 2008. Evapotranspiration of “Superior” grapevines under intermittent irrigation. *Agric. Water Manag.* 95, 301–308.
- Ben-Asher, J., Tsuyuki, I., Bravdo, B.-A., Sagih, M., 2006. Irrigation of grapevines with saline water: I. Leaf area index, stomatal conductance, transpiration and photosynthesis. *Agric. Water Manag.* 83, 13–21.
- Ben-Gal, A., Shani, U., 2002. A highly conductive drainage extension to control the lower boundary condition of lysimeters. *Plant Soil* 239, 9–17.
- Bhaskaran, K., Gasparrini, A., Hajat, S., Smeeth, L., Armstrong, B., 2013. Time series regression studies in environmental epidemiology. *Int. J. Epidemiol.* 42, 1187–1195.
- Bloomfield, P., Royle, J.A., Steinberg, L.J., Yang, Q., 1996. Accounting for meteorological effects in measuring urban ozone levels and trends. *Atmos. Environ.* 30, 3067–3077.
- Box, G.E.P., Cox, D.R., 1964. An analysis of transformations. Source: *J. R. Stat. Soc. Ser. B (Methodol.)* 26, 211–252.
- Box, G.E.P., Pierce, D.A., 1970. Distribution of residual autocorrelations in autoregressive-integrated moving average time series models. Source: *J. Am. Stat. Assoc.* 65 (332), 1509–1526. <https://doi.org/10.1080/01621459.1970.10481180>.
- Brockwell, P.J., Davis, R.A., 2002. *Introduction to Time Series and Forecasting*, second ed. Springer, New York, NY.
- Cowpertwait, P.S.P., Metcalfe, A.V., 2009. *Introductory Time Series with R*. Springer-Verlag.
- Croxford, R., 2016. *Restricted Cubic Spline Regression: A Brief Introduction*. Institute for Clinical Evaluative Sciences, Toronto.
- Day, M.E., 2000. Influence of temperature and leaf-to-air vapor pressure deficit on net photosynthesis and stomatal conductance in red spruce (*Picea rubens*). *Tree Physiol.* 20, 57–63.
- Dominici, F., McDermott, A., Zeger, S.L., Samet, J.M., 2002. On the use of generalized additive models in time-series studies of air pollution and health. *Am. J. Epidemiol.* 156, 193–203.
- Dragoni, D., Lakso, A.N., Piccioni, R.M., Tarara, J.M., 2006. Transpiration of grapevines in the humid northeastern United States. *Am. J. Enol. Vitic.* 57, 460–467.
- Durrleman, S., Simon, R., 1989. Flexible regression models with cubic splines. *Stat. Med.* 8, 551–561.
- Eilers, P.H.C., Marx, B.D., 2002. Generalized linear additive smooth structures. *J. Comput. Graph. Stat.* 11, 758–783.
- Evans, R.G., Spayd, S.E., Wample, R.L., Kroeger, M.W., Mahan, M.O., 1993. Water use of *Vitis vinifera* grapes in Washington. *Agric. Water Manag.* 23, 109–124.
- Greer, D.H., 2012. Modelling leaf photosynthetic and transpiration temperature-

- dependent responses in *Vitis vinifera* cv. Semillon grapevines growing in hot, irrigated vineyard conditions. *AoB Plants* 2012, pls009.
- Greer, D.H., Weedon, M.M., 2013. The impact of high temperatures on *Vitis vinifera* cv. Semillon grapevine performance and berry ripening. *Front. Plant Sci.* 4, 491.
- Griggs, W., 2013. Penalized Spline Regression and Its Applications.
- Hammer, B., Frasco, M., Ledell, E., 2018. Package “Metrics” – Evaluation Metrics for Machine Learning.
- Hargreaves, G.H., 1974. Estimation of Potential and Crop Evapotranspiration. *Trans. ASAE*.
- Hastie, T., Tibshirani, R., 1986. Generalized additive models. *Stat. Sci.* 1, 297–310.
- Hunter, J.J., Visser, J.H., 2017. The effect of partial defoliation, leaf position and developmental stage of the vine on the photosynthetic activity of *Vitis vinifera* L. cv Cabernet Sauvignon. *South African J. Enol. Vitic.* 9.
- Johnson, R.S., Williams, L.E., Ayars, J.E., Trout, T.J., 2005. Weighing lysimeters aid study of water relations in tree and vine crops. *Calif. Agric.* 59, 133–136.
- Kriedemann, P.E., Kliewer, W.M., Harris, J.M., 1970. Leaf age and photosynthesis in *Vitis vinifera* L. *Vitis* 9, 97–104.
- Kuhn, M., 2008. Building predictive models in R using the caret package. *J. Stat. Softw.* 28, 1–26.
- Laurinec, P., 2018. T Sprepr R package: time series representations. *Int. J. Open Source Softw. Process.* 3, 577.
- Van Leeuwen, C., Trégoat, O., Choné, X., Bois, B., Pernet, D., Gaudillère, J.-P., 2009. Vine water status is a key factor in grape ripening and vintage quality for red Bordeaux wine. How can it be assessed for vineyard management purposes? *J. Int. des Sci. la vigne du vin* 43, 121.
- López-Urrea, R., Martín de Santa Olalla, F., Fabeiro, C., Moratalla, A., 2006. Testing evapotranspiration equations using lysimeter observations in a semiarid climate. *Agric. Water Manag.* 85, 15–26.
- López-Urrea, R., Montoro, a., Mañas, F., López-Fuster, P., Fereres, E., 2012. Evapotranspiration and crop coefficients from lysimeter measurements of mature ‘Tempranillo’ wine grapes. *Agric. Water Manag.* 112, 13–20.
- Lu, Z., Percy, R.G., Qualset, C.O., Zeiger, E., 1998. Stomatal conductance predicts yields in irrigated Pima cotton and bread wheat grown at high temperatures. *J. Exp. Bot.*
- Maindonald, J., 2010. Smoothing Terms in GAM Models.
- Martínez-Lüscher, J., Kizildeniz, T., Vučetić, V., Dai, Z., Luedeling, E., van Leeuwen, C., Gomès, E., Pascual, I., Irigoyen, J.J., Morales, F., Delrot, S., 2016. Sensitivity of grapevine phenology to water availability, temperature and CO₂ concentration. *Front. Environ. Sci.* 4, 48.
- Montoro, A., López-urrea, R., Manuel SÁNCHEZ, J., 2017. Meteorological parameters effect on diurnal and nocturnal transpiration and stomatal conductance grapevine. *Internet J. Viticult. Enol.*
- Montoro, A., López Urrea, R., Mañas, F., López Fuster, P., Fereres, E., 2008. Evapotranspiration of grapevines measured by a weighing lysimeter in La Mancha Spain. *Acta Hortic.* 459–466.
- Montoro, A., Mañas, F., López-Urrea, R., 2016. Transpiration and evaporation of grapevine, two components related to irrigation strategy. *Agric. Water Manag.* 177, 193–200.
- Moritz, S., Bartz-Beielstein, T., 2017. imputeTS: time series missing value imputation in R. *R J.* 9, 207–218.
- Munitz, S., Netzer, Y., Schwartz, A., 2016. Sustained and regulated deficit irrigation of field grown Merlot grapevines. *Aust. J. Grape Wine Res.* 23, 87–94.
- Munitz, S., Schwartz, A., Netzer, Y., 2019. Water consumption, crop coefficient and leaf area relations of a *Vitis vinifera* cv. “Cabernet Sauvignon” vineyard. *Agric. Water Manag.* 219, 86–94.
- Naor, A., Gal, Y., Bravdo, B., 1997. Crop load affects assimilation rate, stomatal conductance, stem water potential and water relations of field-grown Sauvignon blanc grapevines. *J. Exp. Bot.* 48 (314), 1675–1680.
- Netzer, Y., Munitz, S., Shtein, I., Schwartz, A., 2019. Structural memory in grapevines: early season water availability affects late season drought stress severity. *Eur. J. Agron.* 105, 96–103.
- Netzer, Y., Yao, C., Shenker, M., Bravdo, B.-A., Schwartz, A., 2009. Water use and the development of seasonal crop coefficients for Superior Seedless grapevines trained to an open-gable trellis system. *Irrig. Sci.* 27.
- Ohana-Levi, N., Munitz, S., Ben-Gal, A., et al., 2020. Multiseasonal grapevine water consumption – Drivers and forecasting. *Agric. For Meteorol.* 280, 107796. <https://doi.org/10.1016/j.agrformet.2019.107796>.
- Pereira, A.B., Villa Nova, N.A., Pires, L.F., Alfaro, A.T., 2011. Transpiration of irrigated apple trees and citrus from a water potential gradient approach in the leaf-atmosphere system. *Rev. Bras. Meteorol.* 26, 181–188.
- Pereira, L.S., Allen, R.G., Smith, M., Raes, D., 2015. Crop evapotranspiration estimation with FAO56: past and future. *Agric. Water Manag.* 147, 4–20.
- Petrie, P.R., Trought, M.C.T., Howell, G.S., 2000. Influence of leaf ageing, leaf area and crop load on photosynthesis, stomatal conductance and senescence of grapevine (*Vitis vinifera* L. cv. Pinot noir) leaves. *Vitis* 39, 31–36.
- Picón-Toro, J., González-Dugo, V., Uriarte, D., Mancha, L.A., Testi, L., 2012. Effects of canopy size and water stress over the crop coefficient of a “Tempranillo” vineyard in south-western Spain. *Irrig. Sci.* 30, 419–432.
- Pieruschka, R., Huber, G., Berry, J.A., 2010. Control of transpiration by radiation. *Proc. Natl. Acad. Sci. U. S. A.* 107, 13372.
- R Core Team, 2013. R: A Language and Environment for Statistical Computing.
- Ramsay, T.O., Burnett, R.T., Krewski, D., 2003. The effect of concurrency in generalized additive models linking mortality to ambient particulate matter. *Epidemiology* 14, 18–23.
- Rana, G., Katerji, N., 2000. Measurement and estimation of actual evapotranspiration in the field under Mediterranean climate: a review. *Eur. J. Agron.* 13, 125–153.
- Rogiers, S.Y., Coetzee, Z.A., Walker, R.R., Deloire, A., Tyerman, S.D., 2017. Potassium in the grape (*Vitis vinifera* L.) berry: transport and function. *Front. Plant Sci.* 8, 1629.
- Schubert, A., Restagno, M., Lovisolo, C., 1996. Net photosynthesis of grapevine leaves of different age exposed to high or low light intensities. *Adv. Hortic. Sci.*
- Shtein, I., Hayat, Y., Munitz, S., Harcavi, E., Akerman, M., Drori, E., Schwartz, A., Netzer, Y., 2017. From structural constraints to hydraulic function in three *Vitis* rootstocks. *Trees* 31, 851–861.
- Signorell, A., Aho, K., Alfons, A., An-deregg, N., Aragon, T., Arppe, A., Baddeley, A., Barton, K., Bolker, B., Borchers, H.W., Caeiro, F., Champely, S., Ches-sel, D., Chhay, L., Cummins, C., Dewey, M., Do-ran, H.C., Dray, S., Dupont, C., Eddelbuettel, D., Enos, J., Ekstrom, C., Eff, M., Erguler, K., Farebrother, R.W., Fox, J., Fran-cois, R., Friendly, M., Galili, T., Gamer, M., Gastwirth, J.L., Gel, Y.R., Gross, J., Grothendieck, G., Harrell Jr, F.E., Heiberger, R., Hoehle, M., Hoffmann, C.W., Hojsgaard, S., Hothorn, T., Huerzeler, M., Hui, W.W., Hurd, P., Hyndman, R.J., Villacorta Iglesias, P.J., Jackson, C., Kohl, M., Korpela, M., Kuhn, M., Labes, D., Tem-ple Lang, D., Leisch, F., Lemon, J., Li, D., Maechler, M., Magnus-son, A., Malter, D., Marsaglia, G., Marsaglia, J., Matei, A., Meyer, D., Miao, W., Millo, G., Min, Y., Mitchell, D., Naepflin, M., Navarro, D., Nilsson, H., Nordhausen, K., Ogle, D., Ooi, H., Parsons, N., Pavoine, S., Plate, T., Rapold, R., Revelle, W., Rinker, T., Ripley, B.D., Rodriguez, C., Russell, N., Sabbe, N., Se-shan, V.E., Snow, G., Smithson, M., Soetaert, K., Stahel, W.A., Stephenson, A., Stevenson, M., Templ, M., Themeau, T., Tille, Y., Trapletti, A., Ul-rich, J., Ushey, K., VanDerWal, J., Venables, B., Verzani, J., Warnes, G.R., Wellek, S., Wickham, H., Wilcox, R.R., Wolf, P., Wollschlaeger, D., Wu, Y., Yee, T., Maintainer, Zeileis, Andri Signorell, A., 2019. Package “DescTools” – Tools for Descriptive Statistics.
- Smoyer, K.E., Kalkstein, L.S., Greene, J.S., Ye, H., 2000. The impacts of weather and pollution on human mortality in Birmingham, Alabama and Philadelphia, Pennsylvania. *Int. J. Climatol.* 20, 881–897.
- Syvertsen, J.P., Levy, Y., 1982. Diurnal changes in Citrus leaf thickness, leaf water potential and leaf to air temperature difference. *J. Exp. Bot.* 33, 783–789.
- Verdenal, T., Zufferey, V., Dienes-Nagy, A., Gindro, K., Belcher, S., Lorenzini, F., Rösti, J., Koestel, C., Spring, J.-L., Viret, O., 2017. Pre-flowering defoliation affects berry structure and enhances wine sensory parameters. *Oeno One* 51.
- Wang, S., Zhu, G., Xia, D., Ma, J., Han, T., Ma, T., Zhang, K., Shang, S., 2019. The characteristics of evapotranspiration and crop coefficients of an irrigated vineyard in arid Northwest China. *Agric. Water Manag.* 212, 388–398.
- Wieling, M., 2018. Analyzing dynamic phonetic data using generalized additive mixed modeling: a tutorial focusing on articulatory differences between L1 and L2 speakers of English. *J. Phon.* 70, 86–116.
- Williams, L.E., Ayars, J.E., 2005. Grapevine water use and the crop coefficient are linear functions of the shaded area measured beneath the canopy. *Agric. For. Meteorol.* 132, 201–211.
- Williams, L.E., Baeza, P., Vaughn, P., 2012. Midday measurements of leaf water potential and stomatal conductance are highly correlated with daily water use of Thompson Seedless grapevines. *Irrig. Sci.* 30, 201–212.
- Williams, L.E., Phene, C.J., Grimes, D.W., Trout, T.J., 2003. Water use of mature Thompson Seedless grapevines in California. *Irrig. Sci.* 22, 11–18.
- Wood, S.N., 2012. Stable and efficient multiple smoothing parameter estimation for generalized additive models. *J. Am. Stat. Assoc.* 99, 673–686.
- Wood, S.N., 2017. Generalized Additive Models: An Introduction with R, 2nd editio. ed. Chapman and Hall/CRC.
- Wright, I.R., 1990. A lysimeter for the measurement of evaporation from high altitude grass. Hydrology in Mountainous Regions. I-Hydrological Measurements; The Water Cycle. IAHS Publ, Lausanne.
- Zeileis, A., Grothendieck, G., 2005. zoo:S3 Infrastructure for Regular and Irregular Time Series. *J. Stat. Softw.* 14, 1–27.
- Zhang, B., Kang, S., Li, F., Tong, L., Du, T., 2010. Variation in vineyard evapotranspiration in an arid region of northwest China. *Agric. Water Manag.* 97, 1898–1904.
- Zhang, Y., Kang, S., Ward, E.J., Ding, R., Zhang, X., Zheng, R., 2011. Evapotranspiration components determined by sap flow and microlysimetry techniques of a vineyard in northwest China: dynamics and influential factors. *Agric. Water Manag.* 98, 1207–1214.

2.6: Chapter 6:

Structural memory in grapevines: Early season water availability affects late season drought stress severity.

Yishai Netzer, Sarel Munitz, Ilana Shtein and Amnon Schwartz

Published in European journal of agronomy February 2019



Structural memory in grapevines: Early season water availability affects late season drought stress severity

Yishai Netzer^{a,b,c,1,*}, Sarel Munitz^{a,b,1}, Ilana Shtein^{a,b}, Amnon Schwartz^a

^a R.H. Smith Institute of Plant Science and Genetics in Agriculture, Faculty of Agriculture, Food and Environment, The Hebrew University of Jerusalem, Rehovot 76100, Israel

^b Department of Chemical engineering, Biotechnology and Materials, Ariel University, Israel

^c The Eastern Regional Research and Development Center, Science Park, 40700, Ariel, Israel

ARTICLE INFO

Keywords:

Vitis vinifera
Xylem anatomy
Vessel diameter
Water potential
Drought stress

ABSTRACT

In the future drought events are expected to occur more frequently, with unpredictable rain and heat events. In current research we investigated how different water availability patterns influenced late season plant water status in *Vitis vinifera*.

‘Cabernet Sauvignon’ grapevines were grown for three consecutive years. We compared the response to five water availability regimes: High, Intermediate, Low (along all season) and High-to-Low (High during the beginning of vegetative seasons switched to low during the rest of season) and Low-to-High (opposite treatment). Midday stem water potential (SWP) was measured weekly to determine the seasonal pattern of drought stress. Xylem anatomy was investigated by trunk vessel diameter measurements, and specific axial xylem conductivity was calculated according to Hagen-Poiseuille's law.

Vines exposed to high water availability treatment showed improved seasonal water status along the season, compared to vines in the low treatment. Vines exposed to High-to-Low water regime showed a markedly improved water status at the beginning of the season, but became the most severely stressed toward the end of season. The SWP values were more negative in the High-to-Low regime even when compared to the Low water regime. Water availability at the beginning of the season (during main period of cambial activity) determined the vessel characteristics: high water availability during cambial activity increased vessel diameter and thus specific hydraulic conductivity.

Our data strongly indicates that regulated drought stress can be induced by manipulating xylem structural parameters via controlling water availability during the period of stem cambial activity.

1. Introduction

Inducing drought stress in the vineyards during late season is favorable in quality red wine production, as long as reasonable photosynthetic rates are maintained, and has become a common practice (Chaves et al., 2007; Leeuwen, n.d.; Romero and Ignacio, 2010). In rainy regions, limiting water availability at the beginning of the season, aims to control vigorous growth and restrict high yields. In dry regions controlling water availability aims to simultaneously optimize water use and obtain superior quality yields. In all cases, when determining the appropriate amount and timing of irrigation, the correct balance must be found between drought stress and yet optimal yield.

Impaired plant water status is indicated by extremely negative stem water potential, decreased stomatal conductance and photosynthetic

assimilation rate (Romero et al., 2010). Drought stress conditions reduce shoot and branch axial growth (Buesa et al., 2017; Lovisolo and Schubert, 1998; Munitz et al., 2016; Pellegrino et al., 2005; Williams, 2012) as well as stem thickening (Intrigliolo and Castel, 2007; Selles et al., 2005). As a result, drought stressed plants have a lower xylem cross-sectional area and hydraulic conductivity (Gerzon et al., 2015; Hochberg et al., 2015; Lovisolo and Schubert, 1998; Munitz et al., 2018). Observations on intact vines using visualization techniques (microCT/NMR, Brodersen and Roddy, 2016) indicated that *Vitis vinifera* is relatively hydraulically vulnerable, when SWP values of -1.4 to -1.7 MPa inducing 30–80% loss of stem hydraulic conductivity (Alsiná et al., 2007; Charrier et al., 2016; Choat et al., 2010; Hochberg et al., 2016; Jacobsen and Pratt, 2012). A vine exposed to prolonged dehydration sheds its basal leaves (after being embolised) in order to

* Corresponding author at: Department of Chemical engineering, Biotechnology and Materials, Ariel University, Israel.

E-mail address: ynetzer@gmail.com (Y. Netzer).

¹ These authors contributed equally to this work and share first authorship.

minimize the embolism of younger leaves and stems (Gerzon et al., 2015; Hochberg et al., 2017).

In *Vitis vinifera* most of the vascular cambial activity in the trunk occurs during the six weeks after bud break (Pratt, 1974), which occurs during May and June in Israel's conditions (Bernstein and Fahn, 1960).

The vascular cambium is a cylinder of meristematic cells that produces secondary xylem towards the pith of the stem or root of conifers and dicots. In general, xylem is a compound tissue made of parenchyma (living cells), fibers and mature dead conduits (tracheids and vessel elements). In the formation of young stems primary xylem is formed. At the beginning narrow and small protoxylem elements are formed (characterized by the ability to elongate with the elongation of the stem), and later metaxylem elements are formed. Metaxylem are wider cells and have a defined pattern of cell wall thickening. In mature vines at the beginning of the growing season the cambium produces wide vessels, and much smaller ones later on (Pratt, 1974), this seasonal pattern produces the annual rings (ring porous wood). *Vitis vinifera* is characterized by a bi-modal distribution pattern of xylem vessels (Ewers et al., 1990; Wheeler and LaPasha, 1994). However, the pattern of distribution of vessel diameters varies between different *V. vinifera* cultivars (Chatelet et al., 2011; Chouzouri and Schultz, 2005; Hochberg et al., 2015; Shtein et al., 2016). *Vitis vinifera* vessels remain hydraulically active for one to three years after they are formed, and are completely inactivated by tyloses after seven years (Pratt, 1974; Pratt and Jacobsen, 2018; Tibbetts and Ewers, 2000). Hydraulic architecture is known to affect water balance in numerous species (*Dodonaea* (Shtein et al., 2011), *Quercus* (Lo Gullo and Salleo, 1991), *Chorisia* (Salleo and Gullo, 1986)). In different *Vitis vinifera* cultivars it was reported that isohydric and anisohydric behaviour could be regulated by structure derived hydraulic conductance (Gerzon et al., 2015; Schultz, 2003).

The main question arising from "drought stress practices" concerns the prolonged effects on the plant, and especially on the water conductive tissue – the xylem. If plant water status does affect vessel anatomy and thus water conductivity, what are the consequences for development of drought stress late in the growing season when the soil is dry, the canopy is wide, potential evapotranspiration is maximal and water availability is minimal? Also, it is not clear how a water availability regime applied three years earlier would affect plant drought stress in the current season.

The objectives of the present research were:

- (1) To examine how xylem vessel characteristics are affected by plant water status.
- (2) To determine the most crucial phenological stages in which plant water status may affect characteristics of xylem anatomy and development of drought stress late in the season.

2. Materials and methods

2.1. Plant material

A three-year (2009–2011) study was conducted in a 0.27 ha commercial vineyard of *Vitis vinifera* L. 'Cabernet Sauvignon' grafted onto 140 'Ruggeri' rootstock (*V. berlandieri* x *V. rupestris*). The vines were planted in April 1999 in the mountainous region of central Israel (31.5°N, 35.0°W) at an elevation of 430 m above sea level. The soil at the experimental site is loamy sand (56.4% sand, 26.6% silt, 17% clay) with pronounced rock content. The climate is Mediterranean, with dry summers and daily maximum summer temperatures of 35 °C. Average annual winter rainfall at the experimental site is 528 mm; there were no summer rains in the experimental plot during the period of the trial. Vine spacing was 1.3 m within rows and 3 m between rows (2564 vines per hectare). Rows were oriented north–south and the vines were trained to a Vertical Shoot Positioned trellis system with two foliage wires on each side. The vineyard was drip-irrigated twice a week using a computer-controlled drip irrigation system (Dream 1, Talgil, Israel) with five separate electronic valves and five mechanical flowmeters

Table 1

Dates and day of the year (in parentheses) of phenological stages during each year of the trial.

Year	Fruit set	Bunch closure	Veraison	Harvest
2009	21 May (141)	23 June (174)	27 July (208)	28 Sept. (271)
2010	10 May (130)	4 June (155)	19 July (200)	2 Sept. (245)
2011	19 May (139)	13 June (164)	12 Aug. (224)	21 Sept. (264)

(one per treatment). One line (16 mm) per row and 2.4 L h⁻¹ in-line, pressure-compensated drippers spaced 0.5 m apart were used (Uni-ram, Netafim, Israel).

2.2. *Vitis vinifera* phenology

Vitis vinifera growth period can be divided into three major phenological stages, according to berry development (Coombe, 1995; Kennedy and Kennedy, 2002): stage I (fruit set to bunch closure); stage II (bunch closure to veraison); stage III (veraison to harvest). Adjusting the level of drought stress according to a plant's phenological stages is termed Regulated Deficient Irrigation (RDI) (Munitz et al., 2017; Romero et al., 2010). Examination of phenological stages across the years of the trial shows a difference of 11 days in fruit set date between 2009 and 2010 (Table 1).

2.3. Water availability treatments

Five water availability treatments were applied in the vineyard (Table 2). Each treatment consisted of four replicates in a randomized block design with eight measured vines per replicate; each replicate was surrounded by 22 border vines that received the same water availability treatment. The irrigation control unit was manually set to satisfy 50% of ET_c (vine evapotranspiration) in the high-volume water availability treatment (High), 35% of ET_c in the Intermediate-volume water availability treatment (Intermediate) and 20% of ET_c in the Low-volume water availability treatment (Low) (Table 2). The other two water availability treatments varied the volume of water application according to the phenological stage (Table 1, 2). In the Low-to-High treatment, irrigation was set to satisfy 20% of ET_c during stages I and II and increased to 50% of ET_c during stage III. In the High-to-Low-treatment, irrigation was set to satisfy 50% of ET_c during stage I and decreased to 20% of ET_c during stages II and III. The irrigation schedule was determined twice a week according to a modified Leaf Area Index - Crop coefficient relationship (Munitz et al., 2014; Netzer et al., 2009). The daily ET_c (mm day⁻¹) was calculated by multiplying daily reference evapotranspiration (ET_o) (mm day⁻¹) by Crop coefficient (K_c) (Doorenbos and Pruitt 1977; Allen et al. 1998). Total irrigation amounts at each phenological stage are presented in Table 2. ET_o was calculated according to the Penman-Monteith equation as modified for the ASCE (American Society of Civil Engineers). The meteorological data used for calculating ET_o were obtained from a weather station located 1.2 km from the vineyard. The average amount of water applied in the Low water availability treatment (20% ET_c) was 119.1 mm per season with the greatest amount applied during stages II and III

Table 2

Average water amounts (mm) applied in each irrigation treatment at each phenological stage 2009–2011.

Treatment	Fruit set – Bunch closure	Bunch closure–Veraison	Veraison – Harvest	Total
Low	25.3 ± 3.7	25.3 ± 5.2	34.4 ± 6.0	119.1 ± 7.0
Intermediate	45.1 ± 6.1	45.1 ± 7.9	58.7 ± 13.8	192.7 ± 11.7
High	62.5 ± 9.6	62.5 ± 11.3	83.2 ± 18.9	263.4 ± 18.1
Low-to-High	25.3 ± 3.7	25.3 ± 5.0	84.3 ± 22.5	171.2 ± 22.7
High-to-Low	63.0 ± 9.3	63.0 ± 4.2	33.6 ± 7.7	155.0 ± 11.8

(Table 2). The Intermediate (35% ET_c) and High (50% ET_c) water availability treatments received 62% and 122% more water, respectively, compared to the Low treatment. Similarly, the Low-to-High and High-to-Low treatments received 44% and 33% more water, respectively, compared to the Low treatment (Table 2).

2.4. Midday stem water potential (Ψ_s)

Midday stem water potential (Ψ_s) was measured weekly prior to irrigation at solar noon (from 12:00 to 14:30), using a portable pressure chamber (model Arimad 2, Kfar Charuv, Israel) mounted on a portable cart, according to the procedures of Boyer (1995). Twelve sunlit, mature, fully-expanded leaves (at the sixth to ninth position from shoot apex) from each treatment (three leaves from three vines per replicate) were double bagged (plastic bags covered with aluminum foil) 1.5 h prior to measurement. The leaves were disconnected from the vines by sharp cutting of the leaf petiole and quickly placed in the pressure chamber. The time elapsing between leaf excision and chamber pressurization was less than 25 s.

2.5. Leaf Area Index (LAI)

The leaf area index (LAI) represents the leaf area (one side) per unit of ground surface area (Munitz et al., 2017; Netzer et al., 2009). The LAI values of vines (three per replicate) were estimated several times during the growing seasons using a non-destructive canopy analysis system (SunScan model SS1-R3-BF3; Delta-T Devices, Cambridge, UK). The canopy analysis system uses a line quantum sensor array that is sensitive to photosynthetically active radiation (PAR). This method of estimating LAI (gap fraction inversion) is based on light measurements beneath the canopy. The analyzer was operated using the standard protocol recommended by the manufacturer. Each sample consisted of equally spaced readings (20 cm apart) at ground level, starting from the center of the row to half the distance to the adjacent row, with the linear probe positioned parallel to the rows.

LAI values obtained using this non-destructive method were verified by direct measurement of leaf area following leaf removal from one vine. Leaf area was then measured using an area meter (model 3100; Li-Cor, Lincoln, NE, USA). Leaf areas of 38 vines were measured at different times along the growing seasons. Estimated and measured LAI values were highly correlated with one another. $y = 0.674x + 0.16$, $R^2 = 0.922$, $P < 0.0001$, $n = 38$ (Fig. S1).

2.6. Xylem anatomy

To examine whether the characteristics of xylem vessels differ between water availability regimes, trunk xylem cores were taken 50 cm above the base of the trunk, from three representative vines in each plot (12 per treatment, total of 60 vines sampled) during January 2012 (at the dormant period of the winter). Cores of trunk xylem samples were collected using an increment borer (5.15 mm Core 3-Thread Increment Borer, 8", HagÖlf, Sweden) and stored at 5°C in water until sectioning. The cores were sectioned with a sliding microtome (NR 17 800 Reichert, Austria) at a thickness of 90 µm. The sections were stained with Phloroglucinol and washed with distilled water. Photographs of the sections were taken at X8 magnification with a light microscope (SZ2-ILST, Olympus, Tokyo, Japan) equipped with a digital camera (U-TZ0.5xC-3, Olympus, Tokyo, Japan). Images were acquired with image analysis software (LCmicro 5.1, Olympus, Tokyo, Japan).

The width of the 4 recent annual growing rings, vessel diameter and number of vessels per mm², were measured using ImageJ software (Rasband, W.S., ImageJ, U. S. National Institutes of Health, Bethesda, Maryland, USA, <http://imagej.nih.gov/ij/>, 1997–2015). Diametric classes of 30 µm were used for describing the distribution of the vessels and for determining hydraulic conductivity. Theoretical specific hydraulic conductivity (K_s ; kg m⁻¹ MPa⁻¹ s⁻¹) was calculated using the

modified Hagen–Poiseuille's law (Tyree and Ewers, 1991):

$$K_s = (\pi\rho/128\eta A_w) \sum_{i=1}^n (d_i^4)$$

Where K_s is the specific hydraulic conductivity, ρ is the density of the fluid in kg m⁻³ (assumed to be 1000 kg m⁻³), η is the dynamic viscosity of the fluid in MPa s⁻¹ (assumed to be 1×10^{-9} MPa s⁻¹), A_w is the area (m²) of the xylem cross-section measured, d is the diameter (m) of the i th vessel and n is the total number of the vessels in the measured area. Mean hydraulic vessels diameter (d_h) was calculated after Tyree and Zimmermann (2002) using the equation: $d_h = (\Sigma d^4/N)^{1/4}$.

2.7. Statistical analyses

The data were consisted of the averages of samples (3 samples per plot) within each replicated plot (4 plots per treatment), and it was subjected to Analysis of variance (ANOVA) (JMP Pro 11 Statistical Software; SAS Institute Inc., Cary, NC, USA). Tukey post-hoc test was used to determine the significance of differences between treatment means at $p \leq 0.05$.

3. Results

3.1. Physiological parameters

Midday stem water potential (SWP) shows a trend of declining water status as the season progresses (Fig. 1 and 2). Examination of the three "constant" treatments (Low, Intermediate and High) in 2009 shows that at the beginning of stage I SWP in all treatments was -0.5 MPa. Later in the season, as harvest approached, SWP decreased to -1.2 MPa in the High treatment. In the Intermediate and Low treatments SWP decreased to -1.4 MPa already in stage II, with drought stress in the Low treatment further decreasing to ~ -1.6 MPa in a localized incident on day 255 (Fig. 1A). Examination of the High-to-Low treatment shows that throughout stage I, when this treatment was comparable to the High treatment, SWP was nearly identical to that of the High treatment (Fig. 1A). From the beginning of stage II, when irrigation amounts were reduced to Low, a sharp drop in SWP was observed. Surprisingly, significantly more negative values (compared to the low treatment) were measured in this treatment throughout stage III (on 6 out of the 8 measurement days). The inverse mixed treatment Low-to-High, was very similar to the Low treatment in terms of SWP values during stages I and II. However, once the irrigation was raised, the water status improved during stage III until it reached values similar to those of the High treatment towards the end of stage III (Fig. 1B). The consistency of SWP during 2010 and 2011 seasons can be seen in the comparison between the two extreme treatments and the High-to-Low treatment (Fig. 2). In 2010 drought stress became more pronounced in comparison to 2009 (Fig. 2A). However, trends were very similar to the 2009 trends, where at the end of stage II, SWP values in the High-to-Low treatment was significantly more negative than in the Low treatment. The extreme drought stress conditions in this treatment during pre-harvest are indicated by SWP values reaching -1.9 MPa. A slightly different seasonal scenario was observed in 2011 with dramatically improved SWP in the High treatment, yet very similar trends between the Low treatment and the High-to-Low treatment (Fig. 2B). Gas exchange parameters at the end of stage II is indicative for drought stress in the low and the High-to-Low and Low-to-High treatments (S3).

3.2. The effect of water amounts on xylem anatomy

The bimodal distribution pattern (large vs. small vessels) typical for climbing plants (lianas) is clearly shown in the vessel distribution (Fig. 3A). Examination of frequency distribution by size groups (each group at a range of 30 µm), shows that nearly 40% of all the vessels are

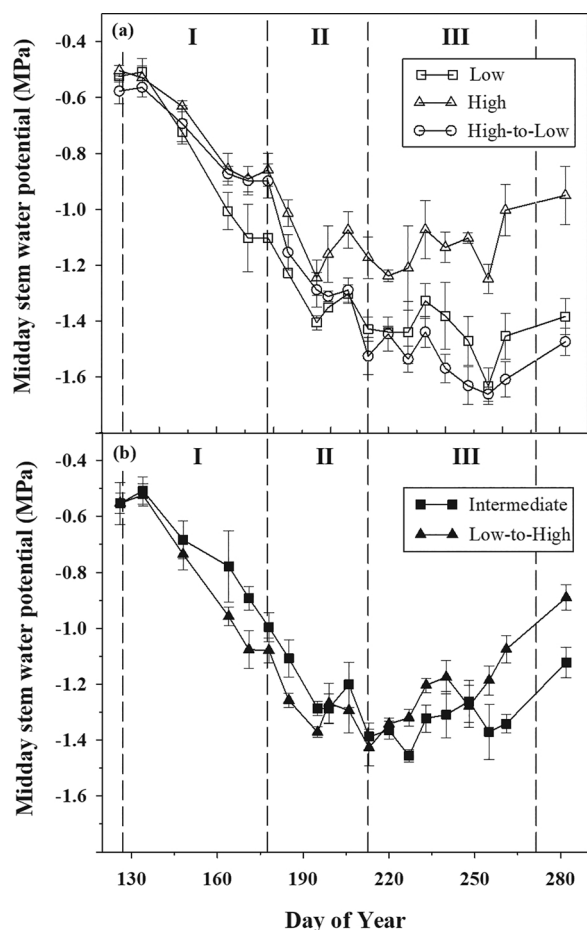


Fig. 1. Seasonal pattern of midday stem water potential of vines exposed to five different irrigation treatments during the 2009 growing season. Measurements were taken at midday on the day before irrigation was applied. Each point is the mean of four replicates \pm SE. The value of each replicate was the average of the measurements of three randomly sampled vines per plot.

within the smallest size group of 10–40 μm (Fig. 3A), and 73% are within the small group ($\leq 100 \mu\text{m}$). Examination of the hydraulic conductivity distribution by size group shows that the small vessels, despite their large number, reflect only 2% of the total calculated hydraulic conductivity, while the sparse large vessels ($> 100 \mu\text{m}$) account for ~98% of the total calculated specific hydraulic conductivity (Fig. 3B). From the data it appears that in the Low and the Low-to-High treatments there is a clear tendency towards narrower vessels, on the other hand in the High and the High-to-low treatments the pattern is shifted towards wider vessels (Fig. 3B). Xylem annual ring width (Fig. 4A), affecting the cross-sectional area of the ring, was significantly greater in the High treatment compared to the Low and Intermediate treatments. The mean hydraulic vessel diameter differs significantly between High and treatment subjected to low water availability during stage I (Low, Low-to-High, Fig. 4B). In the specific hydraulic conductivity more pronounced trends can be seen, where High and High-to-low treatments exhibit ~40% higher (and statistically significant) values compared to the Low and the Low-to-high treatments (Fig. 4C).

Examination of the relationship between total annual water amount applied and the specific hydraulic conductivity (Fig. 5), shows a weak linear relationship ($R^2 = 0.35$). However, water amount during stage I and specific hydraulic conductivity shows a strong linear relationship ($R^2 = 0.81$) (Fig. 6).

Measurements of vegetative growth conducted throughout the growing season (expressed by Leaf Area Index) shows no significant differences between the irrigation treatments, with the exception of two

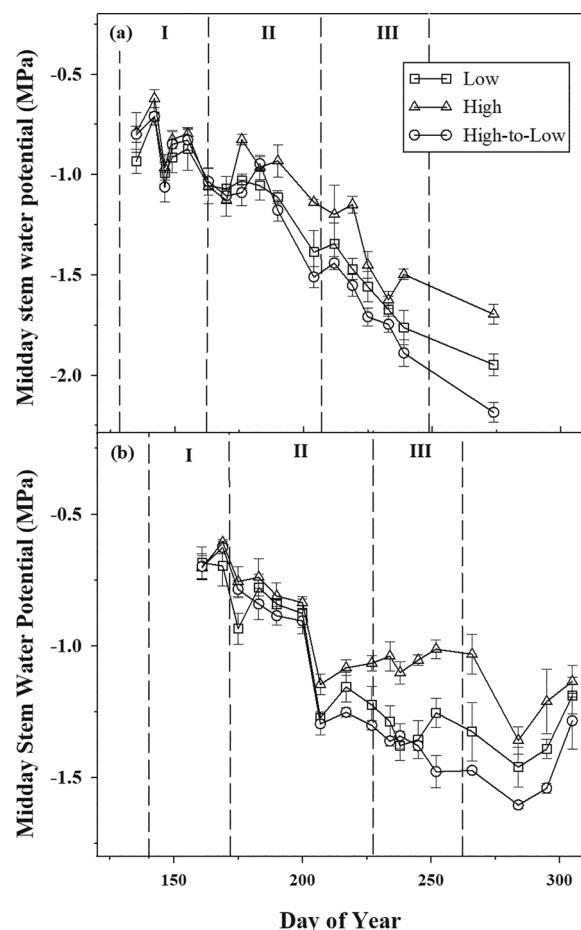


Fig. 2. Seasonal pattern of midday stem water potential of vines exposed to different irrigation amounts during the 2010 (A) and 2011 (B) growing seasons. Measurements were taken at midday on the day before irrigation was applied. Each point is the mean of four replicates \pm SE. The value of each replicate was the average of the measurements of three randomly sampled vines per plot.

sampling dates (Fig. 7) in the range of DOY 200–220.

In the three "constant" treatments, yield, bunch number and berry mass increased significantly with an increasing amount of irrigation (Table 3). Both Mixed treatments that received a similar amount of seasonal water, had similar yield, but the Low-to-High vines had higher berry mass (6%, not significant) compared to that of the High-to-Low vines. Seasonal trends of berry growth is presented in Fig. S2. Among all treatments no significant difference was observed for the number of berries per bunch.

4. Discussion

Adequate plant water status allows the plant to maintain regular photosynthesis, essential mineral uptake, appropriate turgor pressure and leaf evaporative cooling. At the beginning of the vine growing season in the spring, under adequate soil moisture and normal plant water status, a rapid vegetative growth occurs. In mid-summer vine water consumption may reach 60 L day^{-1} in table grapes (Netzer et al., 2009) and 33 L day^{-1} in wine grapes (Munitz et al., 2014). To enable rapid and efficient transport of large volumes of water (via a relatively small conductive area as compared with other trees), lianas must have an improved hydraulic system, i.e., wide vessels (Tyree and Ewers, 1991).

Vitis, like other climbing plants, is characterized by exceptionally wide vessels, alongside very small vessels and tracheids (Adkinson, 1913; Carlquist, 1985; Ewers et al., 1990; Pratt, 1974). This pattern can

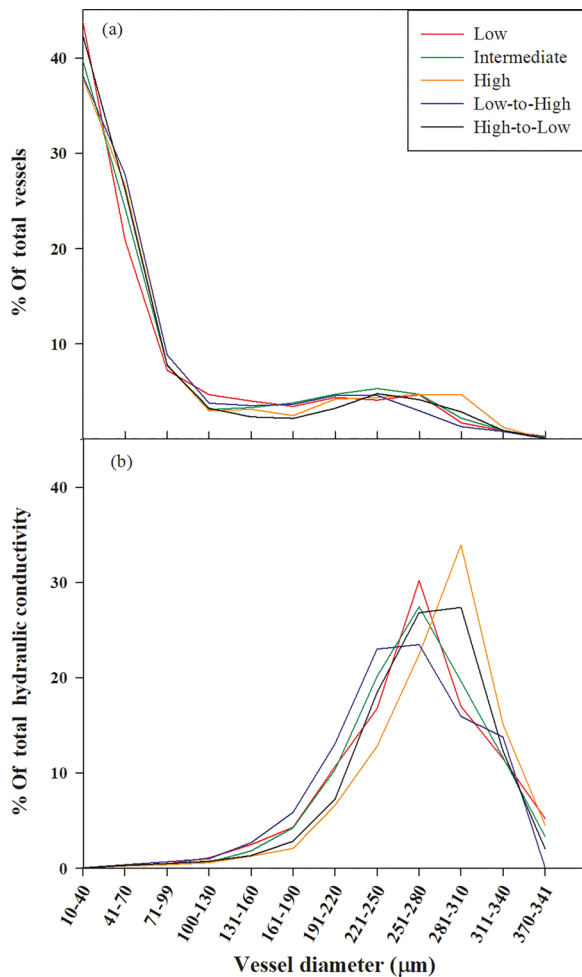


Fig. 3. Distribution frequency according to diameter class (μm) of xylem vessels (A) and total calculated conductivity (B), in the trunk of Cabernet Sauvignon vines. The latest three annual rings in each of the five treatments were analyzed. The data was based on 12 samples for each treatment, in total 6761 vessels were measured.

be referred to as bi-modal (Carlquist, 1985; Ewers et al., 1990; Wheeler and LaPasha, 1994). In *Vitis rotundifolia* stem maximum vessel size is in the range of 179–337 μm (Ewers et al., 1990) and in *Vitis labrusca* is 300 μm (Zimmermann and Jeje, 1981). In the current study on 'Cabernet Sauvignon', the maximum measured vessel diameter in the stem exceeded 300 μm (0.3 mm). Such wide vessels can be easily observed with the naked eye. The force that drives the water upstream is the atmospheric demand creating tension within xylem vessels. Large-diameter vessels provide the plant with improved hydraulic conductivity that can support vigorous vegetative growth. However, they also pose a risk under drought stress conditions. When the plant is exposed to drought stress with increasing negative water potential, large diameter vessels can be hydraulically impeding. Studies of the relationship between vessel diameter and hydraulic conductivity within the same species, shows that the larger the xylem vessel, the greater the risk of embolism formation (Cai and Tyree, 2010; Lo Gullo and Salleo, 1991; Patakas et al., 2005; Tyree and Sperry, 1989). One possible explanation for this phenomenon is termed the 'rare pit hypothesis' (Christman et al., 2012; Wheeler and LaPasha, 1994; Wheeler et al., 2005). Based on this theory, air seeding pressure originates from the most leaking pit. So, more pit area per vessel means more cavitation vulnerability, and on the other hand greater hydraulic conductivity. Different plant species with improved hydraulic systems (long and wide vessels) also have a greater pitted wall area, which are prone to air seeding. Hence, the

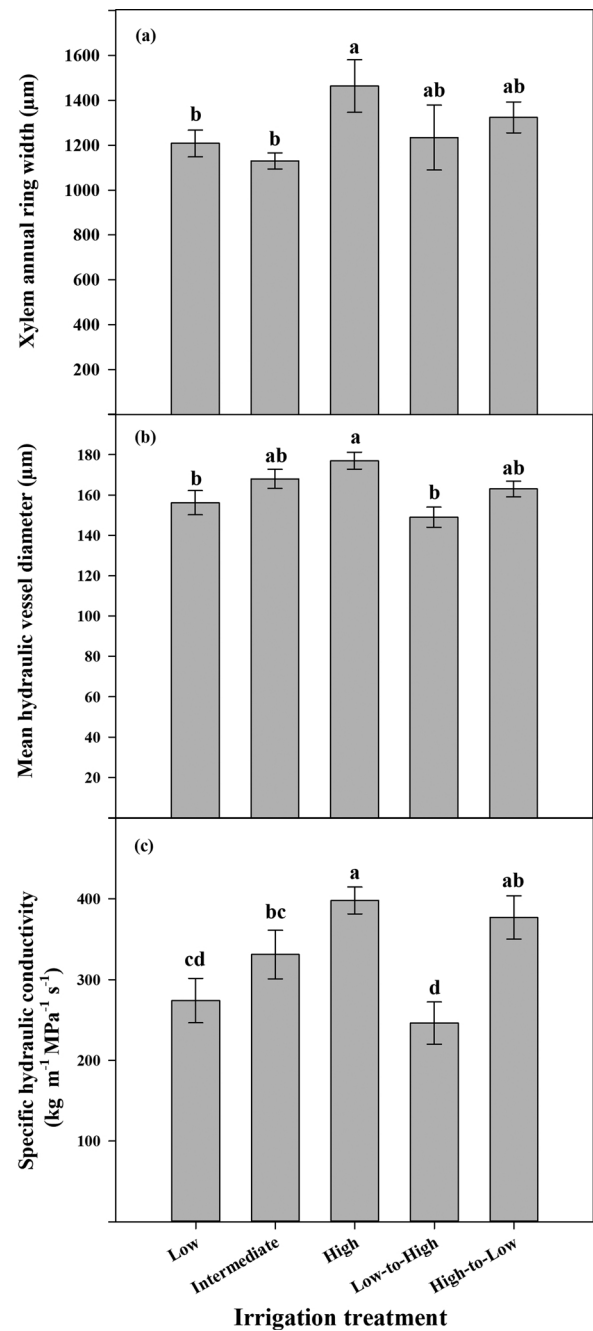


Fig. 4. Hydraulic anatomy of vines exposed to five different irrigation treatments. Annual xylem ring width (A), hydraulic diameter of all vessels (B) and calculated specific hydraulic conductivity (C). Different letters indicate significantly different treatments, $p < 0.05$.

more protected the xylem transport system is against embolism formation, the less efficient it is in water conductance (Tyree and Sperry, 1989; Venturas et al., 2017). Recent studies applying advanced technologies expose the precise dynamics of air bursting from the gas-filled conduits into the adjacent vessels via the pits, including the repair process in which air cavities are expelled from the xylem vessels (Brodersen et al., 2011, 2010; Cochard et al., 2014).

This study shows a trend of declining plant water status as the season progresses (Fig. 1). This trend is a derivative of a well-known deficit irrigation practice in wine grape cultivation (Feres and Soriano, 2007; Munitz et al., 2017; Romero and Martinez-Cutillas, 2012; Santesteban et al., 2011). Unsurprisingly, in the present study, an increasingly-widening gap could be observed between the High and

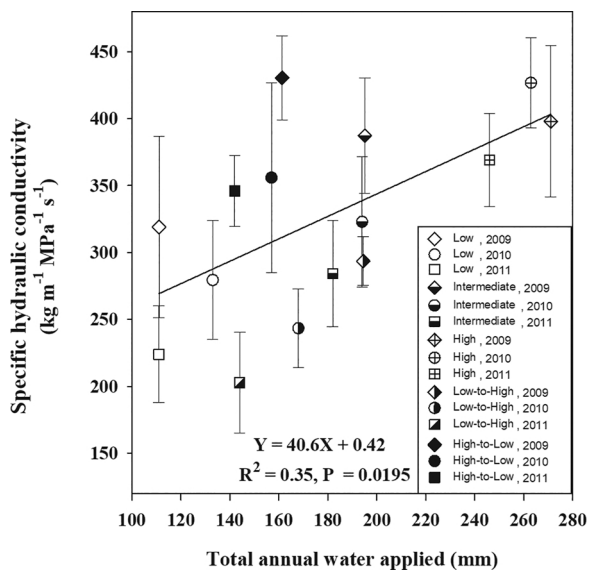


Fig. 5. Relationship between annual water amounts applied and specific hydraulic conductivity. Each point is the mean of four replicates \pm SE. Each replicate was comprised of an average of three samples from three randomly sampled vines (12 leaves from different vines measured from 4 replicates, $n = 20$).

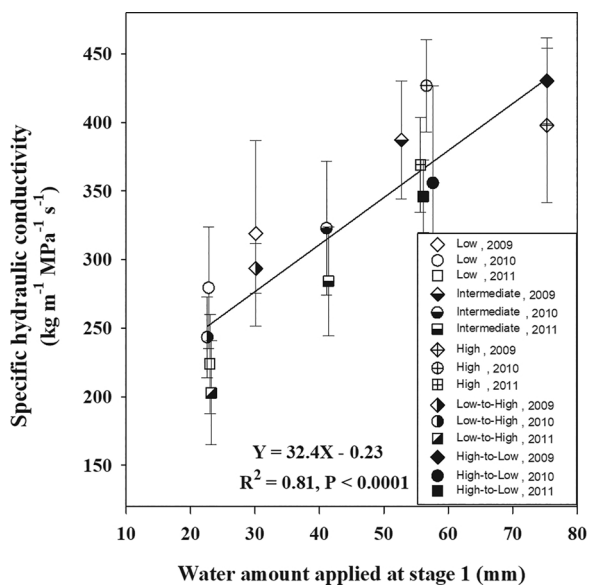


Fig. 6. Relationship between water amounts applied during stage I (from fruit set to bunch closure) and specific hydraulic conductivity. Each point is the mean of four replicates \pm SE. Each replicate was comprised of an average of three samples from three randomly sampled vines (12 leaves from different vines measured from 4 replicates, $n = 20$).

Low treatments from early in the season (Fig. 1 and 2). The SWP values measured in the current work are similar to values reported in the literature: -1.5 MPa in Cv. 'Merlot' (Munitz et al., 2017) -1.5 MPa in Cv. 'Sauvignon Blanc' (Naor A et al., 1994) -1.4 MPa in Cv. 'Malbec' (Shellie and Bowen, 2014) -1.65 MPa in 'Tempranillo' and 'Manto Negro' (Medrano et al., 2003). The degree of drought stress can be defined on the bases of midday SWP Values: -0.9 to -1.1 MPa weak drought stress, and above -1.4 MPa severe stress (Leeuwen et al., 2009).

As the season advanced, canopy area and reference evapotranspiration increased, leading to greater plant drought stress. The most surprising effect was observed during stage III, when stem water

potential in the High-to-Low treatment indicated even more severe drought stress compared to the Low treatment. This effect was already observed during the first year of the study (Fig. 1B) and was maintained (with slight variations) in the following years (Fig. 2A, B). Interestingly, in the High-to-Low treatment the seasonally water amount applied was 44% higher compared to the Low treatment (Table 2).

These findings raise the question how the vine water status during stage I affects physiological parameters during stage III. It was exposed to when the season commenced. Our intuitive assumption regarding this effect has to do with the plant water status during the vegetative growth period which overlaps stage I. A possible explanation could be that leaf area in the High-to-Low treatment was larger than in the Low treatment, which eventually caused a greater vine water consumption that yielded a more stressed vine. This assumption was rejected because the wine grape growing practice involves control of canopy dimensions through a series of canopy management practices (non-fertile shoot removing, hedging and topping). When observing at the overall leaf area, the slight difference in growth rates is unnoticeable (Fig. 7).

The explanation offered for this effect is the influence of improved water status in stage I on cambial activity and the final vessel diameter. In fact there is clear overlap between stage I and stem thickening following cambial activity (Bernstein and Fahn, 1960; Smart, 1974). This point was illustrated by data obtained from 20 dendrometers installed in the plot in later seasons (data not shown). The results of this study shows the influence of vine water status on the width of the annual growing ring (Fig. 4A) as already shown in other studies (Bernstein and Fahn, 1960; Myburgh, 1996; Ton and Kopyt, 2004). Yet clearly, the key factor influencing the specific hydraulic conductivity (Fig. 4C) is the diameter of the vessels (Fig. 4B). Significant differences found by us in calculated hydraulic conductivity can indicate on actual distinction, since there is a good correlation between measured and calculated hydraulic conductivity (Hargrave et al., 1994; Lovisolo and Schubert, 1998; Nolf et al., 2017; Salleo et al., 1985). Plant water status influences the nature of cambial activity and dramatically affects final hydraulic vessel diameter and hydraulic parameters. On one hand, an improved hydraulic system will be favorable in non-stress conditions, but on the other hand, when vine water availability is dramatically decreased those "pampered" plants will suffer from the worst drought stress, as shown in our case during stage III. This strengthens our understanding that stage I is the critical phenological stage (being the stage of main cambial activity), and it determines the hydraulic function of the plant throughout the growing season. In a way, the water availability during cambial growth is translated into hydraulic anatomy and into hydraulic function- thus serving as structural memory.

5. Conclusions

In summary, as cambial activity is renewed at the beginning of each growing season, a new set of active xylem vessels is produced. The frequency diameter distribution of these vessels is essentially genetically-based, yet environmental conditions and water availability can also affect xylem anatomy (Chatelet et al., 2011; Munitz et al., 2018). Our current study clearly shows that vessel diameters can be increased by manipulating plant water status. It is reasonable that a successive elevation of water amount applied increases both yield and berry weight, the last known by its negative effect on red wine quality (Bravdo et al., 1985; Munitz et al., 2016). From our data it is shown that improved plant water status during stage I, increased vessel diameter and specific hydraulic conductivity. Since drought stress during stage III is desired in red wine cultivation, we were curious to understand the effects of mixed treatments, especially the High-to-Low treatment. As larger diameter vessels (formed during stage I) are more prone to the risk of embolism formation, water availability can be reduced towards the end of the growing season. Thus, inducing even greater plant water stress than in vines that received Low irrigation and were anatomically acclimated to a limited water availability conditions. The results

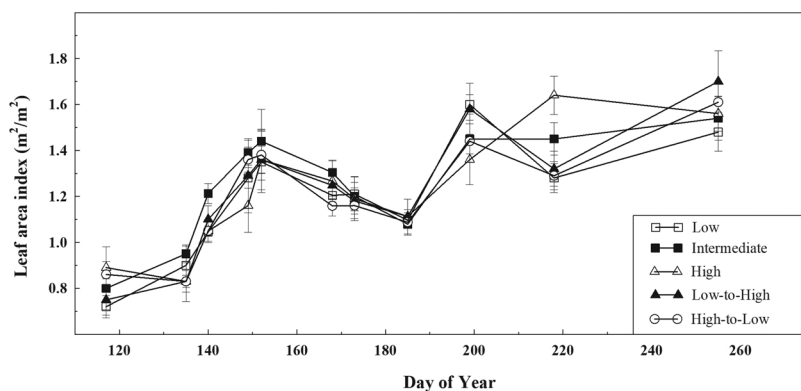


Fig. 7. The multi-seasonal course of leaf area index (LAI) of vines exposed to different irrigation amounts during the 2009–2011. Measurements were taken using a SunScan-canopy analysis system. Measurements were taken at midday when the zenith angle was $< 30^\circ$. Each point is the mean of four replicates \pm SE. The value of each replicate was the average of the measurements of three randomly sampled vines per plot.

Table 3

Effect of irrigation treatments on yield components. Values are averages of three years data recorded during the trial years (2009–2011) in ‘Dolev’ Cabernet Sauvignon vineyard.

Irrigation treatment	Water amount (mm season-1)	Yield (kg vine-1)	Bunch (number vine-1)	Berry mass (gr)	Berries (number bunch-1)
Low	118	4.99b	58.8	1.15c	72.6
Intermediate	190	6.19a	63.4	1.26b	78.0
High	260	6.30a	63.9	1.35a	73.2
Low-to-High	169	5.78a	61.3	1.25b	76.1
High-to-Low	153	5.89a	62.4	1.18bc	80.8

Values represent means ($n = 20$). Within each column, means followed by letters are significantly different ($P < 0.05$) according to Tukey’s test.

indicates that in High-to-Low treatment the best combination between yield, small berry size and desired drought stress is achieved.

The influence of water status on the hydraulic anatomy has extensive ecological and agricultural implications. In the wine grape industry where drought stress has a cardinal effect on both yield and quality of red wines, it is highly important to recognize the within-season and between-season implications. This is especially important in the light of current climate change with decreasing worldwide water availability, as such changes will have a strong effect on plant structure and function (Escalona et al., 2013; Torres-Ruiz et al., 2017). In climatic regions where vineyards rely exclusively on irrigation, agro-technical manipulation of xylem structure could be used by growers as a significant tool to influence water status and determine wine quality. In other climatic regions that enjoy spring and summer rains, a prolonged drought stress events at the middle or at the end of the growing season could result an extremely stressed vines due to the fact that the vines were not acclimated properly. From controlled agriculture practice much could be learnt in order to understand future climatic and water availability changes.

Source of funding

This research was supported by the Israeli Ministry of Agriculture and Rural Development (Project No. 837 - 0067 - 012); and by the Israeli Wine Council.

Acknowledgments

We thank Yair Eldar, Zivan Shavit, Eli Vilga, Bat-el Vaknin, Or Bumatz, Yakov Hening, Dror Dotan and Yechezkel Harosh, for assistance in the field and laboratory. We particularly acknowledge Marc Perel for providing meteorological data. We also thank the vine grower Shlomi Cohen and his assistants Mundir Nofel and Mutea Nofel for technical help, and the "Netafin" company for help with the irrigation system, and the "Phytech" company for help with the dendrometers.

Appendix A. Supplementary data

Supplementary material related to this article can be found, in the online version, at doi:<https://doi.org/10.1016/j.eja.2019.02.008>.

References

- Adkinson, J., 1913. Some features of the anatomy of the Vitaceae. *Ann. Bot.* 27, 133–139.
- Alsina, M.M., De Herralde, F., Aranda, X., Savé, R., Biel, C., 2007. Water relations and vulnerability to embolism are not related: experiments with eight grapevine cultivars. *Vitis - J. Grapevine Res.* 46, 1–6.
- Bernstein, Z., Fahn, A., 1960. The effect of annual and Bi-annual pruning on the seasonal changes in xylem formation in the grapevine. *Ann. Bot.* 24, 159–171.
- Boyer, J., 1995. *Water Relations of Plants and Soils*. Academic Press, San Diego, CA, USA.
- Bravdo, B., Hepner, Y., Loinger, C., Cohen, S., Tabacman, H., 1985. Effect of irrigation and crop level on growth, yield and wine quality of Cabernet Sauvignon. *Am. J. Enol. Vitic.* 36, 132–139.
- Brodersen, C.R., Roddy, A.B., 2016. New frontiers in the three-dimensional visualization of plant structure and function. *Am. J. Bot.* 103, 184–188. <https://doi.org/10.3732/ajb.1500532>.
- Brodersen, C.R., McElrone, A.J., Choat, B., Matthews, M.a, Shackel, Ka, 2010. The dynamics of embolism repair in xylem: in vivo visualizations using high-resolution computed tomography. *Plant Physiol.* 154, 1088–1095. <https://doi.org/10.1104/pp.110.162396>.
- Brodersen, C., Lee, E., Choat, B., Jansen, S., Phillips, R., Shackel, Ka, McElrone, A.J., Matthews, Ma, 2011. Automated analysis of three-dimensional xylem networks using high-resolution computed tomography. *New Phytol.* 191, 1168–1179.
- Buesa, I., Pérez, D., Castel, J., Intrigliolo, D., Castel, J., 2017. Effect of deficit irrigation on vine performance and grape composition of *Vitis vinifera* L. cv. Muscat of Alexandria. *Aust. J. Grape Wine Res.* 23, 251–259. <https://doi.org/10.1111/ajgw.12280>.
- Cai, J., Tyree, M.T., 2010. The impact of vessel size on vulnerability curves: data and models for within-species variability in saplings of aspen, *Populus tremuloides* Michx. *Plant Cell Environ.* 33, 1059–1069. <https://doi.org/10.1111/j.1365-3040.2010.02127.x>.
- Carlquist, S., 1985. Observations on functional wood histology of vines and lianas: vessel dimorphism, tracheids, vascentric tracheids, narrow vessels, and parenchyma. *Aliso* 11, 139–157.
- Charrier, G., Torres-Ruiz, J.M., Badel, E., Burtlett, R., Choat, B., Cochard, H., Delmas, C.E.L., Domec, J.-C., Jansen, S., King, A., Lenoir, N., Martin-StPaul, N., Gambetta, G.A., Delzon, S., 2016. Evidence for hydraulic vulnerability segmentation and lack of xylem refilling under tension. *Plant Physiol.* 172, 1657–1668. <https://doi.org/10.1104/pp.16.01079>.
- Chatelet, D.S., Wistrom, C.M., Purcell, A.H., Rost, T.L., Matthews, M.a, 2011. Xylem structure of four grape varieties and 12 alternative hosts to the xylem-limited bacterium *Xylella fastidiosa*. *Ann. Bot.* 108, 73–85. <https://doi.org/10.1093/aob/mcr106>.

- Chaves, M.M., Santos, T.P., Souza, C.R., Ortuño, M.F., Rodrigues, M.L., Lopes, C.M., Maroco, J.P., Pereira, J.S., 2007. Deficit irrigation in grapevine improves water-use efficiency while controlling vigour and production quality. *Ann. Appl. Biol.* 150, 237–252. <https://doi.org/10.1111/j.1744-7348.2006.00123.x>.
- Choat, B., Drayton, W.M., Brodersen, C., Matthews, M.A., Shackel, K.A., Wada, H., McElrone, A.J., 2010. Measurement of vulnerability to water stress-induced cavitation in grapevine: a comparison of four techniques applied to a long-vesselled species. *Plant Cell Environ.* 33, 1502–1512. <https://doi.org/10.1111/j.1365-3040.2010.02160.x>.
- Chouzouri, A., Schultz, H., 2005. Hydraulic anatomy, cavitation susceptibility and gas-exchange of several grapevine cultivars of different geographic origin. *Acta Hort* 689, 325–332.
- Christman, M.A., Sperry, J.S., Smith, D.D., 2012. Rare pits, large vessels and extreme vulnerability to cavitation in a ring-porous tree species. *New Phytol.* 193, 713–720. <https://doi.org/10.1111/j.1469-8137.2011.03984.x>.
- Cochard, H., Delzon, S., Badel, E., 2014. X-ray microtomography (micro-CT): a reference technology for high-resolution quantification of xylem embolism in trees. *Plant Cell Environ.* <https://doi.org/10.1111/pce.12391>.
- Coombe, B.G., 1995. Adoption of a system for identifying grapevine growth stages. *Aust. J. Grape Wine Res.* 1, 104–110.
- Escalona, J.M., Fuentes, S., Tomás, M., Martorell, S., Flexas, J., Medrano, H., 2013. Responses of leaf night transpiration to drought stress in *Vitis vinifera* L. *Agric. Water Manag.* 118, 50–58. <https://doi.org/10.1016/j.agwat.2012.11.018>.
- Ewers, F.F.W., Fisher, J.B.J., Chiu, S.T., 1990. A survey of vessel dimensions in stems of tropical lianas and other growth forms. *Oecologia* 84, 544–552. <https://doi.org/10.1007/BF00328172>.
- Fereres, E., Soriano, M.A., 2007. Deficit irrigation for reducing agricultural water use. *J. Exp. Bot.* 58, 147–159. <https://doi.org/10.1093/jxb/erl165>.
- Gerzon, E., Biton, I., Yaniv, Y., Zemach, H., Netzer, Y., Schwartz, A., Fait, A., Ben-Ari, G., 2015. Grapevine anatomy as a possible determinant of isohydric or anisohydric behavior. *Am. J. Enol. Vitic.* 66, 340–347. <https://doi.org/10.5344/ajev.2015.14090>.
- Hargrave, K., Klob, K., Ewers, F., Davis, S., 1994. Conduit diameter and drought-induced embolism in *Salvia mellifera* Greene (Labiatae). *New Phytol.* 126, 695–705.
- Hochberg, U., Degu, A., Gendler, T., Fait, A., Rachmilevitch, S., 2015. The variability in the xylem architecture of grapevine petiole and its contribution to hydraulic differences. *Funct. Plant Biol.* 42, 357–365. <https://doi.org/10.1071/FP14167>.
- Hochberg, U., Albuquerque, C., Rachmilevitch, S., Cochard, H., David-Schwartz, R., Brodersen, C.R., McElrone, A., Windt, C.W., 2016. Grapevine petioles are more sensitive to drought induced embolism than stems: evidence from in vivo MRI and microcomputed tomography observations of hydraulic vulnerability segmentation. *Plant Cell Environ.* 39, 1886–1894. <https://doi.org/10.1111/pce.12688>.
- Hochberg, U., Windt, C.W., Ponomarenko, A., Zhang, Y.-J., Gersony, J., Rockwell, F.E., Holbrook, N.M., 2017. Stomatal closure, basal leaf embolism and shedding protect the hydraulic integrity of grape stems. *Plant Physiol.* <https://doi.org/10.1104/pp.16.01816>. 01816.2016.
- Intrigliolo, D.S., Castel, J.R., 2007. Evaluation of grapevine water status from trunk diameter variations. *Irrig. Sci.* 26, 49–59. <https://doi.org/10.1007/s00271-007-0071-2>.
- Jacobsen, A.L., Pratt, R.B., 2012. No evidence for an open vessel effect in centrifuge-based vulnerability curves of a long-vesselled liana (*Vitis vinifera*). *New Phytol.* 194, 982–990. <https://doi.org/10.1111/j.1469-8137.2012.04118.x>.
- Kennedy, J., Kennedy, B.Y.J., 2002. Understanding grape berry development. *Pract. Winer. Vineyard* 4, 1–5.
- Leeuwen, C., Van, Tregooat, O., Chon, X., Bois, B., Pernet, D., Gaudillre, J.P., 2009. Vine water status is a key factor in grape ripening and vintage quality for red bordeaux wine. How can it be assessed for vineyard management purposes? *J. Int. des Sci. la Vigne du Vin* 43, 121–134. <https://doi.org/10.20870/oeno-one.2009.43.3.798>.
- Lo Gullo, M.A., Salleo, S., 1991. Three different methods for measuring xylem cavitation and embolism: a comparison. *Ann. Bot.* 67, 417–424.
- Lovisol, C., Schubert, A., 1998. Effects of water stress on vessel size and xylem hydraulic conductivity in *Vitis vinifera* L. *J. Exp. Bot.* 49, 693–700. <https://doi.org/10.1093/jxb/49.321.693>.
- Medrano, H., Escalona, J.M., Cifre, J., Bota, J., Flexas, J., 2003. A ten-year study on the physiology of two Spanish grapevine cultivars under field conditions: effects of water availability on leaf photosynthesis to grape yield and quality. *Funct. Plant Biol.* 30, 607–619. <https://doi.org/10.1071/FP02110>.
- Munitz, S., Schwartz, A., Netzer, Y., 2014. Evaluation of seasonal water use and crop coefficients for cabernet sauvignon grapevines as the base for skilled regulated irrigation. *Acta Hort* IV 33–40. <https://doi.org/10.17660/ActaHortic.2016.1115.6>.
- Munitz, S., Netzer, Y., Schwartz, A., 2016. Sustained and regulated deficit irrigation of field-grown Merlot grapevines. *Aust. J. Grape Wine Res.* 23, 87–94. <https://doi.org/10.1111/ajgw.12241>.
- Munitz, S., Netzer, Y., Schwartz, A., 2017. Sustained and regulated deficit irrigation of field-grown Merlot grapevines. *Aust. J. Grape Wine Res.* 23, 87–94. <https://doi.org/10.1111/ajgw.12241>.
- Munitz, S., Netzer, Y., Shetin, I., Schwartz, A., 2018. Water availability dynamics have long-term effects on mature stem structure in *Vitis vinifera*. *Am. J. Bot.* 105. <https://doi.org/10.1111/ijlh.12426>. Accepted for publication.
- Myburgh, P.A., 1996. Response of *Vitis vinifera* L. cv. Barlinka/Ramsey to soil water depletion levels with particular reference to trunk growth parameters. *S. Afr. J. Enol. Vitic.* 17.
- Naor, A., Bravdo, B., Gelobter, J., 1994. Gas exchange and water relations in field-grown Sauvignon Blanc grapevines. *Am. J. Enol. Vitic.* 45, 423–428.
- Netzer, Y., Yao, C., Shenker, M., Bravdo, B.-A., Schwartz, A., 2009. Water use and the development of seasonal crop coefficients for Superior Seedless grapevines trained to an open-gable trellis system. *Irrig. Sci.* 27, 109–120. <https://doi.org/10.1007/s00271-008-0124-1>.
- Nolf, M., Lopez, R., Peters, J.M.R., Flavel, R.J., Koloadin, L.S., Young, I.M., Choat, B., 2017. Visualization of xylem embolism by X-ray microtomography: a direct test against hydraulic measurements. *New Phytol.* 214, 890–898. <https://doi.org/10.1111/nph.14462>.
- Patakas, A., Noitsakis, B., Chouzouri, A., 2005. Optimization of irrigation water use in grapevines using the relationship between transpiration and plant water status. *Agric. Ecosyst. Environ.* 106, 253–259. <https://doi.org/10.1016/j.agee.2004.10.013>.
- Pellegrino, A., Lebon, E., Simonneau, T., Wery, J., 2005. Towards a simple indicator of water stress in grapevine (*Vitis vinifera* L.) based on the differential sensitivities of vegetative growth components. *Aust. J. Grape Wine Res.* 11, 306–315.
- Pratt, C., 1974. Vegetative anatomy of cultivated grapes—a review. *Am. J. Enol. Vitic.* 25, 131–150.
- Pratt, R.B., Jacobsen, A.L., 2018. Identifying which conduits are moving water in woody plants: a new HRC-based method. *Tree Physiol.* 00, 1–13. <https://doi.org/10.1093/treephys/tpy034>.
- Romero, P., Ignacio, F., 2010. Physiological thresholds for efficient regulated deficit-irrigation management in winegrapes grown under semiarid conditions. *Am. J. Enol. Vitic.* 3, 300–312.
- Romero, P., Martínez-Cutillas, A., 2012. The effects of partial root-zone irrigation and regulated deficit irrigation on the vegetative and reproductive development of field-grown Monastrell grapevines. *Irrig. Sci.* 30, 377–396. <https://doi.org/10.1007/s00271-012-0347-z>.
- Romero, P., Fernández-Fernández, J.I., Martínez-Cutillas, A., 2010. Physiological thresholds for efficient regulated deficit-irrigation management in winegrapes grown under semiarid conditions. *Am. J. Enol. Vitic.* 61, 300–312.
- Salleo, S., Gullo, M.A., 1986. Xylem cavitation in nodes and internodes of whole *Chorisia insignis* H.B. Et K. Plants subjected to water stress: relations between xylem conduit size and cavitation. *Ann. Bot.* 58, 431–441. <https://doi.org/10.1093/annbot/58.4.431>.
- Salleo, S., Lo Gullo, M.A., Oliveri, F., 1985. Hydraulic parameters measured in 1-year-old-twins of some Mediterranean species with diffuse-porous wood: changes in hydraulic conductivity and their possible functional significance. *J. Exp. Bot.* 36, 1–11.
- Santesteban, L.G., Miranda, C., Royo, J.B., 2011. Regulated deficit irrigation effects on growth, yield, grape quality and individual anthocyanin composition in *Vitis vinifera* L. cv. “Tempranillo”. *Agric. Water Manag.* 98, 1171–1179. <https://doi.org/10.1016/j.agwat.2011.02.011>.
- Schultz, H.R., 2003. Differences in hydraulic architecture account for near- isohydric and anisohydric behaviour of two old-grown. *Plant Cell Environ.* 26, 1393–1406. <https://doi.org/10.1046/j.1365-3040.2003.01064.x>.
- Selles, G., Ferreyra, R., Ahumada, R., Muñoz, I., Silva, H., 2005. Use of trunk growth rate as criteria for automatic irrigation scheduling on table grapes cv. crimson seedless. *Irrigated by Drip. Frutic* 5, 12–16.
- Shellie, K.C., Bowen, P., 2014. Isohydrodynamic behavior in deficit-irrigated Cabernet Sauvignon and Malbec and its relationship between yield and berry composition. *Irrig. Sci.* 32, 87–97. <https://doi.org/10.1007/s00271-013-0416-y>.
- Shtein, I., Meir, S., Riou, J., Philosoph-Hadas, S., 2011. Interconnection of seasonal temperature, vascular traits, leaf anatomy and hydraulic performance in cut *Dodonaea “dana”* branches. *Postharvest Biol. Technol.* 61, 184–192. <https://doi.org/10.1016/j.postharvbio.2011.03.004>.
- Shtein, I., Hayat, Y., Munitz, S., Harcavi, E., Akerman, M., Drori, E., Schwartz, A., Netzer, Y., 2016. From structural constraints to hydraulic function in three *Vitis* rootstocks. *Trees* 31, 851–861. <https://doi.org/10.1007/s00468-016-1510-6>.
- Smart, R.E., 1974. Aspects of water relations of the grapevine (*Vitis vinifera*). *Am. J. Enol. Vitic.* 25, 84–91.
- Tibbetts, T., Ewers, F., 2000. Root pressure and specific conductivity in temperate lianas: exotic *Celastrus orbiculatus* (Celastraceae) vs. native *Vitis riparia* (Vitaceae). *Am. J. Bot.* 87, 1272–1278.
- Ton, Y., Kopyt, M., 2004. Phytomonitoring in realization of irrigation strategies for wine grapes. *Acta Hort.* 652, 167–173.
- Torres-Ruiz, J.M., Cochard, H., Choat, B., Jansen, S., López, R., Tomášková, I., Padilla-Díaz, C.M., Badel, E., Burtlett, R., King, A., Lenoir, N., Martin-StPaul, N.K., Delzon, S., 2017. Xylem resistance to embolism: presenting a simple diagnostic test for the open vessel artefact. *New Phytol.* 215, 489–499. <https://doi.org/10.1111/nph.14589>.
- Tyree, M., Ewers, F., 1991. The hydraulic architecture of trees and other woody plants. *New Phytol.* 119, 345–360.
- Tyree, M.T., Sperry, J.S., 1989. Vulnerability of xylem to cavitation and embolism. *Annu. Rev. Plant Biol.* 40, 19–38. <https://doi.org/10.1146/annurev.pp.40.060189.000315>.
- Venturas, M.D., Sperry, J.S., Hacke, U.G., 2017. Plant xylem hydraulics: what we understand, current research, and future challenges. *J. Integr. Plant Biol.* 59, 356–389. <https://doi.org/10.1111/jipb.12534>.
- Wheeler, E.A., LaPasha, C.A., 1994. Woods of the Vitaceae—fossil and modern. *Rev. Palaeobot. Palynol.* 80, 175–207. [https://doi.org/10.1016/0034-6667\(94\)90001-9](https://doi.org/10.1016/0034-6667(94)90001-9).
- Wheeler, J.K., Sperry, J.S., Hacke, U.G., Hoang, N., 2005. Inter-vessel pitting and cavitation in woody Rosaceae and other vesselless plants: a basis for a safety versus efficiency trade-off in xylem transport. *Plant Cell Environ.* 28, 800–812. <https://doi.org/10.1111/j.1365-3040.2005.01330.x>.
- Williams, L.E., 2012. Interaction of applied water amounts and leaf removal in the fruiting zone on grapevine water relations and productivity of Merlot. *Irrig. Sci.* 30, 363–375. <https://doi.org/10.1007/s00271-012-0355-z>.
- Zimmermann, M., Jeje, A., 1981. Vessel-length distribution in stems of some American woody plants. *Can. J. Bot.* 59, 1882–1892.

2.7: Chapter 7:

From structural constraints to hydraulic function in three *Vitis* rootstocks

Ilana Shtein, Yair Hayat, Sarel Munitz, Eran Harcavi, Michal Akerman, Elyashiv Drori, Amnon Schwartz and Yishai Netzer

Published in *Trees* December 2016

From structural constraints to hydraulic function in three *Vitis* rootstocks

Ilana Shtein² · Yair Hayat^{1,2} · Sarel Munitz^{1,2} · Eran Harcavi³ · Michal Akerman⁴ · Elyashiv Drori¹ · Amnon Schwartz² · Yishai Netzer¹ 

Received: 10 August 2016 / Accepted: 12 December 2016
© Springer-Verlag Berlin Heidelberg 2016

Abstract

Key message Narrow stem size in limiting *Vitis* rootstocks imposes a morphological constraint on the scion via reduced annual ring size, and thus reduces hydraulic conductivity and subsequently physiological performance and yield.

Abstract Graft is a union between two separate species or cultivars, which produces a chimera plant with new qualities—as rootstock affects scion growth, yield, and adaptability to different environmental conditions. In *Vitis*, it is possible to generate rootstock/scion combinations that produce a desired drought stress effect crucial for high-quality wine production, though the mechanisms for such interactions are complex and poorly understood. The current study was done on vines with an identical scion (*Vitis vinifera* ‘Cabernet Sauvignon’) grafted on three different rootstocks—either Riparia Gloire, Paulsen 1103 or 420A—in attempt to explain the differences in water status by examining the underlying anatomical constraints and calculated theoretical hydraulic conductivity. There was a significant difference in physiological responses and yield

between the grafts. Riparia Gloire grafts had the lowest water potentials and the highest quality grapes, together with low root, scion stem, and branch theoretical hydraulic conductivity. In scions grafted on Riparia Gloire, the annual growth rings were significantly narrower than in the other two grafts, causing a significantly lower theoretical hydraulic conductivity per annual ring. The narrow annual ring size in scion stem was imposed by the morphological constraint of the stem size. In hydraulically inferior Riparia Gloire grafts, the difference was disproportionately large, with a wide scion grafted on a very narrow rootstock, and Paulsen 1103 had the smoothest graft union. Our results indicate that the ability to develop stronger drought stress in *Vitis* grafts depends on rootstock-imposed morphological restriction of hydraulic conductivity.

Keywords Functional anatomy · Xylem · Hydraulic conductivity · Grafts · *Vitis vinifera*

Introduction

We thus see that although there is a clear and fundamental difference between the mere adhesion of grafted stocks and the union of the male and female elements in the act of reproduction, yet that there is a rude degree of parallelism in the results of grafting and of crossing distinct species (Charles Darwin 1859).

Graft is a union between two separate species or cultivars, which produces a chimera plant with new qualities—as rootstock affects scion growth, yield, and adaptability to different environmental conditions. Though rootstocks have been extensively used for fruit tree propagation for at

Communicated by A. Nardini.

✉ Yishai Netzer
ynetzer@gmail.com

¹ Agriculture Research Department, Eastern Region Research and Development Center, Ariel 40700, Israel

² The Robert H. Smith Institute of Plant Sciences and Genetics in Agriculture, The Hebrew University of Jerusalem, The Robert H. Smith Faculty of Agriculture, Food and Environment, 76100 Rehovot, Israel

³ The Agricultural Extension Service of Israel, Jerusalem, Israel

⁴ Tabor Winery, Kfar Tavor, Israel

least 2000 years (Webster 1995), their effects on scion physiology are still not fully understood. Over the years, several attempts of mechanistic explanations of this phenomenon were presented. Those can be roughly divided into three categories: (1) hormonal effects (*Lycopersicum*, Albacete et al. 2009; *Gossypium*, Dong et al. 2008; *Vitis*, Skene and Antcliff 1972), (2) assimilate and nutrient movement (*Vitis*, Tardaquila et al. 1995; *Malus*, Jones 1976), and (3) water status (*Malus*, Cohen and Naor 2002; *Olea*, Nardini et al. 2006; *Vitis*, Alsina et al. 2011; Tombesi et al. 2010a). The overall picture is quite complex and the data are sometimes contradictory.

Vitis grafting is a routine agricultural practice. *Vitis vinifera* is the commonly grown *Vitis* species in the Old World, while in North America, *Vitis riparia*, *Vitis labrusca*, and *Vitis rotundifolia* are frequently used for grape and wine production. Cross breeding among *V. berlandieri*, *V. riparia*, and *V. rupestris* has produced several widely used rootstocks. Currently, many commercial rootstocks are available, each having well-known characteristics. Rootstocks are selected on the basis of their performance in different soil types, water requirements, and disease susceptibility—while the scion is selected mainly on the basis of vigor and yield quality. In red grapevine cultivation, yield quality (rather than quantity) is the critical element, which depends mainly on the development of a mild drought stress during growth period—while excessive irrigation induces vigorous canopy growth that leads to both shading and reduced carbohydrate partitioning to reproductive organs (Bravdo and Hepner 1987). Drought stressed vines produce grapes with higher phenol and anthocyanin content that are essential for high-quality red wine production (Bravdo et al. 1985; Kennedy 2002; Castellarin et al. 2007). For instance, a mild drought stress of down to -1.2 MPa at midday for *V. vinifera* cv. Cabernet Sauvignon was shown to be the most effective threshold to optimize soil water availability, irrigation scheduling, yield, and grape quality (Acevedo-Opazo et al. 2010). Drought stress can be induced by reducing irrigation, but this is not always achievable due to either high precipitation or soil structure (terroir). It is possible to generate rootstock/scion combinations that produce a more desired wet soil tolerance (Christensen 2003), though the mechanisms for these beneficial effects are complex and poorly understood.

In the study reported here, significant differences in water status and subsequently yield parameters were found in vines with the identical scion (*V. vinifera* cv. ‘Cabernet Sauvignon’) grafted on three different rootstocks in clay soil with relatively high water content. The current study explains the differences in hydraulic performance by analyzing the underlying anatomical structure of the scion-graft combinations in roots, stems, and branches (shoots).

We undertook an indirect approach of assessing the hydraulic conductivity (calculated based on anatomical measurements)—as a direct measurement of hydraulic conductivity is not feasible in grapevine trunks. In grafted vines, the trunks are the most important structural element, which both combine the rootstock with the scion and integrate the multi-annual hydraulic history of the plant. Though theoretical calculated axial hydraulic conductivity is by no means fully comparable to measured values, they have been found to have a close correlation in *Vitis* branches (Lovisolo and Schubert 1998; Lovisolo et al. 2002).

Materials and methods

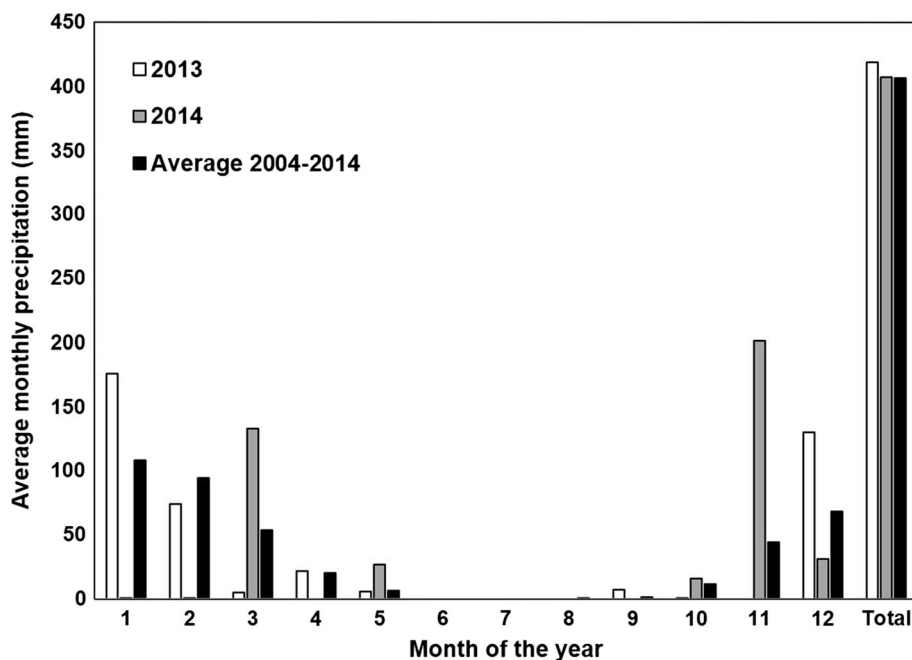
Experimental site

The vineyard examined in this study over two successive years (2013–2014) was planted in 2007. The experimental vineyard was a part of large commercial vineyard, located in the Judean mountain region, with deep clay soil with high stoniness and medium calcite (lime) content. Climatic data were obtained from regional meteorological station located 3 km from the experimental site. The region has semi-arid climate with winter dominant rainfall (Fig. 1). There was a large difference in monthly precipitation between 2013 and 2014, with 2014 being an unusual year (minimal mid-winter rains and pronounced late-winter rains), though the total annual precipitation was similar (Fig. 1).

Plants and agricultural practice

Three treatment groups were examined (graft combinations): *V. vinifera* L. ‘Cabernet Sauvignon’ was grafted on either (1) Riparia Gloire (*V. riparia*), (2) Paulsen 1103 (*Vitis berlandieri* × *Vitis rupestris*), or (3) 420A (*V. berlandieri* × *V. riparia*) rootstock. The grapevines were trained onto a two-wire vertical trellis system. Row direction was east/west, and vine and row spacing were 1.5 and 3 m, respectively (4.5 m² per vine). Winter pruning was conducted according to local practice (15 spurs per vine, two nodes per spur), thus rendering the plant height almost similar. Due to agricultural practice of uniform pruning, variance in canopy structure between the plants was negligible—which rather simplified the experimental design. Pest management and fertilization in the vineyard were performed according to local agricultural standard practice. Irrigation was minimal, 24–30 mm per season applied during August–September (12–18 mm before harvest during 2013 and 2014, respectively, and additional 12 mm after harvest). Irrigation was applied by an above-ground drip line positioned near the row. Harvest was conducted in October.

Fig. 1 Monthly precipitation during the years of the research, compared to a multiple years average of 2004–2014. Climatic data were obtained from regional meteorological station located 3 km from the experimental site



Experimental design

The experimental layout was a completely randomized block design with three treatments (rootstocks) each replicated six times, where each block consisted of one row. In each block, treatments comprised of 15 vines per plot with the outer two vines from each side being border vines and measurements conducted on the inner 11 vines (a total of 198 measurement vines, i.e., 11 vines \times 3 treatments \times 6 replicates). At each plot, three vines, representative of canopy size and trunk diameter, were marked and used for physiological measurements.

The growing season was divided into three phenological stages according to Kennedy (2002): stage I (from bloom to bunch closure), stage II (from bunch closure to veraison), and stage III (from veraison to harvest). The physiological parameters and leaf area index were measured at the end of each stage, yield parameters were measured at the end of stage III, and the anatomical parameters were measured 1 month after harvest.

Leaf area index (LAI)

Leaf area index (LAI) is the ratio of total green surfaces, including leaves, shoots, and fruit (when present), to unit of land area allocated for each vine. Leaf area of three representative vines per plot was determined at the end of each phenological stage using a non-destructive SunScan canopy analysis system (model SS1- R3-BF3, Delta-T Devices, Cambridge, UK). Eight radiation measurements were taken underneath each vine (spaced every 20 cm

covering the soil surface completely under a given vine (for details, see Netzer et al. 2009). To verify the LAI values obtained using this non-destructive method, a leaf area validation was performed using a destructive method. Direct measurement of leaf area was performed on different plants following leaf defoliation from 35 vines at different phenological stages for several different cultivars from different vineyards. Leaf area was then measured using an area meter (model LI-3100, Li-Cor, Lincoln, NE, USA). Estimated and measured LAI values were highly correlated with one another ($y = 0.663x + 0.17$, $r^2 = 0.911$, $p < 0.0001$, $n = 35$).

Physiological parameters

Midday stem water potential (Ψ_s) was measured at solar noon, using pressure chamber (Arimad-3000, MRC, Holon, Israel) according to Kramer and Boyer (1995). Two sunlit, mature, fully expanded leaves from each plot (12 leaves per treatment) were bagged 2 h prior to measurement in plastic bags covered with aluminum foil. The time passed between leaf excision and chamber pressurization was less than 30 s.

Leaf net CO_2 assimilation rate (A) and stomatal conductance (g_s) were measured on 3–4 leaves per plot (18 leaves per treatment), using a portable gas exchange system (LI-6400, Li-Cor, Lincoln, NE, USA). Gas exchange parameters were recorded, and at the same time, Ψ_s measurements were taken; leaves with similar characteristics were chosen for Ψ_s and gas exchange measurements. All physiological measurements were taken 1 day before irrigation.

Yield measurements

The yield measurements were done between the years 2011–2014, thus including two additional years prior to the start of the main research, as a part of a preliminary study. Each plot was harvested when the berry total soluble solids (TSS) reached 23.5°Brix. All 11 measuring vines within each plot were harvested, and number of clusters and yield per vine were recorded. A week before harvest, 36 bunches per plot, randomly chosen, were hand crushed for determination of total soluble solids and pH. At the end of stage III, 100 berries per plot were randomly sampled and weighted, and berry mass was determined.

Anatomy

Sampling

The samples for the anatomical observations were obtained 1 month after the end of stage III. Due to practical considerations, a destructive sampling was not possible, and the sampling was as unobtrusive as possible. *Roots*: Six root samples were sampled with a hoe from every treatment 20 cm from the plant stem, below the drip line. The roots were sampled as uniform as possible, without strong visible suberisation and of similar diameter. The root samples were immediately fixed in FAA (5:5:90, formalin:acetic acid:70% ethanol). *Branches*: Six 6–7-month-old branches (shoots) were sampled and put into polyethylene bags with wet paper towels until further processing in the lab. Branches were sampled with pruning shears; uniform branches were taken from between internodes two and three. *Stems*: Twelve stem cores per treatment were sampled and put into polyethylene bags with wet paper towels until further processing in the lab. Stem cores were taken both from rootstock and from scion. Trunk diameters at the drilling location were measured to calculate annual ring area later. Core samples were collected with 5 mm diameter increment borer (5.15 mm Core 3-Thread Increment Borer, 8", Hagölf, Sweden) and stored at 4 °C temperature in distilled water until sectioned. Rootstock stems were sampled 1 cm above the ground. Scion stems were sampled 50 cm above the ground. Two plants were sampled for each plot (1 scion + 1 rootstock sample per plant; 6 per treatment × 3 blocks, total 82 samples).

Histology

FAA fixed root fragments were dehydrated in a graded alcohol series and then embedded in paraffin wax (Paraplast plus, Leica). Cross sections (12 µm) were cut using a rotary microtome (Leica, Germany) and stained with Toluidine Blue O (O'Brien et al. 1964). Branch cross

sections were obtained by hand sectioning of fresh plant material. Stems were cross sectioned by sliding microtome (NR17800, Reichert, Austria) at thickness of 90 µm. Stem and branch sections were stained with phloroglucinol-HCl (Ruzin 1999). The sections were viewed and photographed under a stereo microscope (Olympus SZ2-ILST) equipped with a camera (Olympus LC20).

Image analysis

Image analysis was done using the ImageJ software (Rasband, W.S., ImageJ, U. S. National Institutes of Health, Bethesda, MD, USA, <http://imagej.nih.gov/ij/>, 1997–2015). Analysis of the roots and the branches was done on the whole section. Analysis of stem cross sections was performed by quantifying various parameters in the visible field separately for the three last annual growth rings (2012–2014). Thousands of vessels were measured simultaneously using Analyze Particles option, while the measured parameters were vessel area (A) and number (N). Vessel area (A) was later converted to diameter (d), as: $d = \sqrt{\frac{4A}{\pi}}$. Vessel number (N) was used to calculate density (D) as: $D = \frac{N}{A}$. Ring and bark diameter were measured in stem sections and used for ring area calculations. Vascular area (A_w) was measured in roots and branches—as the area excluding bark, cambium, and vascular cylinder/pith.

Specific hydraulic conductivity calculations

Theoretical specific hydraulic conductivity (k_s ; $\text{kg m}^{-1} \text{MPa}^{-1} \text{s}^{-1}$) was calculated using the modified Hagen-Poiseuille's equation (Tyree and Ewers 1991):

$$k_s = (\pi\rho/128\eta A_w) \sum_{i=1}^n (d_i^4),$$

where k_s is the specific hydraulic conductivity, ρ is the density of the xylem sap (assumed to be 1000 kg m^{-3}), η is the dynamic viscosity of the xylem sap (assumed to be $1 \times 10^{-9} \text{ MPa s}^{-1}$), A_w is the area (m^2) of the xylem cross section measured, d is the diameter (m) of the i th vessel, and n is the total number of the vessels in the measured area. Hydraulic conductivity per annual ring ($\text{kg m}^{-1} \text{MPa}^{-1} \text{s}^{-1}$) was achieved by multiplying the theoretical xylem-specific hydraulic conductivity by annual growth ring area.

Statistical analysis

Analysis of variance (ANOVA) (JMP Pro 11 Statistical Software; SAS Institute Inc., Cary, NC, USA) was used to determine differences between treatments at $p \leq 0.05$. Tukey post hoc means comparisons were made to compare the significantly different treatments.

Results

Graft physiology and general observations

Visual observation of the different grafts revealed noticeable differences in stem morphology (Fig. 2a). There was a very large difference in stem diameter between Riparia Gloire rootstock and scion (almost 15 mm), a small but significant difference in 420A, while in Paulsen1103, rootstock and scion stem diameters were not significantly different (Fig. 2b). Paulsen1103 rootstock had the widest stem diameter and Riparia Gloire rootstock had the narrowest one. Interestingly, in Paulsen 1103 grafts, the scion diameter was also significantly the widest.

There were significant differences in various yield parameters between the grafts (Table 1). The yield parameters were taken over four consecutive years (2011–2014), including 2 years (2011–2012) of preliminary study. The general trends were preserved during the whole period. Plants grafted on 420A had the highest yield and cluster number, and Paulsen had the highest berry weight. 420A berries had the lowest sugar content (°Brix). Plants grafted on Riparia Gloire had lower yields, which yielded fewer berry clusters with smaller berries. Small berries are known to develop under drought stress (Bravdo et al. 1985) and are considered superior because of their higher skin-to-pulp ratio. In addition, Riparia Gloire berries had a significantly higher sugar content (°Brix) as compared to other two grafts—which is also an indicator of earlier ripening as a consequence of a drought stress (Munitz et al. 2016).

Different physiological parameters were examined during two consecutive years, 2013 and 2014 (Fig. 3). There were clear differences between the years, probably due to

high variation in precipitation distribution pattern. Though the physiological measurements in both years were made during the dry season (May–September), in 2014, the rains were unusually late and overlapped with the measuring season. In 2014, the leaf area index was higher as compared to 2013 (Fig. 3a, b). It is important to note that the decrease in leaf area index (LAI) during the measuring season was caused by routine green hedging (pruning) of the plant's canopy: the hedging was performed in July in 2013 (Fig. 3a), and in June in 2013 (Fig. 3b). The leaf area index was not significantly different between the rootstocks treatments in both years, though Riparia Gloire repeatedly showed the lowest values and Paulsen 1103 the highest ones. Leaf biomass was found to be an important factor in different hydraulic performance of grafted citrus trees (Rodríguez-Gamir et al. 2010), but in the current study, this parameter was equalized by canopy management agricultural practice.

In 2013, there were significant differences between the grafts in several physiological parameters. Riparia Gloire had significantly lower stem water potential (Fig. 3c), stomatal conductance (Fig. 3e), and CO₂ assimilation rate (Fig. 3g). On the other hand, in 2014, only stem water potential was significantly different between the grafts—when Riparia Gloire again had the lowest stem water potential of the three (Fig. 3d). In 2014, Riparia Gloire had lower values of stomatal conductance (Fig. 3f) and CO₂ assimilation rate (Fig. 3h), though the differences were not large and statistically insignificant. Paulsen 1103 had the highest physiological performance of the three grafts during 2013 (Fig. 3c, e, g). In 2014, the plants failed to develop a drought stress; all the water status values were higher than in 2013. In 2014, only in Riparia Gloire, the water potential approached -1 MPa, being much less

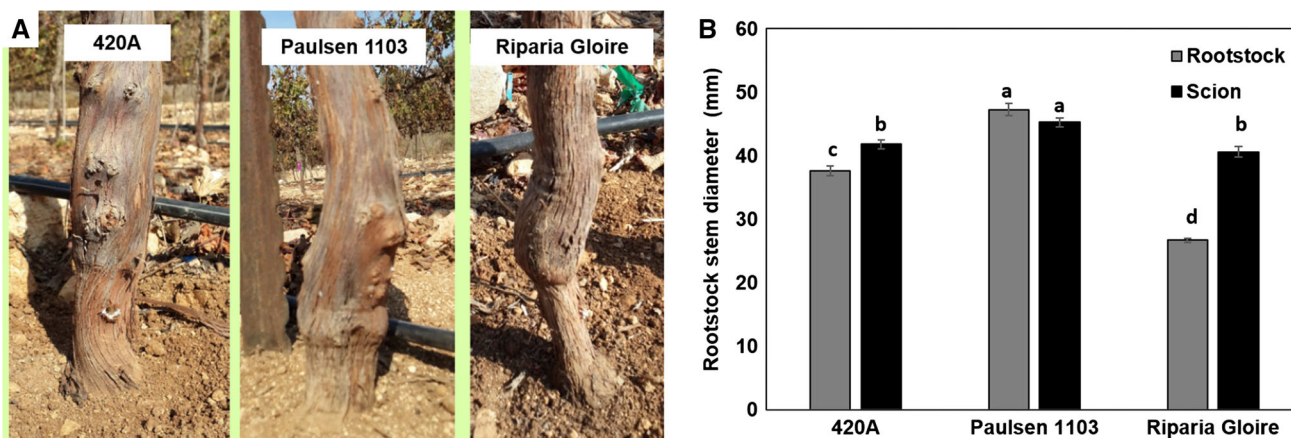


Fig. 2 Stem diameter in grafts of *Vitis vinifera* cv. Cabernet Sauvignon scions on three different rootstocks (420A, Paulsen 1103, and Riparia Gloire). **a** Examples of stem appearance at the graft union, **b** measured stem diameters. Each value is the mean of 12

vines of the same graft (12 rootstock stems + 12 scion stems) \pm standard error. Different letters indicate significant differences between rootstock versus scion at $p \leq 0.05$

Table 1 Yield parameters of *Vitis vinifera* cv. Cabernet Sauvignon scions grafted on three different rootstocks (420A, Paulsen 1103 and Riparia Gloire) in the years 2011–2014

	Year	Rootstocks		
		420A	Paulsen 1103	Riparia Gloire
Yield/plant (kg)	2011	9.90 a	9.40 ab	8.90 b
	2012	6.82 a	6.67 a	5.78 b
	2013	5.67 a	5.16 a	5.14 a
	2014	7.35 a	5.86 b	6.29 ab
Grape cluster N/plant	2011	52 a	49 a	47 a
	2012	37.5 a	38.3 a	35.5 a
	2013	26 a	25 a	25 a
	2014	35 a	30 ab	27 b
100 Berry weight (g)	2012	147 b	158 a	157 a
	2013	155 a	152 a	152 a
	2014	134 a	136 a	128 a
Grape must total soluble solids (°Brix)	2011	22.4 b	23.0 ab	23.8 a
	2012	25.0 b	25.7 a	25.9 a
	2013	24.42 b	24.96 ab	25.04 a
	2014	22.4 b	23.5 b	25.0 a
Grape must pH	2011	3.44 b	3.49 ab	3.51 a
	2012	3.56 a	3.53 ab	3.49 b
	2013	3.52 b	3.57 ab	3.58 a
	2014	3.71 b	3.79 a	3.64 c

Different letters indicate significant differences between rootstocks at $p \leq 0.05$

negative in Paulsen1103 and 420A—around -0.7 MPa (Fig. 3d). In comparison, during 2013, all the rootstocks reached a low water potential of about -1 MPa (Fig. 3c).

Anatomical characteristics and hydraulic conductivity

To understand the structure differences that underlay the variation in physiology, we examined the xylem anatomy of stems, roots, and branches. The rootstock stem vessel diameters were different, while the scion vessel diameters were very similar (Fig. 4). We analyzed both the average vessel diameter and separately large (over $100 \mu\text{m}$) vessel diameter—as large vessels have a significant impact on hydraulic conductivity (Tyree and Ewers 1991). Riparia Gloire rootstock stems had the widest vessel diameter (Fig. 4a) and the widest large ($>100 \mu\text{m}$) vessel diameter (Fig. 4b). Paulsen 1103 rootstock stems had the smallest maximal vessel diameter and fewer large vessels than the other rootstocks (Fig. 4c). Scion stems of all the grafts had similar vessel diameters (Fig. 4a, b). Similar trends could be seen in vessel size distribution frequencies (Fig. 4c, d). Rootstock stems had a large variation in vessel size frequency. Paulsen 1103 rootstock stems had less very small vessels (under $60 \mu\text{m}$) and less very large vessels (over $160 \mu\text{m}$) than the other two rootstocks, and the vessel distribution did not show the classical bimodal curve

(Fig. 4c). 420A and Riparia Gloire rootstock stems both showed a bimodal distribution, with Riparia Gloire having a larger percentage of both very small and very large vessels (Fig. 4c). Scion stem vessels were very similar in all the grafts (Fig. 4a, b, d), showing bimodal vessel distribution (Fig. 4d). Vessel distribution frequency in scions seemed most similar to 420A rootstocks. Vessel diameters in scion stems were larger than in the rootstock stems—vessels of over $280 \mu\text{m}$ were inexistent in rootstocks but comprised over 4% of the vessels in scions.

Stem hydraulic parameters showed very interesting tendencies (Fig. 5). Theoretical hydraulic conductivity per annual ring was significantly lower in the rootstocks as compared to scions, with 420A rootstock having the lowest conductivity (Fig. 5a). In scions, vines grafted on Riparia Gloire had the lowest conductivity. As hydraulic conductivity is influenced both by vessel size, vessel density, and growth ring area, it is important to inspect those parameters as well. The vessel density was similar between the rootstocks and the scions, with all the rootstocks having a slightly higher vessel density than the scions (Fig. 5b). This difference was highest in Riparia Gloire. Annual ring area was the smallest in Riparia Gloire as compared to other two grafts—both in rootstock and in scion (Fig. 5c). Paulsen 1103 rootstock had a significantly larger (though not by a large margin) annual ring area as compared to the Paulsen 1103 graft scion (Fig. 5c).

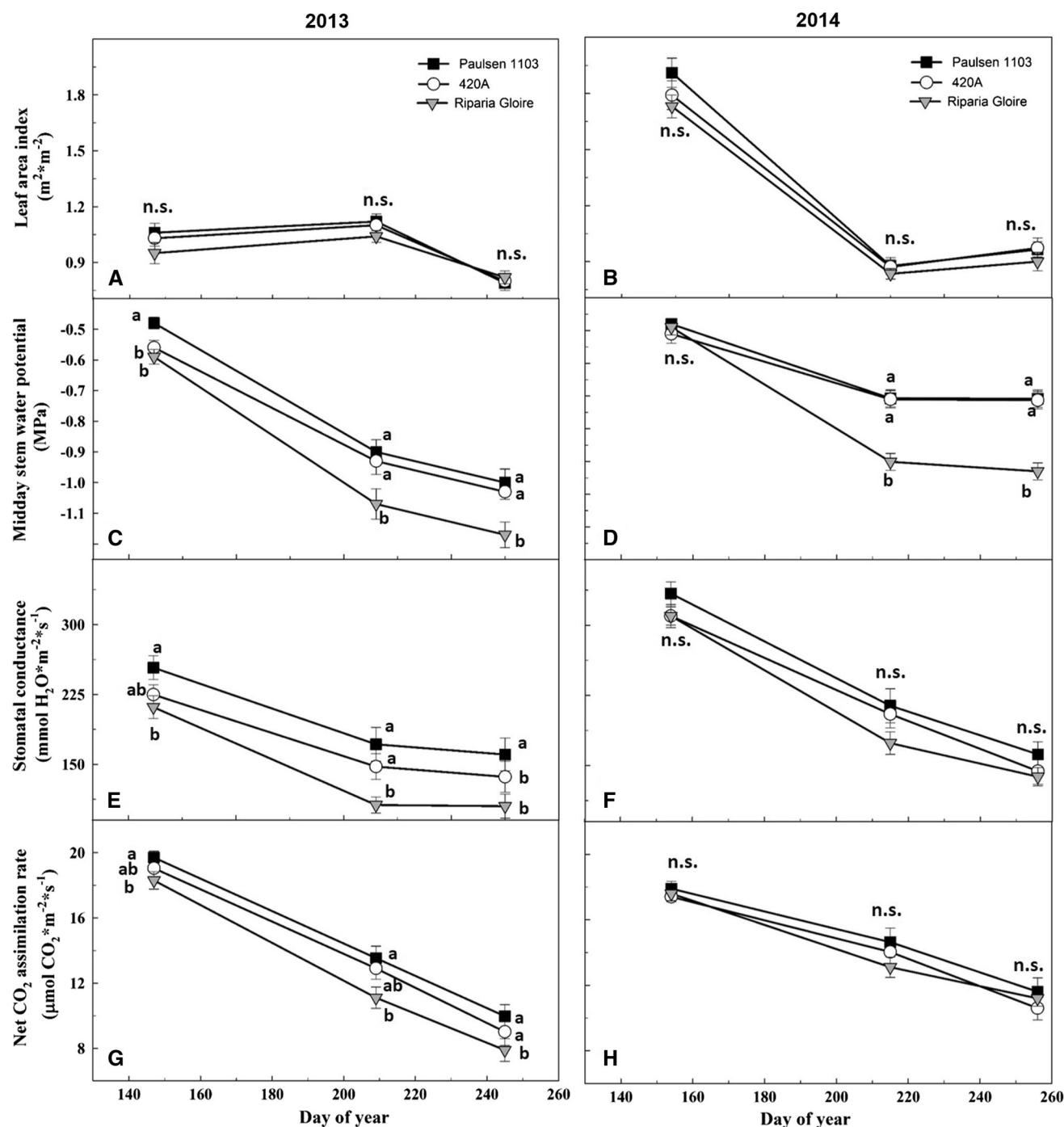


Fig. 3 Physiological parameters in grafts of *Vitis vinifera* cv. Cabernet Sauvignon scions on three different rootstocks (420A, Paulsen 1103 and Riparia Gloire) during the growth season in the years 2013 (a, c, e, g) and 2014 (b, d, f, h). Leaf area index (a, b), midday stem water potential (c, d), stomatal conductance (e, f), and

net CO₂ assimilation rate (g, h). The measurements were made during the dry season (May–September). Each value is the mean of 12 vines of the same graft \pm standard error. Different letters indicate significant differences between rootstocks at $p \leq 0.05$

We also examined the vascular anatomy and calculated hydraulic conductivity of roots and branches (Fig. 6). In general, in all grafts roots had higher specific hydraulic conductivity than branches (Fig. 6). Such axial decrease in hydraulic conductivity is a known phenomenon, that was

reported for different woody species (Domec et al. 2010; Kotowska et al. 2015). Both roots and branches of plants grafted on Riparia Gloire had significantly lowest specific hydraulic conductivity, while those grafted on 420A had the highest ones (Fig. 6a, b). Accordingly, Riparia Gloire

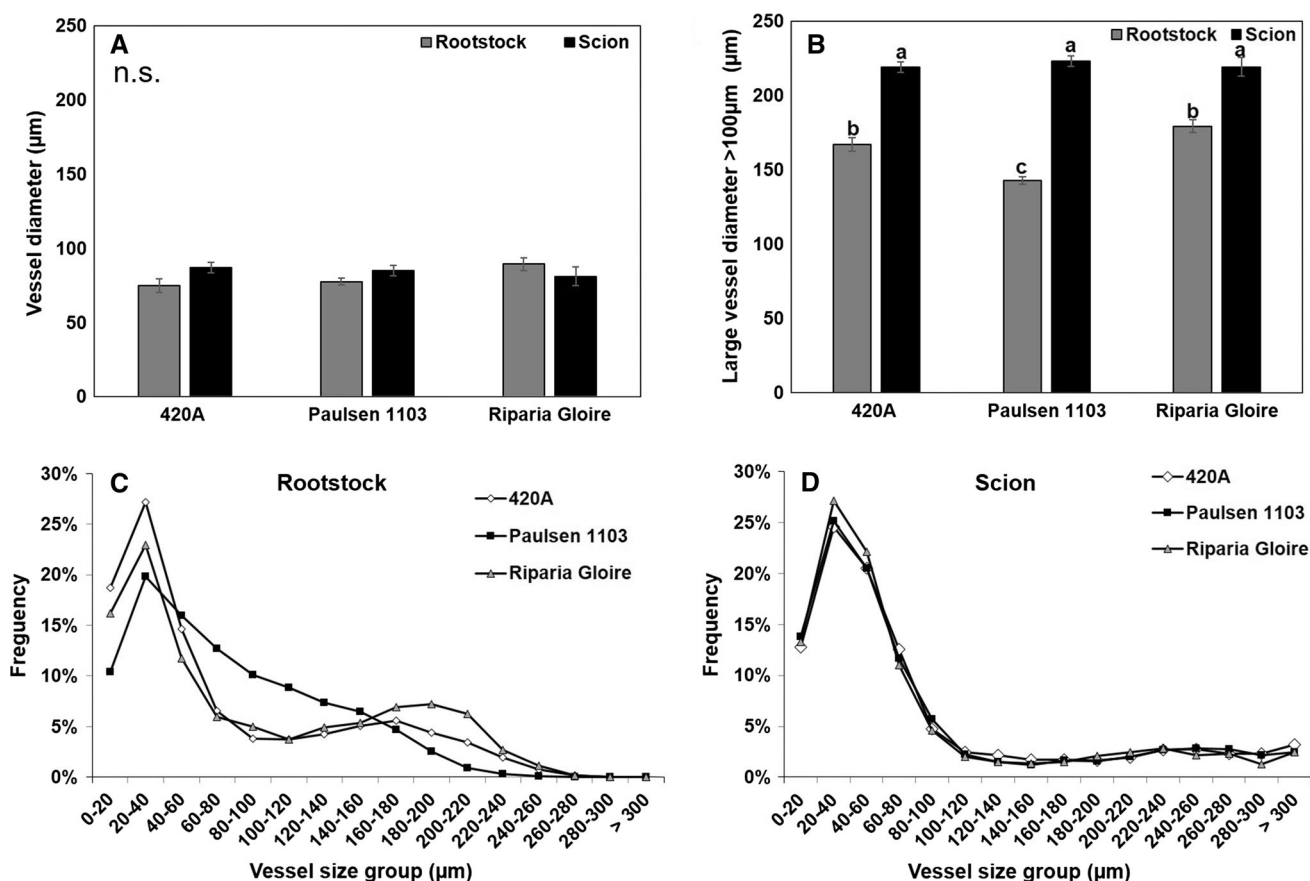


Fig. 4 Stem vessel characteristics in grafts of *Vitis vinifera* cv. Cabernet Sauvignon scions on three different rootstocks (420A, Paulsen 1103 and Riparia Gloire). **a** average vessel diameters, **b** average large (>100 µm) vessel diameters. Each value is the mean

of 12 vines of the same graft (12 rootstock stems + 12 scion stems) ± standard error. Different letters indicate significant differences between rootstocks at $p \leq 0.05$. **c**, **d** Vessel size distribution for all the vessels in rootstock and scion stem, respectively

grafts had the lowest vessel diameters (Fig. 6c, d). The vascular area showed an inconsistent trend—in roots, it was lowest in Paulsen 1103 and highest in 420A (Fig. 6e), and in branches was very similar in all three grafts (Fig. 6f).

Discussion

It is fascinating that scions of the same species and cultivar—*V. vinifera* cv. Cabernet Sauvignon—acquired very different structural and physiological characteristics when grafted on rootstocks of different *Vitis* species. When grown in clay soil with relatively high water content, Riparia Gloire (*V. riparia*) grafts were the most drought stressed (Fig. 3) and, therefore, had the highest yield quality and the lowest quantity (Table 1). The other two grafts were less drought stressed and even failed to reach the required low water potential threshold in the second trial year (Fig. 3d) and thus had an inferior yield quality. Such relationship between drought stress and yield quality

is well documented (Castellarin et al. 2007; Leeuwen et al. 2009; Acevedo-Opazo et al. 2010; Munitz et al. 2016); Riparia Gloire rootstock is, indeed, a restricting rootstock, suitable for inducing drought stress in water excess conditions. However, what is the mechanistic explanation of this phenomenon?

Riparia Gloire graft roots had the lowest specific hydraulic conductivity (Figs. 5a, 6a, b). Similarly, root xylem vessels' diameter was smaller in kiwifruit rootstocks of inferior quality (Wang et al. 1994). Reduced root conductivity was found in dwarfing rootstock in olive (Nardini et al. 2006) and apple (Atkinson et al. 2003); it was considered responsible for the restricting effect of these rootstocks. However, neither calculated nor measured root conductivity can represent the whole root system. We wish to emphasize that although the roots hydraulic parameters were significantly different, only a small sample of the whole root system was measured—six roots per treatment and we do not know the size of the whole root system. For instance, the aquaporins, radial conductivity, root pressure, total roots area, and xylem-to-phloem ratio should be

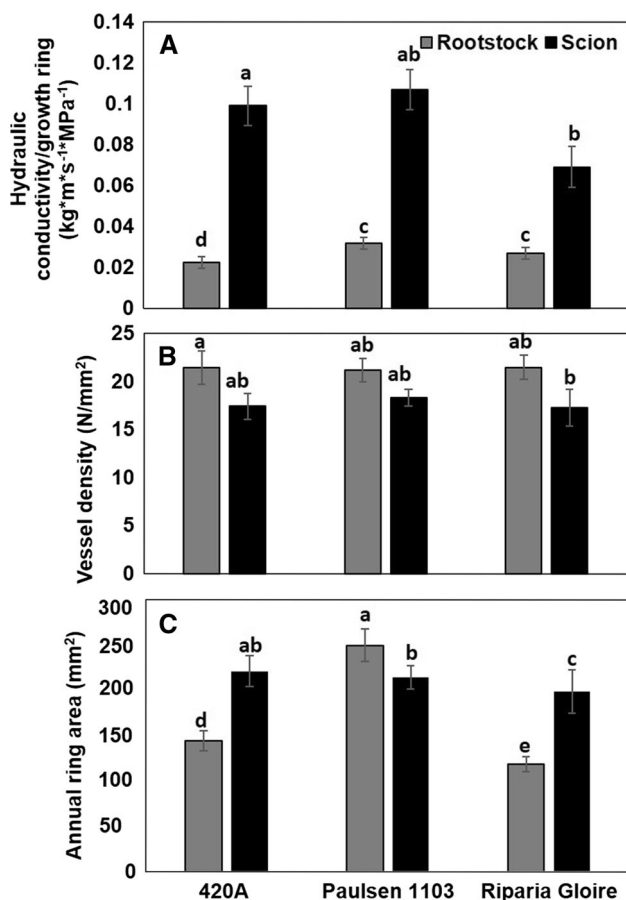


Fig. 5 Stem hydraulic parameters in grafts of *Vitis vinifera* cv. Cabernet Sauvignon scions on three different rootstocks (420A, Paulsen 1103 and Riparia Gloire). Each value is the mean of 12 vines of the same graft (12 rootstock stems + 12 scion stems) \pm standard error. Different letters indicate significant differences between rootstocks at $p \leq 0.05$

considered to describe the root systems complexity (Eshel 1998; Clearwater et al. 2007; Iwanami et al. 2009; Eshel and Grünzweig 2013; Gambetta et al. 2013). In addition, though 420A grafts were intermediate in their physiological performance (Fig. 3) and their quality parameters (Table 1), their roots had the highest hydraulic conductivity and vascular area (Fig. 6a), thus inconsistent with the theory that the roots are the major restricting factor.

It is important to note that all the stems (except Paulsen rootstocks) showed a bimodal vessel size distribution, with numerous small vessels and numerous large vessels, with a decrease in medium-sized vessels frequency. Such bimodal distribution is typical for vines and climbing plants (Carlquist 1985), and is thought to increase both conductivity and safety. The different rootstock stems had large variation in vessel size distribution (Fig. 4c), as they, indeed, belong to different species/hybrids. On the other hand, scion vessel size distribution was very similar between grafts (Fig. 4d), all of them being the same cultivar—*V.*

vinifera ‘Cabernet Sauvignon’. Similarly, in peach grafts, the rootstocks had very little effect on scion vascular anatomy (Tombesi et al. 2010a, 2012). The main significant anatomical difference in scion stems in different grafts was the growth ring area (Fig. 5c). In stems of scions grafted on Riparia Gloire rootstock, the growth rings were significantly narrower than in the other two grafts. Though the vessel frequency and size were not significantly different as compared to the other two grafts, narrow growth rings significantly reduced the water conducting area. Subsequently, in Riparia Gloire scion stems, the hydraulic conductivity per annual ring was the lowest (Fig. 5a). This low conductivity was preserved downstream in Riparia Gloire graft branches as well. It seems that the restricting action of Riparia Gloire rootstock is akin to the mechanism of dwarfing rootstocks, which induce a lower hydraulic conductivity in the scion (Cohen and Naor 2002; Tombesi et al. 2010b). Narrow growth rings were found to be an important anatomical parameter in slow-growing dwarf woody plants (Baas et al. 1984), and were reduced in water-deficient conditions in *Potentilla diversifolia* (Von Arx et al. 2012). Thus, the ability to develop drought stress in Riparia Gloire grafts was probably due to narrow annual rings that limited the downstream water flow capacity.

The narrow annual ring size in scion stem was imposed by the morphological constraint of the stem size. It seems that the hydraulic restriction point was basically the diameter difference between rootstock and scion stems (Fig. 2). In hydraulically inferior Riparia Gloire (*V. riparia*) grafts, the stem diameter difference was disproportionately high, with a wide scion growing on a very narrow rootstock. To adapt itself to growing on a narrow rootstock stem, the scion is forced to limit its stem size by narrowing the annual rings. Thus, such simple morphological constraint causes more elaborate anatomical and physiological changes. It is important to emphasize that Riparia rootstocks did not have a low hydraulic conductivity as compared to the other two rootstocks (Fig. 5); thus, the restricting effect was not due to reduced conductivity between the rootstock and scion, but rather due to structural constraint. Interestingly, (Webber 1948) considered the graft union shape in citrus as the definitive indicator of grafting success—while a smooth graft union was regarded as more successful. However, the major restricting effect might not be due to the decreased hydraulic conductivity in the scion stem itself. The axial portion of the stem pathway contributes a relatively small proportion of the total hydraulic resistance, while the most resistance typically resides in the fine roots, branches, and leaves. In Riparia grafts, the low conductivity was preserved downstream, in the branches (Fig. 6a), and it is possible that the overall restricting effect, while initiating at the morphological constraint at the graft junction, was due to increased

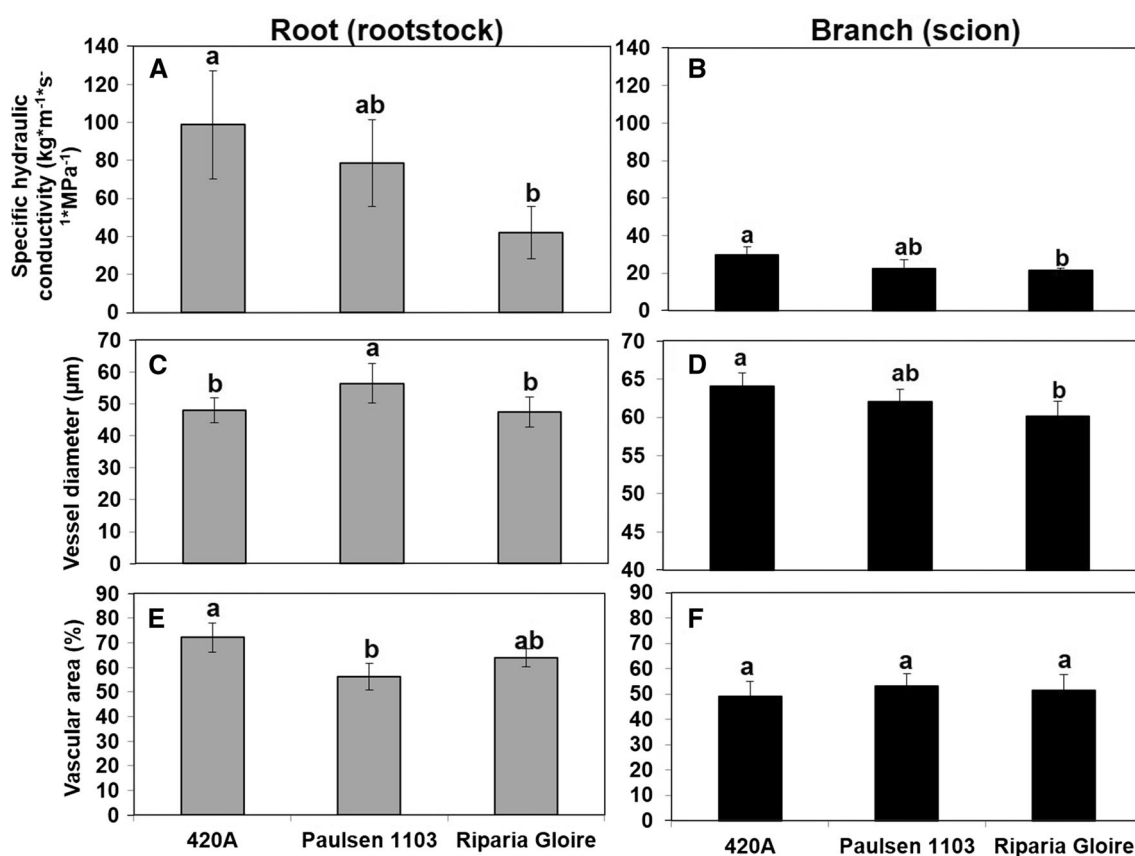


Fig. 6 Root (a, c, e) and branch (b, d, f) hydraulic parameters in grafts of *Vitis vinifera* cv. Cabernet Sauvignon scions on three different rootstocks (420A, Paulsen 1103 and Riparia Gloire). Each

value is the mean of 6 (roots) or 5 (branches) \pm standard error. Different letters indicate significant differences between rootstocks at $p \leq 0.05$

resistance in the end point of the soil to leaf pathway. Unfortunately, it is almost impossible to reliably measure transpiration of a whole plant in the field, and directly show the link between the xylem conductivity to water demand.

Graft is a union of two distinct species, which produces a chimera individual with combined qualities. Such close interaction between two organisms presents numerous difficulties, as they must adapt structurally to each other and function as a single whole. Our results demonstrate that the relationship between the graft and the scion requires compromises. The scion has to adapt structurally to the rootstock, and the extent of compromise needed possibly will determine the vitality of the grafted plant as a whole.

Author contribution statement IS—acquisition and analysis of data, writing, YH—acquisition and analysis of data, SM—acquisition and analysis of data, EH—design of the work, analysis of data, MA—acquisition of data, ED—analysis of data, AS—design of the work, YN—design of the work, acquisition and analysis of data, and writing.

Acknowledgements This work was supported by the Israeli Wine Council. We wish to thank Uri Goren for his help with data processing. We are very grateful to Prof. Amram Eshel for the critical reading of our manuscript.

Compliance with ethical standards

Conflict of interest The authors declare that they have no conflict of interest.

References

- Acevedo-Opazo C, Ortega-Farias S, Fuentes S (2010) Effects of grapevine (*Vitis vinifera* L.) water status on water consumption, vegetative growth and grape quality: an irrigation scheduling application to achieve regulated deficit irrigation. *Agric Water Manag* 97:956–964. doi:10.1016/j.agwat.2010.01.025
- Albacete A, Martínez-Andújar C, Ghanem ME et al (2009) Rootstock-mediated changes in xylem ionic and hormonal status are correlated with delayed leaf senescence, and increased leaf area and crop productivity in salinized tomato. *Plant Cell Environ* 32:928–938. doi:10.1111/j.1365-3040.2009.01973.x
- Alsina MM, Smart DR, Bauerle T et al (2011) Seasonal changes of whole root system conductance by a drought-tolerant grape root system. *J Exp Bot* 62:99–109. doi:10.1093/jxb/erq247
- Atkinson CJ, Else MA, Taylor L, Dover CJ (2003) Root and stem hydraulic conductivity as determinants of growth potential in grafted trees of apple (*Malus pumila* Mill.). *J Exp Bot* 54:1221–1229. doi:10.1093/jxb/erg132
- Baas P, Xinying Z, Chenglee L et al (1984) Some effects of dwarf growth on wood structure. *IAWA J* 5:45–63. doi:10.1163/22941932-90000855

- Bravdo B, Hepner Y (1987) Water management and effect on fruit quality on grapevines. In: Lee TF (ed) Proceedings of the 6th Australian wine industry technical conference. Australian Industrial Publications, Adelaide, pp 150–158
- Bravdo B, Hepner Y, Loinger C et al (1985) Effect of irrigation and crop level on growth, yield and wine quality of cabernet sauvignon. *Am J Enol Vitic* 36:132–139
- Carlquist S (1985) Observations on functional wood histology of vines and lianas: vessel dimorphism, tracheids, vasicentric tracheids, narrow vessels, and parenchyma. *Aliso* 11:139–157
- Castellarin SD, Matthews MA, Di Gaspero G, Gambetta GA (2007) Water deficits accelerate ripening and induce changes in gene expression regulating flavonoid biosynthesis in grape berries. *Planta* 227:101–112. doi:10.1007/s00425-007-0598-8
- Christensen L (2003) Rootstock Selection. In: Christensen L, Dokoozlian N, Walker M, Wolpert J (eds) Wine grape varieties in California. ANR Pub 3419, Oakland, pp 12–15
- Clearwater MJ, Blattmann P, Luo Z, Lowe RG (2007) Control of scion vigour by kiwifruit rootstocks is correlated with spring root pressure phenology. *J Exp Bot* 58:1741–1751. doi:10.1093/jxb/erm029
- Cohen S, Naor A (2002) The effect of three rootstocks on water use, canopy conductance and hydraulic parameters of apple trees and predicting canopy from hydraulic conductance. *Plant Cell Environ* 25:17–28. doi:10.1046/j.1365-3040.2002.00795.x
- Darwin C (1859) On the origin of species by means of natural selection. Murray, London
- Domec JC, Schafer K, Oren R et al (2010) Variable conductivity and embolism in roots and branches of four contrasting tree species and their impacts on whole-plant hydraulic performance under future atmospheric CO₂ concentration. *Tree Physiol* 30:1001–1015. doi:10.1093/treephys/tpq054
- Dong H, Niu Y, Li W, Zhang D (2008) Effects of cotton rootstock on endogenous cytokinins and abscisic acid in xylem sap and leaves in relation to leaf senescence. *J Exp Bot* 59:1295–1304. doi:10.1093/jxb/erm035
- Eshel A (1998) On the fractal dimensions of a root system. *Plant Cell Environ* 21:247–251. doi:10.1046/j.1365-3040.1998.00252.x
- Eshel A, Grünzweig JM (2013) Root-shoot allometry of tropical forest trees determined in a large-scale aeroponic system. *Ann Bot* 112:291–296. doi:10.1093/aob/mcs275
- Gambetta GA, Fei J, Rost TL et al (2013) Water uptake along the length of grapevine fine roots: developmental anatomy, tissue-specific aquaporin expression, and pathways of water transport. *Plant Physiol* 163:1254–1265. doi:10.1104/pp.113.221283
- Iwanami H, Moriya S, Abe K (2009) Relationships between sap flow, hydraulic conductivity, and the anatomical characteristics of stems and roots in apple rootstocks of different vigour. *J Hortic Sci Biotechnol* 84:632–638. doi:10.1080/14620316.2009.11512578
- Jones OP (1976) Effect of dwarfing interstocks on xylem sap composition in apple trees: effect on nitrogen, potassium, phosphorus, calcium and magnesium content. *Ann Bot* 40:1231–1235
- Kennedy BYJ (2002) Understanding grape berry development. *Pract Winer Vineyard*, pp 1–5
- Kotowska MM, Hertel D, Rajab YA et al (2015) Patterns in hydraulic architecture from roots to branches in six tropical tree species from cacao agroforestry and their relation to wood density and stem growth. *Front Plant Sci* 6:1–16. doi:10.3389/fpls.2015.00191
- Kramer PJ, Boyer JS (1995) Pressure chamber. Water relations of plants and soils. Academic Press, San Diego, pp 13–48
- Lovisolio C, Schubert A (1998) Effects of water stress on vessel size and xylem hydraulic conductivity in *Vitis vinifera* L. *J Exp Bot* 49:693–700. doi:10.1093/jxb/49.321.693
- Lovisolio C, Schubert A, Sorce C (2002) Are xylem radial development and hydraulic conductivity in downwardly-growing grapevine shoots influenced by perturbed auxin metabolism? *New Phytol* 156:65–74. doi:10.1046/j.1469-8137.2002.00492.x
- Munitz S, Netzer Y, Schwartz A (2016) Sustained and regulated deficit irrigation of field-grown Merlot grapevines. *Aust J Grape Wine Res* 1:1–8. doi:10.1111/ajgw.12241
- Nardini A, Gascó A, Raimondo F et al (2006) Is rootstock-induced dwarfing in olive an effect of reduced plant hydraulic efficiency? *Tree Physiol* 26:1137–1144. doi:10.1093/treephys/26.9.1137
- Netzer Y, Yao C, Shenker M et al (2009) Water use and the development of seasonal crop coefficients for Superior Seedless grapevines trained to an open-gable trellis system. *Irrig Sci* 27:109–120. doi:10.1007/s00271-008-0124-1
- O'Brien TP, Feder N, McCully ME (1964) Polychromatic staining of plant cell walls by toluidine blue O. *Protoplasma* 59:368–373. doi:10.1007/BF01248568
- Rodríguez-Gamir J, Intrigliolo DS, Primo-Millo E, Forner-Giner MA (2010) Relationships between xylem anatomy, root hydraulic conductivity, leaf/root ratio and transpiration in citrus trees on different rootstocks. *Physiol Plant* 139:159–169. doi:10.1111/j.1399-3054.2010.01351.x
- Ruzin S (1999) Plant microtechnique and microscopy. Oxford University Press, New York
- Skene KGM, Antcliff AJ (1972) A comparative study of cytokinin levels in bleeding sap of *Vitis vinifera* (L.) and the two grapevine rootstocks, Salt Creek and 1613. *J Exp Bot* 23:283–293
- Tardaquila J, Bertamini M, Giulivo C, Scienza A (1995) Rootstock effect on growth, dry weight partitioning and mineral nutrient concentration of grapevine. *Acta Hort* 388:111–116
- Tombesi S, Johnson RS, Day KR, Dejong TM (2010a) Interactions between rootstock, inter-stem and scion xylem vessel characteristics of peach trees growing on rootstocks with contrasting size-controlling characteristics. *AoB Plants*. doi:10.1093/aob/mcp281
- Tombesi S, Johnson RS, Day KR, Dejong TM (2010b) Relationships between xylem vessel characteristics, calculated axial hydraulic conductance and size-controlling capacity of peach rootstocks. *Ann Bot* 105:327–331. doi:10.1093/aob/mcp281
- Tombesi S, Marsal J, Basile B et al (2012) Peach tree vigor is a function of rootstock xylem anatomy and hydraulic conductance. *Acta Hort* 932:483–490
- Tyree M, Ewers F (1991) The hydraulic architecture of trees and other woody plants. *New Phytol* 119:345–360. doi:10.1111/j.1469-8137.1991.tb00035.x
- Van Leeuwen C, Tregoat O, Choné X et al (2009) Vine water status is a key factor in grape ripening and vintage quality for red bordeaux wine. How can it be assessed for vineyard management purposes? *J Int des Sci la Vigne du Vin* 43:121–134
- Von Arx G, Archer SR, Hughes MK (2012) Long-term functional plasticity in plant hydraulic architecture in response to supplemental moisture. *Ann Bot* 109:1091–1100. doi:10.1093/aob/mcs030
- Wang Z-Y, Gould KS, Patterson KJ (1994) Comparative root anatomy of five *Actinidia* species in relation to rootstock effect in kiwifruit flowering. *Ann Bot* 73:403–413
- Webber HJ (1948) Rootstocks: their character and reactions. In: Batchelor LD, Webber HJ (eds) The Citrus Industry, vol 2. University of California Press, Berkeley, pp 69–168
- Webster AD (1995) Rootstock and interstock effects on deciduous fruit tree vigour, precocity, and yield productivity. *N Z J Crop Hortic Sci* 23:373–382. doi:10.1080/01140671.1995.9513913

3. Discussion and conclusions

3.1.1 water consumption and crop coefficient

This experiment was intentionally conducted in a commercial vineyard and lysimeters were constructed in the second row, even though considerable technical difficulties were expected. This approach reflected our desire to measure water consumption of wine grapevines in a way that most accurately represents water consumption of "real" vines growing in "real" commercial vineyard conditions. Similarly, canopy area and water status were always compared between lysimeter vines and field vines. The ET_c of 715 mm season⁻¹ recorded in this study was measured in a region with total ET_o of 1237 mm season⁻¹, thus the seasonal ET_c/ET_o ratio is 0.58. This level of water consumption is in the range reported in the literature for wine grapevines. López-Urrea et al. (2012) reported water consumption (using weighting lysimeters) of 477 mm season⁻¹ for "Tempranillo" grapevines grown under climatic conditions of ET_o of 895 mm season⁻¹ giving an ET_c/ET_o ratio of 0.53. For the same grape cultivar, Picón-Toro (2012) obtained (using weighting lysimeters) water consumption of 834 mm season⁻¹ with ET_o of 1159 mm season⁻¹ giving an ET_c/ET_o ratio of 0.72. It is important to note that both López-Urrea et al. (2012) and Picón-Toro (2012) measured minimal evaporation of dry soil, while in the current study the soil was always completely wet (accepted procedure for drainage lysimeters irrigated at 1-hour intervals). In general, ordinary patterns of ET_c in early season (bud break to bloom) and at late season (stage III, approaching harvest) were mostly influenced by leaf area dynamics, while in mid-season they were highly affected by temperature. The maximal K_c values below 1 obtained in this study are reasonable for VSP-trained wine grapevines with limited canopy area. Our maximal K_c values of 0.8 - 0.9 are in good agreement with other reported K_c values for wine grapevine cultivars. Picón-Toro et al. (2012) reported maximal K_{cb} (dry soil) values around 1 for "Tempranillo" (using weighting lysimeters). Intrigliolo et al. (2009) obtained maximal K_{cb} values of 0.55 for field grown "Riesling" (using a canopy chamber). Higher values of K_c (above 1) have been reported for table grapes with a much wider canopy ($LAI = 5 \text{ m}^2 \text{ m}^{-2}$, Netzer et al, 2009). In "Thompson seedless", Williams et al. (2003) found maximal K_c above 1, and in "Superior Seedless", Netzer et al. (2009) and Wang et al. (2019) reported maximal K_c of 1.2 - 1.3.

3.1.2 Evaporation : transpiration ratio

The average percent evaporation from total evapotranspiration measured in this study was 18%. This is in good agreement with evaporation values reported by others in vineyards. In "Tempranillo" vines, Montoro et al. (2016) calculated 26 - 31% evaporation (using FAO 56

methodology) from total evapotranspiration. In "Cabernet Sauvignon" vines, Kool et al. (2014) reported 8 – 17% evaporation (using eddy correlation) of total evapotranspiration. In table grapes with a much wider canopy that shades the soil, lower evaporation/evapotranspiration ratios were found. In "Thompson seedless", 13% was reported (Williams and Fidelibus, 2016), and in "Superior Seedless", 7% (Netzer et al., 2009). It is important to note that our evaporation results overestimate vineyard evaporation since our lysimeter soil was always wet; nevertheless, our evaporation results underestimate vineyard evaporation since our lysimeter soil surface is only 1.1 m² while the soil surface per vine in the vineyard is 4.5 m².

3.1.3 Leaf area index and crop coefficient relationship

The linear correlation between LAI and K_c reported in this study has a steeper slope (higher K_c for similar LAI) than that of relationships reported for table grapes (Netzer et al., 2009; Williams and Ayars, 2005). This is because the VSP trellis systems used for wine grapes receive much greater sun exposure compared to the vines trailed onto open gable / overhead systems used for table grapes. As mentioned above, K_c is affected by canopy shape and trellising architecture (Williams and Ayars, 2005; Williams and Fidelibus, 2016). We converted the canopy cover percentage data of López-Urrea et al. (2012) to LAI, using correlations from Williams and Ayars (2005) and converted their basal crop coefficient (K_{cb} , only transpiration) to crop coefficient (K_c , transpiration + evaporation, using their own data). The resulting LAI to K_c relationship resembles our correlation, but with a decline in the slope. The slope of the LAI to K_{cb} relationship obtained for wine grapes by Picón-Toro et al. (2012) is quite similar to slopes reported previously for table grapes (Netzer et al., 2009; Williams and Ayars, 2005).

3.2.1 Water availability effect on physiological parameters

In general, the vines physiological parameters were strongly affected by the irrigation regime, e.g. irrigation initiation timing.

The seasonal trend of decreasing values of Ψ_s along the growing seasons is typical for deficit irrigated vineyards, where there is a continuous depletion of available soil water content (Intrigliolo and Castel, 2010; Munitz et al., 2016; Netzer et al., 2019; Olivo et al., 2008; Romero et al., 2010b). The vines of the early irrigation treatments (Budbreak & -0.6 MPa) had consistently significantly higher values of Ψ_s compared to those of the late irrigation treatments (-1.0 MPa & -1.2 MPa, Fig. 2), reinforcing the findings that Ψ_s is a sensitive indicator of vine water status (Acevedo-Opazo et al., 2010; Choné et al., 2001; Munitz et al., 2016; Patakas et al., 2005; Santesteban et al., 2019; Williams and Araujo, 2002). The range of Ψ_s values measured in this

study in the lysimeter vines (-0.3 to -0.65 MPa), are typical for non-stressed grapevines. Picón-Toro (2012) reported Ψ_s of -0.35 to -0.8 MPa in non-stressed "Tempranillo" vines. Patakas et al. (2005) obtained Ψ_s of -0.4 to -0.6 MPa in non-stressed "Malagouzia" vines. Picón-Toro (2012) calculated that in grapevines, evapotranspiration is maximal down to Ψ_s of -0.5 to -0.6 MPa, and then begins to decrease. Our lysimeter vines maintained Ψ_s of -0.6 MPa and higher throughout all growing seasons, meaning that their evapotranspiration was kept maximal as required by FAO paper 56 for ET_c calculation (Allen et al., 1998). The similar Ψ_s of field-grown vines and lysimeter vines during the spring period demonstrates that lysimeter vines represent field-grown vines during high water availability periods. A phenomenon that had emerged over the trial years is that vines of the late irrigation treatments reached their thresholds points (that determined irrigation start point) earlier as the trial years passed, in contrast to vines of the early irrigation treatments that reached a stabilized threshold timeframe. This may imply on increased drought stress sensitivity derived from prolong exposure to a deficit irrigation regime. SWP value of -1.4 MPa is considered as an indicator of severe drought stress (Leeuwen et al., 2009; Romero et al., 2010b), and was not crossed by any of the vines in all irrigation treatments during 2014 & 2015. In contrast, the -1.4 MPa threshold was crossed by all vines in all irrigation treatments during the beginning of stage III in 2016 and during the middle of stage II in 2017 & 2018. This phenomenon cannot be explained by differences in evapotranspiration and precipitation, neither by canopy area. Severe drought stress conditions that are evident earlier along the growing season as trial year's advance, can be derived from the long-term effect of deficit irrigation.

Significant differences in values of g_s and A_n between vines of the early and the late irrigation treatments were present from DOY 140 to 180, but they were less pronounced compared to differences in the Ψ_s values. When g_s values decreased beneath the severe drought stress threshold of $50 \text{ mmol H}_2\text{O m}^{-2} \text{ s}^{-1}$ (Flexas et al., 2002; Medrano et al., 2002), the differences between vines of different irrigation treatments were obscured, even though significant differences in Ψ_s values were still present during that time. When A_n values declined beneath the threshold of $4 \text{ } \mu\text{mol CO}_2 \text{ m}^{-2} \text{ s}^{-1}$, the same phenomenon was recorded, thus it can be considered as A_n severe drought stress threshold. The meaning of this, is that Ψ_s is a clearer vine water status indicator compared to gas exchange parameters, especially during periods in which severe drought stress conditions prevail. A commencement of decline in g_s and A_n values was recorded at DOY 160 - 170 during 2014 - 2015 in vines of all irrigation treatments, while during 2016 - 2018 it was present already at DOY 130 - 145 (Fig. 3). Again, this can be interpreted as long-term effect of photosynthesis downregulation caused by a prolonged deficit irrigation regime. Since in it was found by us that drought stress effects anatomical structure and hydraulic conductivity (Munitz et al., 2018; Netzer

et al., 2019), it can give good explanation of the long term additive effect of drought stress on physiological parameters.

3.2.2 Drought stress effect on vegetative growth

In general, vegetative growth occurred mainly during springtime (stage I), in which late irrigation vines received minimal irrigation, resulting in decreased vegetative growth in those vines. As the experiment period advanced, a reduction in seasonal vegetative development was recorded in all vines, nevertheless it was more pronounced in the late irrigation vines.

The growth of vine trunk diameter occurring during the period of early season (mainly stage I), is also reported by others for wine grapevines (Edwards and Clingeleffer, 2013; Intrigliolo and Castel, 2007; Montoro et al., 2011; Myburgh, 1996; Ton and Kopyt, 2004) and is consistent with spring time cambium activity (Bernstein and Fahn, 1960). During the trunk widening period, the late irrigation vines received almost no irrigation, explaining the multiseasonal gradual deceleration in their trunk growth compared to the early irrigation vines. Interestingly, a sharp decrease in annual width growth in the late irrigation treatments trunks was recorded over 2017, enlarging by nearly a third compared to trunk growth of the early irrigation treatments. This also suggests a cumulative effect of drought stress conditions on vegetative growth. The fluctuations in trunk width during the dormancy period of the vines can be attributed to temperature variation effect on dendrometers and to changes in the phloem and outer bark width as a result of wetting/drying cycles. To our knowledge, this is the first multiseasonal curve of trunk's dendrometry of wine grapevines reported in the literature.

Vine canopy area (measured as LAI) development usually takes place from bud break until the end of stage I (bunch closure) as observed in this current study. This is consistent with documented results (Munitz et al., 2019, 2016; Netzer et al., 2019, Ben-Asher et al., 2006; Edwards and Clingeleffer, 2013; Intrigliolo et al., 2009; Peacock et al., 1987; Romero and Martinez-Cutillas, 2012). The range of maximal LAI values (0.75 to 1.45 m² m⁻²), is in agreement with others that conducted LAI measurements (using several different methods) at deficit irrigated vineyards trained on a VSP trellis system (Buesa et al., 2017; Intrigliolo and Castel, 2010; Johnson et al., 2003; Romero et al., 2010b). Similar LAI values of lysimeter and field vines indicate that the lysimeter vines are well representative of field-grown vines. LAI was shown to have a strong effect on ET_c (Munitz et al., 2019). Ohana-Levi et al. (2019) analyzed the dataset derived from the lysimeters and related the influence of meteorological variables and LAI on ET_c. It was found that LAI had a relative influence over ET_c ranging between 62 and 86% compared to the impact of the meteorological variables. Pruning mass values recorded in this work (0.8 to 1.0 kg vine⁻¹) are

complementary to those reported by others in VSP trained vines (Bou Nader et al., 2019; Buesa et al., 2017; Edwards and Clingeleffer, 2013; Intrigliolo and Castel, 2007; Reynolds et al., 1996; Turkington et al., 1980). The vines treated with early irrigation had significantly heavier pruning mass compared to the late irrigation vines, supporting the findings that pruning mass is a well-established indicator of seasonal vegetative growth (Bravdo et al., 1984; Buesa et al., 2017; Chaves et al., 2007; Kliewer and Dokoozlian, 2005; Poni et al., 1994; Williams et al., 2003). The significantly heavier pruning mass was derived from heavier shoot mass, while there was no increase in shoot number. Interestingly, the "Budbreak" vines had 20% heavier pruning mass compared to the -0.6 MPa vines (not significant), even though they received during springtime only an additional 18 mm in average. Annual ring width and area, which represent annual vegetative growth, were found to be positively correlated with high water availability early in the season (Stage I). The dominance of early season vegetative growth in *Vitis vinifera* can be explained by the fact that cambial activity to produce new vascular elements takes place mainly during the early stage of the growing season (until 20 days after bunch closure, Bernstein and Fahn, 1960).

3.2.3 Water availability effect on anatomical structure.

As cambial activity is renewed at the beginning of each growing season, a new set of active xylem vessels is produced. The frequency diameter distribution of these vessels is essentially genetically-based, yet environmental conditions and water availability can also affect xylem anatomy (Chatelet et al., 2011; Munitz et al., 2018). Our current study clearly shows that vessel diameters can be increased by manipulating plant water status. From our data it is shown that improved water availability during stage I, increased vessel diameter and specific hydraulic conductivity. As larger diameter vessels (formed during stage I) are more prone to the risk of embolism formation, water availability can be reduced towards the end of the growing season. Thus, inducing even greater plant drought stress than in vines that were exposed all season to low water availability and were anatomically acclimated to those conditions. The influence of water status on the hydraulic anatomy has extensive ecological and agricultural implications. In the wine grape industry where drought stress has a cardinal effect on both yield and quality of red wines, it is highly important to recognize the within-season and between-season implications. This is especially important in the light of current climate change with decreasing worldwide water availability, as such changes will have a strong effect on plant structure and function (Escalona et al., 2013; Torres-Ruiz et al., 2017). In climatic regions where vineyards rely exclusively on irrigation, agro-technical

manipulation of xylem structure could be used by growers as a significant tool to influence water status and determine wine quality.

3.2.4 Irrigation regime effect on yield components

The range of yield that was recorded (4.3 to 6.1 kg vine⁻¹) complies with values reported by other studies for high quality vineyards planted in similar densities (Guidoni et al., 2002; Keller et al., 2008; Medrano et al., 2003; Shellie and Bowen, 2014), and is also representative for local premium commercial vineyards. The crucial effect of water availability during spring time on yield levels, found in this current work, is consistent with a recent study (Munitz et al., 2016). Yield increase in early irrigation treatment vines was a result of increased berry mass and to lesser extent due to higher bunch number. The values of berry mass obtained by us (1.20 to 0.95 gr) are typical for deficit irrigated field-grown 'Cabernet Sauvignon' vines (Bravdo et al., 1985; Chalmers et al., 2010; Edwards and Clingeleffer, 2013; Shellie and Bowen, 2014). The classical "double sigmoid" berry growth pattern reported by others (Coombe et al., 1992; Coombe and McCarthy, 2000; Hardie and Considine, 1976) was not present in current study. Interestingly, over the seasons with more extreme drought stress levels (2016 - 2018) differences in berry mass of vines that received different irrigation treatments were more pronounced compared to seasons in which higher water availability prevailed (2014 – 2015). As shown in other studies (Bahar et al., 2011; Bonada et al., 2013; Fuentes et al., 2010), we found that the occurrence of shriveled berries is significantly positively affected ($p < 0.05$) by drought stress.

4. Reference

- Acevedo-Opazo, C., Ortega-Farias, S., Fuentes, S.,** 2010. Effects of grapevine (*Vitis vinifera L.*) water status on water consumption, vegetative growth and grape quality: An irrigation scheduling application to achieve regulated deficit irrigation. *Agric. Water Manag.* **97**, 956–964. <https://doi.org/10.1016/j.agwat.2010.01.025>
- Allen, R.G., Pereira, L., Raes, D.,** 2006. Crop evapotranspiration. Guidelines for computing crop water requirements., in: FAO Irrigation and Drainage Paper. ROME.
- Allen, R.G., Pereira, L.S., Raes, D., Smith, M.,** 1998. Crop evapotranspiration. Guidelines for computing crop water requirements. FAO irrigation and drainage paper no. 56, FAO irrigation and drainage paper no. 56. ROME. <https://doi.org/10.1016/j.eja.2010.12.001>
- Bahar, E., Carbonneau, A., Korkutal, I.,** 2011. The effect of extreme water stress on leaf drying limits and possibilities of recovering in three grapevine (*Vitis vinifera L.*) cultivars. *Afr. J. Agric. Res.* **6**, 1151–1160. <https://doi.org/10.5897/AJAR10.778>
- Ben-Asher, J., Tsuyuki, I., Bravdo, B.-A., Sagih, M.,** 2006. Irrigation of grapevines with saline water I. Leaf area index, stomatal conductance, transpiration and photosynthesis. *Agric. Water Manag.* **83**, 13–21. <https://doi.org/10.1016/j.agwat.2006.01.002>
- Ben-Gal, A., Kool, D., Agam, N., van Halsema, G.E., Yermiyahu, U., Yafe, A., Presnov, E., Erel, R., Majdop, A., Zipori, I., Segal, E., Rüger, S., Zimmermann, U., Cohen, Y., Alchanatis, V., Dag, A.,** 2010. Whole-tree water balance and indicators for short-term drought stress in non-bearing “Barnea” olives. *Agric. Water Manag.* **98**, 124–133. <https://doi.org/10.1016/j.agwat.2010.08.008>
- Bernstein, Z., Fahn, A.,** 1960. The Effect of Annual and Bi-annual Pruning on the Seasonal Changes in Xylem Formation in the Grapevine. *Ann. Bot.* **24**, 159–171.
- Bonada, M., Sadras, V., Moran, M., Fuentes, S.,** 2013. Elevated temperature and water stress accelerate mesocarp cell death and shrivelling, and decouple sensory traits in Shiraz berries. *Irrig. Sci.* **31**, 1317–1331. <https://doi.org/10.1007/s00271-013-0407-z>
- Bou Nader, K., Stoll, M., Rauhut, D., Patz, C.D., Jung, R., Loehnertz, O., Schultz, H.R., Hilbert, G., Renaud, C., Roby, J.P., Delrot, S., Gomès, E.,** 2019. Impact of grapevine age on water status and productivity of *Vitis vinifera L.* cv. Riesling. *Eur. J. Agron.* **104**, 1–12. <https://doi.org/10.1016/j.eja.2018.12.009>
- Bravdo, B., Hepner, Y., Loinger, C., Cohen, S., Tabacman, H.,** 1984. Effect of crop level on growth, yield and wine quality of a high yielding Carignane vineyard. *Am. J. Enol. Vitic.* **35**, 247–252.
- Bravdo, B., Hepner, Y., Loinger, C., Cohen, S., Tabacman, H.,** 1985. Effect of irrigation and crop level on growth, yield and wine quality of Cabernet Sauvignon. *Am. J. Enol. Vitic.* **36**, 132–139.
- Buesa, I., Pérez, D., Castel, J., Intrigliolo, D., Castel, JR,** 2017. Effect of deficit irrigation on vine performance and grape composition of *Vitis vinifera L.* cv. Muscat of Alexandria. *Aust. J. Grape Wine Res.* **23**, 251–259. <https://doi.org/10.1111/ajgw.12280>
- Bureau, S.M., Baumes, R.L., Razungles, A.J.,** 2000. Effects of vine or bunch shading on the glycosylated flavor precursors in grapes of *Vitis vinifera L.* Cv. Syrah. *J. Agric. Food Chem.* **48**, 1290–1297. <https://doi.org/10.1021/jf990507x>
- Carrasco-Benavides, M., Ortega-Farías, S., Lagos, L.O., Kleissl, J., Morales, L., Poblete-Echeverría, C., Allen, R.G.,** 2012. Crop coefficients and actual evapotranspiration of a drip-irrigated Merlot vineyard using multispectral satellite images. *Irrig. Sci.* **30**, 485–497. <https://doi.org/10.1007/s00271-012-0379-4>
- Chalmers, Y.M., Downey, M.O., Krstic, M.P., Loveys, B.R., Dry, P.R.,** 2010. Influence of sustained deficit irrigation on colour parameters of Cabernet Sauvignon and Shiraz microscale wine fermentations. *Aust. J. Grape Wine Res.* **16**, 301–313. <https://doi.org/10.1111/j.1755-0238.2010.00093.x>
- Chatelet, D.S., Rost, T.L., Matthews, M. a, Shackel, K. a,** 2008. The peripheral xylem of grapevine (*Vitis vinifera*) berries. 2. Anatomy and development. *J. Exp. Bot.* **59**, 1997–2007. <https://doi.org/10.1093/jxb/ern061>
- Chaves, M., Zarrouk, O., Francisco, R., Costa, J., Santos, T., Regalado, A., Rodrigues, M., Lopes, C.,** 2010. Grapevine under deficit irrigation: hints from physiological and molecular data. *Ann. Bot.* **105**, 661–76.

<https://doi.org/10.1093/aob/mcq030>

- Chaves, M.M., Santos, T.P., Souza, C.R., Ortuño, M.F., Rodrigues, M.L., Lopes, C.M., Maroco, J.P., Pereira, J.S.**, 2007. Deficit irrigation in grapevine improves water-use efficiency while controlling vigour and production quality. *Ann. Appl. Biol.* **150**, 237–252. <https://doi.org/10.1111/j.1744-7348.2006.00123.x>
- Choné, X., Leeuwen, C. Van, Dubourdieu, D., Gaudillere, J.P.**, 2001. Stem water potential is a sensitive indicator of grapevine water status. *Ann. Bot.* **87**, 477–483.
- Chorti, E., Guidoni, S., Ferrandino, A., Novello, V.**, 2010. Effect of different cluster sunlight exposure levels on ripening and anthocyanin accumulation in Nebbiolo grapes. *Am. J. Enol. Vitic.* **61**, 23–30.
- Consoli, S., D’Urso, G., Toscano, A.**, 2006. Remote sensing to estimate ET-fluxes and the performance of an irrigation district in southern Italy. *Agric. Water Manag.* **81**, 295–314. <https://doi.org/10.1016/j.agwat.2005.04.008>
- Coombe, B.G.G., McCarthy, M.G., Kennedy, B.Y.J.**, 1992. Research on Development and Ripening of the Grape Berry. *Am. J. Enol. Vitic.* **43**, 101–110. <https://doi.org/10.1111/j.1755-0238.2000.tb00171.x>
- Coombe, B.G.G., McCarthy, M.G.G.**, 2000. Dynamics of grape berry growth and physiology of ripening. *Aust. J. Grape Wine Res.* **6**, 131–135. <https://doi.org/10.1111/j.1755-0238.2000.tb00171.x>
- Deidda, P., Dettori, S., Filigheddu, M., Viridis, F., Pala, M.**, 1990. Lysimetric analysis of water requirements for young table-olive trees. *Acta Hort.* **286**, 259–261.
- Di, H., Cameron, K.**, 2002. Nitrate leaching in temperate agroecosystems: Sources, factors and mitigating strategies. *Nutr. Cycl. Agroecosystems* **64**, 237–256. <https://doi.org/10.1023/A:1021471531188>
- Doorenbos, J., Pruitt, W.**, 1977. Guidelines for predicting crop water requirements. *FAO Irrig. Drain. Pap.* **24**.
- Edwards, E.J., Clingeleffer, P.R.**, 2013. Interseasonal effects of regulated deficit irrigation on growth, yield, water use, berry composition and wine attributes of Cabernet Sauvignon grapevines. *Aust. J. Grape Wine Res.* **19**, 261–276. <https://doi.org/10.1111/ajgw.12027>
- Esteban, M.A., Villanueva, M.J., Lissarrague, J.R.**, 2001. Effect of irrigation on changes in the anthocyanin composition of the skin of cv Tempranillo (*Vitis vinifera* L) grape berries during ripening. *J. Sci. Food Agric.* **81**, 409–420. [https://doi.org/10.1002/1097-0010\(200103\)81:4<409::AID-JSFA830>3.0.CO;2-H](https://doi.org/10.1002/1097-0010(200103)81:4<409::AID-JSFA830>3.0.CO;2-H)
- Evans, R.G., Spayd, S.E., Wample, R.L., Kroeger, M.W., Mahan, M.O.**, 1993. Water use of *Vitis vinifera* grapes in Washington*. *Agric. Water Manag.* **23**, 109–124. [https://doi.org/10.1016/0378-3774\(93\)90035-9](https://doi.org/10.1016/0378-3774(93)90035-9)
- Fereres, E., Evans, R.G.**, 2006. Irrigation of fruit trees and vines: An introduction. *Irrig. Sci.* **24**, 55–57. <https://doi.org/10.1007/s00271-005-0019-3>
- Fernandes-Silva, A., Oliveira, M., A. Paço, T., Ferreira, I.**, 2019. Deficit Irrigation in Mediterranean Fruit Trees and Grapevines: Water Stress Indicators and Crop Responses, in: *Irrigation in Agroecosystems*. pp. 1–35. <https://doi.org/10.5772/intechopen.80365>
- Flexas, J., Escalona, J.M., Evain, S., Gulías, J., Moya, I., Osmond, C.B., Medrano, H.**, 2002. Steady-state chlorophyll fluorescence (Fs) measurements as a tool to follow variations of net CO₂ assimilation and stomatal conductance during water-stress in C₃ plants, in: *Phys.* pp. 231–240.
- Fuentes, S., Sullivan, W., Tilbrook, J., Tyerman, S.**, 2010. A novel analysis of grapevine berry tissue demonstrates a variety-dependent correlation between tissue vitality and berry shrivel. *Aust. J. Grape Wine Res.* **16**, 327–336. <https://doi.org/10.1111/j.1755-0238.2010.00095.x>
- Gao, Y., Cahoon, G.A.**, 1994. Cluster shading effects on fruit quality, fruit skin color, and anthocyanin content and composition in Reliance (*Vitis* hybrid). *Vitis* **33**, 205–209.
- García-Tejero, I.F., Hernandez, A., Rodriguez, V., Ponce, J., Ramos, V., Muriel, J., Duran-Zuazo, V.H.**, 2015. Estimating Almond Crop Coefficients and Physiological Response to Water Stress in Semiarid Environments (SW Spain). *J. Agric. Sci. Technol.* **17**, 1255–1266.
- Girona, J., del Campo, J., Mata, M., Lopez, G., Marsal, J.**, 2011. A comparative study of apple and pear tree water consumption measured with two weighing lysimeters. *Irrig. Sci.* **29**, 55–63. <https://doi.org/10.1007/s00271-010-0217-5>

- Girona, J., Marsal, J., Mata, M., Del Campo, J., Basile, B.**, 2009. Phenological sensitivity of berry growth and composition of Tempranillo grapevines (*Vitis vinifera* L.) to water stress. *Aust. J. Grape Wine Res.* **15**, 268–277. <https://doi.org/10.1111/j.1755-0238.2009.00059.x>
- Grimes, D.W., Williams, L.E.**, 1990. Irrigation Effects on Plant Water Relations and Productivity of Thompson Seedless Grapevines. *Crop Sci.* **30**, 255–260. <https://doi.org/10.2135/cropsci1990.0011183X003000020003x>
- Guidoni, S., Allara, P., Schubert, A.**, 2002. Effect of cluster thinning on berry skin anthocyanin composition of *Vitis vinifera* cv. Nebbiolo. *Am. J. Enol. Vitic.* **53**, 224–226.
- Hardie, W., Considine, J.**, 1976. Response of grapes to water-deficit stress in particular stages of development. *Am. J. Enol. Vitic.* **27**, 55–61.
- Heilmeier, H., Wartinger, A., Erhard, M., Zimmermann, R., Horn, R., Schulze, E.D.**, 2002. Soil drought increases leaf and whole-plant water use of *Prunus dulcis* grown in the Negev Desert. *Oecologia* **130**, 329–336. <https://doi.org/10.1007/s004420100808>
- Intrigliolo, D.S., Castel, J.R.**, 2010. Response of grapevine cv. ‘Tempranillo’ to timing and amount of irrigation: water relations, vine growth, yield and berry and wine composition. *Irrig. Sci.* **28**, 113–125. <https://doi.org/10.1007/s00271-009-0164-1>
- Intrigliolo, D.S., Castel, J.R.**, 2007. Evaluation of grapevine water status from trunk diameter variations. *Irrig. Sci.* **26**, 49–59. <https://doi.org/10.1007/s00271-007-0071-2>
- Intrigliolo, D.S., Lakso, A.N., Piccioni, R.M.**, 2009. Grapevine cv. ‘Riesling’ water use in the northeastern United States. *Irrig. Sci.* **27**, 253–262. <https://doi.org/10.1007/s00271-008-0140-1>
- Jagtap, S., Jones, J.**, 1989. stability of crop coefficients under different climate and irrigation Management Practices *. *Irrig. Sci.* **10**, 231–244.
- Johnson, L., Roczen, D., Youkhana, S., Nemani, R., Bosch, D.**, 2003. Mapping vineyard leaf area with multispectral satellite imagery. *Comput. Electron. Agric.* **38**, 33–44.
- Keller, M.**, 2005. Deficit irrigation and vine mineral nutrition. *Am. J. Enol. Vitic.* **56**, 267–283.
- Keller, M., Smithyman, R., Mills, L.**, 2008. Interactive effects of deficit irrigation and crop load on Cabernet Sauvignon in an arid climate. *Am. J. Enol. Vitic.* **59**, 221–234. <https://doi.org/10.5344/ajev.2011.10103>
- Kliewer, W., Dokoozlian, N.**, 2005. Leaf area/crop weight ratios of grapevines: influence on fruit composition and wine quality. *Am. J. Enol. Vitic.* **56**, 170–181.
- Kool, D., Ben-Gal, A., Agam, N., Šimůnek, J., Heitman, J., Sauer, T., Lazarovitch, N.**, 2014. Spatial and diurnal below canopy evaporation in a desert vineyard: Measurements and modeling. *Water Resour. Res.* **50**, 7035–7049. <https://doi.org/10.1002/2014WR015409>
- Leeuwen, C. Van, Tregoat, O., Chone, X., Bois, B., Pernet, D., Gaudillere, J.P.**, 2009. Vine water status is a key factor in grape ripening and vintage quality for red bordeaux wine. How can it be assessed for vineyard management purposes? *J. Int. des Sci. la Vigne du Vin* **43**, 121–134. <https://doi.org/10.20870/oenone.2009.43.3.798>
- Lopes, C., Monteiro, A., Rückert, F.E., Gruber, B., Steinberg, B., Schultz, H.R., Braun, P., Schmid, J., Campos, I., Neale, C.M.U., Calera, A., Balbontín, C., González-Piqueras, J., Ferreyra, R., Sellés, G., Ruiz, R., Sellés, Im.**, 2010. Assessing satellite-based basal crop coefficients for irrigated grapes (*Vitis vinifera* L.). *Agric. Water Manag.* **98**, 45–54. <https://doi.org/10.1016/j.agwat.2010.07.011>
- López-Urrea, R., Montoro, a., Mañas, F., López-Fuster, P., Fereres, E.**, 2012. Evapotranspiration and crop coefficients from lysimeter measurements of mature ‘Tempranillo’ wine grapes. *Agric. Water Manag.* **112**, 13–20. <https://doi.org/10.1016/j.agwat.2012.05.009>
- Lorite, I., Santos, C., Testi, L., Fereres, E.**, 2012. Design and construction of a large weighing lysimeter in an almond orchard. *Spanish J. Agric. Res.* **10**, 238. <https://doi.org/10.5424/sjar/2012101-243-11>
- Medrano, H., Escalona, J.M., Bota, J., Gulías, J., Flexas, J.**, 2002. Regulation of photosynthesis of C3 plants in response to progressive drought: Stomatal conductance as a reference parameter. *Ann. Bot.* **89**, 895–905. <https://doi.org/10.1093/aob/mcf079>

- Medrano, H., Escalona, J.M., Cifre, J., Bota, J., Flexas, J.,** 2003. A ten-year study on the physiology of two Spanish grapevine cultivars under field conditions: effects of water availability from leaf photosynthesis to grape yield and quality. *Funct. Plant Biol.* **30**, 607–619. <https://doi.org/10.1071/FP02110>
- Montoro, A., Mañas, F., López-Urrea, R.,** 2016. Transpiration and evaporation of grapevine, two components related to irrigation strategy. *Agric. Water Manag.* **177**, 193–200. <https://doi.org/10.1016/j.agwat.2016.07.005>
- Montoro, A., Urrea, R.L., Manas, F., Fuster, L.L.,** 2011. Dendrometric measurements in grapevine (*Vitis vinifera* L. 'Tempranillo' and 'Cabernet sauvignon') under regulated deficit irrigation. *Acta Hort* 113–122.
- Morrison, J.C., Noble, A.C.,** 1990. The effects of leaf and cluster shading on the composition of Cabernet Sauvignon grapes and on fruit and wine sensory properties. *Am. J. Enol. Vitic.* **41**, 193–200.
- Mpelasoka, B., Behboudian, M., Green, S.,** 2001. Water use, yield and fruit quality of lysimeter-grown apple trees: Responses to deficit irrigation and to crop load. *Irrig. Sci.* **20**, 107–113. <https://doi.org/10.1007/s002710100041>
- Munitz, S., Netzer, Y., Schwartz, A.,** 2016. Sustained and regulated deficit irrigation of field-grown Merlot grapevines. *Aust. J. Grape Wine Res.* **23**, 87–94. <https://doi.org/10.1111/ajgw.12241>
- Munitz, S., Netzer, Y., Shetin, I., Schwartz, A.,** 2018. Water availability dynamics have long-term effects on mature stem structure in *Vitis vinifera*. *Am. J. Bot.* **105**, 1–10. <https://doi.org/10.1111/ijlh.12426>
- Munitz, S., Schwartz, A., Netzer, Y.,** 2019. Water consumption, crop coefficient and leaf area relations of a *Vitis vinifera* cv. "Cabernet Sauvignon" vineyard. *Agric. Water Manag.* **219**, 86–94. <https://doi.org/10.1016/j.agwat.2019.03.051>
- Myburgh, P.A.,** 1996. Response of *Vitis vinifera* L. cv. Barlinka/Ramsey to soil water depletion levels with particular reference to trunk growth parameters. *South African J. Enol. Vitic.* **17**.
- Netzer, Y., Munitz, S., Shtein, I., Schwartz, A.,** 2019. Structural memory in grapevines : Early season water availability affects late season drought stress severity. *Eur. J. Agron.* **105**, 96–103. <https://doi.org/10.1016/j.eja.2019.02.008>
- Netzer, Y., Yao, C., Shenker, M., Bravdo, B.-A.B.-A., Schwartz, A.,** 2009. Water use and the development of seasonal crop coefficients for Superior Seedless grapevines trained to an open-gable trellis system. *Irrig. Sci.* **27**, 109–120. <https://doi.org/10.1007/s00271-008-0124-1>
- Ohana-Levi, N., Munitz, S., Ben-Gal, A., Netzer, Y.,** 2019a. Evaluation of within-season grapevine evapotranspiration patterns and drivers using generalized additive models. *Agric. water Manag.* **228**. <https://doi.org/10.5331/seppyo.33.215>
- Ohana-Levi, N., Munitz, S., Ben-Gal, A., Schwarz, A., Peeters, A., Netzer, Y.,** 2019b. Multiseasonal grapevine water consumption – drivers and forecasting. *Agric. For. Meteorol.* **280**.
- Oliver, H., Sene, K.,** 1992. Energy and water balances of developing vines. *Agric. For. Meteorol.* **61**, 167–185. [https://doi.org/10.1016/0168-1923\(92\)90048-9](https://doi.org/10.1016/0168-1923(92)90048-9)
- Olivo, N., Girona, J., Marsal, J.,** 2008. Seasonal sensitivity of stem water potential to vapour pressure deficit in grapevine. *Irrig. Sci.* **27**, 175–182. <https://doi.org/10.1007/s00271-008-0134-z>
- Padgett-Johnson, M., Williams, L., Walker, M.,** 2003. Vine water relations, gas exchange, and vegetative growth of seventeen *Vitis* species grown under irrigated and nonirrigated conditions in California. *J. Am. Soc.* **128**, 269–276.
- Patakas, A., Noitsakis, B., Chouzouri, A.,** 2005. Optimization of irrigation water use in grapevines using the relationship between transpiration and plant water status. *Agric. Ecosyst. Environ.* **106**, 253–259. <https://doi.org/10.1016/j.agee.2004.10.013>
- Peacock, W., Christensen, L., Andris, H.,** 1987. Development of a drip irrigation schedule for average canopy vineyards in the San Joaquin valley. *Am. J. Enol. Vitic.* **38**, 113–119.
- Pellegrino, A., Lebon, E., Simonneau, T., Wery, J.,** 2005. Towards a simple indicator of water stress in grapevine (*Vitis vinifera* L.) based on the differential sensitivities of vegetative growth components. *Aust. J. Grape Wine Res.* **11**, 306–315.

- Picón-Toro, J., González-Dugo, V., Uriarte, D., Mancha, L., Testi, L.**, 2012. Effects of canopy size and water stress over the crop coefficient of a “Tempranillo” vineyard in south-western Spain. *Irrig. Sci.* **30**, 419–432. <https://doi.org/10.1007/s00271-012-0351-3>
- Picón, J., Uriarte, D., Mancha, L.A., Blanco, J., Prieto, M.H.**, 2012. Seasonal crop coefficients and relationships with measures of canopy development for “Tempranillo” grapevines in south-western Spain, in: *Acta Horticulturae*. pp. 235–242.
- Poni, S., Lakso, A., Turner, J., Melious, R.E.**, 1994. Interactions of crop level and late season water stress on growth and physiology of field-grown Concord grapevines. *Am. J. Enol. Vitic.* **45**, 252–258.
- Prior, L.D., Grieve, A.M.**, 1987. Water use and irrigation requirements of grapevine, in: Sixth Australian Wine Industry Technical Conference. pp. 165–168.
- Reynolds, A.G., Wardle, D.A., Naylor, A.P.**, 1996. Impact of training system, vine spacing, and basal leaf removal on riesling. Vine performance, berry composition, canopy microclimate, and vineyard labor requirements. *Am. J. Enol. Vitic.* **47**, 63–76. <https://doi.org/10.1071/PP9960115>
- Ro, H.M.**, 2001. Water use of young “Fuji” apple trees at three soil moisture regimes in drainage lysimeters. *Agric. Water Manag.* **50**, 185–196. [https://doi.org/10.1016/S0378-3774\(01\)00099-3](https://doi.org/10.1016/S0378-3774(01)00099-3)
- Romero, P., Fernández-Fernández, J.I., Martínez-Cutillas, A.**, 2010a. Physiological Thresholds for Efficient Regulated Deficit-Irrigation. *Am. J. Enol. Vitic.* **61**, 400–401.
- Romero, P., Fernández-Fernández, J.I., Martínez-Cutillas, A., Ignacio, F., Fernández-Fernández, J.I., Martínez-Cutillas, A.**, 2010b. Physiological thresholds for efficient regulated deficit-irrigation management in winegrapes grown under semiarid conditions. *Am. J. Enol. Vitic.* **61**, 300–312.
- Romero, P., Gil-Muñoz, R., del Amor, F.M., Valdés, E., Fernández, J.I., Martínez-Cutillas, A.**, 2013. Regulated Deficit Irrigation based upon optimum water status improves phenolic composition in Monastrell grapes and wines. *Agric. Water Manag.* **121**, 85–101. <https://doi.org/10.1016/j.agwat.2013.01.007>
- Romero, P., Martínez-Cutillas, A.**, 2012. The effects of partial root-zone irrigation and regulated deficit irrigation on the vegetative and reproductive development of field-grown Monastrell grapevines. *Irrig. Sci.* **30**, 377–396. <https://doi.org/10.1007/s00271-012-0347-z>
- Rozenstein, O., Haymann, N., Kaplan, G., Tanny, J.**, 2018. Estimating cotton water consumption using a time series of Sentinel-2 imagery. *Agric. Water Manag.* **207**, 44–52. <https://doi.org/10.1016/j.agwat.2018.05.017>
- Santesteban, L.G., Miranda, C., Marín, D., Sesma, B., Intrigliolo, D.S., Mirás-Avalos, J.M., Escalona, J.M., Montoro, A., de Herralde, F., Baeza, P., Romero, P., Yuste, J., Uriarte, D., Martínez-Gascuña, J., Cancela, J.J., Pinillos, V., Loidi, M., Urrestarazu, J., Royo, J.B.**, 2019. Discrimination ability of leaf and stem water potential at different times of the day through a meta-analysis in grapevine (*Vitis vinifera* L.). *Agric. Water Manag.* **221**, 202–210. <https://doi.org/10.1016/j.agwat.2019.04.020>
- Santesteban, L.G., Miranda, C., Royo, J.B.**, 2011. Regulated deficit irrigation effects on growth, yield, grape quality and individual anthocyanin composition in *Vitis vinifera* L. cv. “Tempranillo.” *Agric. Water Manag.* **98**, 1171–1179. <https://doi.org/10.1016/j.agwat.2011.02.011>
- Scholander, P., Hammel, H., Bradstreet, E., Hemmingsen, E.**, 1965. Sap pressure in vascular plants. *Science* (80-.). **148**, 339–346.
- Shellie, K.C., Bowen, P.**, 2014. Isohydrodynamic behavior in deficit-irrigated Cabernet Sauvignon and Malbec and its relationship between yield and berry composition. *Irrig. Sci.* **32**, 87–97. <https://doi.org/10.1007/s00271-013-0416-y>
- Shtein, I., Hayat, Y., Munitz, S., Harcavi, E., Akerman, M., Drori, E., Schwartz, A., Netzer, Y.**, 2016. From structural constraints to hydraulic function in three *Vitis* rootstocks. *Trees* **31**, 851–861. <https://doi.org/10.1007/s00468-016-1510-6>
- Ton, Y., Kopyt, M.**, 2004. Phytomonitoring in realization of irrigation strategies for wine grapes. *Acta Hort.* **652**, 167–173.
- Turkington, C.R., Peterson, J.R., Evans, J.C.**, 1980. A Spacing, Trellising, and Pruning Experiment with Muscat Gordo Blanco Grapevines. *Am. J. Enol. Vitic.* **31**, 298–302.

- Van Zyl, J., Van Huyssteen, L.**, 1980. Comparative studies on wine grapes on different trellising systems: I. Consumptive water use. *South African J. Enol. Vitic.* **1**, 7–14.
- Vanino, S., Pulighe, G., Nino, P., De Michele, C., Bolognesi, S., D'Urso, G.**, 2015. Estimation of Evapotranspiration and Crop Coefficients of Tendone Vineyards Using Multi-Sensor Remote Sensing Data in a Mediterranean Environment. *Remote Sens.* **7**, 14708–14730. <https://doi.org/10.3390/rs71114708>
- Wang, S., Zhu, G., Xia, D., Ma, J., Han, T., Ma, T., Zhang, K., Shang, S.**, 2018. The characteristics of evapotranspiration and crop coefficients of an irrigated vineyard in arid Northwest China. *Agric. Water Manag.* **212**, 388–398. <https://doi.org/10.1016/j.agwat.2018.09.023>
- Watts, D.G., Hergert, G.W., Nichols, J.T.**, 1991. Plant and Environment Interactions. Nitrogen Leaching Losses from Irrigated Orchardgrass on Sandy Soils. *J. Environ. Qual.* **20**, 355–362.
- Williams, L.E., Araujo, F.J.**, 2002. Correlations among predawn leaf, midday leaf, and midday stem water potential and their correlations with other measures of soil and plant water status in *Vitis vinifera*. *J. Am. Soc.* **127**, 448–454.
- Williams, L.E., Ayars, J.E.**, 2005. Water use of Thompson Seedless grapevines as affected by the application of gibberellic acid (GA3) and trunk girdling - Practices to increase berry size. *Agric. For. Meteorol.* **129**, 85–94. <https://doi.org/10.1016/j.agrformet.2004.11.007>
- Williams, L.E., Fidelibus, M.W.**, 2016. Measured and estimated water use and crop coefficients of grapevines trained to overhead trellis systems in California's San Joaquin Valley. *Irrig. Sci.* **34**, 431 - 441. <https://doi.org/10.1007/s00271-016-0513-9>
- Williams, L.E., Phene, C.J., Grimes, D.W., Trout, T.J.**, 2003. Water use of mature Thompson Seedless grapevines in California. *Irrig. Sci.* **22**, 11–18. <https://doi.org/10.1007/s00271-003-0067-5>
- Yunusa, I.A.M., Walker, R.R., Lu, P.**, 2004. Evapotranspiration components from energy balance, sapflow and microlysimetry techniques for an irrigated vineyard in inland Australia. *Agric. For. Meteorol.* **127**, 93–107. <https://doi.org/10.1016/j.agrformet.2004.07.001>

5. Hebrew summary (תקציר בעברית)

כרמי ענבי היין המיועדים לגידול ענבים עבור ייצור יין איכותי מושקים במנות מים נמוכות, העומדות בין 70 ל-200 מ"ק לדונם לעונה, מכיוון שפרקטיקת הגידול מחייבת השריית עקת יובש. יישום מנות מים גבוהות מוביל ליבולים גבוהים יחסית, אך מצד שני גורם ליצירת פרי באיכות נמוכה מבחינה ייננית (Bravdo and Hepner, 1987). המגמה הכללית בארץ בשנים האחרונות היא הרחבה מואצת של שטחי כרמים המיועדים לייצור ענבי איכות (שומרון, גולן, גליל והרי יהודה). יחד עם ההבנה שהשקיה מושכלת היא כלי רב עוצמה בקביעת איכות היין, קיימים עדיין פערי ידע משמעותיים במיוחד בתחום קביעת גודל מנות המים לאורך עונת הגידול ומועד תחילת ההשקיה. מטרת המחקר הנוכחי היא פיתוחו של מודל השקיה עבור ענבי יין המבוסס על מדידת צריכת מים יומית באמצעות ליזימטרים ולימוד ההשפעה של מדדי אקלים וגודל הנוף. ליבת המודל היא חישובו של מקדם הגידול הספציפי עבור ענבי יין וייחוסו לגודל העלווה של הגפנים (LAI). חישוב מקדם הגידול (K_c) מתבצע על ידי חלוקה של צריכת המים האמיתית של הגפנים (ET_c) בהתאדות המחושבת על פי נוסחת פנמן-מונטית (ET_0). צריכת המים האמיתית של שישה גפני יין מהזן "קברנה סובניון" נמדדה החל מעונת גידול 2012 בכרם מסחרי באזור שילה באמצעות מערך של שישה ליזימטרי שטיפה, וההתאדות הפוטנציאלית חושבה ע"י מדדים מטאורולוגיים המתקבלים מתחנה מטאורולוגית סמוכה. בניית הקשר בין מקדם הגידול (K_c) לגודל הנוף, מאפשרת את חישוב מקדם הגידול בכרמים אחרים בהם נמדד גודל הנוף בלבד. מאחר ובארץ פרוסות תחנות מטאורולוגיות רבות, ניתן לקבל נתונים מטאורולוגיים מהימנים אשר על פיהם ניתן יהיה לחשב את ההתאדות הפוטנציאלית באזור הכרם. לאחר שמקדם הגידול (K_c) וההתאדות המחושבת (ET_0) נמצאו ניתן לחשב את צריכת המים עבור הכרם המסוים על פי הנוסחה: $ET_c = ET_0 \times K_c$. מכיוון שכאמור בגידול גפן יין דרושה עקת יובש בכדי לקבל יבול איכותי (חומרי צבע וטעם) המתאים לייצור יין, נהוג ליישם השקיה באחוז מסוים מצריכת המים המקסימלית (ET_c), על ידי הכפלת צריכת המים המקסימלית במקדם עקה (K_s). ניסויים רחבי היקף נערכו בעבר על ידי קבוצת המחקר שלנו בכדי לבחון את השפעת גובה מקדם העקה והשינוי שלו לאורך עונת הגידול. נקודה חשובה נוספת הנדרשת ליישמו המושכל של מודל ההשקיה היא המועד בעונת הגידול בו מתחילים להשקות את הגפנים. בעבודה זו נבחנו מועדי תחילת השקיה שונים הנקבעים על פי ספים פיזיולוגיים של הגפן (פוטנציאל מים בגזע בצהרי היום) וההשפעה שלהם על מדדים פיזיולוגיים ואנטומים. הניסוי נערך בכרם מסחרי הסמוך למערך הליזימטרים, והוקם בעונת הגידול 2014. נקבעו חמישה ערכי סף של פוטנציאל המים בגזע לתחילת ההשקיה: לבלוב, 0.6 MPa, -0.8 MPa, -1 MPa, -1.2 MPa (ערכי פוטנציאל מים בגזע בצהרי היום). הטיפולים השונים מפוזרים בכרם בארבע חזרות בתבנית של בלוקים באקראי, כאשר כל חזרה בנויה משלוש שורות (שתי שורות גבול ובניהם שורת מדידה). בתוך כל חזרה, כל טיפול בנוי מ-16 גפנים, שמתוכן 12 הגפנים המרכזיות נמדדות (2 גפני גבול מכל צד). לאורך עונת הגידול נלקחים באופן רציף המדדים הפיזיולוגיים הבאים: פוטנציאל המים בגזע בצהרי היום, קצב קיבוע פחמן, מוליכות פיוניות, גודל הנוף, קוטר הגזע ומשקל הגרגרים באשכול. בנוסף לכך מדדים אנטומיים (קוטר טרכיאיות, מוליכות הידראולית) נמדדים ומחושבים בחלקי הגפן השונים (פטוטר, זמורה, גזע). בסוף כל עונת גידול נמדד גובה היבול ומספר האשכולות בכל גפן בנפרד ומכל חזרה מוכן יין בשיטת מיקרוויניפיקציה ביקב מחקרי של מו"פ שומרון. טעימה עיוורת של כל 20 היינות נערכת על ידי פנל של ייננים מומחים מכל היקבים המובילים בארץ. בניסוי הליזימטרים נמצא כי בין מקדם הגידול (K_c) לבין שטח העלווה (LAI) ישנו יחס ישר ומובהק $(K_c = 0.54 \cdot LAI + 0.16, R^2 = 0.66)$. כמו כן לגפני הליזימטרים היו תפקודים פיזיולוגיים (פוטנציאל מים, שטח עלווה, חילוף גזים, משקל גזם) כמו אלו של גפני השדה בתקופת האביב (בה יש זמינות מים גבוהה).

בניסוי מועד תחילת ההשקיה נמצא כי ככל שמתחילים להשקות את הגפנים מוקדם יותר לאורך עונת הגידול – כך הצימוח הווגטטיבי, המדדים הפיזיולוגיים, גודל הגרגר וגובה היבול – עולים. לעומת זאת, ככל שמתחילים להשקות מאוחר יותר לאורך עונת הגידול- כך מתקבל גרגר קטן יותר ואיכות יין גבוהה יותר. ניתן להסיק כי ניתן להשתמש בשטח העלווה כבסיס לחישוב מקדם הגידול עבור יישום מודל השקיה מושכל בכרמי יין. במקרים בהם רצוי יבול מקסימלי יש להתחיל ליישם את המודל הזה כבר מהלבלוב של הגפנים, ובכרמים בהם רצויה איכות יש להשהות את מועד פתיחת ההשקיה לשלבים מתקדמים יותר של עונת הגידול (בהתאם לזן, כנה, סוג הקרקע, כמות המשקעים, ההתאדות הפוטנציאלית ועוד).

**השימוש בליזימטרים לקביעת מקדם הגידול (K_c) של גפן
יין מהזן "קברנה סוביניון" ובדיקת השפעת מועד תחילת
ההשקיה על מדדים פיסולוגיים ואנטומיים.**

חיבור לשם קבלת דוקטור לפילוסופיה מאת

שראל מוניץ

הוגש לסנט האוניברסיטה העברית בירושלים

כסלו תש"פ דצמבר 2019

**השימוש בליזימטרים לקביעת מקדם הגידול (K_c) של גפן
יין מהזן "קברנה סוביניון" ובדיקת השפעת מועד תחילת
ההשקיה על מדדים פיסולוגים ואנטומים.**

חיבור לשם קבלת דוקטור לפילוסופיה מאת

שראל מוניץ

הוגש לסנט האוניברסיטה העברית בירושלים

כסלו תש"פ דצמבר 2019